Characterization of wheat cuticle and wheat cuticle-related transcription factor genes in relation to drought

Huihui Bi

A thesis submitted to The University of Adelaide in fulfilment of the requirements for the degree of Doctor of Philosophy

Faculty of Sciences

School of Agriculture, Food and Wine

The University of Adelaide

September 2016

Table of contents

Abstract

The plant cuticle forms a hydrophobic layer covering the epidermis of aerial organs of a plant, and plays important roles in plant development and protection against environmental stresses. The primary role of the cuticle is to resist non-stomatal water loss. Several studies have explored the role of cuticle structure and composition in determining the cuticle's ability to resist water loss. A number of transcription factor (TF) genes have been identified that regulate the biosynthesis of the cuticle, and many of these genes were found to play important roles in drought tolerance. However, little information was available on the drought-related composition, structure and function of the cuticle or on the regulatory genes involved in cuticle synthesis in wheat. This PhD project was designed to explore such relationships in wheat, to examine the impact of drought on the wheat leaf cuticle, and to identify and characterise drought-responsive wheat TF genes encoding regulators of cuticle biosynthesis.

To fulfil the first two aims, residual transpiration rates, cuticle structure and cuticular wax composition were examined in five elite Australian wheat lines with contrasting glaucousness and drought tolerance, grown under conditions of sufficient or limited watering. Residual transpiration rates of non-glaucous and drought-sensitive Kukri were found to be much higher than those of the four glaucous and drought-tolerant lines, Excalibur, Drysdale, RAC875 and Gladius. No significant differences existed in the thickness of the cuticle between the five genotypes. Considerable variation was detected in the content of C31 β-diketone, which was well correlated with the respective levels of glaucousness. The amount of alkanes was increased under drought stress in all examined wheat lines while the thickness of the cuticle was increased in Drysdale and RAC875.

Six wheat genes encoding MYB TFs and five homeologues of two wheat *WXPL* genes were cloned. Tissue specific and drought-responsive expression of four *MYB* genes and two *WXPL* homeologues were examined in Kukri and RAC875. The involvement of MYB and WXPL TFs in the regulation of cuticle biosynthesis was confirmed by their activation of the promoters derived from wheat genes encoding cuticle synthesis enzymes and the SHN1/WIN1 TF. Two functional MYB-responsive DNA *cis*-elements were localized in the *TdSHN1* promoter, which was specifically activated by TaMYB74 but not by other MYB TFs characterised in this study. The different binding preferences of TaWXPL1D and TaWXPL2B for three stress-responsive DNA *cis*-elements were

demonstrated using the yeast one-hybrid assay. Schemes which indicated the roles of wheat MYB and WXPL TFs in the regulation of cuticle biosynthetic genes under drought stress were proposed.

To examine the function of TaSHN1 TF in wheat, transgenic wheat lines overexpressing the *TaSHN1* gene were produced. Significant decreases were detected in the stomatal density on the abaxial surfaces of flag leaves of transgenic plants compared to control plants, grown under well-watered conditions and drought. Water loss rates of flag leaves detached from transgenic lines grown under drought were much lower than those from control plants. Overexpression of *TaSHN1* decreased the content of C31 β-diketones but increased the content of C29/C31 alkanes, C26/C28 aldehydes and C24/C26 primary alcohols in cuticular wax. Promising changes in plant biomass and yield were seen in transgenic lines grown in controlled environments but these results require field confirmation. The results strongly suggested that TaSHN1 played a role in wax synthesis and/or deposition, and in plant water conservation. However, variation in the examined traits were observed between independent transgenic lines, which might result from different strengths of transgene expression in the selected lines.

Declaration

I certify that this work contains no material which has been accepted for the award of any other degree or diploma in my name in any university or other tertiary institution, and to the best of my knowledge and belief, contains no material previously published or written by another person, except where due reference has been made in the text. In addition, I certify that no part of this work will, in the future, be used in a submission in my name for any other degree or diploma in any university or tertiary institution without the prior approval of the University of Adelaide and where applicable, any partner institution responsible for the joint-award of this degree.

I give consent to this copy of my thesis when deposited in the University Library, being made available for loan and photocopying, subject to the provisions of the Copyright Act 1968.

The author acknowledges that copyright of published works contained within this thesis (as named in "Publications arising from this thesis") resides with the copyright holder(s) of those works.

I also give permission for the digital version of my thesis to be made available on the web, via the University's digital research repository, the Library Search and also through web search engines, unless permission has been granted by the University to restrict access for a period of time.

Signature **Date** 15/09/2016

Acknowledgements

First of all, I would like to express my sincere gratitude to my supervisors Professor Peter Langridge, Dr. Penny Tricker and Professor Maria Hrmova for their excellent guidance, constant support, and invaluable understanding and encouragement.

I am very grateful to Dr. Sergiy Lopato and Dr. Nikolai Borisjuk for their initiation of this project and for their supervision during the early stage of my candidature, and for their continuous help.

I acknowledge the University of Adelaide, the China Scholarship Council and the Australian Centre for Plant Functional Genomics for offering me this study opportunity and providing financial support.

I am grateful to Professor Dabing Zhang for offering me an opportunity to visit his lab in Shanghai Jiao Tong University where I performed GC-MS analyses of some of my samples.

I especially thank Dr. Yuri Shavrukov for his guidance and assistance in the lab. I am also grateful to Larissa Chirkova and Natalia Bazanova for their help in the lab. I thank Dr. Gwenda Mayo for suggestions and help with electron microscopic analysis.

I would like to extend my gratitude to all of the friendly people at the Australian Centre for Plant Functional Genomics, particularly, Dr. Nataliya Kovalchuk, Dr. Ryan Whitford, Dr. Stuart Roy, Dr. Ute Baumann, Dr. Delphine Fleury, Dr. Ursula Langridge, Yuan Li, Hui Zhou, Anzu Okada, Margaret Pallotta, Melissa Pickering, Priyanka Kalambettu and Raghuveeran Anbalagan.

I would also like to acknowledge my friends Jannatul, Ming, Yunfei, Pauline, Habtamu, Taj, Shani, Shashi and Fabio for making my PhD journey more enjoyable.

At last, I must thank my parents and grandparents for all the efforts and sacrifices they made to bring me and my brother up. I am grateful to my partner Yue Zhao for waiting for me while I was away from him. His perseverance and optimism offered me strength to accomplish this journey.

Abbreviations

ABA	abscisic acid
ACPFG	The Australian Centre for Plant Functional Genomics
AD	activation domain
AP2/ERF	APETALA2/ ethylene responsive factor
At	*Arabidopsis thaliana*
BD	binding domain
bp	base pair
CDS	coding sequence
CRT	C-repeat
DR	drought
DRE	dehydration-responsive element
DREB	drought responsive element binding protein
ERF	ethylene responsive factor
GC-MS	gas chromatography-mass spectrometry
IWGSC	International Wheat Genome Sequencing Consortium
MYB	myeloblastosis
NCBI	the National Centre for Biotechnology Information
QTL	quantitative trait loci
Q-PCR	quantitative real-time PCR
RTR	residual transpiration rate
SD	synthetic defined
SEM	scanning electron microscopy
Ta	*Triticum aestivum*
TEM	transmission electron microscopy
TF	transcription factor
VLCFA	very long chain fatty acid
WIN1/SHN1	*Arabidopsis* wax inducer 1 or SHINE1
WT	wild type
WW	well-watered
WXP	WAX PRODUCTION
Y1H	yeast one-hybrid

Publications arising from this thesis

1. Bi H, Luang S, Li Y, Bazanova N, Morran S, Song Z, Perera MA, Hrmova M, Borisjuk N, Lopato S. Identification and characterization of wheat drought-responsive MYB transcription factors involved in the regulation of cuticle biosynthesis. Journal of Experimental Botany, doi:10.1093/jxb/erw298. Feature article with a front cover photograph.

2. Bi H, Luang S, Li Y, Bazanova N, Hrmova M, Borisjuk N, Lopato S. Wheat drought-responsive WXPL transcription factors regulate cuticle biosynthesis genes. Submitted to Plant Molecular Biology.

3. Bi H, Kovalchuk N, Langridge P, Tricker P, Lopato S, Borisjuk N. The impact of drought on wheat leaf cuticle properties. Ready for submission.

4. Bi *et al*. Molecular and functional characterization of the wheat SHN1 transcription factor. Manuscript in preparation.

Chapter 1 Introduction and literature review

1.1 Introduction

Common wheat (*Triticum aestivum*) is one of the three most important and most produced grain crops in the world with maize and rice being the other two. Wheat grain contains 8-15% protein, which, as a staple food, might represent a considerable proportion of protein used for human consumption in less developed countries (Shewry 2009).

Abiotic stresses, such as drought, high temperature and salinity, considerably impair grain yields and quality. Drought is one of the most complex stresses, and it has been shown that breeding for drought resistant cultivars is a challenging task (Mickelbart *et al.* 2015). Tolerance mechanisms often vary with environmental conditions and it is difficult to establish screening approaches, which have to cover all variations related to drought. In addition, the genetic control of drought tolerance is complex as it has a multigenic/multiloci nature, and low heritability and high interaction between genotype and environment (Fleury *et al.* 2010; Mickelbart *et al.* 2015).

Crops adopt three main strategies to resist drought, namely, drought escape, drought avoidance and drought tolerance (reviewed in Bodner *et al.* 2015; Levitt 1980). Tolerance is more a mechanism of developing specialised physiological processes, while avoidance uses the competency of general physiological processes to provide mechanical and morphological apparatus to protect plants from the effects of severe environmental stimuli (Shepherd and Wynne Griffiths 2006). Drought avoidance is achieved *via* enhancement of water uptake or reduction of water loss.

Accumulation and/or alteration of epicuticular waxes on the surfaces of plants has been shown to be an effective way to decrease water loss and increase drought resistance (Aharoni *et al.* 2004; Bourdenx *et al.* 2011; Lee *et al.* 2014; Zhang *et al.* 2005; Zhang *et al.* 2007). Drought stress often induces alterations in plant cuticle, such as increases in the amount of wax and thickening of the cuticle layer (Cameron *et al.* 2006; Jäger *et al.* 2014; Kim *et al.* 2007a; Kim *et al.* 2007b; Kosma *et al.* 2009). All of this evidence suggests that the cuticle represents an important adaptation to drought.

A number of transcription factors (TFs) involved in plant cuticle regulation have been identified; overexpression of these TFs altered cuticle composition and content, and in many cases enhanced drought tolerance (Aharoni *et al.* 2004; Seo *et al.* 2011; Zhang *et al.* 2005; Zhang *et al.* 2007). Most of these TFs were identified and characterised in *Arabidopsis* (reviewed in Borisjuk *et al.* 2014). Little information is available on the transcriptional regulation of cuticle biosynthesis in wheat.

1.2 Drought resistance strategies of plants

According to Levitt (1980), plants use three main strategies to resist drought stress or water deficit (Fig 1.1), namely drought escape, drought avoidance and drought tolerance. Drought escape is the ability of a plant to finish its life cycle before serious water stress. This mechanism, mainly used by annual species, occurs in different forms including early maturity, developmental plasticity and remobilisation of pre-anthesis assimilates to grain (Turner 1979). Flowering time has been widely used as a measure of drought escape (Kooyers 2015). Drought avoidance, also referred to as dehydration avoidance, is the ability of a plant to maintain high water potential during dry periods (Blum 1988). It occurs when plants increase the efficiency of water use, which is achieved either through increasing water uptake, for example, by increasing rooting depth and penetration rate, or through reducing water loss by stomatal closure, leaf rolling and decrease of epidermal transpiration. This mechanism often applies to mild or moderate drought during a growing season, and frequent/cyclic mild droughts (Kooyers 2015). Drought tolerance, or desiccation tolerance, is the ability of a plant to endure water deficit at low plant water potential. Adaptive traits corresponding to this survival mechanism include osmotic adjustment, accumulation of protective solutes and increased cell membrane stability (Bodner *et al.* 2015).

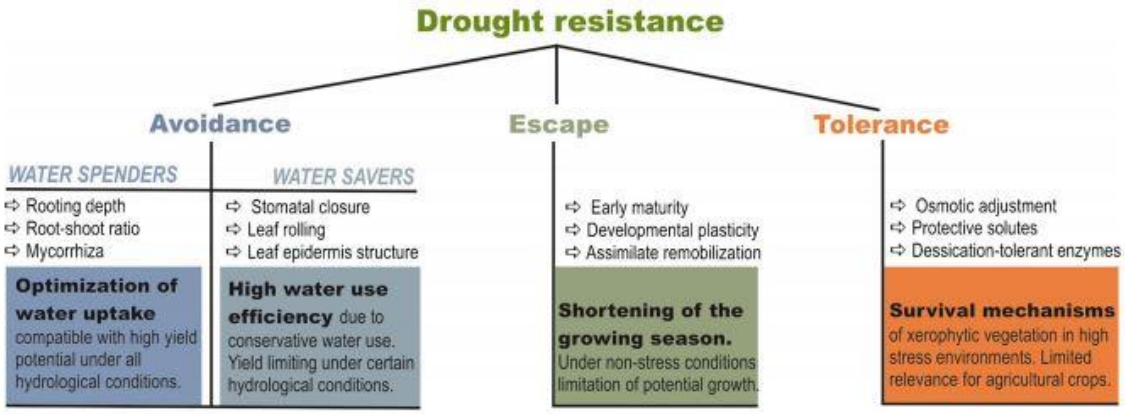

Figure 1.1 Drought resistance strategies according to Levitt (1980).

Figure is sourced from Bodner *et al.* (2015). Examples of adaptive traits for each of the resistance strategies and their potential application/limitation for agricultural crops are listed.

1.3 The cuticle

1.3.1 Cuticle structure

The plant cuticle is a waxy layer of a composite structure. It is divided into cuticle proper and cuticular layer, based on histochemical staining and chemical composition (reviewed in Pollard *et al.* 2008; Yeats and Rose 2013). The cuticle proper is cutin embedded with intracuticular waxes, while the cuticular layer contain cutin and associated polysaccharides. Epicuticular waxes accumulate on the surface of the cuticle and confer specific appearances to plant surfaces, such as a shiny green leaf surface in the Arabidopsis *shn* mutant (Aharoni *et al.* 2004), a glossy surface in the maize *Glossy 15* (*Gl15*) mutant (Moose and Sisco 1996), and glaucous surfaces on leaves and spikes of wheat (Adamski *et al.* 2013).

Barthlott *et al.* (1998) investigated the structures of epicuticular waxes using scanning electron microscopy in over 13,000 species, and identified 23 types of wax crystals. In particular, platelets and tubules were the most common wax structures, followed by rodlets and films. Some representative wax structures reported by these authors are shown in Figure 1.2. Furthermore, it was suggested that a correlation exists between diverse wax microstructures and particular chemical components. While platelets resulted from the presence of primary alcohols, tubules, the best known crystalloids, were divided into nonacosan-10-ol dominated tubules and β-diketone dominated tubules. The crystalline structures of the epicuticular waxes in 35 plant species were examined by Ensikat *et al.* (2006) *via* electron and X-ray powder diffraction studies. It was revealed that waxes exhibited three different crystalline structures, orthorhombic (of most waxes), triclinic (of secondary alcohols tubules), and hexagonal (of β-diketone tubules).

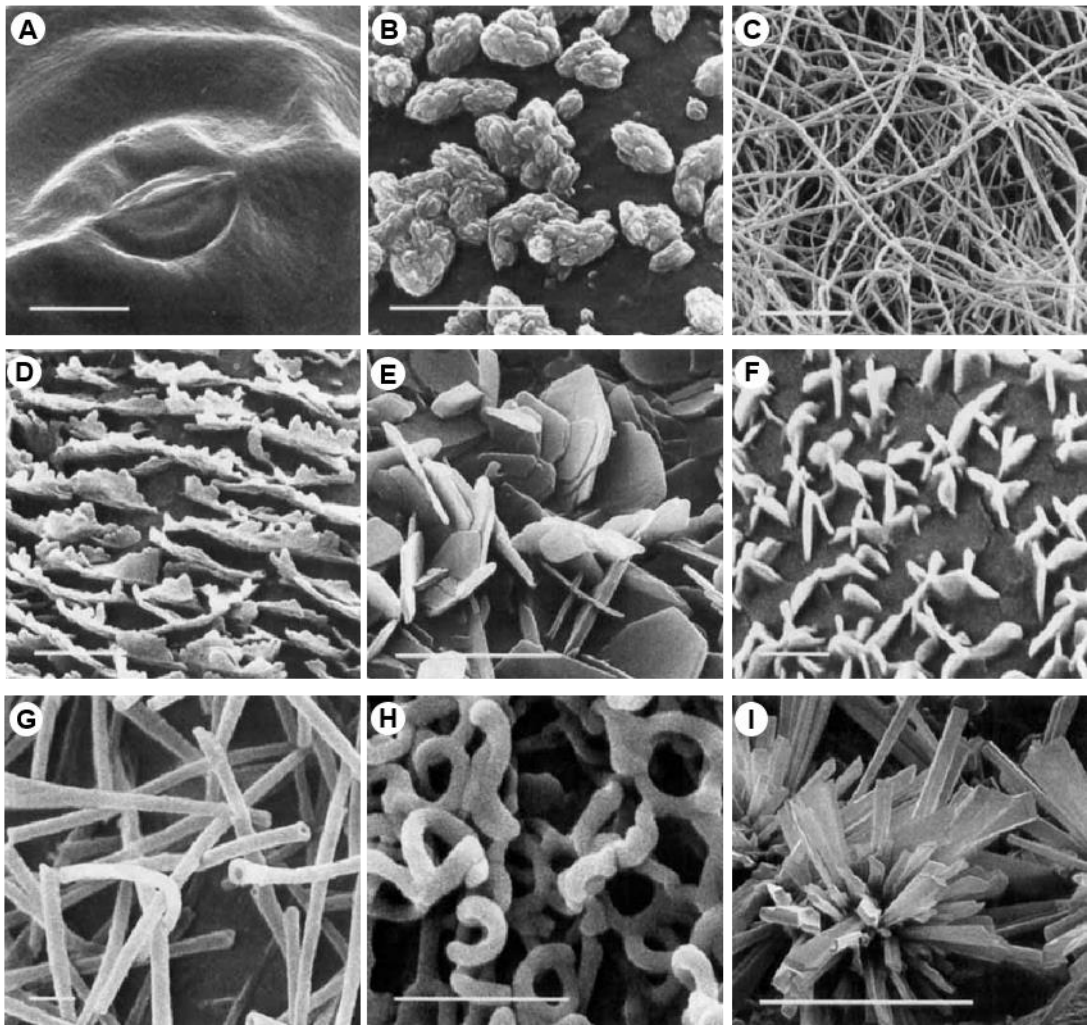

Figure 1.2 Representative wax structures in different plant species.

Images were sourced and re-arranged from Barthlott *et al*. (1998). (A) *Hydrocotyle bonariensis* Lam.. (Apiaceae): film. Scale bar = 10 µm. (B) *Aegiceras corniculatum* (L.) Blanco (Aegiceratataceae): granules. Scale bar = 5 µm. (C) *Drosera burmanni* Vahl (Droseraceae): threads. Scale bar = 2 µm. (D) *Grevillea bipinnatifida* R.Br. (Proteaceae): non entire platelets. Scale bar = 1 µm. (E) *Lecythis chartacea* Berg (Lecythidaceae): plates. Scale bar = 5 µm. (F) *Calliandra haematoma* (Bert) Benth. (Fabaceae): rosettes. Scale bar = 1 µm. (G) *Columellia oblonga* Ruiz & Pav. ssp. *sericea* (Kunth) Brizicki (Columelliaceae): tubules. Scale bar = 1 µm. (H) *Buxus sempervirens* L. (Buxaceae): coiled rodlets. Scale bar = 1 µm. (I) *Daphne tangutica* Maxim. (Thymelaeaceae): clusters of rodlets. Scale bar = 10 µm.

1.3.2 Role of the cuticle in drought

The cuticle was developed in terrestrial plants to prevent water diffusing into the atmosphere (Goodwin and Jenks 2005). It is a crucial barrier that, in concert with stomata, controls plant water status and helps plants survive under drought (Javelle *et al.* 2011).

The cuticle delays the onset of cellular dehydration stress under drought and is therefore considered an important component of plant drought resistance (reviewed in Goodwin and Jenks 2005; Kosma and Jenks 2007). During water deficit, stomata close and the cuticle becomes the primary barrier to plant water loss. Non-stomatal water loss through the cuticle may represent up to 50% of total water loss in wheat plants under drought during the daytime and 100% at night (Rawson and Clarke 1988). The cuticle plays an important role in osmotic signalling and tolerance. An *Arabidopsis* mutant, which was incapable of responding to osmotic stresses, was revealed to result from a mutation in an allele of *BODYGUARD* gene, which has been shown to be essential for the cuticle biosynthesis (Wang *et al.* 2011). Further, it was found that abscisic acid biosynthesis genes also could not be induced by osmotic stress in other cutin mutants. In addition, epicuticular waxes, an important component of the cuticle, can enhance leaf reflectance of light, which decreases radiation absorbance and thus leaf temperature. This may decrease vapour pressure differences between the leaf and the ambient air, which may reduce transpirational losses (Blum 1975).

Enhancement of leaf cuticular wax production appears to represent a prevalent response to water deficit across the terrestrial plant kingdom (Kosma and Jenks, 2007; Figure 1.3). For instance, a 75% increase in total wax amount per unit of leaf area was reported in *Arabidopsis* under water deficit (Kosma *et al.* 2009), and drought induced an over 150% increase in leaf total wax accumulation in tree tobacco (Cameron *et al.* 2006). Water deficit also increased the leaf cuticle thickness in *Arabidopsis*, by 49% (Kosma *et al.* 2009). The changes in *Arabidopsis* cuticle were associated with decreased cuticle permeability measured as reductions in rates of water loss and chlorophyll leaching from detached leaves (Kosma *et al.* 2009). Elevated cuticle membrane thickness in the *Arabidopsis cer9* (*eceriferum 9*) mutant correlated with lower transpiration rates and improved water use efficiency (Lü *et al.* 2009). In addition, increased amounts of cuticular waxes have been linked to enhanced drought tolerance of plants, such as *Arabidopsis* (Aharoni *et al.* 2004), alfalfa (Zhang *et al.* 2005) and Camelina (Lee *et al.* 2014).

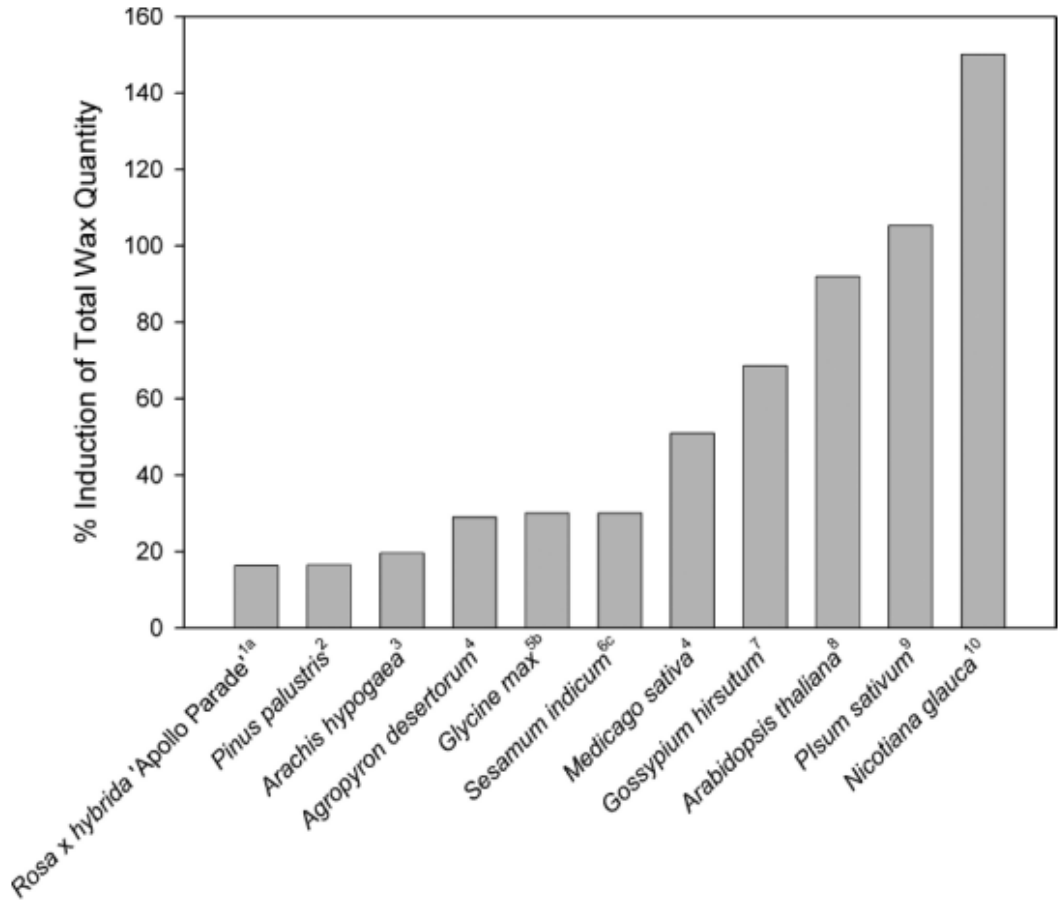

Figure 1.3 Percent induction (relative to non-treated controls) of total leaf cuticular wax amount in several plant species resulting from drought treatment.

Figure is sourced from Kosma and Jenks (2007). References: 1. (Jenks *et al.* 2001), 2. (Prior *et al.* 1997), 3. (Samdur *et al.* 2003), 4. (Jefferson *et al.* 1989), 5. (Kim *et al.* 2007b), 6. (Kim *et al.* 2007a), 7. (Bondada *et al.* 1996), 8. (Kosma *et al.*, unpublished), 9. (Sánchez *et al.* 2001), 10. (Cameron *et al.* 2006). Notes: [a] maximum induction on the most responsive cultivar; [b] mean of 18 cultivars; [c] mean of 18 cultivars.

Accumulation of epicuticular waxes on surfaces of some plant species results in a bluish-white colouration termed glaucousness, which is a visible form of densely distributed epicuticular wax crystalloids. Glaucousness increases radiation reflectance and reduces leaf temperatures and transpiration (Febrero *et al.* 1998; Richards *et al.* 1986). Richards *et al.* (1986) showed that a glaucous durum wheat isogenic line had a greater reduction in transpiration than photosynthesis, which led to an increased water use efficiency. The glaucousness in wheat starts to develop from about the time of meiosis, and reaches the full range when spike growth is greatest and crop water use is approaching a maximum. For these two main reasons, glaucousess was considered as an important adaptive trait for dryland wheat (Richards *et al.* 1986). Clarke and Richards (1988) reported a 33%

lower rate of residual transpiration in a glaucous wheat isogenic line than in the nonglaucous one. Glaucousness has been demonstrated as a positive factor for yield, especially in dry environments (Febrero *et al.* 1998; Johnson *et al.* 1983; Merah *et al.* 2000). In barley, a glaucous line exhibited a higher stable isotope ^{13}C discrimination than the non-glaucous line, suggesting these glaucous plants had lower transpiration efficiency, defined as the ratio of net photosynthesis to transpiration, over the long term (Febrero *et al.* 1998).

It is well accepted that the primary function of the cuticle is to resist water loss. However, which aspects of the cuticle determine its water barrier property is still unclear. Despite the fact that the induction of cuticular waxes is a common response of a plant to drought, there are also cases when the amounts of waxes are not inversely correlated with epidermal transpiration (Ristic and Jenks 2002; Schreiber and Riederer 1996). Particular wax species and the resulting cuticle matrix appear to be a relevant factor to water resistance features of the cuticle (reviewed in Yeats and Rose 2013). In an effort to evaluate the effects of the amount and the composition of leaf epicuticular waxes of species from the Caatinga and Cerrado, Oliveira *et al.* (2003) found that wax constituents were important determinants of water barrier properties of the cuticle, while increased wax deposits were not. Particularly, alkanes, a common wax component in many plant species, were found to be one of the most efficient barriers to water evaporation. In *Arabidopsis*, alkanes account for up to 70% of the total leaf wax amount, and overexpression of *Arabidopsis ECERIFERUM1* (*CER1*), a gene encoding a key enzyme involved in alkane biosynthesis, significantly increased the content of alkanes, reduced cuticle permeability and the susceptibility to water deficit (Bourdenx *et al.* 2011). Using an advanced backcross population derived from two *Capsicum* species with contrasting rates of post-harvest water loss, Parsons *et al.* (2012) found a negative correlation between water loss rates and the percentage of alkanes in total epicuticular wax amounts. Their results also provided evidence for the notion that straight-chain aliphatic components of the cuticle form stronger barriers than isoprenoid-based constituents.

Unlike cuticular waxes, the content of almost all cutin monomers in leaves of *Arabidopsis* were increased by drought, indicating that more total cutin, rather than more of specific cutin monomers, may be important in the response of *Arabidopsis* to water deficit (Kosma *et al.* 2009). This supports the notion that cutin and the corresponding ester-linkage play a major role in establishing barrier properties by providing the framework in which the cuticular waxes are arranged (reviewed in Goodwin and Jenks 2005; Kosma and Jenks

2007). The abnormal formation of cutin does dramatically affects the capacity of a plant to retain water. A natural-occurring mutation in the HvABCG31 transporter led to a low capacity to retain leaf water. This defect was associated with a reduction of cutin deposition and a thin layer of cuticle (Chen *et al.* 2011).

1.3.3 Other functions of the cuticle

The cuticle also acts as a physical barrier to protect plants from UV radiation and invasions of pathogens and pests. As a part of UV radiation, UV-B radiation (280-320 nm region) can cause damage to plant DNA and cell membranes and damage affecting photosynthesis, and influence levels of phytohormones (Rozema *et al.* 1997). Plants have developed a variety of defence mechanisms against such damage, which include filtering UV-B by phenolics in epidermal cells and by the cuticle, and absorption of UV-B by pigments, for example, flavonoids, which are typically localised in epidermal cells (Rozema *et al.* 1997). In *Dudleya brittonii*, a succulent rosette plant, glaucous leaves (leaves covered with a whitish and powdery wax coating), reflect more than 83% of light in the UV-B region; by contrast, non-glaucous leaves reflect less than 10% in the same region (Mulroy 1979). The reduction in epicuticular waxes and alterations in the cuticle structure increased sensitivity to the fungal pathogen *Exserohilum turcicum*, as revealed in the analysis of *Sorghum bicolor* bloomless (*bm*) mutants (Jenks *et al.* 1994). *Medicago truncatula irg1/palm1* mutants are deprived of abaxial leaf epicuticular waxes, which causes negative effects on spore differentiation of pathogens (Uppalapati *et al.* 2012). In wheat, infestation by Hessian fly, a worldwide pest, results in changes in wheat leaf cuticle properties, including alterations in cuticular wax composition and cutin monomer composition, suggesting that the integrity of the cuticle might be an important defence mechanism of wheat to Hessian fly (Kosma *et al.* 2010).

More and more evidence has accumulated on the involvement of the cuticle in plant development. Firstly, the cuticle functions in organ separation and avoidance of organ adhesion. A number of plant mutants have been reported showing the relationship between alterations of the plant cuticle and organ fusions. Such mutants include mutations in cuticle-related biosynthetic genes, such as *bodyguard* (Kurdyukov *et al.* 2006) and *lacs1 lacs2* mutants (Weng *et al.* 2010), mutations in transporter genes responsible for cutin and wax secretion, such as the *atwbc11* mutant (Luo *et al.* 2007) and *gpat4 gpat8 pec1* triple mutant (Fabre *et al.* 2016), and also mutations in regulatory genes, such as the maize *fused leaves1* (*fdl1*) (La Rocca *et al.* 2015). In addition, the cuticle in the reproductive organs was shown to be essential for pollen development. For example, a

rice male-sterile mutant was found to be caused by a mutation in *wax-deficient anther1* (*Wda 1*) gene, the absence of which caused significant defects in the biosynthesis of cuticular waxes on the anther walls and thus defective formation of pollen exine, which eventually disrupted microspore development (Jung *et al.* 2006). Similarly, defects in anther cutin biosynthesis were also shown to disrupt the formation of pollen exine and thus the fertility of rice (Li *et al.* 2010).

Recently, the cuticle was revealed to be involved in physical dormancy. By characterising *Medicago truncatula* mutants that lost physical dormancy, Chai *et al.* (2016) found that a nondormant seed mutant had an impaired cuticle layer in the seed coat. Chemical analysis revealed alterations of cutin monomer composition in the mutant. An important cutin biosynthetic gene, *CYP86A*, was identified as one of the downstream genes of *KNOX4*, the gene where mutation occurred. These results suggested that KNOX4-regulated cuticle formation was at least one of the mechanisms of KNOX4 controlling physical dormancy (Chai *et al.* 2016).

1.3.4 Cuticular wax composition

Plant cuticles are composed of a polymer matrix of cutin and organic solvent soluble cuticular waxes. The composition and content of plant cuticular waxes is complex and dynamic. They vary with plant species, organs and developmental stages. For instance, β-diketones are a major class of waxes in glaucous varieties of wheat and barley, but they are absent in many other plant species, such as *Arabidopsis*, tomato and rice. In wheat, β-diketones are not produced until the stage of stem elongation (Richards *et al.* 1986). Arabidopsis leaves contain 10 times less cuticular waxes than stems when 25-days old (Jenks *et al.* 1995). In addition, a series of environmental factors, such as light, temperature and humidity, influence wax constituents (reviewed in Shepherd and Wynne Griffiths 2006).

In general, cuticular waxes are a diverse mixture of aliphatics, namely, very long chain fatty acids (VLCFAs) and their derivatives with 20-34 carbons, including free fatty acids, primary and secondary alcohols, alkanes, aldehydes, ketones and esters (reviewed in Borisjuk *et al.* 2014; Kunst and Samuels 2009; Nawrath 2006; Yeats and Rose 2013). In many plant species, other wax constituents have been identified, such as triterpenoids on leaves of *Kalanchoe daigremontiana* (Jetter and Sodhi 2011) and fruits of tomato (*Lycopersicon esculentum*) (Vogg *et al.* 2004), and alkylresorcinol on leaves of wheat (Adamski *et al.* 2013).

1.3.5 Cuticular wax biosynthesis

The biosynthesis of cuticular waxes (Figure 1.4) begins with *de novo* C16 or C18 long-chain fatty acid synthesis in the plastids of epidermal cells catalysed by a fatty acid synthase (FAS), using an acyl carrier protein (ACP) as a cofactor (reviewed in Borisjuk *et al.* 2014; Li-Beisson *et al.* 2013). The end products, 16:0-ACP and 18:0-ACP, are hydrolysed by a fatty acyl thioesterase A or B (FATA or FATB) to free fatty acids before export outside of the plastid. The released C16 or C18 fatty acids are activated to C16/C18-CoA by a long-chain acyl-CoA synthase (LACS). These C16/C18-CoA compounds are transferred to the endoplasmic reticulum (ER), where they become a substrate for the fatty acid elongase (FAE) complex and give rise to VLCFAs with 20-34 carbons. The FAE complex, which catalyses four sequential reactions, consists of a β-ketoacyl-CoA synthase (KCS), a β-ketoacyl-CoA reductase (KCR), a β-hydroxyacyl-CoA dehydratase (HCD), and an enoyl-CoA reductase (ECR) (reviewed in Bernard and Joubes 2013; Kunst and Samuels 2009). The KCS enzyme was revealed to be rate-limiting because the introduction of KCS alone in yeast and plants was sufficient for the production of VLCFAs, and the introduction of additional copies of KCS produced more VLCFAs (Millar and Kunst 1997). By contrast, the activities of other three enzymes appear to be ubiquitous throughout plants and were not rate-limiting (Millar and Kunst 1997). Furthermore, it was revealed that KCS controls the length of VLCFAs *via* a molecular caliper mechanism (Denic and Weissman 2007).

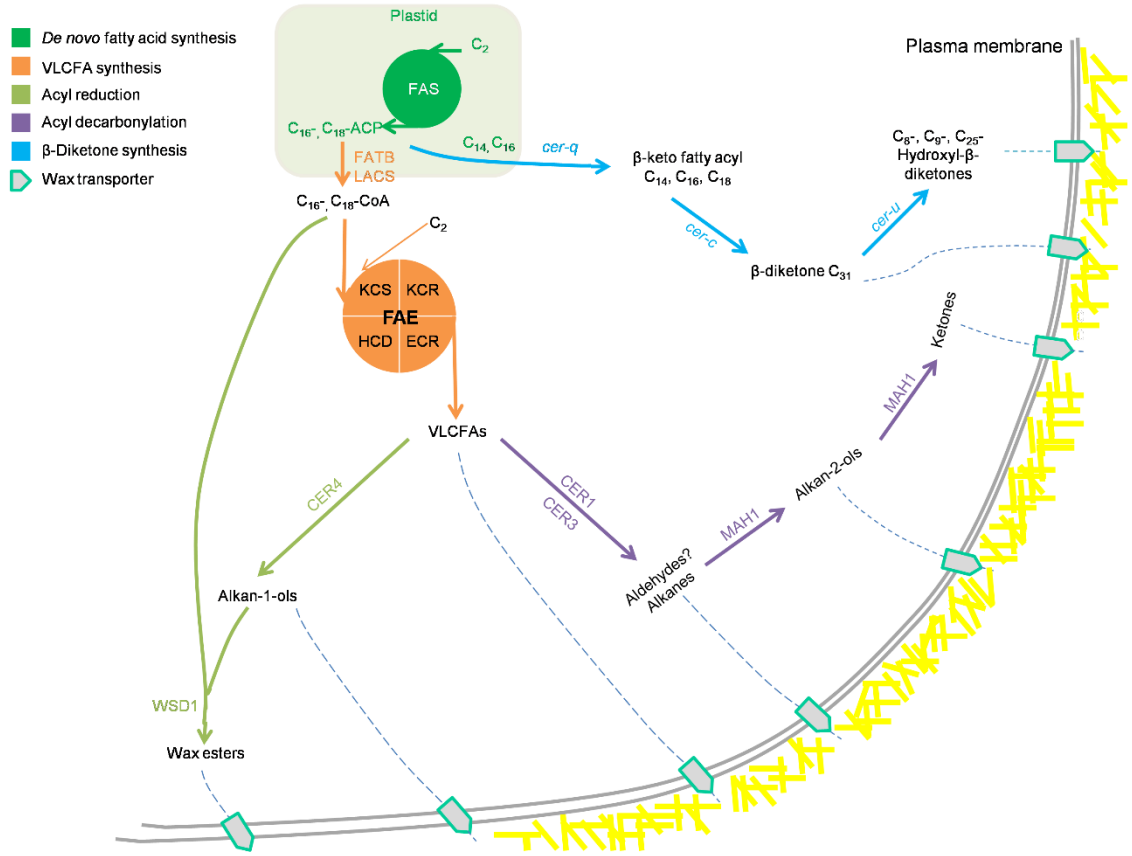

Figure 1.4 A diagram showing the cuticular wax biosynthesis and deposition.
Figure is sourced from Zhang *et al.* (2013).

VLCFAs are converted into aliphatic VLCFA derivatives through two biosynthetic pathways: the acyl reduction pathway (or alcohol-forming pathway) from which primary alcohols and wax esters are generated, and the decarbonylation pathway (or alkane-forming pathway), the products of which include alkanes, aldehydes, secondary alcohols and ketones. A number of genes involved in these two pathways have been identified. CER4, an alcohol forming fatty acyl-CoA reductase (FAR), was shown to be able to produce alcohols specifically from VLCFAs and was responsible for the biosynthesis of primary alcohols in the epidermal cells of *Arabidopsis* leaves, stems and roots (Rowland *et al.* 2006). A bifunctional wax ester synthase/diacylglycerol acyltransferase gene, *WSD1*, was found to be required for the biosynthesis of wax esters in the stem of *Arabidopsis* (Li *et al.* 2008). The amounts of wax esters in the stem wax of *wsd1* mutants were significantly decreased. An *in vitro* assay of protein activity demonstrated that WSD1 exhibited a high level of wax synthase activity; in contrast, the level of diacylglycerol acyltransferase activity was about 10-fold lower. Furthermore, the expression of the *WSD1* gene in yeast led to the accumulation of wax esters, but not

triacylglycerols. Overall, the work of Li *et al.* (2008) indicated that *WSD1* was primarily a wax synthase gene.

In the alkane-forming pathway, *CER1*, *CER3* and *WAX2* genes have been suggested to be the key components through the wax composition analysis of mutants and overexpression lines (Aarts *et al.* 1995; Bourdenx *et al.* 2011; Chen *et al.* 2003; Jenks *et al.* 1995). However, all attempts to examine CER1 biochemical activity in a yeast heterologous expression system failed (Bourdenx *et al.* 2011). Another work performed by the same research group revealed a mechanistic model for alkane formation; in this model CER1 interacted with CER3 and CYTB5s, cytochrome b5 isoforms (Bernard *et al.* 2012). Co-expression of *CER1* and *CER3* in transgenic *Arabidopsis* led to the accumulation of alkanes, and the addition of *CYTB5s* enhanced alkane production of CER1/CER3. The last two steps of the decarbonylation pathway, from alkanes to secondary alcohols and from secondary alcohols to ketones, were revealed to be catalysed by a cytochrome P450 enzyme CYP96A15, the midchain alkane hydroxylase 1 (MAH1). T-DNA insertional mutants of MAH1/ CYP96A15 contained no, or much lower, levels of secondary alcohols and ketones in stem waxes; conversely, the amounts of alkanes were increased in mutants (Greer *et al.* 2007). The overexpression of *MAH1* could partially complement the wax phenotypes in mutants under the control of both native and 35S constitutive promoters. Moreover, the 35S-MAH1 overexpression resulted in the production of alcohols and ketones in the leaf of *Arabidopsis*, whereas only low amounts of both constituents were identified in the wild type plants.

In *Triticeae*, like wheat and barley, as well as in some dicot plants, such as *Eucalyptus*, a third cuticular wax biosynthetic pathway was discovered. This pathway yields mainly β-diketones, the high content of which makes plants look glaucous. Our understanding of this pathway was mainly based on the biochemical and genetic analyses of a vast collection of *Eceriferum* (*cer*) mutants in barley, *cer-c*, *cer-q*, *cer-u* and their double and triple mutants (von Wettstein-Knowles 1972; von Wettstein-Knowles 1979; von Wettstein-Knowles 1995; von Wettstein-Knowles 2012). In hexaploid wheat, glaucousness is predominantly controlled by four loci, the wax production loci *W1* and *W2* and the wax inhibition loci *Iw1*and *Iw2* (Tsunewaki 1962; Tsunewaki and Ebana 1999; Zhang *et al.* 2013). With recent advances in barley genomic resources and mapping populations, Schneider *et al.* (2016) revealed that three barley genes (*Cer-c*, *Cer-q* and *Cer-u*) are a polyketide synthase, a lipase/carboxyl transferase and a P450 enzyme, respectively. Shortly after this report, Hen-Avivi *et al.* (2016) identified three wheat genes

as strong candidates for the wheat wax production (glaucousness) gene locus *W1* through the analyses of glaucousness traits, surface waxes and the transcriptome analysis of chromosome-arm substitution wheat lines. These three genes were designated as *Diketone Metabolism-PKS* (*DMP*), *Diketone Metabolism-Hydrolase* (*DMH*) and *Diketone Metabolism-CYP450* (*DMC*). The roles of *DMP* and *DMH* in the wheat β-diketone biosynthetic pathway were confirmed *in planta via* Virus-Induced Gene Silencing (VIGS). Heterologous expression in *E. coli* suggested that DMH is a 3-ketoacyl-ACP thioesterase and uses 3-ketoacyl-ACP as a substrate, rather than 3-ketoacyl-CoA. Furthermore, querying the three wheat genes (*DMP, DMH* and *DMC*) against the barley genome led to three top hits, MLOC_59804, MLOC_13397 and MLOC_12151, which actually are *Cer-c*, *Cer-q* and *Cer-u*, respectively, as revealed by Schneider *et al.* (2016). Contrasting with the suggested function of its wheat counterpart DMH, Cer-q was proposed to be a lipase/carboxyl transferase based on protein homology (Schneider *et al.* 2016).

1.3.6 Known TFs regulating cuticle biosynthesis

Many studies have revealed that the cuticular wax biosynthesis is regulated at transcriptional (mainly by TFs), post-transcriptional (*e.g.*, *via* small RNA) and post-translational (*e.g.*, *via* ubiquitination) levels (reviewed in Lee and Suh 2015a). A number of cuticle biosynthesis-related TFs have been identified. Most of them belong to two large families of plant TFs, which are APETALA2/Ethylene Responsive Factor (AP2/ERF) and myeloblastosis (MYB) families (reviewed in Borisjuk *et al.* 2014).

Overexpression of these TFs alters cuticle deposition and/or composition, and often increases stress tolerance of transgenic plants (Aharoni *et al.* 2004; Seo *et al.* 2011; Seo and Park 2011; Zhang *et al.* 2005; Zhang *et al.* 2007).

1.3.6.1 AP2/ERF TFs

AP2/ERF constitutes one of the largest families of TFs in plants and includes TFs that contain one or two AP2 DNA binding domains (reviewed in Licausi *et al.* 2013). Based on the number of AP2 domains and the presence of other DNA binding domains, members of this superfamily were divided into the AP2, ERF, DREB (dehydration-responsive element-binding) and RAV (Related to ABI3/VP1) subfamilies (reviewed in Mizoi *et al.* 2012). The members of ERF and DREB subfamilies contain a single AP2 domain. ERFs usually binds an ethylene responsive *cis*-element, known as a GCC-box (AGCCGCC) (Ecker 1995). In some cases, ERFs can also bind dehydration-

responsive element (DRE; ACCGAC) and C-repeat element (CRT; GCCGAC) (Lee *et al.* 2004; Zhang *et al.* 2009), which are usually recognised by DREB proteins (Sakuma *et al.* 2002). Both ERFs and DREBs are involved in the regulation of plant development and responses to biotic and abiotic stresses (reviewed in Licausi *et al.* 2013; Mizoi *et al.* 2012; Xu *et al.* 2011). According to Nakano *et al.* (2006), *Arabidopsis* wax inducer/SHINE (WIN/SHN) TFs and *Medicago* WAX PRODUCTION (WXP) TFs that are reviewed here, belong to the ERF and DREB subfamilies, respectively.

Arabidopsis wax inducer 1 or *SHINE1* (*WIN1/SHN1*) was the first identified TF gene in plants whose product regulates the biosynthesis of cuticular waxes (Aharoni *et al.* 2004; Broun *et al.* 2004). Multiple genes involved in wax biosynthesis, particularly, CER1, CER2 and KCS1, were up-regulated in transgenic lines overexpressing *WIN1/SHN1* (Broun *et al.* 2004). Kannangara *et al.* (2007) found that *WIN1/SHN1* overexpression caused changes in cutin composition and the overall amount of cutin in both leaves and flowers. Gene expression profiling showed that five cutin biosynthesis genes, which are *CYP86A7*, *CYP86A4*, *LACS2*, *HTH-like*, and *GPAT4*, were activated by WIN1/SHN1 in transgenic *Arabidopsis*. The promoter of *LACS2*, a cutin pathway gene that encodes a long-chain acyl-CoA synthetase, was directly bound by WIN1/SHN1 *in planta*.

Overexpression of two other members (*SHN2* and *SHN3*) of the SHN clade exhibited a similar phenotype to *SHN1* overexpression, which included a shiny green leaf colour, leaf curling and distorted petal structure (Aharoni *et al.* 2004). Further, through silencing of all three SHNs *via* a microRNA approach, it was revealed that three SHNs act redundantly in surface patterning of flower organs, especially in petals, in *Arabidopsis via* controlling cuticular lipids and modifying cell wall properties, such as regulating epidermal cell elongation and nanoridge formation (Shi *et al.* 2011). Using a transient expression assay, the authors showed that SHN TFs act by direct binding to promoters of genes encoding cutin and/or suberin and cell wall associated proteins, such as CYP86A7, CYP86A4, BDG3, FAR1, RXF26 and GRP.

In addition to alterations in the cuticle and organ surface patterning, *WIN1/SHN1* gene overexpression increased cuticle permeability, reduced stomatal density and significantly enhanced drought tolerance (Aharoni *et al.* 2004). In an attempt to disclose the molecular mechanisms underlying the association between wax induction and drought tolerance, Yang *et al.* (2011) applied a gene switching approach to regulate expression of the *WIN1/SHN1* gene. They confirmed that induced drought tolerance by WIN1/SHN1 was caused by cuticular wax accumulation and a decreased number of stomata. More recently,

a role of *AtWIN1/SHN1* and *SlWIN/SHN3* (*Solanum lycopersicum*) in plant defence responses to pathogens was reported (Buxdorf *et al.* 2014; Sela *et al.* 2013).

Another important function of WIN/SHN TFs is mediation of organ adhesion and separation. A very specific expression of *SHN2* in the dehiscence zones of anther and silique of *Arabidopsis* suggested a role of the *SHN2* gene at the interface between cells and cell layers (Aharoni *et al.* 2004). Co-silencing of all three *SHN* genes resulted in postgenital fusions of reproductive organs, particularly, in petals (Shi *et al.* 2011). Co-silencing of two different pairs of target genes of SHNs all caused severe floral organ fusions and alterations in cell shape and decoration. These two pairs of genes were *CYP86A4* with *CYP86A7*, and *At5g33370* (a putative GDSL-lipase) with its close homolog *LTL1*; genes within each pair belong to the same family and have been shown in the same study to be putative target genes of the SHN TFs.

The gene in the *nud* locus that controls adhering hulls in barley grains was revealed to be a homologue of *AtWIN1/SHN1* (Taketa *et al.* 2008). These authors showed that hulless caryopses were not stained by Sudan black B, a lipophilic dye, during all examined stages, while dehulled caryopses of the control (naturally with a hull) were stained at 2- and 3-week old stages. This suggested that a lipid layer on the epidermis of a pericarp was critical for the formation of hulled barley.

Other AP2/ERF TFs that regulate cuticle biosynthesis are the products of *WAX PRODUCTION* (*WXP1* and *WXP2*) genes from the legume *Medicago truncatula*. These TFs have a low level of amino acid sequence identity to the members of the WIN/SHN clade of the ERFs (Zhang *et al.* 2005; Zhang *et al.* 2007). Expression of both *WXP* genes was ABA-dependent and controlled by drought.

Strong constitutive expression of *WXP1* in transgenic *Medicago sativa* as well as expression of both *WXP1* and *WXP2* in transgenic *Arabidopsis* significantly increased cuticular wax deposition on plant leaves, which could be visually detected (Zhang *et al.* 2005; Zhang *et al.* 2007). The metabolomics analysis of cuticles in *WXP1* and *WXP2* transgenic *Arabidopsis* plants demonstrated differences in the contents and chain length distributions of various wax components. For example, the amount of n-alkanes, the major wax component of *Arabidopsis* leaves, increased significantly in both *WXP1* and *WXP2* transgenic *Arabidopsis* compared to control plants. However, the content of primary alcohols increased in *WXP1* transgenic plants but decreased in *WXP2* transgenic plants. Changes were also detected in physical properties of cuticles. A chlorophyll leaching assay showed no changes in the leaf cuticle permeability of the *WXP1*

Arabidopsis plants and decrease in the permeability of *WXP1* transgenic alfalfa, but increase in the permeability of the *WXP2 Arabidopsis* plants. Expression of three *fatty acid elongase* (*FAE*)-like genes and two *LACERATA* (*LCR*, encoding cytochrome P450 monooxygenases) genes was up-regulated in *WXP1* transgenic alfalfa plants compared to control plants (Zhang *et al.* 2005). Drought tolerance of all alfalfa and *Arabidopsis* transgenic *WXP* lines was significantly enhanced compared to control plants. Expression of *WXP1* in alfalfa and *WXP2* in *Arabidopsis* interfered significantly with the growth and development of transgenic lines, however, no such interference was observed when *WXP1* was expressed in *Arabidopsis*. These results suggested that *WXP1* and *WXP2* under appropriate conditions could be interesting candidate genes for genetic improvement of drought tolerance (Zhang *et al.* 2005; Zhang *et al.* 2007).

1.3.6.2 MYB TFs

MYB TFs comprise a large family of TFs in plants, members of which contain one or several MYB DNA-binding domains of 52 amino-acid residues (Baldoni *et al.* 2015; Dubos *et al.* 2010; Stracke *et al.* 2001). According to the number of repeated MYB domains the MYB TF family is divided into four subfamilies: 4R-MYB, 3R-MYB (R1R2R3-MYB), 1R-MYB or MYB-related proteins and R2R3-MYB. R2R3-MYB represents the largest subfamily of MYBs, and are involved in plant development and plant response to various biotic and abiotic stresses (Baldoni *et al.* 2015; Dubos *et al.* 2010). The DNA-binding domain of this MYB subfamily regulates gene expression by binding to MYB-recognition (MYBR) sites, YAACKG or CNGTTR (Abe *et al.* 2003; Urao *et al.* 1993). So far, all reported MYB-type regulators of cuticle biosynthesis belong to the R2R3-MYB subfamily of TFs. These are AtMYB41, AtMYB96, AtMYB30, AtMYB94, AtMYB16, AtMYB106 and SlMYB12 (Adato *et al.* 2009; Cominelli *et al.* 2008; Lee and Suh 2015b; Oshima *et al.* 2013; Raffaele *et al.* 2008; Seo *et al.* 2011).

The A*tMYB41* gene had a low level of expression in all analysed organs of *Arabidopsis* in the absence of stress, but it was strongly induced by ABA, drought, and high salinity (Cominelli *et al.* 2008). Overexpression of *AtMYB41* in transgenic *Arabidopsis* plants led to increased cuticle permeability. The expression of a number of genes related to lipid biosynthesis and transport, cuticle metabolism, and cell wall biosynthesis were found to be affected by overexpression of *AtMYB41* in transgenic *Arabidopsis* plants (Cominelli *et al.* 2008). *AtMYB41* controls primary metabolism and negatively regulates short-term transcriptional responses to osmotic stress (Lippold *et al.* 2009). It was shown that

AtMYB41 was induced by osmotic stress and ABA in a way similar to induction of known ABA-responsive genes, such as *AtAil1*, *AtRab18*, *AtRd29b* and *AtAia1*, which are a part of the AREB regulon (Fujita *et al.* 2005; Lippold *et al.* 2009). More recently, Kosma *et al.* (2014) demonstrated that AtMYB41 can activate ectopic synthesis and deposition of suberin in leaves of transgenic *Arabidopsis* and tobacco. Although pleiotropic effects of strong transgene overexpression occurred, the significantly elevated level of expression of genes associated with biosynthesis, transport and assembly of lamellar suberin in transgenic plants strongly supported the role of AtMYB41 in the regulation of suberin production. In addition, these authors demonstrated that the *AtMYB41* promoter was not active in unstressed plants, but it was activated in the endodermis by ABA and high salinity. Phosphorylation of AtMYB41 by mitogen-activated protein kinase 6 (MPK6) through Ser251 enhanced its binding to the promoter of a *LTP* gene (Hoang *et al.* 2012). Transgenic *Arabidopsis* plants overexpressing wild type *AtMYB41* showed enhanced salt tolerance, while overexpression of mutated *AtMYB41S251A* in transgenic plants led to decreased salt tolerance during seed germination and initial root growth. These results suggested an important role of phosphorylation in the biological function of AtMYB41 (Hoang *et al.* 2012).

Another well studied cuticle-related TF is AtMYB96, which was initially identified as a regulator of drought stress responses in *Arabidopsis* that integrated ABA and auxin signals (Seo *et al.* 2009). Expression of *AtMYB96* was induced by ABA, drought and high salinity. Constitutive overexpression of *AtMYB96* conferred drought tolerance to transgenic *Arabidopsis* plants, while a knockout mutant was more sensitive to drought than wild type plants (Seo *et al.* 2009). This was confirmed by studies of the loss-of-function mutant *myb96*, which also exhibited sensitivity to drought (Guo *et al.* 2013). Strong constitutive expression of *AtMYB96* has been used to improve drought tolerance of an emerging oilseed crop plant *Camelina sativa* (Lee *et al.* 2014). It has recently been shown that expression of *AtMYB96* is also induced by low temperature. Overexpression of *AtMYB96* in transgenic *Arabidopsis* plants enhanced freezing tolerance by activation of the *CBF* regulon (Guo *et al.* 2013; Lee and Suh 2015a). In addition, AtMYB96-mediated ABA signalling improved plant resistance to pathogens through induction of salicylic acid (SA) biosynthesis (Seo and Park 2010). The transcriptional activation by AtMYB96 of cuticular wax biosynthesis in connection with increased drought tolerance was originally reported by Seo *et al.* (2011). A microarray analysis revealed that AtMYB96 activated a group of genes encoding cuticle wax biosynthetic enzymes, including several enzymes responsible for condensing of VLCFAs (Seo *et al.* 2011). The

cuticular wax depositions in both leaves and stems were significantly increased in the activation-tagged *myb96-1D* mutant and decreased in the loss-of-function *myb96-1* mutant. MYB-recognition *cis*-element TAACTA/G was found in the promoters of target genes, and a direct interaction of AtMYB96 with promoters of several genes encoding wax biosynthetic enzymes was demonstrated using several approaches (Seo *et al.* 2011).

Two closely related TFs of AtMYB96, AtMYB30 and AtMYB94, were also shown to regulate cuticular wax biosynthetic genes (Lee and Suh 2015b; Raffaele *et al.* 2008). The *Arabidopsis* MYB30 TF was originally reported to be a positive regulator of a cell death pathway mediated by hypersensitive plant immune response to pathogen attack (Raffaele *et al.* 2008). Putative target genes of AtMYB30 were identified using comparative microarray analysis of gene expression profiles between transgenic *Arabidopsis* lines with either *AtMYB30* overexpression or antisense RNA silencing and wild type plants. It was found that among putative AtMYB30 targets there were genes that encoded four enzymes forming the acyl-coA elongase complex, which were responsible for the synthesis of VLCFAs (Raffaele *et al.* 2008). The role of AtMYB94 in cuticular wax biosynthesis was confirmed by the analysis of transgenic *Arabidopsis* with constitutive overexpression of this gene. The comparison of transgenic and control plants revealed enhanced expression of cuticular wax biosynthetic genes, increased accumulation of cuticular waxes, and a reduced rate of cuticular transpiration in transgenic plants (Lee and Suh 2015b). It was shown that AtMYB94 activated the expression of wax biosynthetic genes *WSD1, KCS2/DAISY, CER2, FAR3* and *ECR* by binding directly to their promoters. The level of expression of the *AtMYB94* gene under drought was increased approximately nine-fold. An increased accumulation of cuticular waxes reduced the rate of cuticular transpiration in the leaves of AtMYB94 transgenic *Arabidopsis* lines under drought. The analysis of the *fused leaves 1* (*fdl1-1*) mutation in maize revealed involvement of the *Fdl1* gene product, ZmMYB94, in the regulation of cuticle deposition in young seedlings and the establishment of a regular pattern of epicuticular wax deposition on the epidermis of young leaves (La Rocca *et al.* 2015). Lack of *Fdl1* led to developmental defects, such as abnormal coleoptile opening and the presence of curly leaves with areas of fusion between the coleoptile and the first leaf, or between the first and the second leaf.

Two other cuticle-related *MYB* genes, *AtMYB16* and *AtMYB106*, are paralogous genes and are involved in the formation of epidermal cell shape and regulation of cuticle biosynthesis by cooperating with the *WIN1*/*SHN1* gene in *Arabidopsis thaliana* and *Torenia fournieri* (Folkers *et al.* 1997; Gilding and Marks 2010; Jakoby *et al.* 2008;

Oshima *et al.* 2013). Expression in transgenic *Arabidopsis* of *AtMYB106* fused to a repressor domain (Hiratsu *et al.* 2003), as well as the knockout/knockdown of *AtMYB106* and *AtMYB16* genes using RNAi, negatively influenced cuticle formation, and resulted in adhesion of flowering organs (Oshima and Mitsuda 2013; Oshima *et al.* 2013). In addition, a significant overlap in sets of cuticle biosynthetic genes regulated by AtMYB106 and WIN1/SHN1 TFs in transgenic plants was found by the microarray analysis of gene expression (Oshima *et al.* 2013).

Another MYB TF, which is involved in plant cuticle regulation is SlMYB12. Initially, characterisation of the tomato *colorless peel y* mutant lacking the yellow flavonoid pigment demonstrated that SlMYB12 was a key transcriptional regulator of flavonoid accumulation in the cuticle. However, the detailed gene expression and metabolomic analysis of transgenic tomato plants revealed further roles of SlMYB12 in the regulation of tomato fruit cuticle biosynthesis (Adato *et al.* 2009). The *Arabidopsis* homologue of this gene has not yet been characterised.

1.4 Conclusions

Under severe water deficit, plants close their stomata, and the cuticle becomes one of the most influential factors to limit water loss and thus improve plant survival. The water barrier property of the cuticle is well accepted and demonstrated, although it is still unclear which aspects of the cuticle play an important role, due to a high complexity of its composition and regulation of biosynthesis. Drought-induced changes in the cuticle have been reported in many plant species, and some of them were associated with enhanced drought tolerance. However, little information is available on the relationship between drought stress and the structure and composition of the cuticle in wheat, one of the most important crop plants. A number of cuticle biosynthesis-related TFs have been identified. Overexpression of these TFs altered cuticle deposition and/or composition, and often increased the drought tolerance of transgenic plants. Most of these TFs were identified and characterised in *Arabidopsis*. None of cuticle-related TFs has been reported in wheat other than MYB TFs, which constitute Chapter 3 of this thesis.

1.5 Research Aims

The aims of this PhD project were to characterise the wheat leaf cuticle properties as a water barrier, the cuticle structure and composition, and the involvement of TFs in relation to drought. The further goals were to identify critical traits and genes that can potentially be used for genetic improvement of wheat drought tolerance.

Five elite Australian wheat genotypes with contrasting glaucousness and drought tolerance, Kukri, Excalibur, Drysdale, RAC875 and Gladius, were selected to study the wheat leaf cuticle in relation to drought in the course of this PhD candidature. Firstly, we examined the residual transpiration rates in the five lines, which refer to the water loss rates from detached leaves at minimal stomatal transpiration. It was found that the rates of water loss from the non-glaucous and drought-sensitive line Kukri were much higher than those from the four glaucous and drought-tolerant lines. We employed electron microscopy and gas chromatography-mass spectrometry to reveal the thickness of the cuticle layer, and the structure and composition of epicuticular wax in an effort to establish a link between cuticle properties, structure and composition. All the above studies were also performed on plants grown under conditions of limited watering to investigate the impact of drought on leaf cuticle properties (**Chapter 2**).

Homology cloning was used as an approach to identify wheat drought-responsive genes that encode the regulators of cuticle biosynthesis. Several genes that were homologous to the well-studied TF genes of the MYB (**Chapter 3**) and ERF (**Chapter 4**) families from other plant species were cloned. The transcriptional activation activity of cloned genes was confirmed in yeast and in wheat cell cultures, and the identity and positions of activation domain were examined in yeast. The molecular responses of cloned MYB and ERF genes to the conditions of rapid dehydration and slowly-developing drought were investigated in the non-glaucous, drought-sensitive Kukri and the glaucous, drought-tolerant RAC875 genotypes. The roles of TaMYB31, TaMYB74, TaWXPL1D and TaWXPL2B TFs in the regulation of cuticle biosynthesis under drought were proposed.

The biological roles of TaSHN1, a wheat orthologue of Arabidopsis WIN1/SHN1 TF, were examined in transgenic wheat. Drought related traits, such as water loss rates from detached leaves, stomatal density and the leaf cuticular wax composition, as well as yield components, were studied using transgenic lines grown under the conditions of sufficient and limited watering (**Chapter 5**).

The significance of data generated during this PhD candidature and the potential directions for future research based on our findings, were discussed in **Chapter 6**.

Chapter 2 The impact of drought on wheat leaf cuticle properties

Statement of Authorship

Title of Paper	The impact of drought on wheat leaf cuticle properties
Publication Status	☐ Published ☐ Accepted for Publication ☐ Submitted for Publication ☑ Unpublished and Unsubmitted work written in manuscript style
Publication Details	Bi H, Kovalchuk N, Langridge P, Tricker P, Lopato S, Borisjuk N. The impact of drought on wheat leaf cuticle properties.

Principal Author

Name of Principal Author (Candidate)	Huihui Bi
Contribution to the Paper	Designed the experiments with supervisors, performed experiments, analysed data and wrote the manuscript.
Overall percentage (%)	70%
Certification:	This paper reports on original research I conducted during the period of my Higher Degree by Research candidature and is not subject to any obligations or contractual agreements with a third party that would constrain its inclusion in this thesis. I am the primary author of this paper.
Signature	Date 13/09/2016

Co-Author Contributions

By signing the Statement of Authorship, each author certifies that:

i. the candidate's stated contribution to the publication is accurate (as detailed above);
ii. permission is granted for the candidate in include the publication in the thesis; and
iii. the sum of all co-author contributions is equal to 100% less the candidate's stated contribution.

Name of Co-Author	Nataliya Kovalchuk
Contribution to the Paper	Performed stomatal density analyses, assisted in microscopic work and reviewed the manuscript.
Signature	Date 11.09.16

Name of Co-Author	Peter Langridge
Contribution to the Paper	Supervised the development of experiments and analyses of data. Edited the manuscript.
Signature	Date 12/09/2016

Name of Co-Author	Penny Tricker
Contribution to the Paper	Supervised analyses of data, edited the manuscript and will act as the corresponding author.
Signature	Date 11/9/16

Name of Co-Author	Sergiy Lopato
Contribution to the Paper	Supervised the development of experiments and edited the manuscript.
Signature	Date 12/09/2016

Name of Co-Author	Nikolai Borisjuk
Contribution to the Paper	Conceived the idea, designed and supervised the experiments. Analysed and discussed data, edited the manuscript.
Signature	Date 31-8-2016

The impact of drought on wheat leaf cuticle properties

Huihui Bi[1], Nataliya Kovalchuk[1], Peter Langridge[2], Penny Tricker[1]*, Sergiy Lopato[1], Nikolai Borisjuk[1]

[1]*Australian Centre for Plant Functional Genomics, PMB1 Glen Osmond, South Australia 5064, Australia*

[2]*School of Agriculture, Food and Wine, University of Adelaide, PMB1 Glen Osmond, South Australia 5064, Australia*

*Author to whom correspondence should be addressed.

E-mails:

huihui.bi@acpfg.com.au

nataliya.kovalchuk@acpfg.com.au

peter.langridge@adelaide.edu.au

penny.tricker@acpfg.com.au

slv777@hotmail.com

nborisjuk@gmail.com

Abstract

The plant cuticle is the outmost layer covering aerial tissues and is composed of cutin and waxes. The cuticle plays an important role in protection from environmental stresses and glaucousness, the bluish-white colouration of plant surfaces associated with cuticular waxes, has been suggested as a contributing factor in crop drought tolerance. However, the cuticle structure and composition is complex and it is not clear which aspects are important in determining a role in drought tolerance. Therefore, we analysed residual transpiration rates, cuticle structure and epicuticular wax composition under well-watered conditions and drought in five Australian wheat genotypes, Kukri, Excalibur, Drysdale, RAC875 and Gladius, with contrasting glaucousness and drought tolerance. Significant differences were detected in residual transpiration rates between non-glaucous and drought-sensitive Kukri and four glaucous and drought-tolerant lines. No simple correlation was found between residual transpiration rates and the level of glaucousness among glaucous lines. Modest differences in the thickness of cuticle existed between the examined genotypes, while drought significantly increased cuticle thickness in Drysdale and RAC875. Wax composition analyses showed various amounts of C31 β-diketone among genotypes and increases in the content of alkanes under drought in all examined wheat lines. The results provide new information on the relationship between drought stress and the structure and composition of cuticle for this agriculturally important crop plant.

Keywords: cuticle, cuticular wax, β-diketone, drought, glaucousness, residual transpiration rate, stomatal density, water deficit, wheat (*Triticum aestivum*).

Introduction

Bread wheat, *Triticum aestivum*, is the world's most widely grown crop, representing about 30% of the cereal cultivation area and providing 20% of the calories for the human population. Drought significantly limits crop production and the duration of drought periods is increasing due to climate change, declining ground and surface water resources, and warming of air temperature in most of the cereal cropping regions around the world (Lobell and Gourdji 2012). An understanding of the physiological, biochemical, and genetic mechanisms allowing plants to cope with environmental challenges is of vital importance for breeding crops with improved stress tolerance and performance under stress (Langridge and Reynolds 2015).

The plant cuticle evolved as an exterior extension of epidermal cell walls, is a continuous hydrophobic sheet that covers aerial surfaces of all plant organs and acts as an interface in plants' interactions with various biotic and abiotic environmental factors. The cuticle is a crucial barrier that, in concert with stomata, controls plant water status and helps plants survive under drought and high UV radiation (Javelle *et al.* 2011). Structurally, the wheat cuticle is a 0.1–10 μm thick membrane composed principally of a polyester matrix intertwined with a range of long chain hydrocarbons. Based on solubility in organic solvents, the cuticle components are divided into insoluble cutin and soluble cuticular waxes. Intracuticular wax is embedded in the underlying cutin polyester framework and epicuticular wax is overlaid on the cutin matrix and intracuticular wax. The waxes are typically a complex mixture of derivatives of very-long-chain saturated aliphatics, which include fatty acids, alkanes, aldehydes, ketones, and primary and secondary alcohols (Jetter *et al.* 2007; Samuels *et al.* 2008).

Many elements of the cuticle biosynthesis pathways, including cuticle-related genes encoding key enzymes and regulatory transcription factors, were uncovered primarily by characterising numerous cuticle mutants in *Arabidopsis* and mutants in tomato, rice, maize, and barley (reviewed in Borisjuk *et al.* 2014; Lee and Suh 2015a; Yeats and Rose 2013). The biosynthesis of major cuticle constituents begins with *de novo* synthesis of C16-C18 fatty acids in the plastids of epidermal cells. The fatty acids are converted to acyl-CoAs prior to their export to the endoplasmic reticulum, where, acyl-CoAs are transformed into very long chain fatty acyl-CoAs (VLCFAs) by the fatty acid elongation complex (FAE). These saturated VLCFAs containing 22-34 carbons, can be released from the FAE as free fatty acids or serve as precursors for (i) the alcohol-forming pathway for conversion into even-numbered primary alcohols and alkyl esters, for (ii)

the alkane-forming pathway which yields aldehydes, odd-numbered alkanes, secondary alcohols and ketones, and for (iii) the β-diketone pathway which is less prevalent than the other two pathways but represents an important pathway in some plants like wheat and barley (Delude *et al.* 2016; Hen-Avivi *et al.* 2016).

It has been proposed that the main physiological role of the cuticle is the reduction of water loss. The cuticle delays the onset of cellular dehydration stress under drought and is therefore considered an important component of the plant's protection from drought (Goodwin and Jenks 2005; Kosma and Jenks 2007; Samuels *et al.* 2008). During water deficit, stomata close and nanoscale diffusion pathways crossing the cuticle become the primary path of plant water loss. Non-stomatal water loss through the leaf epidermis may account for up to 50% of total loss in drought-stressed wheat plants during the day and 100% during the night (Rawson and Clarke 1988).

Accumulation of epicuticular waxes on plant surfaces often results in a bluish-white colouration termed glaucousness, which is a visible form of densely distributed epicuticular wax crystalloids. Glaucousness is formed in wheat due to the presence of C31 β-diketones on the surfaces of aerial organs (Adamski *et al.* 2013; Bi *et al.* 2016; Tulloch 1973; Zhang *et al.* 2013). Recently, the genes encoding three key enzymes involved in the synthesis of β-diketones have been reported in wheat and barley (Hen-Avivi *et al.* 2016; Schneider *et al.* 2016). Glaucousness increases radiation reflectance and reduces leaf temperatures and transpiration thereby enhancing leaf survival under water stress (Febrero *et al.* 1998; Richards *et al.* 1986). As a classical genetic marker and agronomic trait, glaucousness has been intensively studied in association with drought/heat tolerance and yield in different wheat varieties (Bennett *et al.* 2012; Izanloo *et al.* 2008; Johnson *et al.* 1983; Merah *et al.* 2000). However, the precise value of this trait in relation to maintenance of plant biomass and grain yield under stress remains uncertain because of the complex biochemical and genetic nature of this easily visible trait.

It has been assumed that the amount and specific biochemical makeup of the waxes to a large extent define protective functions of the cuticle (Jenks and Ashworth 1999; Vogg *et al.* 2004). Increased amounts of cuticular waxes in transgenic plants have been associated with improved drought tolerance, such as in *Arabidopsis* (Aharoni *et al.* 2004), alfalfa (Zhang *et al.* 2005) and Camelina (Lee *et al.* 2014). Breeding barley for higher tolerance and yield under drought, led to increased amounts of cuticular waxes, further confirming the connection between drought tolerance and the cuticle (González

and Ayerbe 2010). Another example is the *glossy 1-2* (*gl1-2*) mutant in rice with reduced accumulation of alkanes, aldehydes and fatty acids. The *gl1-2* mutant plants exhibited increased drought sensitivity and cuticular permeability at the reproductive stage (Islam *et al.* 2009).

The genetic, physiological and metabolic determinants influencing crop yield and drought tolerance have been studied in five elite Australian wheat lines, Kukri, Excalibur, Drysdale, RAC875 and Gladius (Bowne *et al.* 2012; Fleury *et al.* 2010; Ford *et al.* 2011; Hill *et al.* 2013; Izanloo *et al.* 2008; Schoppach and Sadok 2012). Kukri has a lower level of drought tolerance than the other four lines, which represent important sources of drought tolerance in the southern Australian environment, and Kukri was used as the drought-sensitive parent in several mapping populations for drought and yield related studies (Fleury *et al.* 2010). Most recently, two of these lines, Kukri and RAC875, have been investigated for cuticle composition and its regulation by drought-responsive transcription factors of the MYB family (Bi *et al.* 2016).

In this work the five wheat lines were used to: (i) examine leaf cuticle properties as a water loss barrier for wheat plants grown under two different watering regimes, (ii) uncover the stomata- and cuticle-related characteristics responsible for differences in water loss and the responses of these traits to drought, and (iii) establish possible links between cuticle composition, permeability and drought tolerance of these wheat lines.

Materials and Methods

Plant growth and sampling

Seeds of five selected lines, Kukri, Excalibur, Drysdale, RAC875 and Gladius, were sown in large containers (112 × 76 × 50 cm) in a glasshouse, with a 14h day/10h night cycle. Air-conditioning in the glasshouse controlled temperature fluctuations and the temperatures were recorded every 15 minutes, which were 19.9 ± 3.3°C (mean ± standard deviation) for the period from planting to sampling of flag leaves for all the analyses. The plants were grown under controlled, well-watered conditions and drought in the containers that were equipped with an automatic watering system and four soil water tensiometers (gypsum blocks) installed at 10 cm and 30 cm soil depths, and connected to a data logger for continuous monitoring of the soil water tension (Amalraj *et al.* 2016). Recorded soil water tension data for both watering regimes were shown in Fig. S1. Flag leaf samples for all the experiments conducted in this study were collected after the

reading of 30 cm tensiometer reached the highest measureable level of 600 kPa. Flag leaves were selected for all the analyses of wheat cuticular waxes, as they are the main source of assimilates for grain development.

Cuticle permeability assay

Flag leaves were detached from each of four plants per line grown in the well-watered container or drought container 20 days after anthesis, and leaf weight was immediately measured using an analytical balance (OHAUS Corporation, Parsippany, USA) before being placed into a collection tube. Leaves in collection tubes were dehydrated at room temperature (23 °C) for 12 hours with leaf weight measured every hour. Leaves were dried in a 37 °C incubator for 72 hours after which leaf weight was measured and taken as the dry weight.

Leaf surface imprints

The leaf surface imprint method, modified from Sinclair and Dhingra (1995), was used to estimate stomatal numbers per unit area. Flag leaves from the main tiller were detached from five plants of each cultivar grown under well-watered conditions or drought 20 days after anthesis, and the middle part between the major vein and the leaf margin and half-way along the long axis of the leaf was used to make impressions of the surfaces. Cyanoacrylate adhesive (Supa glue; Selleys, Padstow, NSW, Australia) was applied to the area and the glued side was placed against a microscope slide. A second slide was placed on top of the leaf in the same direction. The slides were held together with two large bulldog clips for three minutes, after which the two slides were separated and the leaf was peeled off. Leaf imprints were examined under the Leica AS LMD microscope (Leica Microsystems, Wetzlar, Germany) with differential interference contrast (DIC) at 200 times magnification at the Waite Facility of Adelaide Microscopy. Stomatal counts were made from each of three images of each of the imprints from five biological replicates.

Transmission electron microscopy

Flag leaf blades were collected at day 24 after anthesis and several segments close to the major vein of approximately 5mm x 3mm in size were cut from the middle of a leaf from each of three plants. In a fume hood, cut pieces were placed into TEM fixative [4% sucrose, 1x PBS (phosphate buffered saline), 4% paraformaldehyde, and 0.25% glutaraldehyde]. After overnight incubation at 4°C, samples were rinsed twice with 1 x PBS at 4°C to remove fixative. Then samples were dehydrated in an ethanol series: 50%,

70%, 90%, 95% and 100%, each change approximately 1 hour, followed by 2 changes of 100% dry ethanol (on a molecular sieve). Samples were stored in 100% dry ethanol at 4°C until resin infiltration. Samples were first infiltrated in a 50:50 mix of 100% ethanol and LR White Resin (London Resin Co.Ltd., London, UK) for 8 hours, followed by 3 changes of 100% LR White Resin, also for 8 hours each. Next, infiltrated specimens were embedded in fresh 100% LR White Resin in gelatin capsules. Finally, embedded samples were polymerised at 60°C for 24 hours. Prior to sectioning on the ultramicrotome, resin blocks were trimmed with a razor blade to make a trapezoid face. 70 nm thick sections were generated using a diamond knife. Sections were first stained with 4% uranyl acetate for 20 minutes, then with lead citrate for 20 minutes after three rinses in water. After another three rinses in water and air drying, sections were examined under a Philips CM100 transmission electron microscope at the Adelaide Microscopy Waite Facility.

Scanning electron microscopy

The epicuticular wax was examined using a scanning electron microscope in the Adelaide Microscopy Unit (https://www.adelaide.edu.au/microscopy/, University of Adelaide, Australia). Several segments of approximately 4mm x 3mm were cut from the similar location on the same leaf as the TEM samples and examined as described by Bi *et al.* (2016) (See Chapter 3) under a Philips XL30 Field Emission Scanning Electron Microscope, equipped with a Gatan CT1500 HF Cryo-transfer Stage.

Composition analysis of cuticular waxes

For the wax composition analysis of wheat lines, the 6.5cm long lower part of the flag leaf blade from each of three plants was collected at day 24 after anthesis. The weight of each leaf section was measured, and leaves were snap frozen in liquid nitrogen and further stored at -80 °C until wax extraction. Wax extraction and GC-MS analysis were carried out following the same procedures as described by Bi *et al.* (2016) (See Chapter 3). GC-MS analysis was conducted in the W.M. Keck Metabolomics Research Laboratory of Iowa State University (USA) according to the procedure described by Cha *et al.* (2009).

Statistical analysis of data

Data on stomatal density and wax composition were analysed using two-way ANOVA with the Fisher's least significant difference post-hoc test in GenStat (16th Edition; VSN International Ltd, Hemel Hempstead, UK).

Results

Examination of leaf surface permeability

In order to determine the cuticle's ability to act as a barrier against water loss, water losses were assessed using detached flag leaves of the five wheat lines, which were grown under well-watered (WW) conditions or under drought (DR). As shown in Fig. 1A, during the first two hours of dehydration the WW Kukri and Excalibur leaves lost water more rapidly than leaves of RAC875, Drysdale and Gladius. After two hours the water loss rates became stable in all five lines and could be considered residual transpiration rates (RTRs), which are primarily contributed by the cuticle. The RTRs of WW Kukri plants were higher than those of the other four lines (Fig. 1A). Water loss rates from flag leaves detached from plants grown under DR were relatively stable during the entire 12 hours-long test (Fig. 1B). Similar to results obtained for WW wheat plants, the RTRs of Kukri plants grown under drought conditions were higher than those of DR RAC875, Drysdale or Gladius. (Fig. 1B).

Comparison of RTRs of wheat lines under WW and DR conditions revealed that RTRs of DR Kukri, Drysdale, RAC875 and Gladius were lower, and RTR of Excalibur was higher than those of lines grown under WW conditions (Fig. 1C).

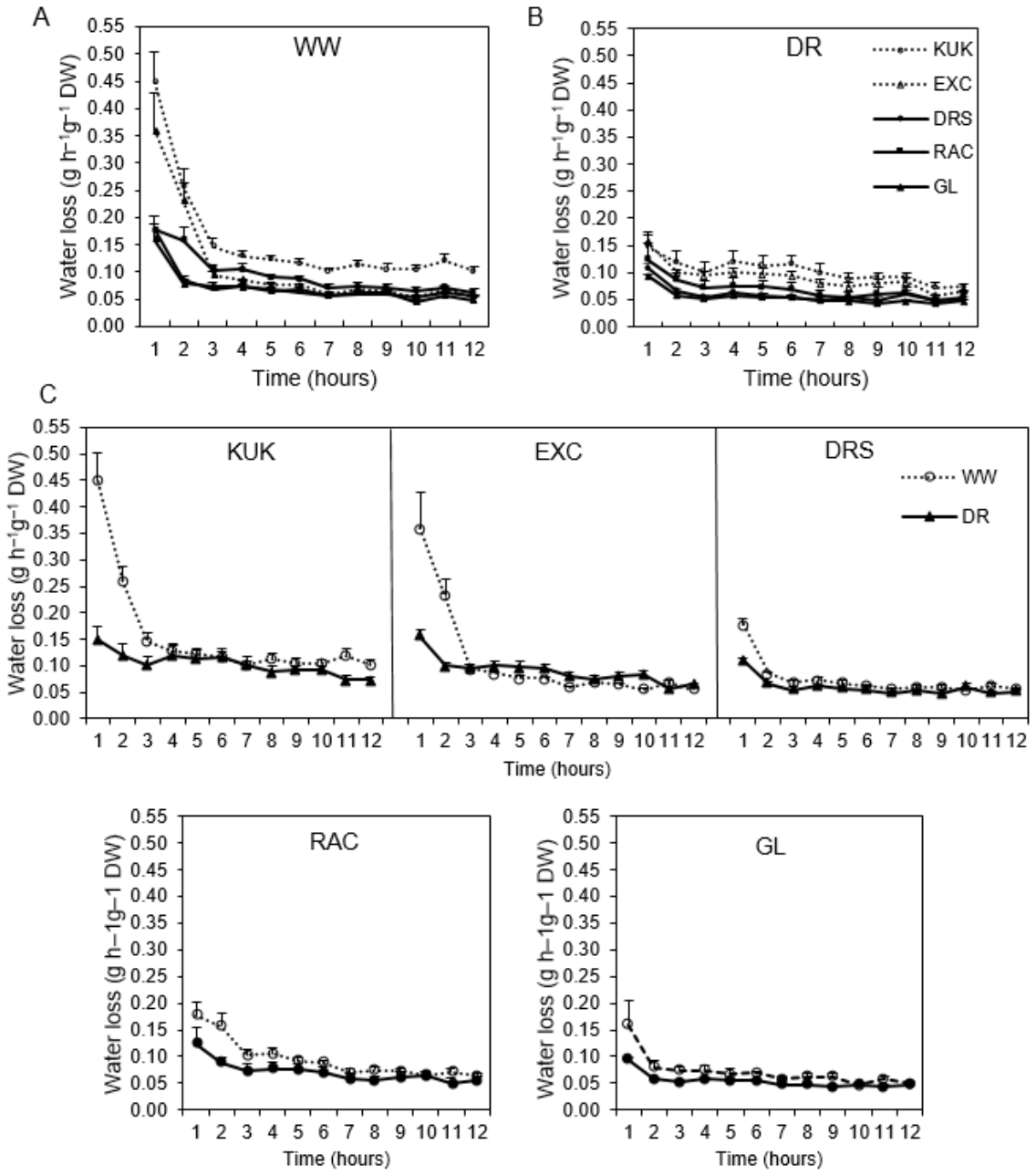

Fig. 1 Water loss rates of flag leaves detached from five wheat lines grown under well-watered (WW) conditions and drought (DR). Water loss rates of flag leaves detached from (A) WW and (B) DR plants over 12 hours. (C) Comparison of water loss rates of WW and DR plants. KUK - Kukri, EXC - Excalibur, DRS - Drysdale, RAC - RAC875, GL - Gladius. Water loss rates were expressed as weight loss per hour per dry weight (DW) of flag leaves. Means and standard errors (indicated by bars) were calculated from four replicates.

Investigation of stomatal density

Stomata are specialized structures on leaf surfaces that control the exchange of water and gases between plants and the environment and therefore stomatal number may affect leaf water loss. More stomata per unit of leaf area existed on the adaxial side of flag leaves than on the abaxial side of the same line, as shown in the non-glaucous and drought sensitive cultivar Kukri and the glaucous and drought tolerant Gladius, representatively (Fig. 2A-2D). Kukri had the lowest number of stomata per unit of leaf surface area on both surfaces of leaves under both control and drought treatment (Fig. 2E, F). Overall, the stomatal density on both sides of flag leaves collected from plants grown under well-watered conditions in all tested lines was 5.9-32.2% lower than that of leaves of plants subjected to drought. An exception was the stomatal density on the abaxial side of flag leaves of RAC875, which under drought was 5.3% lower than the stomatal density on leaves of well-watered plants. However, the stomatal density on the adaxial side of the same leaves was increased by drought by 5.9%.

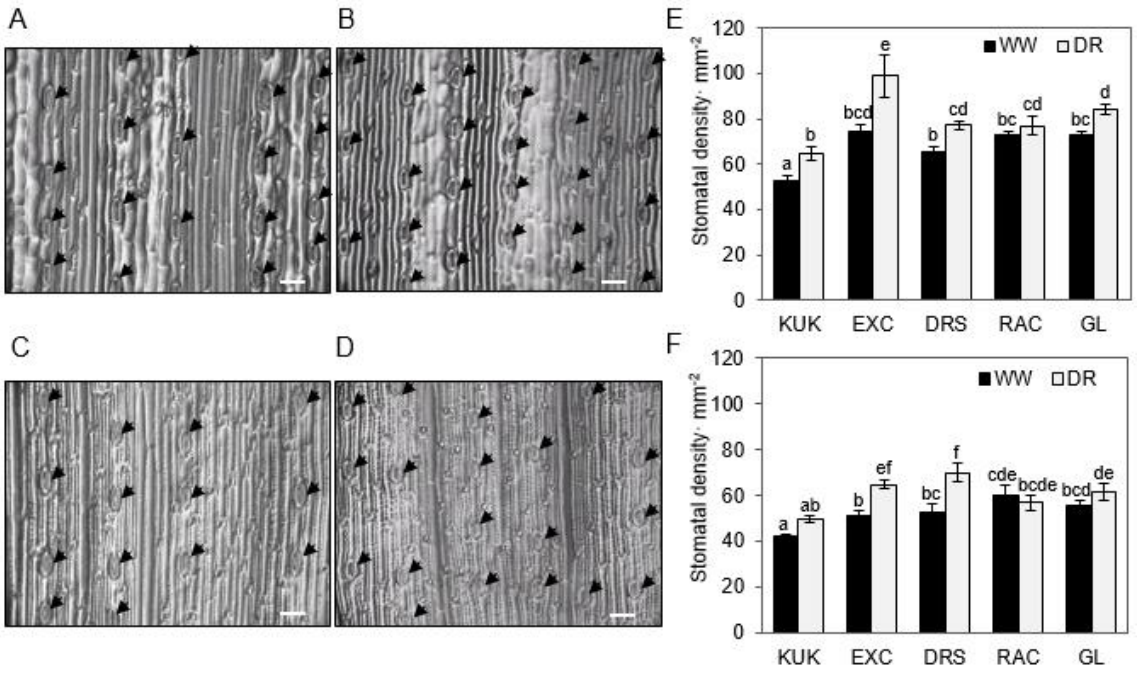

Fig. 2 Stomata and stomatal density on the flag leaves of five wheat lines. (A) Stomata on the adaxial side of a flag leaf in Kukri. Stomata are indicated by arrows. (B) Stomata on the adaxial side of a flag leaf in Gladius. (C) Stomata on the abaxial side of a flag leaf in Kukri. (D) Stomata on the abaxial side of a flag leaf in Gladius. (E) Stomatal density on the adaxial side of flag leaves. (F) Stomatal density on the abaxial side of flag leaves. Means and standard errors were calculated from five plants. Different letters on top of error bars mean significant difference at $P<0.05$. Scale bars represent 50 μm.

Microscopic assessments of leaf surfaces

The thicknesses of the cuticle layer were examined on the abaxial side of flag leaves of five wheat lines grown under the same watering regimes as used for the assessment of stomatal density using transmission electron microscopy. Under WW conditions, modest differences were found in the thickness of the cuticle layer amongst the five genotypes, whereas differences between WW and DR within lines were larger and more obvious (Fig. 3). In particular, the thickness was greatly increased by drought on the abaxial side of Drysdale and RAC875 leaves, slightly increased on the abaxial side of Gladius, and decreased on the abaxial side of Excalibur.

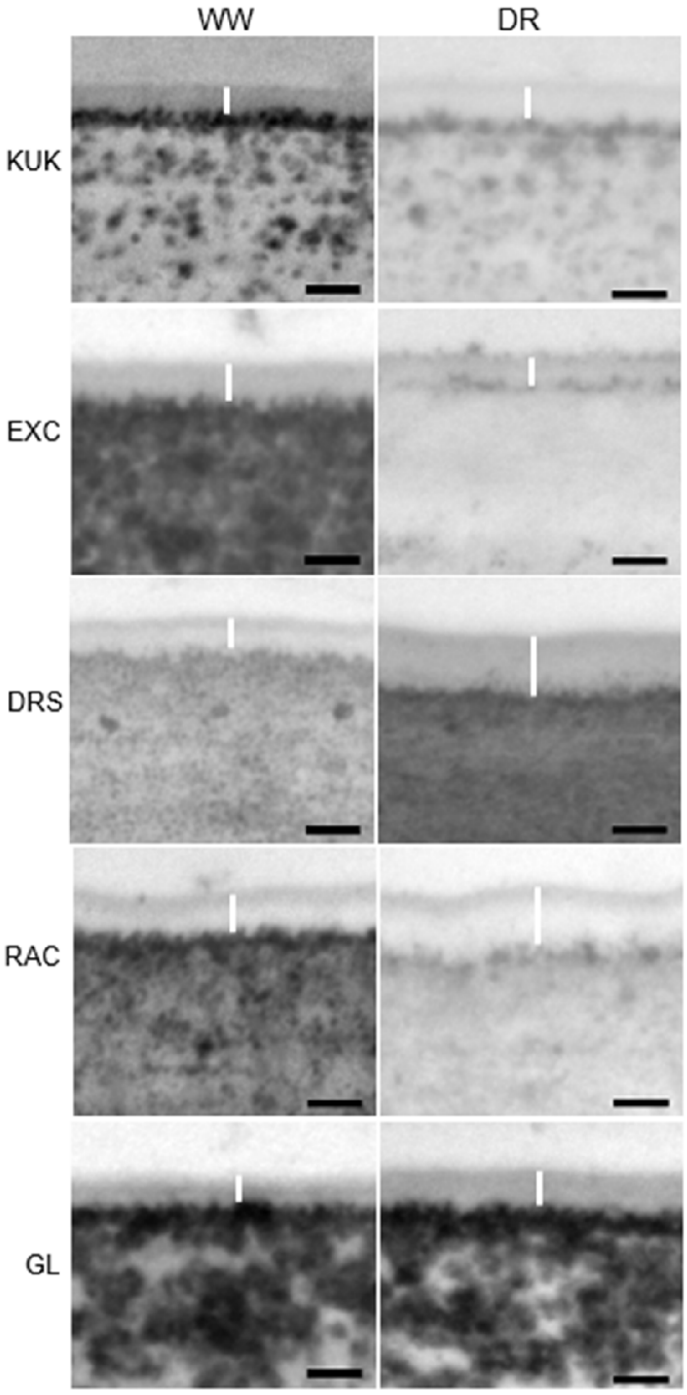

Fig. 3 Transmission electron micrographs of cuticle layers on the abaxial epidermis of flag leaves in five wheat lines. KUK - Kukri, EXC - Excalibur, DRS - Drysdale, RAC - RAC875, GL - Gladius, WW - well-watered conditions, DR - drought. Cuticle layers are marked using white lines. Scale bars = 100 nm.

Accumulation of epicuticular waxes on leaf surfaces confers a whitish and powdery appearance to most modern wheat varieties termed glaucousness. Kukri is a non-glaucous and glossy cultivar, Excalibur has a very low level and Drysdale a medium level of glaucousness, while RAC875 and Gladius were the most glaucous lines examined (Fig. 4). Variations in glaucousness were more noticeable on the abaxial side of leaves than on the adaxial side. When examined under SEM, it was found that wax distribution and structure were different on the adaxial and abaxial sides of leaves. Compared with waxes on the abaxial side, the adaxial side waxes were more densely and evenly deposited. Under SEM, the powdery leaf surfaces of RAC875 and Gladius were clear. The specific structures of waxes were explored under high magnification. No difference was found on the adaxial sides of leaves: the dense platelet-shaped wax crystalloids were dominant in all five lines (Fig. S2). However, different wax shapes were observed on the abaxial side of leaves. The plate-shaped wax crystalloids prevailed on the abaxial side of flag leaves of Kukri, Excalibur and Drysdale (Fig. 5), while long tubule-like crystalloids were the dominant wax structures on the surfaces of the RAC875 and Gladius leaves (Fig. 5). Platelets and tubules are the most frequent types of wax crystalloids found in plants according to the classification and terminology proposed by Barthlott *et al.* (1998).

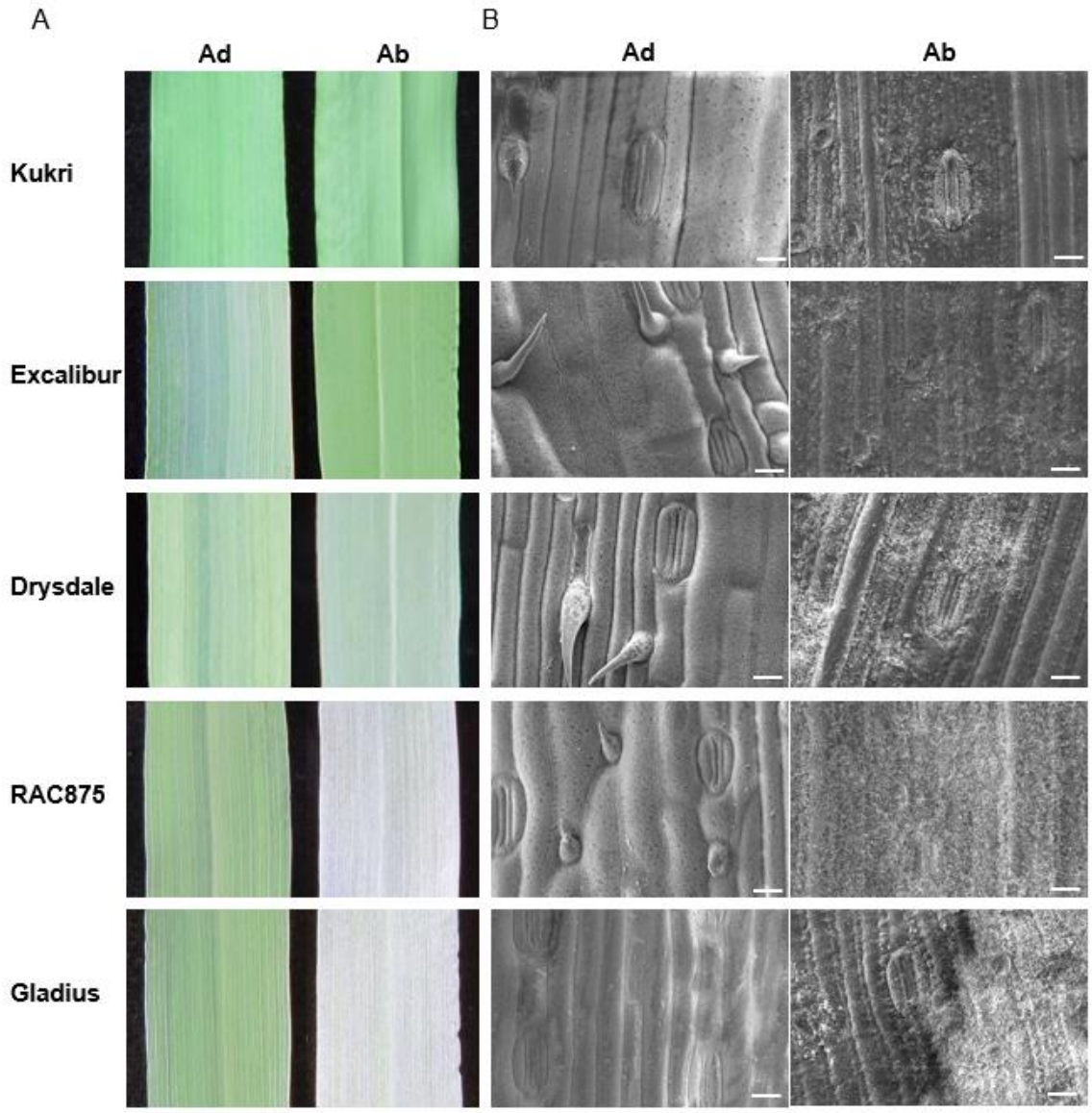

Fig. 4 Visualisation of epicuticular waxes on the flag leaves of five wheat lines. (A) Wax phenotypes on the adaxial (Ad) and abaxial (Ab) sides of flag leaves of Kukri, Excalibur, Drysdale, RAC875 and Gladius. (B) Scanning electron micrographs of the epicuticular waxes on the adaxial (Ad) and abaxial (Ab) sides of flag leaves of Kukri, Excalibur, Drysdale, RAC875 and Gladius. Scale bars = 20 μm.

Genotypic variations in epicuticular waxes and responses of waxes to water deficit

To investigate the association between water loss rates and epicuticular waxes, we analysed the amount and composition of epicuticular waxes on the flag leaves of these five wheat lines using gas chromatography in combination with mass spectrometry (GC-MS). We observed a good correlation in these lines between the content of β-diketones and the predominant presence of long tubule-like crystalloids in wax layers (Fig. 5). The

specific amounts of cuticular waxes of Kukri and RAC875 were presented by Bi *et al.* (2016). Data shown here for Excalibur, Drysdale and Gladius were generated from wheat plants grown under exactly the same conditions as Kukri and RAC875.

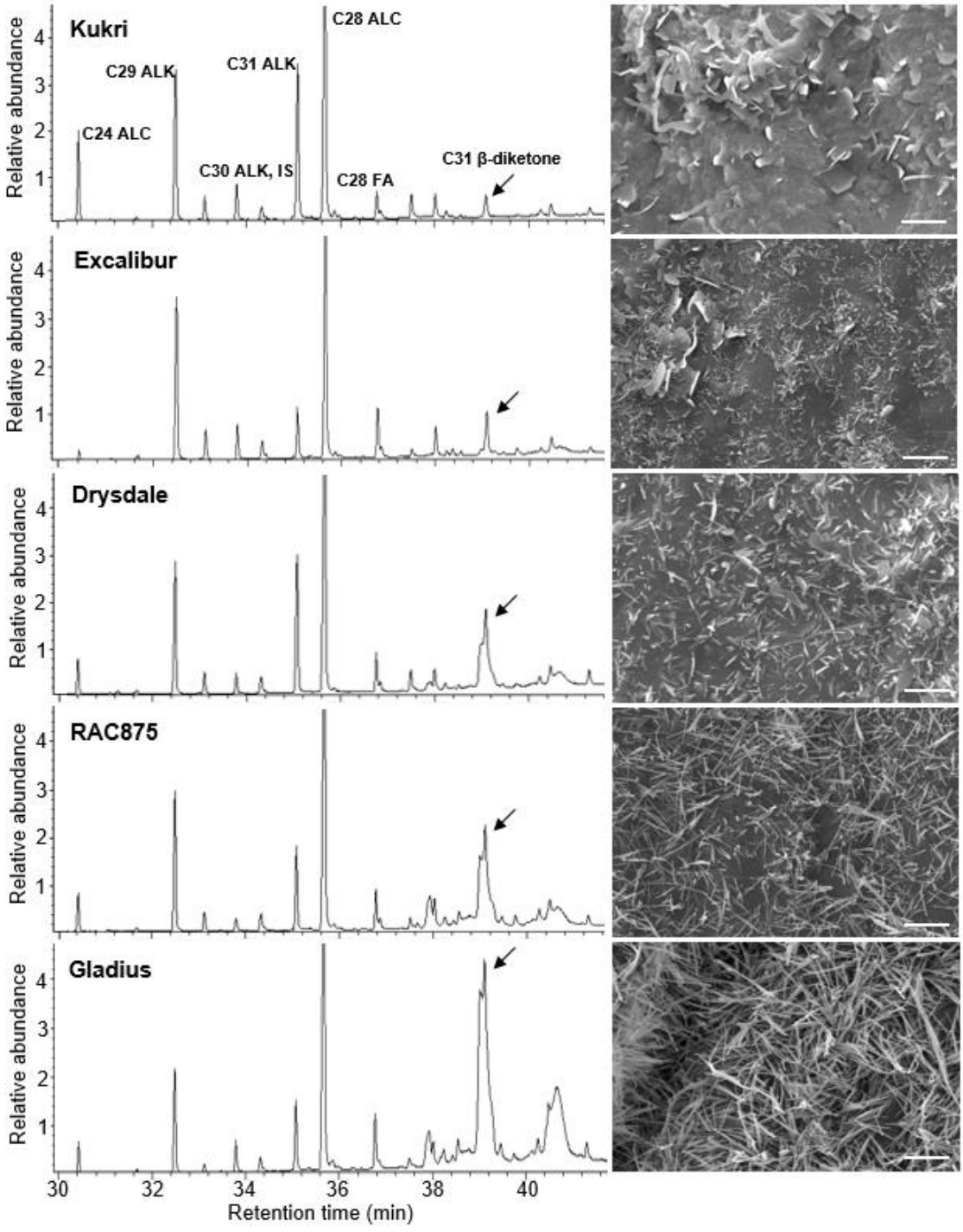

Fig. 5 GC-MS chromatograms representing biochemical compositon of extracted cuticular waxes and SEM images of wax crystalloids on the abaxial side of the flag leaf in the five wheat lines examined. ALC - primary alcohol, ALK – alkane, FA - fatty acid, IS – internal standard. Scale bars = 5 μm. Arrows indicate C31 β-diketone.

Under WW conditions, Gladius had the highest total wax loads on flag leaves; the total amounts of waxes decreased in the order of Drysdale and Excalibur (Fig. 6A). In terms of wax composition, primary alcohols were the most abundant wax species in all three wheat lines, comprising from 40.0 to 51.1% of total wax loads (Fig. 6B). The second most abundant wax species were C31 β-diketone in Gladius (28.2%) and alkanes for the other two wheats. In Excalibur and Drysdale, the contents of β-diketones were much lower, accounting for 1.4% and 4.6% of total wax loads, respectively. The contents of alkanes in the total flag leaf waxes of Excalibur, Drysdale and Gladius were 31.1%, 32.1% and 15.9%, respectively. Among minor components of waxes, which were present on leaves of all examined lines, were fatty acids (9.5 - 12.3%), aldehydes (1.2 - 2.4%) and resorcinols (1.7 - 2.5%).

When comparing total wax loads of plants grown under WW and DR conditions, we found that drought significantly increased total wax loads on flag leaves of Drysdale by 48.5% (Fig. 6A). The wax load was moderately increased on leaves of Excalibur (28.0%) and slightly decreased on leaves of Gladius (-6.8%) (Fig. 6A). The contents of alkanes were increased in all three wheat lines while the amounts of β-diketones were increased in Excalibur and Drysdale but decreased in Gladius (Fig. 6B).

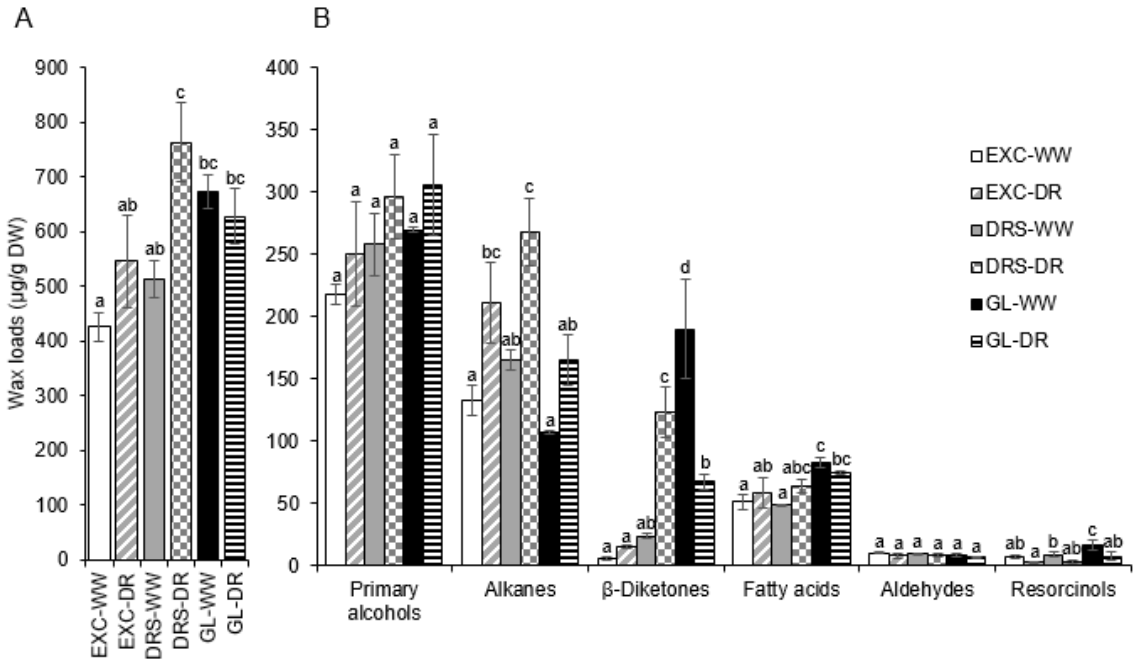

Fig. 6 Wax amounts and composition on flag leaves of wheat lines grown under well-watered (WW) conditions and drought (DR). (A) Total wax loads. (B) Contents of each wax species. EXC - Excalibur, DRS - Drysdale, GL - Gladius. Means and standard errors (indicated by bars) were calculated from three replicates. Different letters on top of error

bars mean significant differences at $P<0.05$. Wax loads were calculated per gram of dry leaf weight (DW).

The distribution of carbon chain lengths of major wax species extracted from flag leaves of wheat lines was examined (Fig. 7). The carbon chain lengths of primary alcohols (Fig. 7A) range from 20 to 34, the β-diketone (Fig. 7B) is 31 carbon-long and alkanes (Fig. 7C) range from 23 to 33. The four most abundant wax components on flag leaves were C28 primary alcohol, C31 β-diketone, and C29 and C31 alkanes. The carbon chain length distribution of three minor wax species (fatty acids, aldehydes and resorcinols) can be found in Fig. S3.

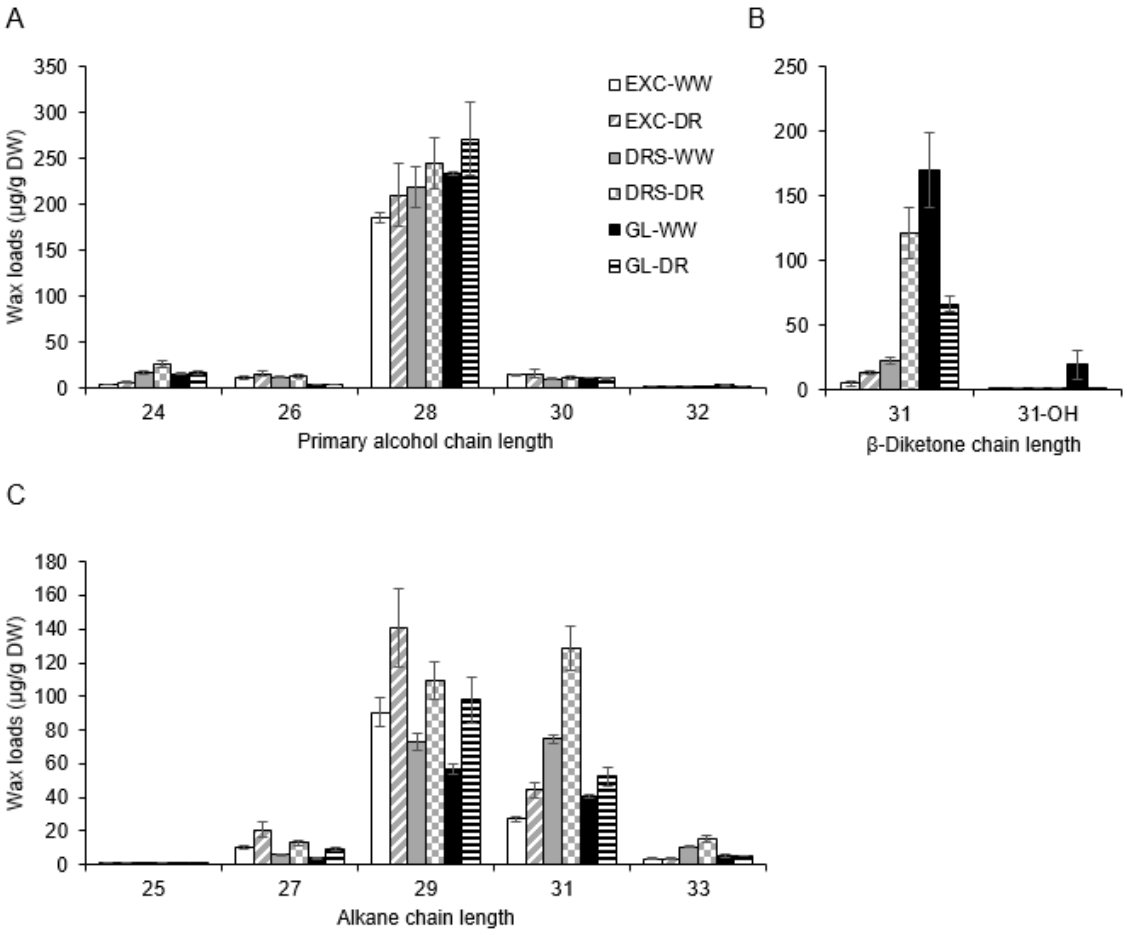

Fig. 7 Carbon chain length distribution of major cuticular wax classes on flag leaves of wheat lines grown under well-watered (WW) conditions and drought (DR). (A) Carbon chain lengths of primary alcohols. (B) Carbon chain length of β-diketones. (C) Carbon chain lengths of alkanes. EXC - Excalibur, DRS - Drysdale, GL - Gladius. Means and standard errors (indicated by bars) were calculated from three replicates. Wax loads were calculated per gram of dry leaf weight (DW). Tiny amounts of 20-, 22- and 34-carbon primary alcohols, and 23-carbon alkane are not shown but used for calculation of total wax loads in Fig. 6.

Increases in the amounts of epicuticular waxes under drought were observed under SEM. However, no structural alterations in waxes were found, as representatively shown in the most drought-responsive cultivar, Drysdale (Fig. 8).

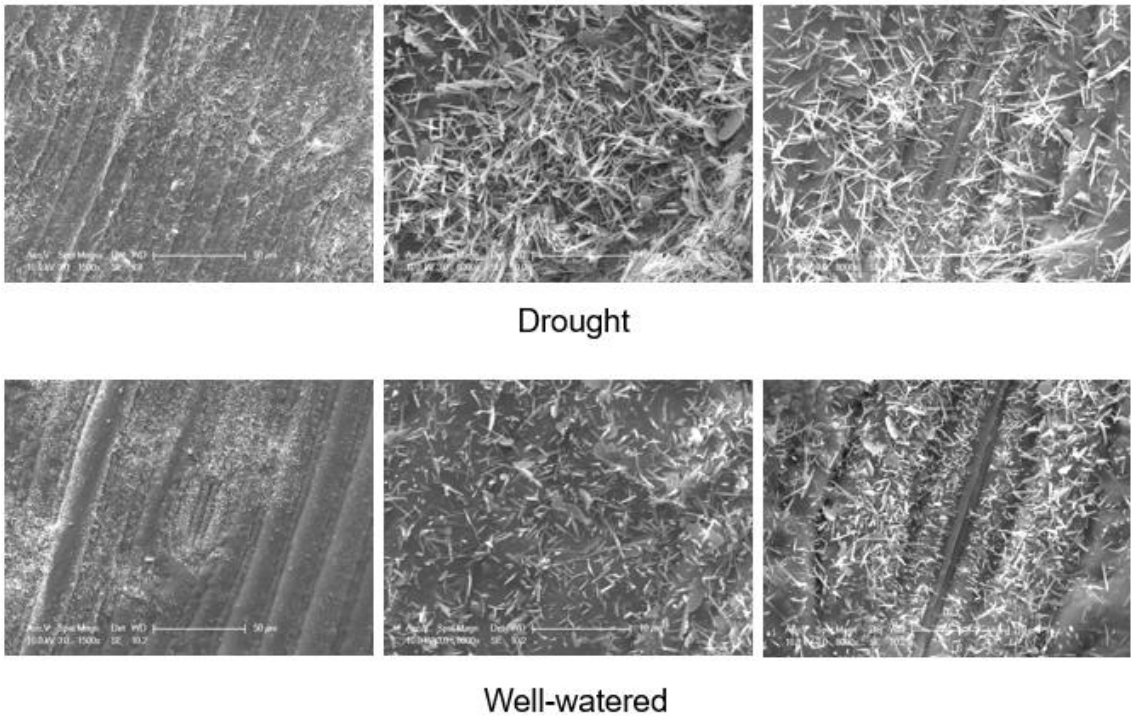

Fig. 8 SEM images for comparison of wax crystalloids on abaxial leaves of Drysdale grown under well-watered conditions and drought. Images in the left-hand column were taken under 1500X magnification. The other four images were taken under 8000X magnification.

Discussion

Glaucousness is an easy trait to select for in a breeding program since it can be readily scored visually. Consequently, if this trait were of major importance for adaptation to hot, dry environments, we would expect to see almost exclusive adoption of glaucous varieties in these environments. However, this is not the case for wheat in regions such as southern Australia where we see a full range of glaucousness, from low to high, in modern varieties. On the other hand, a number of studies have shown that alterations of the cuticle could significantly increase plant drought tolerance. A possible explanation for this apparent contradiction is that glaucousness is only one aspect of cuticle composition and structure and other properties or changes in the cuticle in response to stress may also be important. In this study we sought to tease apart different aspects of the cuticle structure

and deposition in an effort to understand the relationship with drought tolerance of different wheat lines.

Residual transpiration, defined as water loss from detached leaves at minimal stomatal aperture, plays an important role in plant survival under severe water deficit. Rawson and Clarke (1988) found that the cuticle contributed more than 50% of total transpiration when wheat plants were stressed. In our water loss tests the RTRs of Kukri, the least drought tolerant and the only non-glaucous of the examined wheat lines, were significantly higher than those of more drought tolerant and glaucous Drysdale, RAC875 and Gladius, irrespective of whether leaves used in the experiment were detached from plants cultivated under sufficient or water limited conditions (Fig 1A, B). Similarly, Zhang *et al.* (2013) showed that glaucous *W1W2* (*W*: wax production gene) near-isogenic line (NIL) had significantly lower rates of water loss and chlorophyll leaching than the non-glaucous and other glaucous NILs (*W1w2* and *w1W2*).

Jäger *et al.* (2014) found that the most drought tolerant cultivar had the lowest frequency of stomata on wheat flag leaves. In our work, however, the drought-sensitive, non-glaucous cultivar Kukri, which in leaf desiccation tests had the highest water loss rates compared to other four wheat lines, had the lowest stomatal density on both leaf surfaces (Fig. 1 and 2). Higher stomatal density on the leaves of drought tolerant lines RAC875 and Gladius might lead to a higher yield under drought. This would be consistent with results of Xu and Zhou (2008), who found that moderate water deficits increased, while more severe water deficits reduced, stomatal density on leaves of a perennial grass, *Leymus chinensis*. Their results also indicated that an increase in leaf stomatal density was positively associated with leaf–level water use efficiency (*A*/*E*).

Over the past few years there have been various reports on wheat cuticle and glaucousness related genes, and their involvement in protection from biotic and abiotic stresses (Adamski *et al.* 2013; Bennett *et al.* 2012; Kosma *et al.* 2010; Lu *et al.* 2015; Wang *et al.* 2016; Wang *et al.* 2015a; Wang *et al.* 2015b; Zhang *et al.* 2013). Among these reports, it was revealed that β-diketones were associated with glaucousness in wheat (Adamski *et al.* 2013; Zhang *et al.* 2013). Here, we showed a correlation between the amount of β-diketones and long tubule-like wax crystalloids and thus the level of glaucousness in five wheat lines (Fig. 4 and 5). More importantly, we found that the non-glaucous and drought-sensitive Kukri lost water more rapidly than all four glaucous and drought-tolerant lines. These results suggested that glaucous wheat lines had a greater capacity to retain water

than non-glaucous lines although no simple correlation was found between water loss rates and the level of glaucousness among the examined glaucous lines.

Growing wheat plants under conditions of limited water did not influence the morphology of wax crystalloids on the surfaces of flag leaves, although an increase in the density of waxes was observed (Fig. 8). However, a significant increase of cuticle thickness was observed in two of the five lines, Drysdale and RAC875 (Fig. 3). In addition to the highest drought-induced increases in cuticle thickness, these two lines also demonstrated the most significant increases in total wax loads (48.5% and 31.5%, respectively) during plant growth under drought (Fig. 6 and Bi *et al.* (2016)). In contrast, we observed a discrepancy between these two parameters for the cuticle of flag leaves of Excalibur (28% increase in amount of waxes but a decrease in cuticle thickness on the abaxial side of the leaf) and Gladius (6.8% decrease in wax load *versus* an increase in cuticle thickness on the abaxial side of the leaf). These apparent inconsistencies could reflect different responses in the abaxial versus adaxial wax deposition, or the lack of regulation of wax deposition in response to environmental stress.

Enhancement of leaf cuticular wax production and increases in cuticle thickness appear to represent a prevalent response to water deficit across the terrestrial plant kingdom (Kosma and Jenks 2007). For example, a 75% increase in total wax amount per unit of leaf area and 49% increase in cuticle thickness were reported in *Arabidopsis* under water deficit (Kosma *et al.* 2009), and, on leaves of tree tobacco, drought induced over 150% increase in total wax accumulation (Cameron *et al.* 2006). The changes in *Arabidopsis* cuticle were associated with decreased cuticle permeability measured as reductions in water loss and chlorophyll leaching rates of detached leaves (Kosma *et al.* 2009). In addition, elevated cuticle membrane thickness in the *Arabidopsis cer9* (*eceriferum 9*) mutant correlated with lower transpiration rates and improved water use efficiency (Lü *et al.* 2009). Jäger *et al.* (2014) found that both cuticle thickness and stomatal density were relevant contributors to drought tolerance of four European winter wheat cultivars with contrasting behaviour under limited water supply. Synthesis of a larger cutin framework was proposed as a mechanism of drought acclimatisation for *Arabidopsis* (Kosma *et al.* 2009), whereas Vogg *et al.* (2004) demonstrated that the major water permeability barrier of tomato fruit cuticle consisted of intracuticular rather than epicuticular waxes.

In our experiments, the accumulation of free fatty acids remained mostly unaffected by drought, while alkanes increased significantly in all tested wheat lines (Fig. 6 and Bi *et al.* (2016)). These data are in agreement with results from previous studies. Fatty acids

create relatively poor hydrophobic barriers to water diffusion through both natural and artificial cuticular membranes, in contrast with alkanes which represent an effective water permeability barrier (Grncarevic and Radler 1967; Kosma *et al.* 2009). The activation by water stress of biochemical pathways providing components for the biosynthesis of alkanes has been demonstrated for a number of plant species (Kosma and Jenks 2007; Ni *et al.* 2012; Seo *et al.* 2011).

Overall, our results showed that non-glaucous and drought-sensitive Kukri had higher RTRs than glaucous and drought-tolerant Excalibur, Drysdale, RAC875 and Gladius. However, no direct relationship was found between the RTRs and the level of glaucousness among all glaucous lines examined. These results suggested that, to some extent, glaucousness played a role in drought tolerance although its precise value for drought tolerance requires further investigation. The small but obvious changes in RTRs of wheat lines under drought, especially in RTRs of Drysdale and RAC875, correlated well with their levels of drought-induced wax accumulation and thickening of cuticle layers. However, no correlation was found between stomatal density and water loss for the examined lines, and no meaningful changes occurred in stomatal numbers during plant growth under drought.

Conclusions

The basis for this study was to develop an understanding of cuticle structure and deposition of wheat in relation to drought tolerance since there is some evidence, and a reasonable physiological expectation, that the cuticle will play an important role in regulating water loss. Although varying levels of glaucousness are found in modern wheat varieties and glaucousness is an easy, visual trait to score, few breeders would regard it as an important selection target. Overall, our results show that considerable variation exists between genotypes in the composition and structure of the cuticle. The relationship between the cuticle and drought tolerance is not simple and glaucousness is not a unique indicator of tolerance. Rather, specific wax composition, in particular the presence of significant proportions of C31 β-diketone, adaptive changes in composition and amount induced by exposure to drought and wax crystal structure will all influence leaf water loss under conditions of water deficit. These features of cuticle composition and deposition appear important and should provide useful selection criteria although they are more difficult to measure than glaucousness.

Acknowledgements

We thank Gwenda Mayo for suggestions and help with electron microscopic analysis, Zhihong Song and M. Ann Perera (W.M.Keck Metabolomics Research Laboratory, Iowa State University) for the help with analysis of wax composition and Yuriy Onyskiv for technical support in the glasshouse. The China Scholarship Council and the University of Adelaide are acknowledged for providing HB a joint postgraduate scholarship. This work was supported by the Australian Centre for Plant Functional Genomics, and by the Australian Research Council, the Grains Research & Development Corporation and the Government of South Australia.

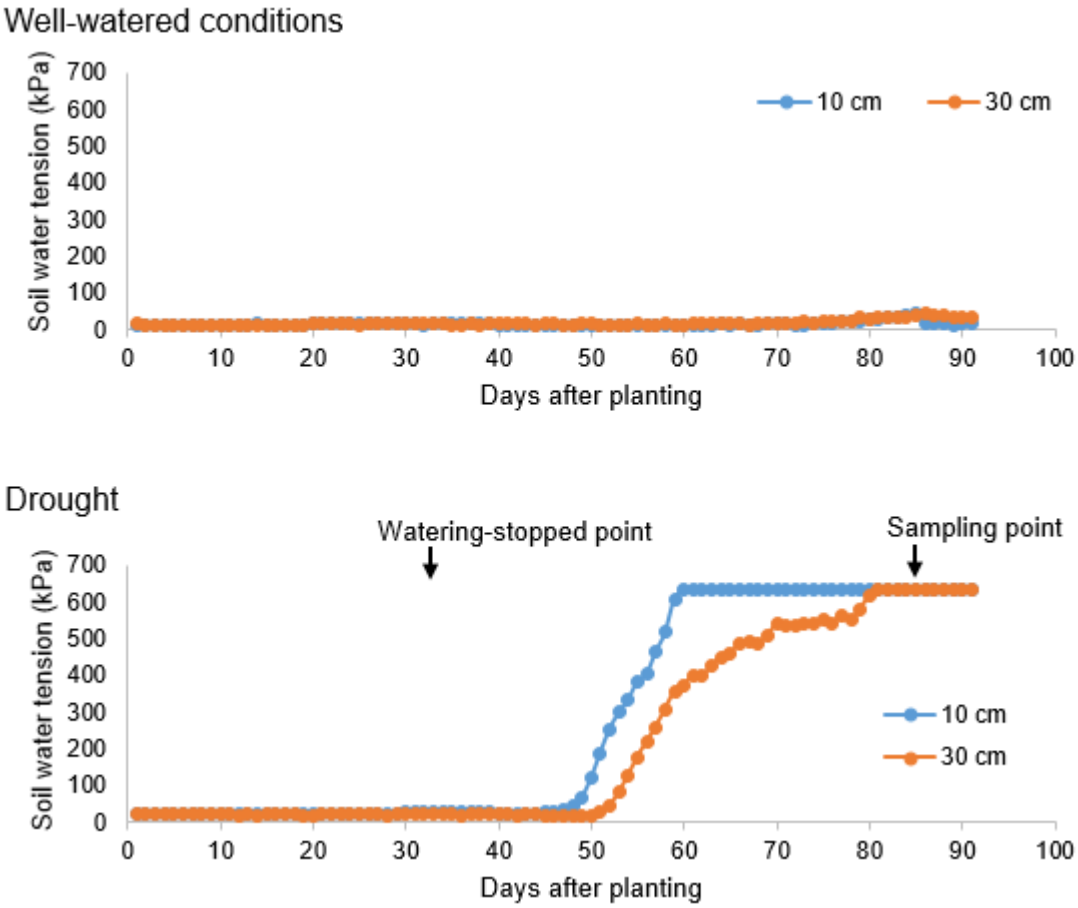

Fig. S1 Soil water tension monitored for well-watered conditions and drought. Soil water tension at 10 cm and 30 cm depths were shown.

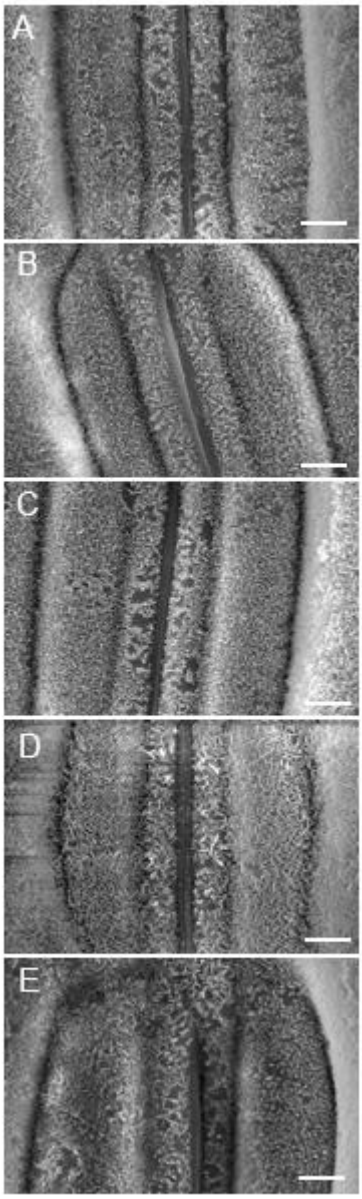

Fig. S2 Scanning electron micrographs of epicuticular waxes on the adaxial side of flag leaves in five wheat lines. (A) Kukri; (B) Excalibur; (C) Drysdale; (D) RAC875 and (E) Gladius. Scale bars represent 5 µm.

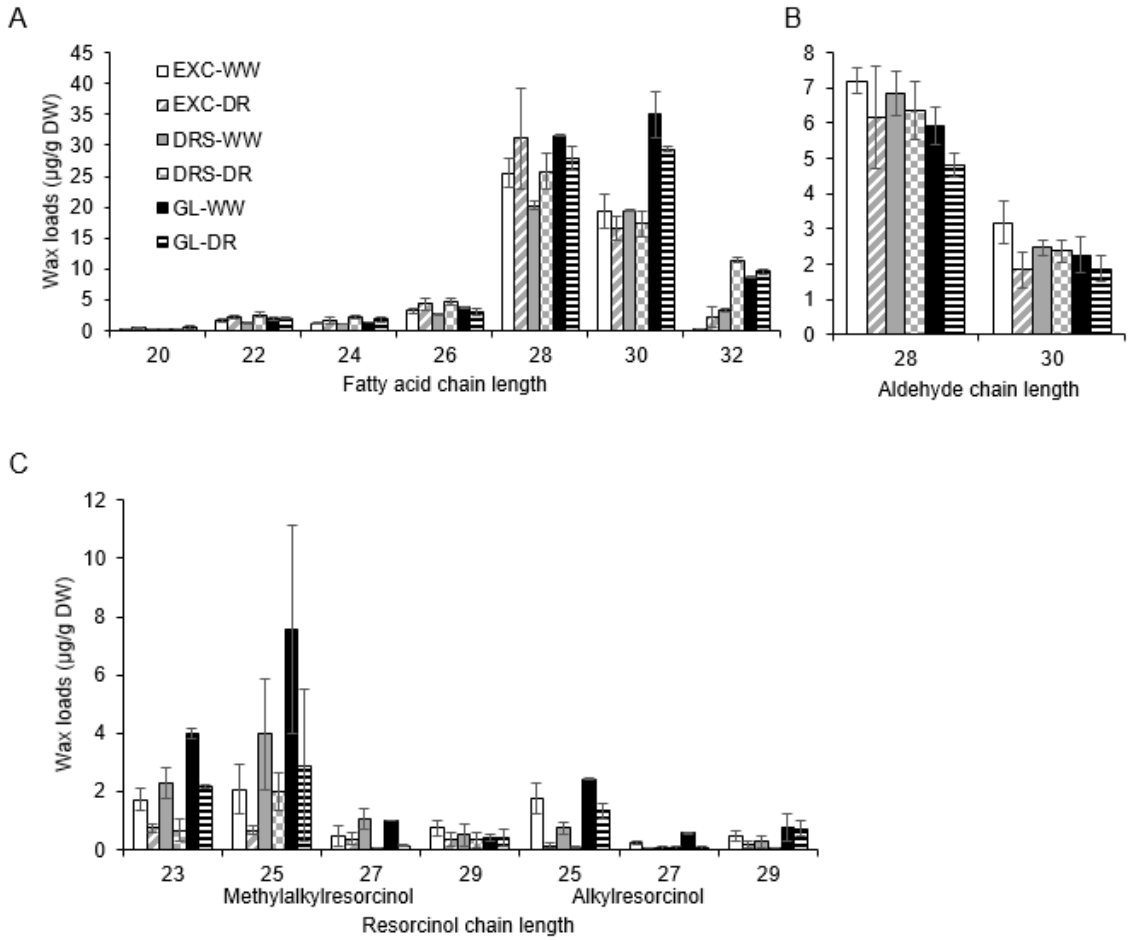

Fig. S3 Carbon chain length distribution of minor cuticular wax species on flag leaves of wheat lines grown under well-watered (WW) condition and drought (DR). (A) Carbon chain length of fatty acids. (B) Carbon chain length of aldehydes. (C) Carbon chain length of resorcinols. EXC - Excalibur, DRS - Drysdale, GL - Gladius. Means and standard errors (indicated by bar) were calculated from three replicates. Wax loads were calculated per gram of dry leaf weight (DW).

Chapter 3 Identification and characterization of wheat drought-responsive MYB transcription factors involved in the regulation of cuticle biosynthesis

Statement of Authorship

Title of Paper	Identification and characterization of wheat drought-responsive MYB transcription factors involved in the regulation of cuticle biosynthesis
Publication Status	☑ Published ☐ Accepted for Publication ☐ Submitted for Publication ☐ Unpublished and Unsubmitted w ork w ritten in manuscript style
Publication Details	Bi H, Luang S, Li Y, Bazanova N, Morran S, Song Z, Perera MA, Hrmova M, Borisjuk N, Lopato S. Identification and characterization of wheat drought-responsive MYB transcription factors involved in the regulation of cuticle biosynthesis. Journal of Experimental Botany, doi:10.1093/jxb/erw298. Feature article with a front cover photograph.

Principal Author

Name of Principal Author (Candidate)	Huihui Bi		
Contribution to the Paper	Designed the experiments with supervisors, performed experiments, analysed data and wrote the manuscript.		
Overall percentage (%)	65%		
Certification:	This paper reports on original research I conducted during the period of my Higher Degree by Research candidature and is not subject to any obligations or contractual agreements with a third party that would constrain its inclusion in this thesis. I am the primary author of this paper.		
Signature		Date	13/09/2016

Co-Author Contributions

By signing the Statement of Authorship, each author certifies that:

i. the candidate's stated contribution to the publication is accurate (as detailed above);
ii. permission is granted for the candidate in include the publication in the thesis; and
iii. the sum of all co-author contributions is equal to 100% less the candidate's stated contribution.

Name of Co-Author	Sukanya Luang		
Contribution to the Paper	Performed and analysed the molecular model of TaMYB74 with MYBR cis-elements.		
Signature		Date	13/09/16

Name of Co-Author	Yuan Li		
Contribution to the Paper	Performed Q-PCR and normalised the data.		
Signature		Date	7/09/16

Name of Co-Author	Natalia Bazanova		
Contribution to the Paper	Performed yeast assay for transcriptional activities of proteins derived from cloned MYB genes.		
Signature		Date	12.09.2016

Name of Co-Author	Sarah Morran		
Contribution to the Paper	Cloned the SHN1 promoter used in the transient expression assays.		
Signature		Date	19/09/2016

Name of Co-Author	Zhihong Song		
Contribution to the Paper	Conducted wax composition analysis.		
Signature		Date	5/09/16

Name of Co-Author	M. Ann Perera		
Contribution to the Paper	Conducted wax composition analysis.		
Signature		Date	5/09/16

Name of Co-Author	Maria Hrmova		
Contribution to the Paper	Supervised the development of experiments and analyses of data, edited the manuscript and acted as the corresponding author.		
Signature		Date	06-09-2016

Name of Co-Author	Nikolai Borisjuk		
Contribution to the Paper	Conceived and designed the experiments, supervised the development of experiments and analyses of data, edited the manuscript.		
Signature		Date	5/09/16

Name of Co-Author	Sergiy Lopato		
Contribution to the Paper	Conceived and designed the experiments, supervised the development of experiments and analyses of data, edited the manuscript.		
Signature		Date	12/09/2016

Journal of Experimental Botany Advance Access published August 3, 2016

Journal of Experimental Botany
doi:10.1093/jxb/erw298
This paper is available online free of all access charges (see http://jxb.oxfordjournals.org/open_access.html for further details)

RESEARCH PAPER

Identification and characterization of wheat drought-responsive MYB transcription factors involved in the regulation of cuticle biosynthesis

Huihui Bi[1], Sukanya Luang[1], Yuan Li[1], Natalia Bazanova[1], Sarah Morran[1], Zhihong Song[2], M. Ann Perera[2], Maria Hrmova[1],*, Nikolai Borisjuk[1] and Sergiy Lopato[1]

[1] Australian Centre for Plant Functional Genomics, School of Agriculture, Food and Wine, University of Adelaide, Glen Osmond, South Australia 5064, Australia
[2] W.M.Keck Metabolomics Research Laboratory, Iowa State University, Ames, IA 50011, USA

* Correspondence: maria.hrmova@adelaide.edu.au

Received 22 April 2016; Accepted 12 July 2016

Editor: Robert Hancock, The James Hutton Institute

Abstract

A plant cuticle forms a hydrophobic layer covering plant organs, and plays an important role in plant development and protection from environmental stresses. We examined epicuticular structure, composition, and a MYB-based regulatory network in two Australian wheat cultivars, RAC875 and Kukri, with contrasting cuticle appearance (glaucousness) and drought tolerance. Metabolomics and microscopic analyses of epicuticular waxes revealed that the content of β-diketones was the major compositional and structural difference between RAC875 and Kukri. The content of β-diketones remained the same while those of alkanes and primary alcohols were increased by drought in both cultivars, suggesting that the interplay of all components rather than a single one defines the difference in drought tolerance between cultivars. Six wheat genes encoding MYB transcription factors (TFs) were cloned; four of them were regulated in flag leaves of both cultivars by rapid dehydration and/or slowly developing cyclic drought. The involvement of selected MYB TFs in the regulation of cuticle biosynthesis was confirmed by a transient expression assay in wheat cell culture, using the promoters of wheat genes encoding cuticle biosynthesis-related enzymes and the SHINE1 (SHN1) TF. Two functional MYB-responsive elements, specifically recognized by TaMYB74 but not by other MYB TFs, were localized in the *TdSHN1* promoter. Protein structural determinants underlying the binding specificity of TaMYB74 for functional DNA *cis*-elements were defined, using 3D protein molecular modelling. A scheme, linking drought-induced expression of the investigated TFs with downstream genes that participate in the synthesis of cuticle components, is proposed.

Key words: Abiotic stress, cuticle, β-diketone, drought, molecular model, MYB and SHINE1 transcription factors, water deficit, wax, wheat.

Introduction

Wheat production is highly sensitive to environmental and climatic variation. Crops are often subjected to the negative influences of abiotic stresses, such as limited water supply, high salinity, and heat; these significantly impair grain yields (Porter and Semenov, 2005). The worst impact of temperature increases created by global warming is predicted to occur at low latitudes, where ~100 Mha of wheat are cultivated. These territories include the major wheat-cropping regions of

Southern and Western Australia (Lobell and Gourdji, 2012). There is a growing consensus that combatting potential yield losses associated with these challenges could be achieved through selection and adaptation of cultivars with improved genetic potential (Reynolds *et al.*, 2012). Understanding the biochemical and molecular mechanisms which allow plants to cope with environmental challenges has a vital significance for improvement of stress tolerance and yield (Hrmova and Lopato, 2014). Towards this aim, two Australian wheat cultivars, Kukri and RAC875, both with excellent performance and superior grain quality, but showing contrasting drought tolerance (RAC875 outyielding Kukri by 24% under cyclic drought), have been subjected to intensive physiological (Izanloo *et al.*, 2008), genetic (Bennett *et al.*, 2012*a*, *b*), and metabolomic (Bowne *et al.*, 2012) investigations. These studies revealed a stronger ability of RAC875 to retain tissue water potential under drought; this trait may be linked to the glaucous appearance (glaucousness) of RAC875 compared with Kukri. Glaucousness is a bluish-white coloration of plant organs, and results from a visual reflection of light by certain epicuticular waxes accumulated in the form of wax crystals on plant surfaces.

The cuticle covers all plant aerial organs and provides protection during plant development and under biotic and abiotic stresses. It is composed of a cutin polyester layer, which is impregnated and covered with waxes composed of various aliphatic carbohydrates (Beisson *et al.*, 2012). Increased amounts of cuticular waxes are associated with improved drought tolerance in several different species (Borisjuk *et al.*, 2014; Baldoni *et al.*, 2015). Breeding for enhanced tolerance and performance under drought can sometimes lead to increased amounts of cuticular waxes (González and Ayerbe, 2010). However, it was found that wax composition is more important than total wax load for the formation of glaucousness in wheat (Zhang *et al.*, 2013). Further points on the role of the cuticle can be found in the Supplementary Introduction at *JXB* online.

Many Arabidopsis genes have been identified to be responsible for cuticular wax biosynthesis, transport, and accumulation (Beisson *et al.*, 2003; Jetter *et al.*, 2007; Jetter and Kunst, 2008; Li-Beisson *et al.*, 2013). Members of several families of transcription factors (TFs) are involved in the regulation of these genes. Most belong to one of three plant TF families: ethylene-responsive factors (ERFs), the myeloblastosis (MYB) family TFs, and homeodomain-leucine zipper class IV (HD-Zip IV) factors (Borisjuk *et al.*, 2014). Overexpression of these TFs alters cuticle deposition and/or composition, and often increases stress tolerance in transgenic plants (Aharoni *et al.*, 2004; Zhang *et al.*, 2005, 2007; Javelle *et al.*, 2010; Seo and Park, 2011; Seo *et al.*, 2011).

MYB TFs comprise one of the largest TF families and are involved in controlling various processes, including responses to biotic and abiotic stresses, development, differentiation, and metabolism (Ambawat *et al.*, 2013; Baldoni *et al.*, 2015). The MYB TF family is subdivided into four subfamilies according to the number of imperfectly repeated R1–R3 DNA-binding domains: 4R-MYB, 3R-MYB (R1R2R3-MYB), 1R-MYB or MYB-related proteins, and R2R3-MYB, which is the largest subfamily of MYB TFs in plants. The residues in the R1–R3 domains contribute to the correct formation of α-helices of MYB TFs and are required for specific base recognition of DNA (Oda *et al.*, 1997). All reported MYB-type regulators of cuticle biosynthesis belong to the R2R3-MYB subfamily of TFs; they are represented by AtMYB41, AtMYB16, AtMYB106, AtMYB96, and AtMYB30 from Arabidopsis, and SlMYB12 from tomato (Cominelli *et al.*, 2008; Raffaele *et al.*, 2008; Adato *et al.*, 2009; Gilding and Marks, 2010; Seo *et al.*, 2011; Oshima *et al.*, 2013).

The *AtMYB41* gene has a low level of expression in all analysed organs of Arabidopsis in the absence of stress, but it is strongly induced by abscisic acid (ABA), drought, and high salinity (Cominelli *et al.*, 2008). Overexpression of *AtMYB41* in transgenic Arabidopsis leads to an increased cuticle permeability. The expression of a number of genes related to lipid biosynthesis and transport, cuticle metabolism, and cell wall biosynthesis were found to be affected by overexpression of *AtMYB41* in transgenic Arabidopsis (Cominelli *et al.*, 2008).

Two other cuticle-related *MYB* genes, *AtMYB16* and *AtMYB106* [also known as *NOK*; the name originates from the Arabidopsis mutant *noeck* (*nok*)], are paralogous genes, involved in the formation of epidermal cell shape and regulation of cuticle biosynthesis by co-operating with the *WAX INDUCER1/SHINE1 (WIN1/SHN1)* gene in *Arabidopsis thaliana* and *Torenia fournieri* (Folkers *et al.*, 1997; Jakoby *et al.*, 2008; Gilding and Marks, 2010; Oshima *et al.*, 2013). Expression in transgenic Arabidopsis of AtMYB106 fused to a repressor domain (Hiratsu *et al.*, 2003), as well as knockout/knockdown of the *AtMYB106* and *AtMYB16* genes using RNAi, negatively influenced the formation of cuticle and resulted in the adhesion of flowering organs (Oshima and Mitsuda, 2013; Oshima *et al.*, 2013).

The Arabidopsis *MYB96* gene was initially identified as a regulator of drought stress responses of plants by integrating ABA and auxin signals; expression of *AtMYB96* was induced by ABA, drought, and high salinity. Constitutive overexpression of *AtMYB96* conferred drought tolerance to transgenic Arabidopsis, while a knockout mutant was more sensitive to drought than wild-type plants (Seo *et al.*, 2009). This was confirmed by studies of the loss-of-function mutant *myb96*, which also had sensitivity to drought (Guo *et al.*, 2013). Transcriptional activation by AtMYB96 of cuticular wax biosynthesis in connection with increased drought tolerance was originally reported by Seo *et al.* (2011). In that study, microarray analysis revealed that AtMYB96 activates a group of genes encoding cuticular wax biosynthetic enzymes, including several enzymes responsible for condensing of very long chain fatty acids (VLCFAs). Cuticular wax depositions in both leaves and stems were significantly increased in the activation-tagged *myb96-1D* mutant and decreased in the loss-of-function *myb96-1* mutant. The MYB recognition *cis*-element (TAACTA/G) was found in the promoters of target genes, and a direct interaction of AtMYB96 with promoters of genes encoding wax biosynthetic enzymes was demonstrated (Seo *et al.*, 2011). Strong constitutive expression of the Arabidopsis gene *AtMYB96* has been used to improve drought tolerance of an emerging oilseed crop plant, *Camelina sativa* (Lee *et al.*, 2014).

Two genes closely related to AtMYB96, AtMYB30 and AtMYB94, were shown to regulate cuticular wax biosynthetic genes (Raffaele *et al.*, 2008; Lee and Suh, 2015*a*). Among the putative AtMYB30 targets, genes were found encoding the four enzymes forming the acyl-coA elongase complex, which are responsible for the synthesis of VLCFAs (Raffaele *et al.*, 2008). Involvement of AtMYB94 in cuticular wax biosynthesis was confirmed by analysis of transgenic Arabidopsis with constitutive overexpression of this gene. A comparison of transgenic and control plants revealed enhanced expression of cuticular wax biosynthesis genes, increased accumulation of cuticular waxes, and a reduced rate of cuticular transpiration in transgenic plants (Lee and Suh, 2015*a*). It was shown that AtMYB94 activates the expression of wax biosynthetic genes *WSD1*, *KCS2*/*DAISY*, *CER2*, *FAR3*, and *ECR* by binding directly to their promoters (Lee and Suh, 2015*b*). The level of expression of the *AtMYB94* gene under drought was increased ~9-fold. An increased accumulation of cuticular waxes reduced the rate of cuticular transpiration in the leaves of *AtMYB94* transgenic Arabidopsis lines under drought (Lee and Suh, 2015*b*). Analysis of the *fused leaves 1* (*fdl1-1*) mutation in maize revealed involvement of the *Fdl1* gene product, ZmMYB94, in the regulation of cuticle deposition in young seedlings and the establishment of a regular pattern of epicuticular wax deposition on the epidermis of young leaves. Lack of *Fdl1* led to developmental defects (La Rocca *et al.*, 2015).

Another MYB TF, which is involved in plant cuticle regulation, is SlMYB12. Detailed gene expression and metabolomics analyses of transgenic tomato plants revealed involvement of SlMYB12 in regulation of tomato fruit cuticle biosynthesis (Adato *et al.*, 2009). The Arabidopsis homologue of this gene has not been characterized.

In this study, we investigated the biochemical background of cuticular waxes in two wheat cultivars, RAC875 and Kukri, grown under well-watered conditions and mild drought. We identified and isolated six *MYB* genes from RAC875, encoding homologues of known cuticle biosynthesis-related Arabidopsis and tomato MYB TFs, and characterized for their involvement in the regulation of cuticle formation in wheat under water deficit.

Materials and methods

Plant material and cultivation

Wheat plants *Triticum aestivum*, cultivars RAC875 and Kukri, previously described by Izanloo *et al.* (2008), were grown in a greenhouse in 112 × 76 × 50 cm containers, equipped with an automatic watering system and continuous monitoring of the soil water potential (Amalraj *et al.*, 2016). For the cyclic drought experiment, drought-tolerant RAC875 and drought-sensitive Kukri were grown as previously described (Harris *et al.*, 2016). A drought treatment was applied to half of the plants, according to a scheme adopted by Bowne *et al.* (2012) and depicted in Supplementary Fig. S1. Watering in the first cycle of drought was withdrawn at flag leaf emergence until the drought-sensitive Kukri showed wilting. Plants were then re-watered to field capacity and again left to dry without watering until Kukri once again reached wilting point. In this experiment, re-watering was done twice: at 15 d and 24 d after flag leaf emergence and the initial withholding of watering (Supplementary Fig. S1). Plant water status was monitored for both cultivars by measuring the relative water content of the detached second leaf, as was described by Izanloo *et al.* (2008).

Cloning of the wheat orthologues of selected MYB TFs

Amino acid and/or nucleotide sequences of selected MYBs (AtMYB41, AtMYB96, AtMYB106, AtMYB16, and SlMYB12) were retrieved from the National Center for Biotechnology Information (NCBI, Bethesda, MD, USA) or the Arabidopsis Information Resource (TAIR, Columbus, OH, USA) databases, using the accession and/or locus numbers summarized by Borisjuk *et al.* (2014). Retrieved sequences were used to search against the latest versions of the wheat genomic and cDNA sequence databases linked to the Blast Portal at the Australian Centre for Plant Functional Genomics (ACPFG, University of Adelaide, Australia) to ensure that the closest wheat genes were identified. The identified wheat sequences were used to design primers (Supplementary Table S1) for gene amplification by nested PCR from cDNA pools prepared from the leaves and spikes of the drought-tolerant wheat cultivar RAC875 subjected to drought. CACC sequences were added to the 5' ends of the forward primers used in the second round of PCR to conduct directional cloning of full-length coding sequences (CDS) of each gene into the pENTR/D-TOPO vector (Life Technologies, Victoria, Australia).

Gene expression analysis in different wheat tissues, under dehydration and cyclic drought

Gene expression of selected MYB genes was investigated in detached leaves subjected to rapid dehydration, and in plants subjected to cyclic drought (described above). To analyse the response of genes to rapid dehydration, flag leaves were cut from four well-watered plants of each of the cultivars RAC875 and Kukri at awn emergence. Leaves were placed in 12 ml open plastic test tubes, incubated at ambient temperature (23 °C) for 0, 2, 4, and 7 h, then frozen in liquid nitrogen and stored at −80 °C for RNA extraction. Flag leaf samples were also collected from both cultivars during the cyclic drought experiment, at 5, 9, 14, 23, and 25 d after initiating the first cycle of drought (Supplementary Fig. S1). A set of samples was collected from well-watered (control) plants at the same time points. Total RNA was isolated from leaf tissues using a Direct-zol RNA MiniPrep Kit (Zymo Research, CA, USA) with an on-column DNase treatment. A 1.5 µg aliquot of purified RNA from each sample was used for cDNA synthesis using a SuperScript III Reverse Transcriptase kit (Life Technologies, Victoria, Australia). Quantitative real-time PCR (Q-PCR) analysis was performed on cDNA samples as described previously (Fletcher, 2014). Three wheat genes, encoding actin, cyclophilin, elongation α factor, and glyceraldehyde-3-phosphate dehydrogenase, were simultaneously used for normalization of expression (Fletcher, 2014). The selection of three genes was based on the pairwise comparison among the three genes mentioned above. To obtain the actual copy numbers of RNA, we generated a standard curve of the copy number in relation to the cycle threshold (Ct) value. The standard curve was constructed using a dilution series, prepared from the purified PCR product of the target gene, covering six orders of magnitudes. To analyse tissue specificity of a selected subset of the genes, we also utilized a cDNA series prepared from different tissues of *T. aestivum* cv. Chinese Spring (Morran *et al.*, 2011). Three biological and three technical replicates were used in all gene expression analysis experiments.

In-yeast activation assays and localization of activation domains

Sets of full-length and partial CDS for *TaMYB16*, *TaMYB24*, *TaMYB31*, *TaMYB74*, *TaMYB77*, and *TaMYB78* were amplified by PCR with *Eco*RI and *Bam*HI restriction sites introduced in forward and reverse primers, respectively, and cloned in the same restriction sites of

the pGBKT7 vector (Scientifix, Victoria, Australia). Each set included the full-length CDS, and versions with truncations at the 3' end. A transcriptional activation assay was performed as previously described by Eini *et al.* (2013). Generated constructs were transformed into yeast (*Saccharomyces cerevisiae*) strain Y187 as described by Pyvovarenko and Lopato (2011). The pGBKT7 vector harbours a tryptophan (Trp) selection gene. The yeast reporter strain, Y187, could not grow on the synthetic defined (SD) medium lacking Trp without introducing a functional *TRP1* gene and could not grow on the SD/-His medium without activation of a *HIS3* gene. Therefore, yeast transformants were first selected on the SD/-Trp medium to prove that transformation of the pGBKT7 construct in yeast cells occurred. The yeast culture was replica-plated onto the SD/-Trp/-His medium. The ability of full-length or truncated wheat MYB proteins to activate expression of the *HIS3* gene led to yeast growth on the selective medium.

Assessment of promoter activation by MYB TFs in a wheat transient expression assay

A transient expression assay was performed using *Triticum monococcum* L. suspension cell culture, according to the procedure established by Eini *et al.* (2013). In this assay, cultivated wheat cells were co-bombarded with vectors expressing one of the *MYB* TF genes in a pair with a construct containing the β-glucuronidase reporter gene (*GUS*) fused to a promoter with potential MYB-binding sites. GUS expression from the MYB-activated promoter was quantified 48 h after bombardment. Promoters of three cuticle biosynthesis-related genes: 3-ketoacyl CoA synthetase (*KCS1*), cytochrome P450 monooxygenase (*ATT1*), and transcription factor *SHN1* (Borisjuk *et al.*, 2014), were selected as targets for activation by MYB TFs. The promoter sequences of the *TaKCS1* and *TaATT1* genes (3235 bp and 2535 bp fragments upstream of the corresponding gene translational sites) were cloned by nested PCR, using primers based on corresponding gene sequences derived from the International Wheat Genome Sequencing Consortium (IWGSC; http://www.wheatgenome.org/) databases, and genomic DNA of *T. aestivum* cv. RAC875 as template. The sequence of the *SHN1* promoter was obtained using a clone from a BAC (bacterial artificial chromosome) library of *Triticum durum* cv. Langdon (Cenci *et al.*, 2003). The full-length CDS of *TaSHN1* (624 bp) was isolated by PCR and used to screen the BAC library by colony hybridization. The plasmid of the selected BAC clone was isolated using a Large Construct Kit (QIAGEN, Hilden, Germany), and the presence of the *TdSHN1* gene was confirmed by PCR using the primers listed in Supplementary Table S1; the BAC clone was sequenced using 454 sequencing technology (Wicker *et al.*, 2006). The obtained sequence was used to design primers and amplify a 2203 bp fragment of the *TdSHN1* promoter. The three promoters, as well as six 5'-deletion variants of the *TdSHN1* promoter, were cloned into the pENTR-D-TOPO vector (Life Technologies, Victoria, Australia) and re-cloned by recombination upstream of the *GUS* gene into the expression vector pMDC164 (Curtis and Grossniklaus, 2003). Vectors for expression of MYB proteins were constructed by recombinational cloning of the *TaMYB24*, *TaMYB31*, *TaMYB74*, and *TaMYB77* CDS into the modified pMDC32 vector (Curtis and Grossniklaus, 2003), where the standard 35S promoter was replaced with a maize polyubiquitin promoter, pUbi (Christensen *et al.*, 1992). The pUbi–green fluorescent protein (GFP) construct was generated in a similar way, by cloning of CDS encoding a GFP in the same vector, and it was used as a negative control in all transient expression experiments. MYB recognition (MYBR) *cis*-elements were predicted using the Plant *Cis*-acting Regulatory DNA Elements database (PLACE, University of Pittsburgh, USA) (Higo *et al.*, 1999) prior to selection and cloning of promoter deletions.

Composition analysis of cuticular waxes

For the wax composition analysis, 6.5 cm long flag leaf segments were collected at 24 d after anthesis. The weight of each leaf was measured, and leaves were immersed in liquid nitrogen for storage at −80 °C. For wax extraction, frozen leaf samples were warmed to ambient temperature for 2 min. Hexadecane (C16 alkane), used as an internal standard, was dissolved in hexane and applied to the surfaces of leaves in amounts of 1 µg per 0.3 g of a leaf sample. At 3–5 min after application of the internal standard, waxes were extracted by dipping into 4 ml of chloroform for 1 min and dried under a stream of nitrogen. GC-MS analysis was conducted in the W.M. Keck Metabolomics Research Laboratory of Iowa State University (USA). The wax extract was dissolved in 200 µl of acetonitrile, spiked with 1 µg of triacontane (dissolved in chloroform), and derivatized with 50 µl of *N,O*-bis(trimethylsilyl)trifluoroacetamide with 1% (v/v) trimethylchlorosilane at 80 °C for 60 min. The sample was dried under a stream of nitrogen; the residue was reconstituted in 100 µl of chloroform and subjected to GC-MS analysis according to the procedure described in Cha *et al.* (2009). GC-MS analysis was performed with an Agilent 6890 GC (Agilent Technologies, CA, USA) interfaced to a 5973 mass spectrometer. The HP-5ms column (30 m×0.25 mm×0.25 µm) was used and a temperature gradient was programmed from 120 °C to 325 °C at 5 °C min^{-1} with a He flow rate at 1.0 ml min^{-1}. Operating parameters for MS were set to 70 eV of ionization voltage and 280 °C of interface temperature. The GC-MS data files were de-convoluted by the NIST AMDIS software and searched using an in-house compound library and the NIST 2014 Mass Spectral Library.

Scanning electron microscopy

The epicuticular wax structure was examined using a scanning electron microscope in the Adelaide Microscopy Unit (https://www.adelaide.edu.au/microscopy/, University of Adelaide, Australia). All analyses of wheat cuticular waxes were performed using flag leaves, the main source of assimilates during grain development (Evans *et al.*, 1975), and the standard subject for cuticle analysis in wheat (Adamski *et al.*, 2013; Zhang *et al.*, 2013). Flag leaf blades were collected 10 d after anthesis, and segments close to the major vein of ~0.4×0.3 cm in size were cut from the middle of leaves and examined under a Philips XL30 Field Emission Scanning Electron Microscope, equipped with a Gatan CT1500 HF Cryo-transfer Stage. Samples were attached to the holder using Tissue-Tek OCT compound mixed with carbon dag in 1:1 ratio (carbon dag is a commonly used name for the conductive carbon paint), after which they were frozen in liquid nitrogen, and transferred under vacuum to the preparation chamber. The temperature of samples was raised to −92 °C, and held for ~2 min, to allow ice on the surface to sublime away. The temperature was lowered to −110 °C (at which sublimation ceased), and the sample was coated with platinum (~2 nm thick layer) to make it electrically conductive. The sample was loaded onto the microscope stage (held at a temperature lower than −150 °C) and examined.

Simulation of evolutionary relationships of MYB proteins

To construct a phylogenetic tree of MYB factors (Fig. 2), we used 103 wheat sequences from the Plant Transcription Factor Database (http://planttfdb.cbi.pku.edu.cn/, Center for Bioinformatics, Peking University, China), 27 wheat R2R3 MYB gene sequences identified by Zhang *et al.* (2012), together with six wheat genes characterized in this study, and five MYB query genes from Arabidopsis and tomato. The evolutionary history of representative MYB proteins was inferred using the Neighbor–Joining method (Saitou and Nei, 1987). Evolutionary distances were computed using the p-distance method (Nei and Kumar, 2000) (with 1000 bootstrap replications), and expressed in units of numbers of residue differences per site. All positions containing gaps and missing data were eliminated. Evolutionary analyses were conducted in MEGA6 (Tamura *et al.*, 2013).

3D protein molecular modelling

Homology modelling of TaMYB74 was performed with Modeller v9.10 (Eswar *et al.*, 2008). The TvMYB2 protein structure from the

protozoan parasite *Trichomonas vaginalis* in complex with MRE-1–12 DNA (5'-AAATATCGTTAT-3'/5'-ATAACGATATTT-3') (Protein Data Bank accession 3OSG) (Jiang *et al.*, 2011) was used as a structural template. The primary sequence of TaMYB74 shares 34.4% identity and 45.6% similarity with the TvMYB2 protein. Selected models displaying the lowest objective function values were analysed by ProSA2003 (Sippl, 1993) and PROCHECK to evaluate stereochemical and G-factor properties (Laskowski *et al.*, 1993). The target DNA *cis*-element for TaMYB74 (denoted as MYBR1: 5'-AGGTGGTTATGC-3'/5'-GCATAACCACCT-3'; the core sequence is underlined) was generated based on the DNA structure of the MRE-1–12 *cis*-element using Coot (Emsley *et al.*, 2010). The most favourable TaMYB74 structural model with a DNA *cis*-element was minimized in YASARA (Krieger *et al.*, 2009) and evaluated. The Ramachandran plot of the DNA–TF complex structure showed that 100% of residues were located in the most favoured and additional allowed regions, with an overall G-factor of −0.17 (PROCHECK) and a *z*-score value of −5.9 (ProSa2003). The overall G-factor for the TvMYB2–DNA structure is 0.24 and the *z*-score value is −7.6. Energy (or conformational stability) analyses were calculated using Fold-X force-field (Schymkowitz *et al.*, 2005).

Statistical analysis of data

Quantification data of wax components and data on gene expression levels under dehydration and cyclic drought were analysed using two-way ANOVA with the Fisher's least significant difference post-hoc test. Transient expression assay data were analysed using one-way ANOVA with the Fisher's least significant difference post-hoc test. All analyses were conducted in GenStat (16th Edition; VSN International Ltd, Hemel Hempstead, UK).

GenBank accession numbers

TaMYB24, KU674896; *TaMYB31*, KU674897; *TaMYB74*, KU674898; *TaMYB16*, KU674899; *TaMYB77*, KU67900; *TaMYB78*, KU67901; *TaSHN1*, KU737577; *TaATT1* promoter, KU737578; *TaKCS1* promoter, KU737579; *TdSHN1* promoter, KU737580.

Results

Microscopic and biochemical characterization of cuticular waxes of Kukri and RAC875 cultivars grown under well-watered and mild drought conditions

Two Australian wheat cultivars, Kukri and RAC875, have contrasting drought and heat tolerance and have been intensively studied at physiological, genetic, and metabolomic levels (Izanloo *et al.*, 2008; Bennett *et al.*, 2012*b*; Bowne *et al.*, 2012). The results of these studies suggest a link between differences in water-retaining capacity and glaucousness. RAC875 has glaucous leaves and is drought tolerant, while Kukri has a non-glaucous phenotype (Fig. 1A). We applied SEM and GC-MS to compare the wax crystal structure and biochemical make-up of leaf blade surfaces in Kukri and RAC875, grown under well-watered and mild drought conditions. Under both well-watered (Fig. 1B) and mild drought conditions (Fig. 1D), tubule-shaped crystals, which have been suggested to result from the high content of β-diketones (Adamski *et al.*, 2013; Zhang *et al.*, 2013), were abundant on the abaxial side of the RAC875 flag leaves. The same surfaces in Kukri had platelet-shaped wax crystals (Fig. 1C, E), suggestive of a high content of primary alcohols (von Wettstein-Knowles, 2012). Under drought conditions, the number of wax crystals on the abaxial side of RAC875 leaves remains unchanged, while the number of those on the abaxial side of the Kukri leaves was slightly increased. However, no changes in crystal shapes were observed (Fig. 1D, E).

To reveal the chemical basis underlying the substantial differences in shape of wax crystals of these two cultivars, we performed GC-MS compositional analysis of extracted wax (Fig. 1F, G; Supplementary Fig. S2). There was a significant increase in total wax loads on leaves of plants grown under drought conditions compared with well-watered plants in RAC875, while a small but definite increase in Kukri was also observed (Fig. 1F). The main difference between the RAC875 and Kukri wax components was the presence of β-diketones in the wax of RAC875. β-Diketones were estimated to comprise ~18% of total waxes in RAC875, but were almost undetectable in Kukri (Fig. 1G). The increase in total wax loads was predominantly defined by an elevated accumulation of alkanes with a chain length of 29 and 31 carbons in both cultivars, and also of primary alcohols in RAC875 with the dominant chain length of 28 carbons (Fig. 1G). No significant difference was observed in the content of β-diketones in RAC875 between well-watered and mild drought conditions.

Gene cloning and the phylogenetic relationships of MYB TFs

Six wheat *MYB* genes were cloned by nested PCR from leaves and spikes of the drought-tolerant wheat cultivar RAC875. The protein sequences of five known cuticle regulators from Arabidopsis and tomato, AtMYB41, AtMYB16, AtMYB106, AtMYB96, and SlMYB12, were used to identify protein and nucleotide sequences of the closest wheat homologues in several wheat databases. Details of the six cloned wheat *MYB* genes, including their names, accession numbers, corresponding Arabidopsis homologues, and their proposed chromosomal locations are summarized in Table 1. Schematic representations of gene structures of the six wheat genes, using the Gene Structure Display Server (GSDS 2.0), are shown in Supplementary Fig. S3. The evolutionary relationship of 141 members, which include four TFs from Arabidopsis and a sequence from tomato together with six wheat homologues/orthologues, as well as 103 wheat MYB sequences from the Plant Transcription Factor Database and 27 wheat R2R3 MYB sequences previously identified by Zhang *et al.* (2012), was inferred by using the Neighbor–Joining method in MEGA6 (Fig. 2). The phylogenetic tree shows that all cloned wheat sequences (indicated by dots in Fig. 2) cluster with their corresponding Arabidopsis protein homologues. The tree confirmed that six wheat and respective Arabidopsis MYB sequences identified in this work are related. Further points on gene cloning and the phylogenetic relationships of MYB TFs can be found in the Supplementary Results.

Domain structure and the activation properties of cuticle-related MYB TFs

Domain organization of the six MYB proteins, encoded by cloned cDNAs, was investigated using the SMART protein

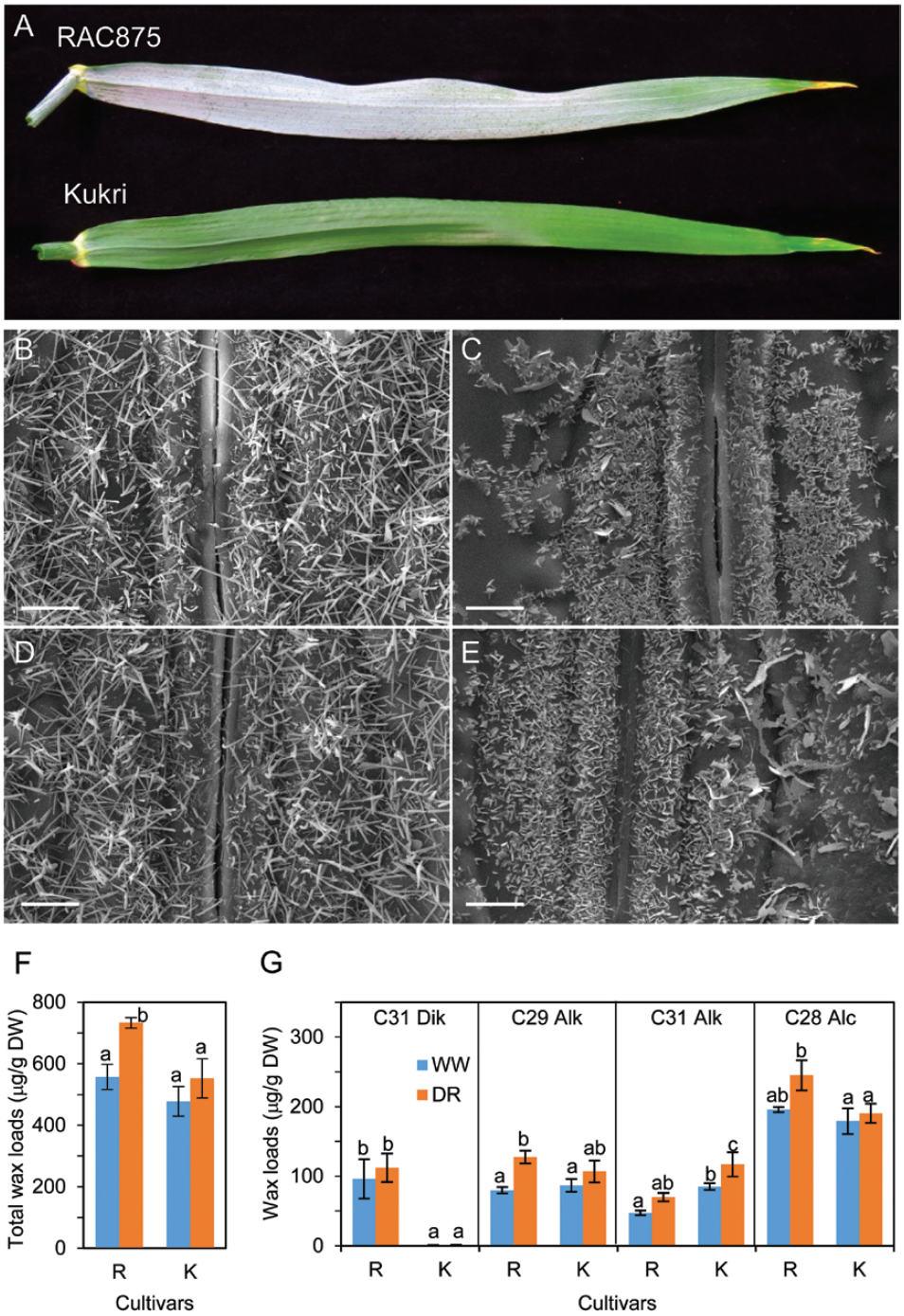

Fig. 1. The visual appearance, ultrastructure, and the wax composition of cuticle on flag leaves of wheat. (A) The appearance of abaxial sides of flag leaves detached from RAC875 and Kukri wheat cultivars grown under well-watered conditions. (B and C) Scanning electron micrographs of the abaxial sides of flag leaves derived from RAC875 and Kukri plants grown under well-watered conditions. (D and E) Scanning electron micrographs of the abaxial side of leaves derived from RAC875 and Kukri plants grown under the conditions of limited watering (mild drought). (F and G) Total wax loads and amounts of the four most abundant wax components on the flag leaves of RAC875 (R) and Kukri (K) under well-watered (WW) and mild drought (DR) conditions. Wax loads were calculated as μg of wax per dry leaf weight (DW). Dik, C31 β-diketones; Alk, alkane; Alc, primary alcohol. Means and SEs were calculated from three replicates. Two-way ANOVA with the Fisher's least significant difference post-hoc test was conducted using GenStat. The same lower case letters on top of error bars indicate differences that are not significant at the 5% level. Scale bars=5 μm.

domain analysis server (Letunic *et al.*, 2015) (http://smart.embl-heidelberg.de/). Each of the wheat MYB TFs contains two adjacent highly conserved SANT DNA-binding domains, localized in the N-terminal part of the protein (Fig. 3), and represent characteristic features of plant R2 and R3 MYB TFs (Stracke *et al.*, 2001).

The presence and positions of activation domains (ADs) in six wheat MYB proteins were examined in yeast. For this purpose, full-length and truncated coding regions of the *MYB* genes were fused to the sequence encoding the binding domain of the yeast GAL4 TF. Constructs were used to transform yeast cells, and the presence of ADs in MYB TFs

Table 1. *Cloned wheat MYB genes*

Gene locations on wheat chromosomes are based on *in silico* analysis using the International Wheat Genome Sequencing Consortium (IWGSC) database. References for each of the query genes are listed in the right column.

Cloned wheat genes	Accession numbers	Query genes	Coding sequence length (bp)	Genetic location	Query sequence references
TaMYB16	KU674899	*AtMYB106*	978	2DL	Oshima *et al.* (2013)
TaMYB24	KU674896	*AtMYB96*	945	2AS	Seo *et al.* (2009, 2011); Seo and Park (2010)
TaMYB31	KU674897	*AtMYB96*	954	5BL	Seo *et al.* (2009, 2011); Seo and Park (2010)
TaMYB74	KU674898	*AtMYB41*	1047	2DS	Cominelli *et al.* (2008)
TaMYB77	KU674900	*AtMYB16*	1059	2DL	Oshima *et al.* (2013)
TaMYB78	KU674901	*SlMYB12*	1041	4AS	Adato *et al.* (2009)

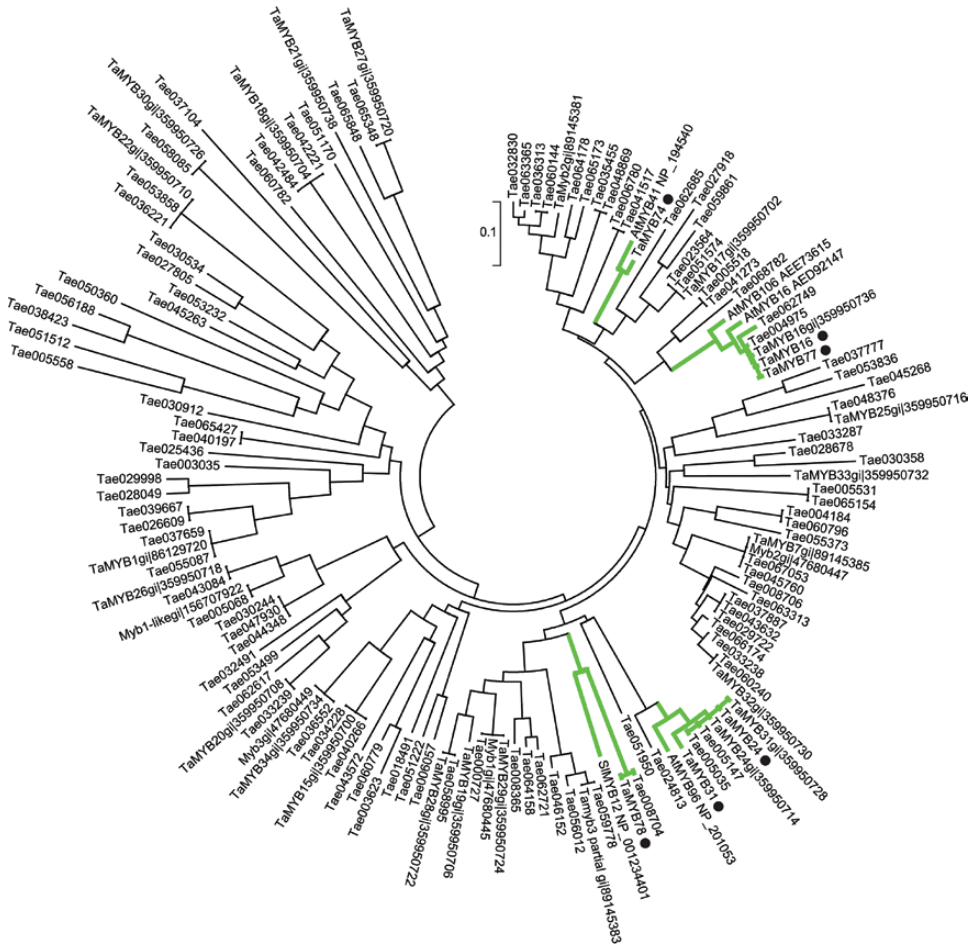

Fig. 2. A phylogenetic tree of MYB TFs. We analysed 141 sequences including six sequences of wheat MYB TFs (indicated by dots) derived from cDNAs cloned in this work, five query Arabidopsis and tomato MYB TFs (GenBank accessions shown in the figure), 103 wheat MYB factors from the Plant Transcription Factor Database (annotated as Tae with a six-figure number) and 27 wheat R2R3 MYB TFs (Zhang *et al.*, 2012). The branches, to which wheat MYB protein sequences studied in this work belong, are indicated with thick grey lines. The number near a scale indicates a residue difference per site. The tree was constructed using the Neighbour–Joining method in MEGA6. (This figure is available in colour at *JXB* online.)

was revealed as the ability of the yeasts to grow on a selective medium. To obtain insights into the position and approximate length of the ADs of wheat MYB TFs, their amino acid sequences were truncated at the C-termini. The predictions of transcriptional ADs (under AD we mean here any sequence which is functionally important for the activation of transcription, rather than a conserved protein domain) in MYB proteins were based on knowledge that ADs are usually (but not always) enriched in acidic amino acid residues and contain glutamine-rich and proline-rich motifs (Johnson *et al.*, 1993).

Three full-length proteins, TaMYB24, TaMYB31, and TaMYB77, provided strong transcriptional activation, and one full-length protein, TaMYB74, resulted in weak transcriptional activation of the yeast *HIS3* gene, the product of which supports yeast growth on the selective medium

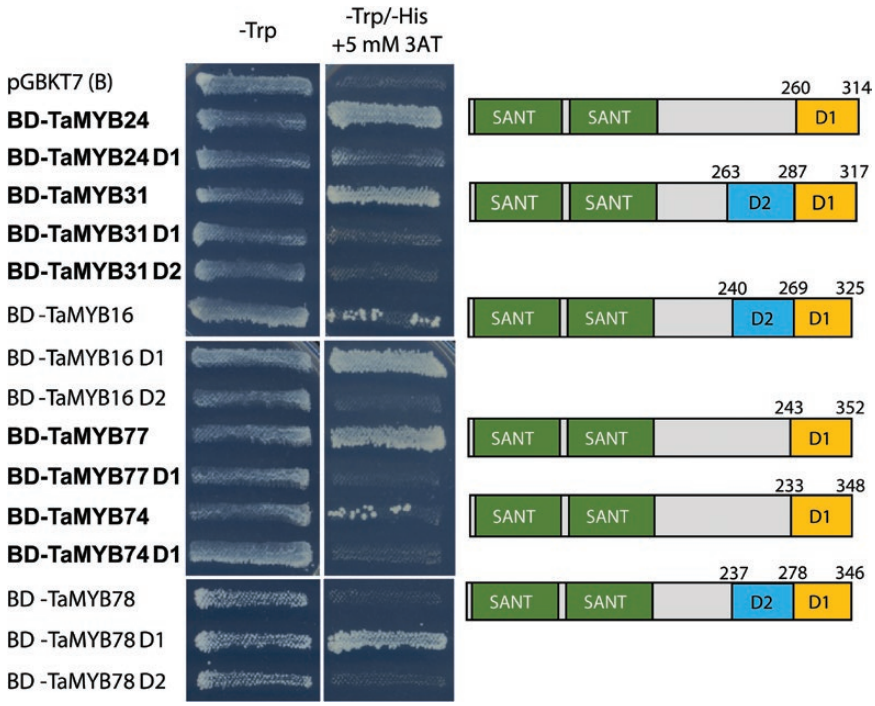

Fig. 3. Transcriptional activation assays and the localization of activation domains of cloned *MYB* genes. The assay was performed in yeast using full-length and C-terminal truncated MYB TFs fused to a binding domain (BD) of yeast GAL4 TF. An empty pGBKT7 plasmid was used as a negative control. -Trp represents the synthetic defined (SD) medium lacking tryptophan (selection for plasmid presence) and -Trp/-His refers to the SD medium without tryptophan and histidine (selection for activation of the yeast *HIS3* gene). Drought-responsive MYBs and their truncations are shown in bold. Domain structures and positions of truncations are indicated in the right part of the figure. SANT: *S*wi3, *A*da2, *N*-Cor, and *T*FIIIB DNA-binding domains. D1 and D2 represent removed protein fragments; D2 truncation included the removal of D1. The residue positions of truncations are indicated. (This figure is available in colour at *JXB* online.)

deficient in histidine (Fig. 3). For the truncations, truncation D1 removed significant parts of predicted ADs in TaMYB24 and TaMYB31, and completely removed the ability of TaMYB77 and TaMYB74 to activate the reporter gene. Surprisingly, the full-length TaMYB16 showed weak activation of the *HIS3* gene and full-length TaMYB78 did not show any transcriptional activity in yeast. However, D1 removal in both proteins released their strong activator properties, suggesting either the presence of repressor motifs in D1, or changes in folding patterns of proteins. D2 removal, however, totally abolished the activation properties of TaMYB16 and TaMYB78, suggesting that the whole or the significant part of protein sequences responsible for transcriptional activation are located in D2.

Selection of MYB genes that are regulated by water deficit

To identify cuticle biosynthesis-related regulatory genes responsive to water deficiency, expression of each of the cloned *MYB* genes was analysed by Q-PCR: (i) in detached flag leaves of RAC875 and Kukri that were subjected to rapid dehydration; and (ii) in flag leaves of the same two cultivars growing under cyclic drought.

Two out of six examined genes, *TaMYB16* and *TaMYB78*, had no detectable gene expression in leaves during a rapid dehydration experiment (Fig. 4). Expression of these two *MYB* genes was not tested during the cyclic drought experiment because flag leaves of a similar developmental stage were used in both experiments. Of the remaining four genes, *TaMYB24* and *TaMYB77* were down-regulated, and *TaMYB31* and *TaMYB74* were up-regulated during rapid dehydration and under drought (Figs 4, 5). Induction of the expression of the *TaMYB24*, *TaMYB31*, *TaMYB74*, and *TaMYB77* genes was investigated in the flag leaves of wheat cultivars Kukri and RAC875 during three consecutive cycles of drought (Fig. 5). Water status during the cyclic drought experiment and the time points of leaf sampling are shown in Supplementary Fig. S1. Further points on the selection of *MYB* genes that are regulated by water deficit can be found in the Supplementary Results.

Expression of MYB genes in wheat tissues

Expression of dehydration- or drought-responsive *MYB* genes was tested in various tissues of *T. aestivum* cv. Chinese spring (Fig. 6). The *TaMYB24* gene showed the highest transcript levels in bracts and pistil before anthesis, and moderate levels in leaves and developing and mature caryopses. In all other tested tissues, the expression levels of *TaMYB24* were low. The expression pattern of the *TaMYB31* gene was similar to that of its homologue, *TaMYB24*, but overall the levels of expression were lower.

The highest expression level of the *TaMYB74* gene was found in roots. Two- to three-fold lower transcript levels were detected in leaves, anthers, pistil, and developing caryopsis.

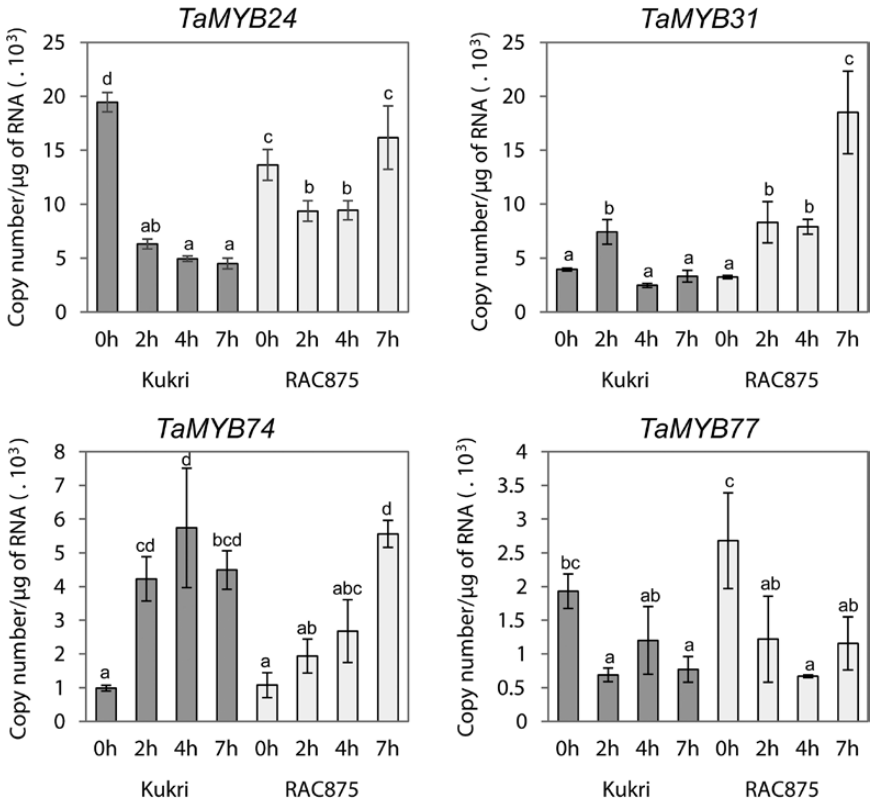

Fig. 4. Expression levels of cloned *MYB* genes in rapidly dehydrating leaves of Kukri and RAC875. Expression of *TaMYB24*, *TaMYB31*, *TaMYB74*, and *TaMYB77* was studied by Q-PCR. Flag leaf samples were sampled at awn emergence. Dehydration was performed at room temperature for 0, 2, 4, and 7 h, after which leaves were snap-frozen in liquid nitrogen. Two-way ANOVA with the Fisher's least significant difference post-hoc test was conducted using GenStat. Error bars indicate the SE of three replicates.

The *TaMYB77* gene had the highest expression levels in leaf, developing caryopsis, and immature inflorescence. The transcript levels of this gene in other tested tissues were low.

Activation of promoters of cuticle biosynthesis-related genes by drought-responsive MYB TFs

Three promoters of cuticle biosynthesis-related genes were cloned either by nested PCR using genomic DNA of *T. aestivum* as template (*TaATT1* and *TaKCS1* promoters), or via screening of a BAC library of *T. durum* (*TdSHN1* promoter). Promoters were cloned upstream of the *GUS* reporter gene and the resulting constructs were used in transient expression assays. These assays were conducted to confirm the involvement of cloned *MYB* genes in the regulation of cuticle biosynthesis. Transient expression assays were performed by co-bombardment of a suspension cell culture of *T. monococcum* L. with constructs containing the *GUS* gene driven by each of tested promoters (reporter constructs), and constructs containing each *MYB* TF gene driven by the constitutive polyubiquitin promoter (effector constructs) (Fig. 7A). The *GFP* gene cloned under the polyubiquitin promoter was used as a negative control to reveal basal levels of promoter activity in wheat cells.

As shown in Fig. 7B, TaMYB74 strongly activated all three tested promoters. A slightly milder activation of *TaATT1* and *TaKCS1* promoters was observed in TaMYB31 and TaMYB24, while TaMYB77 was unable to activate any promoter. The *TdSHN1* promoter was activated only by TaMYB74 (Fig. 7B).

Identification of the functional MYB-responsive cis*-elements in the* TdSHN1 *promoter*

The *TdSHN1* promoter was subjected to *cis*-element analysis using PLACE software (Higo *et al.*, 1999). Five potential MYBR elements were predicted within the 696 bp of the cloned 2203 bp long fragment upstream of the start codon of the *TdSHN1* gene, which will herein be referred to as the full-length promoter. To identify the functional MYBR *cis*-element(s), which is (are) specifically recognized by TaMYB74, a series of promoter deletions was generated at the 5' end of the full-length *TdSHN1* promoter. Deletions were generated in such a way that each of the five predicted MYBR *cis*-elements were removed one by one. As shown in Fig. 8, similar levels of *GUS* expression were initiated by the full-length promoter and by D1, D2, and D3 promoter deletions. However, the level of *GUS* expression driven by the D4 deletion decreased by ~70% compared with that driven by the D3 deletion. The 5'-AGGTGGTTATGC-3'/5'-GCATAACCACCT-3' sequence (the core sequence is underlined) designated here and below as the MYBR1 *cis*-element, predicted to be present on the promoter fragment between the D3 and D4 deletions, was the first (distal) functional MYBR *cis*-element. The second (proximal) functional MYBR *cis*-element, 5'-ATCTAACCACAT-3'/5'-ATGTGGTTAGAT-3'

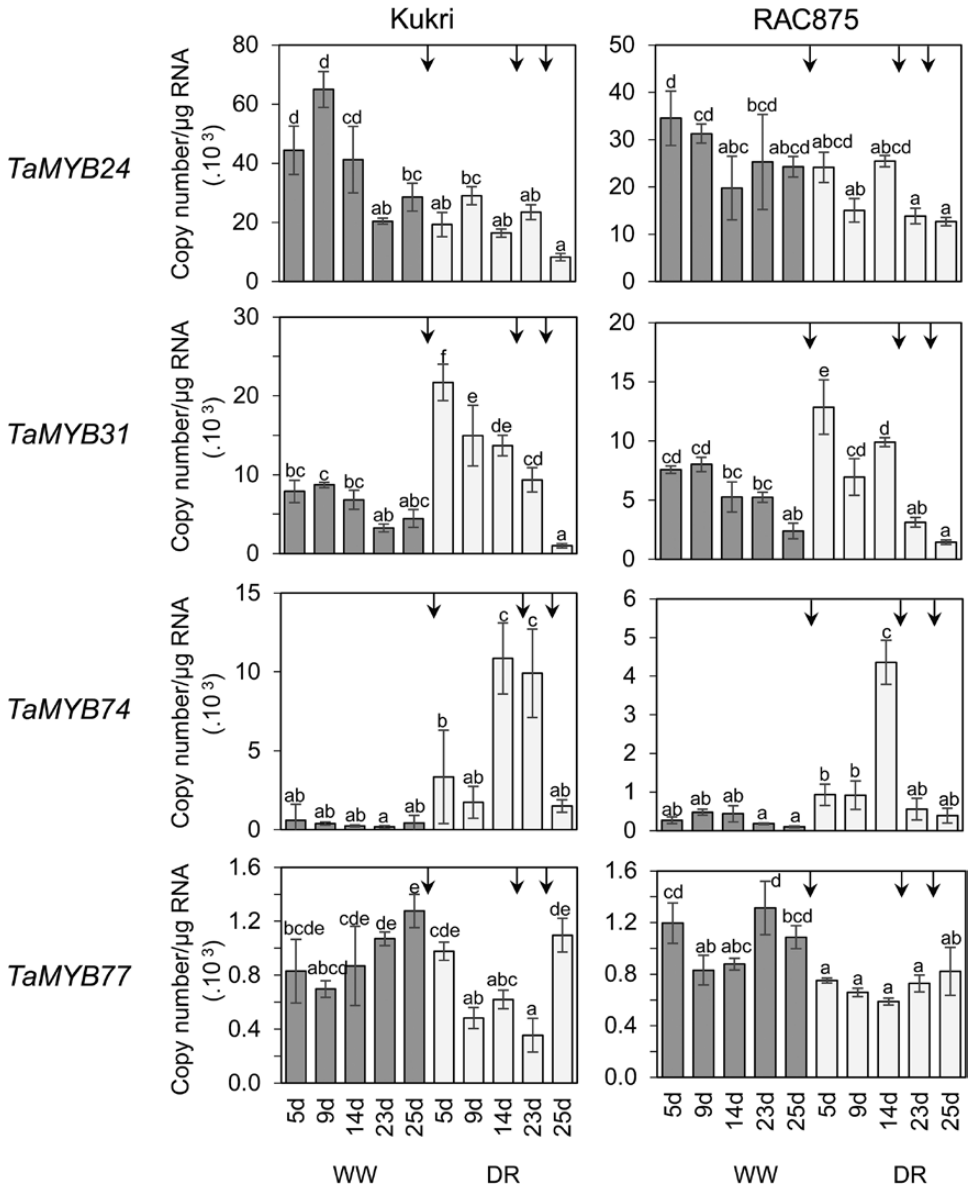

Fig. 5. Expression levels of cloned *MYB* genes under cyclic drought in Kukri and RAC875. Expression of *TaMYB24*, *TaMYB31*, *TaMYB74*, and *TaMYB77* was studied by Q-PCR. Expression of genes was examined after 5, 9, 14, 23, and 25 d, using either well-watered (WW) or cyclic drought-exposed (DR) plants. Three cycles of drought (after watering points 1–3) indicated by arrows were applied at 0, 15, and 24 d as shown in Supplementary Fig. S1. Two-way ANOVA with the Fisher's least significant difference post-hoc test was conducted using GenStat. Error bars indicate the SE of three replicates.

(the core sequence is underlined), designated as MYBR2, is situated between the D5 and D6 deletions. It was responsible for the remaining 30% of the *TdSHN1* promoter activity. The D6 deletion neither contained any MYBR elements nor provided any detectable activation of the *GUS* gene in wheat cells.

Molecular model of TaMYB74 in complex with functional MYBR cis*-elements identified in the* TdSHN1 *promoter*

The TaMYB74 DNA-binding domain contains the conserved R2 and R3 repeats, and adopts a helix–turn–helix conformation with three regularly spaced tryptophan/phenylalanine residues, which form a hydrophobic core of the MYB domain (Fig. 9A, C). The binding domain consists of six α-helices: α1 (Gln19–His32), α2 (Trp37–Asp43), α3 (Gly50–Leu61), α4 (Phe72–Leu85), α5 (Trp89–Arg95), and α6 (Asp101–Arg113). The binding domain binds the MYBR1 DNA element through the α3 helix (R2 motif) and the α6 helix (R3 motif) in the major groove of DNA and makes contacts by forming hydrogen bonds between charged (Lys14, Lys51, and Lys105) and polar residues (Asn102, Asn106, and Asn109) with nucleo-bases (Fig. 9B; Supplementary Table S2). In addition, the hydrogen bonds are mediated by Lys13 and Trp17 at the N-terminus, Arg48, Arg54, and Arg56 of the α3 helix, Asn87, Trp89, and Ser90 of the α5 helix, and Arg115 at the C-terminus, to the sugar-phosphate DNA backbone, to increase the overall stability of the complex (Supplementary Table S2). Hydrogen bond distances between residues and nucleo-bases or sugar-phosphate backbones are between 2.8 Å and 3.6 Å.

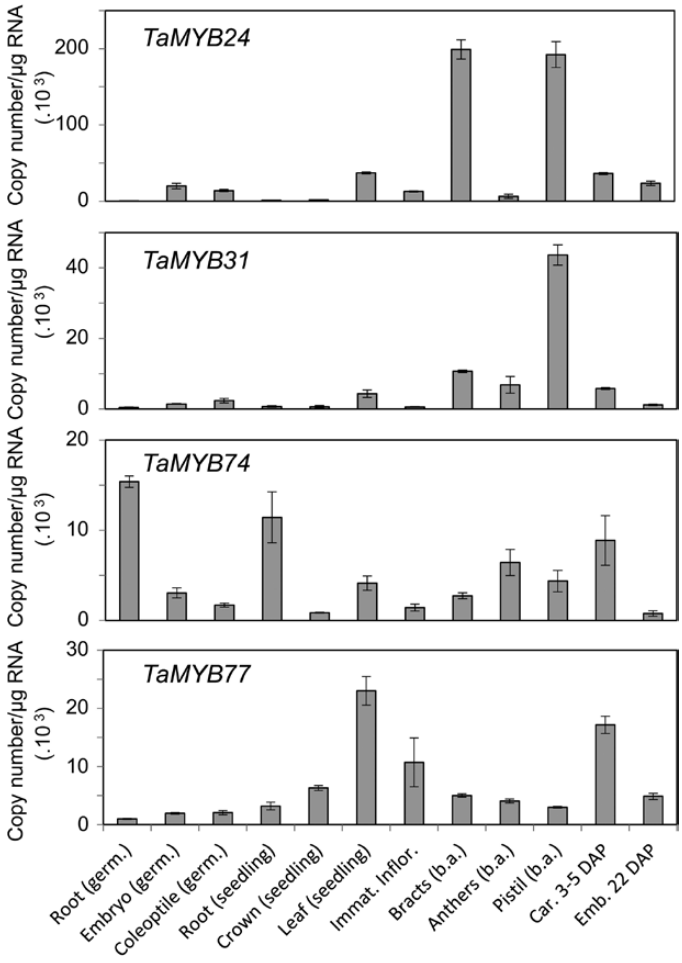

Fig. 6. Expression profiles of *TaMYB24*, *TaMYB31*, *TaMYB74*, and *TaMYB77* in wheat tissues revealed by Q-PCR. germ., germinating seed; Emb., embryo; Immat. Inflor., immature inflorescence; b.a., before anthesis; Car., caryopsis; DAP, days after pollination. Error bars indicate the SE of three replicates.

TaMYB74 also binds to MYBR2. MYBR2 is similar to MYBR1 and contains complementary nucleotides to the core sequence of MYBR1. To analyse which side of the DNA element is bound to the protein, its conformational stability was calculated using Fold-X force-field (Schymkowitz *et al.*, 2005). The free energies (ΔG) of TaMYB74 with 'TGGTTA' and 'TAACCA' were 67.5 kcal mol^{-1} and 74.2 kcal mol^{-1}, respectively, meaning that TaMYB74 is more stable when forming a complex at the 'TGGTTA' site. We predicted why TaMYB74 binds less strongly to MYBR2 than to MYBR1. The differences of DNA sequences in both *cis*-elements affect DNA conformation and orientation. In Supplementary Table S2 we show that nine residues are involved in forming hydrogen bonds to the core sequence of the MYBR1 sense strand. Although MYBR2 also contains the core sequence, the neighbouring nucleotides may affect the conformation of core nucleo bases T_4, T_7, and T_8, and result in a loss of binding to Asn109, Lys14, and Lys51.

The crystal structure of TvMYB2 in complex with MRE-1–12 indicates that the protein interacts with MRE-1–20 DNA via Lys49 (contact with T_3' and T_5), Arg84 (contact with G_5'), Lys138 (contact with G_3), and Asn139 (contact with A_2'), which are responsible for sequence-specific recognition (Jiang *et al.*, 2011). TvMYB2 also interacts with a DNA phosphate backbone via Lys48, Lys49, Gln50, Phe52, Gln85, Arg87, Arg89, Tyr93, Arg120, Trp122, Ala123, and Asn146. Notably, binding affinity is reduced with single residue substitutions at Lys51, Phe52, and Arg87 with alanine. The Arg84Ala change is particularly effective, whereby it completely removes binding to MRE-1–20 (Jiang *et al.*, 2011).

Based on the TvMYB2 crystal structure, we predicted critical residues in TaMYB74 by calculating energy gains (kcal mol^{-1}) upon mutation of specific DNA-binding residues to alanine, using Fold-X force-field (Schymkowitz *et al.*, 2005) (Fig. 9D). The binding affinity of TaMYB74 for the DNA *cis*-element may not change for Asn106Ala, and substitutions of Lys51Ala and Lys105Ala that correspond to Arg84 and Lys139 in TvMYB2, respectively, which are predicted to have little destabilizing effect (Fig. 9D). The most destabilizing substitutions in TaMYB74 are those of Lys14Ala and Trp17Ala, which correspond to Lys49 and Phe52 in TvMYB2, respectively. As for energy contributions, it has been estimated that a loss of 1 kcal mol^{-1} corresponds to approximately one hydrogen bond (Fersht, 1987). There are 15 residues involved in DNA binding in TaMYB74 (Fig. 9B). Two of these, Ser90 and Arg115, are different in TaMYB24 and TaMYB31 (alanine and lysine, respectively; Fig. 9A). Based on calculated free energies, Ser90Ala may not affect protein–DNA interaction, while Arg115Lys is projected to destabilize it slightly (Fig. 9D).

Discussion

It has been established that the primary functions of cuticle and, particularly, of the cuticular waxes is in the protection against excessive solar irradiation and conservation of internal plant water (Yeats and Rose, 2013). Accumulation of epicuticular waxes on plant surfaces often results in a bluish-white coloration termed glaucousness. As a crop trait, glaucousness increases light reflectance and reduces leaf temperature and transpiration, thereby enhancing leaf survival under water deficit and improving water use efficiency (WUE) (Richards *et al.*, 1986; Febrero *et al.*, 1998).

The genetic analysis of variation in flag leaf glaucousness in Australian wheat cultivars has revealed numerous loci influencing this trait (Bennett *et al.*, 2012*a*), indicating complex genetic and metabolic control. However, the extent of deployment of this control within locally adapted germplasm is unknown.

In this work, data on contrasting Australian wheat cultivars, RAC875 (glaucous, drought tolerant) and Kukri (non-glaucous, drought sensitive), previously characterized in terms of stress physiology, genetics, and metabolomics (Izanloo *et al.*, 2008; Bennett *et al.*, 2012*a*, *b*; Bowne *et al.*, 2012), were used with the aim to: (i) uncover the biochemical background of differences in glaucousness; (ii) identify genes coding for MYB TFs that potentially may be involved in the regulation of cuticular wax biosynthesis pathways under drought; (iii) functionally characterize selected MYB

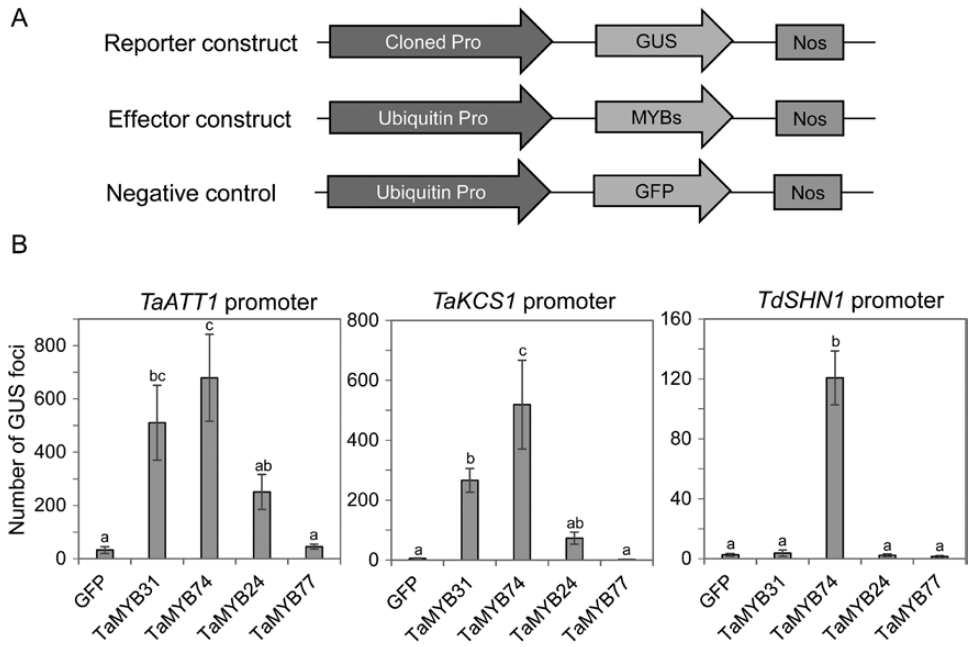

Fig. 7. Activation of promoters of cuticle-related genes *TaATT1*, *TaKCS1*, and *TdSHN1* by drought-responsive MYB TFs. The data were obtained by a transient expression assay in a wheat suspension culture. (A) Schematic showing DNA constructs used in the transient expression assay. The reporter *GUS* gene was driven by one of three promoters of cuticle biosynthesis genes, *TaATT1*, *TaKCS1*, and *TdSHN1*. In effector constructs, wheat *MYB* genes were cloned under the control of the ubiquitin promoter. *GFP* served as a negative control. (B) Activation of *GUS* expression fused with promoters of *TaATT1*, *TaKCS1*, and *TdSHN1* by drought-responsive MYB factors. Each reporter construct was co-bombarded with each effector and *GFP* construct into a wheat suspension culture. One-way ANOVA with the Fisher's least significant difference post-hoc test was conducted using GenStat. Error bars indicate the SE of three replicates.

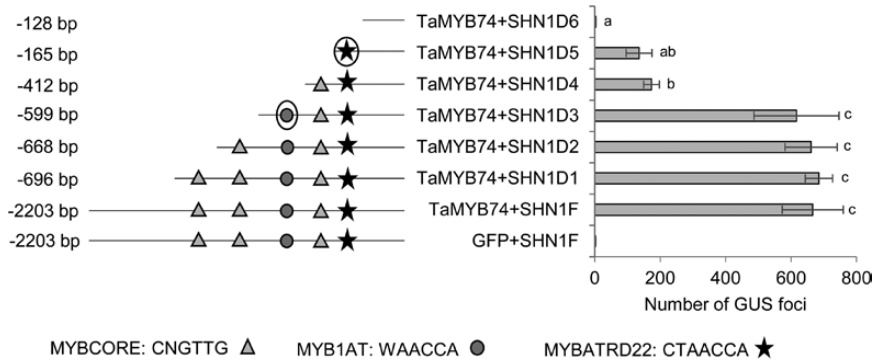

Fig. 8. Identification of functional MYBR *cis*-elements in the *TdSHN1* promoter using a transient expression assay. The full-length *TdSHN1* promoter (F) and six 5'-deletions (D1–D6) were cloned upstream of the *GUS* reporter gene, and co-transformed by biolistic bombardment with either a negative control (pUbi–GFP) or pUbi–TaMYB74 constructs. Promoter deletions and existing MYBR *cis*-elements (MYBCORE, MYB1AT, and MYBATRD22) within 696 bp upstream of the start codon are shown in the left panel. GUS expression quantifications are shown in the right side of the figure. One-way ANOVA with the Fisher's least significant difference post-hoc test was conducted using GenStat. Error bars indicate the SE of three replicates. Functional *cis*-elements are circled.

TFs in their ability to activate promoters of genes involved in cuticle biosynthesis; (iv) develop a 3D molecular model of TF–DNA binding interactions, and (v) establish the link between the activity of characterized MYB TFs and cuticular wax composition.

As a first step, it was demonstrated that the difference in leaf glaucousness of RAC875 and Kukri (leaf waxiness indices are 4 and 5 for RAC875, and 1 and 1.5 for Kukri, grown under well-watered conditions or mild drought conditions, respectively) (Izanloo *et al.*, 2008) is probably caused by the presence of significant amounts of β-diketones in the wax of RAC875 (Fig. 1). A number of studies suggested that β-diketones might be responsible for the glaucous appearance of wheat and barley (Adamski *et al.*, 2013; Zhang *et al.*, 2013), and our study strongly supports this assumption. Moreover, the recently identified gene clusters responsible for accumulation of β-diketones in barley (Schneider *et al.*, 2016) and wheat (Hen-Avivi *et al.*, 2016) were localized in the *W1* locus on chromosome 2BS, which was previously shown to be the determinant for glaucousness. Using a double-haploid population of RAC875 and Kukri, Bennett *et al.* (2012*a*) identified the *QW.aww-2B-1* quantitative trait locus, at a position similar to that of *W1* on chromosome 2B, that affected glaucousness. Combined together, these

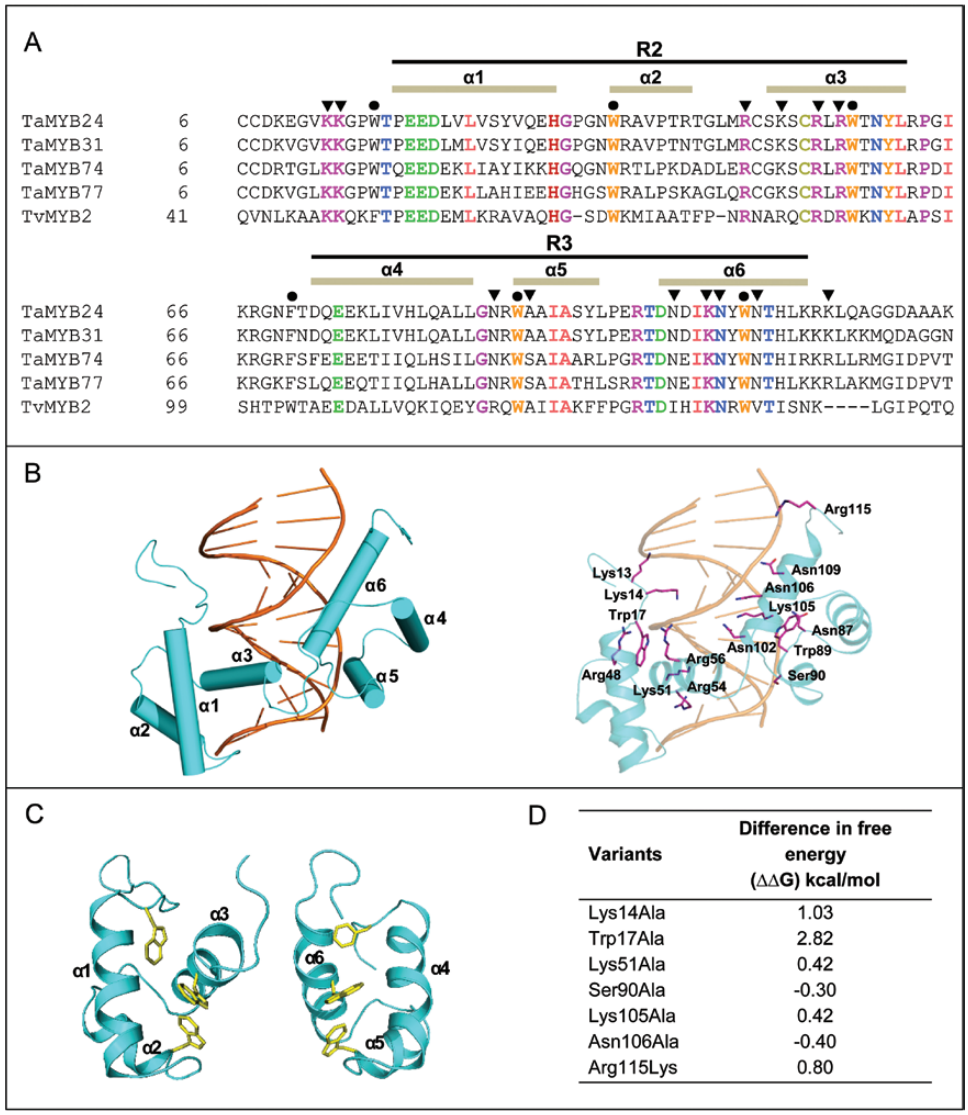

Variants	Difference in free energy (ΔΔG) kcal/mol
Lys14Ala	1.03
Trp17Ala	2.82
Lys51Ala	0.42
Ser90Ala	-0.30
Lys105Ala	0.42
Asn106Ala	-0.40
Arg115Lys	0.80

Fig. 9. Protein sequence analyses and a molecular model of TaMYB74 in complex with the MYBR1 *cis*-element. (A) The protein alignments of the DNA-binding domains of wheat MYB and protozoan TvMYB2 proteins; the latter was used as a template for molecular modelling. Tandem imperfect amino acid repeats R2 and R3 are indicated by lines above the sequences. The conserved residues that form a hydrophobic core and the residues that interact with the DNA *cis*-element are denoted by filled circles and filled inverted triangles, respectively. (B) A cartoon of the TaMYB74 model (cyan) in complex with MYBR1 (orange) (left panel). Predicted residues interacting with DNA (distances between 2.8 Å and 3.6 Å) are shown in magenta sticks (right panel). (C) The orientations and positions of conserved tryptophan and phenylalanine residues, which form a hydrophobic core of TaMYB74. (D) Energy gains (kcal mol^{-1}) upon mutation (into alanine or lysine) of Lys14, Trp17, Lys51, Ser90, Lys105, Asn106, and Arg115, involved in MYBR1 DNA binding, as determined by Fold-X (Schymkowitz *et al.*, 2005).

data open up a new opportunity for further detailed genetic analysis of glaucousness and biosynthesis of β-diketones in Australian wheats.

During growth under limited watering (mild drought), the amounts of waxes increased in both RAC875 and Kukri without changes in the shapes of wax crystals (Fig. 1). While β-diketone content did not increase in response to drought in either RAC875 or Kukri, both cultivars under drought accumulated elevated amounts of primary alcohols and alkanes; this observation correlates well with findings of other plant species in response to a limited water supply (Bernard and Joubès, 2013; Yeats and Rose, 2013). The accumulation of very long chain alcohols (C-28) and alkanes (C-29, C-31) suggested the activation of enzymes involved in fatty acid elongation (FAE) pathways (von Wettstein-Knowles, 2012).

As a second step, we characterized six wheat *MYB* genes, which were cloned from RAC875 based on sequence homology of their products to known cuticle biosynthesis-related MYB TFs from Arabidopsis. To our knowledge, no homologues of these five Arabidopsis MYB TFs from cereals have been yet characterized, with the exception of ZmMYB94 from maize (La Rocca *et al.*, 2015). Expression of the cloned genes was analysed in RAC875 and Kukri under two types of dehydration stresses, as described below. The impact of regulatory genes such as TF genes during stress is often rapid and transient: after some time, the levels of transcripts return to initial levels, even if the stress

factor is persisting. Consequently, if stress develops slowly, as usually occurs in the case of drought in the field, changes in expression of TF genes with a short transient response are often difficult to measure. For these reasons,we used two regimes of dehydration: (i) rapid dehydration of detached leaves at ambient temperature; and (ii) slowly developing (within several days or weeks) and repeatable (cyclic) drought of plants growing in soil (Supplementary Fig. S1). The aim of the first experiment was to detect rapid and transient changes in expression of *MYB* genes. The aim of the second experiment was to compare differences in basal levels of gene expression, and to detect long-lasting and late changes in expression levels under the conditions of two successive cycles of drought.

We found that two TF genes, *TaMYB31* and *TaMYB74*, were up-regulated and two other genes, *TaMYB24* and *TaMYB77*, were down-regulated by both rapid dehydration and slowly developing drought. The remaining two genes, *TaMYB16* and *TaMYB78*, showed no expression in leaves either under well-watered conditions or under drought, and therefore we did not study these further. In all cases, cultivar-specific differences in gene expression were found under rapid dehydration. For example, both *TaMYB31* and *TaMYB74* reached the highest expression levels earlier during dehydration in Kukri than in RAC875, possibly reflecting the sensitivity of these TFs to a common threshold level of dehydration. Detached leaves of Kukri reached the threshold dehydration state earlier than leaves of RAC875. Up-regulation of *TaMYB31* in drought-tolerant RAC875 was stronger than in Kukri, suggesting that higher levels of expression of *TaMYB31* might be one of the reasons for the higher drought tolerance of RAC875. In contrast, a difference in maximal induction levels between the two wheat cultivars was not observed for the *TaMYB74* gene, suggesting a universal requirement for its product under dehydration. The transcript numbers of *TaMYB24* slightly decreased in RAC875 and then rapidly returned to initial levels. This was different from the behaviour of this gene in Kukri, perhaps suggesting that the dehydration response of *TaMYB24* expression is critical for drought tolerance.

The comparison of *TaMYB31* and *TaMYB74* expression levels in plants growing under slowly developing drought revealed significant differences in the time of gene induction during progression of stress, and hence possible dissimilarities in functions of these two genes. *TaMYB31* is an early stress-responsive gene with transient expression, which starts to normalize when a plant is still under strong stress. In contrast, the expression levels of *TaMYB74* were only moderately influenced by mild stress, but were strongly elevated when dehydration became critical (at wilting). In addition, *TaMYB74* did not react on the second cycle of drought in RAC875, which might indicate that the product of this gene is more stable in the drought-tolerant cultivar. These differences between *TaMYB31* and *TaMYB74* expression were less obvious in the rapid leaf dehydration experiment. Up-regulation of *TaMYB74* and *TaMYB31* by both rapid dehydration and cyclic drought were in accordance with the data obtained for their Arabidopsis counterparts, *AtMYB41* and *AtMYB96*. Both Arabidopsis TFs have been reported to be up-regulated by environmental stresses and play multiple roles in response to drought and osmotic stress (Lippold *et al.*, 2009; Seo *et al.*, 2009; Seo and Park, 2010). Besides regulating the amount and quality of cuticle, these TFs might confer drought tolerance through different pathways, such as through the regulation of stomatal development (Yang *et al.*, 2011).

The analysis of gene expression levels in different wheat tissues revealed similarities in the expression patterns of *TaMYB24* and *TaMYB31* (Fig. 6). The only notable difference was observed in the levels of expression in bracts. A similar tissue distribution of *TaMYB24* and *TaMYB31* may reflect their high level of homology (49.5% sequence identity at the protein level); both proteins represent wheat counterparts of MYB96 from Arabidopsis. However, changes in the expression levels of these two genes occurred in opposite directions under stress. Possible explanations for such a different reaction to stress are: (i) these genes have different tissue- or cell layer-specific patterns of expression, which cannot be detected by Q-PCR, and thus would provide different patterns of tissue- or cell layer-specific regulation of the same target genes under stress; or (ii) small variations in protein sequences of DNA-binding domains of *TaMYB24* and *TaMYB31* exist, which are sufficient to provide different DNA binding specificity and hence activation of different groups of target genes.

In the absence of stress, *TaMYB74* was mostly expressed in roots. This finding correlates with recent data about the involvement of its Arabidopsis counterpart, *MYB41*, in the synthesis and deposition of suberin, a polymer which is similar to cutin and is localized mostly in root endodermis and peridermis, and in the seed coat of Arabidopsis (Vishwanath *et al.*, 2013; Kosma *et al.*, 2014). The relatively high levels of *TaMYB74* expression in other tissues, including leaves, as well as strong induction of this gene by drought may suggest its involvement in the regulation of a number of other biochemical and physiological processes in wheat. Similarly to earlier reports for Arabidopsis *MYB16* (Oshima and Mitsuda, 2013), the highest level of expression of *TaMYB77* was found in vegetative tissues. However, expression of this gene in immature inflorescence and developing grain was also elevated compared with other tissues, suggesting the possible involvement of these genes in wheat organ development.

A transient expression assay in wheat suspension cells was used to confirm the participation of drought-affected wheat MYB TFs in transcriptional activation of cuticle-related genes (Fig. 7). For this purpose, the wheat homologues of the Arabidopsis *ATT1* gene, encoding an enzyme from the cutin biosynthetic pathway, the *KCS1* gene, encoding an enzyme from the wax biosynthetic pathway, and *WIN1/SHN1*, encoding the regulator of wax biosynthesis (Yeats and Rose, 2013; Borisjuk *et al.*, 2014), were identified, and promoters of wheat genes were designated as *TaATT1*, *TaKCS1*, and *TdSHN1*, respectively. These were selected for the assay because it was earlier reported that overexpression of *MYB41* in Arabidopsis activated *ATT1* and *WIN1/SHN1* genes, while the *KCS1* gene was activated by overexpression of *MYB96* in both a transcription activation assay

and transgenic Arabidopsis, and overexpression of *MYB16* in transgenic Arabidopsis led to activation of *SHN1* and *KCS1* (Borisjuk *et al.*, 2014). In our assay, three of the four tested wheat TFs, TaMYB74, TaMYB31, and TaMYB24, activated either two or three cloned wheat promoters, and therefore can be considered as true cuticle biosynthesis-related genes in wheat. Surprisingly, these three wheat MYB TFs demonstrated less selectivity in target gene activation than their corresponding Arabidopsis homologues. Each of the wheat MYBs could activate both *TaATT1* and *TaKCS1* promoters, although with variable efficiency. On the other hand, no activation of the *TdSHN1* gene was seen with TaMYB77, although *SHN1* is reported to be the target gene of the Arabidopsis homologue AtMYB16. An absence of activation by TaMYB31 and TaMYB24 can be explained by the absence of the TAACTA/G type of MYBR *cis*-elements in the *TdSHN1* promoter, which are specifically recognized by Arabidopsis MYB96 and might also be specific for the wheat homologues (Seo *et al.*, 2011).

A transient expression assay has been used in this work in combination with molecular modelling for the identification of possible differences in the recognition of MYBR *cis*-element(s) in the *TdSHN1* promoter. Mapping of the promoter, using a series of promoter deletions, revealed two similar MYBR elements which were specifically recognized only by TaMYB74 (Fig. 8). The distal element, designated MYBR1, was responsible for ~70% of promoter activation by TaMYB74, while the proximal element (MYBR2) accounted for the remaining 30%.

The molecular model of TaMYB74 in complex with functional *cis*-elements from the *TdSHN1* promoter suggested that small, but central differences in nucleotides that are adjacent to the same core sequence TGGTTA, may explain differences in the apparent efficiency of promoter activation through MYBR1 and MYBR2 *cis*-elements. However, no significant differences were found between the DNA-binding domains of TaMYB74 and TaMYB24, TaMYB31 and TaMYB77, that would explain the selectivity of recognition of the *TdSHN1* promoter (Fig. 9). A mechanistic explanation for why the *TdSHN1* promoter was activated only by TaMYB74 remains to be determined.

Scheme 1 summarizes our findings on activation of cuticle biosynthetic pathways in wheat by the TFs TaMYB31 and TaMYB74, homologues of the well-characterized cuticle biosynthesis regulators AtMYB96 (Seo *et al.*, 2011) and AtMYB41 (Cominelli *et al.*, 2008). Expression of both wheat MYB TFs was up-regulated by drought (Fig. 5), and both TFs activated *ATT1* and *KCS1* genes through direct binding to their promoters (Fig. 7). Activation of the *TaKCS1* gene that encodes a key enzyme in the FAE pathway (Bernard and Joubès, 2013) may explain the increased accumulation of very long chain alkanes and primary alcohols in response to drought. In a cyclic drought experiment (Fig. 5), the expression levels of *TaMYB31* peaked much earlier (day 5) compared with those of TaMYB74 (day 14); these observations are consistent with its more specialized role in the regulation of a cutin biosynthesis, which under drought starts earlier than the biosynthesis of cuticular waxes (Bernard and Joubès, 2013).

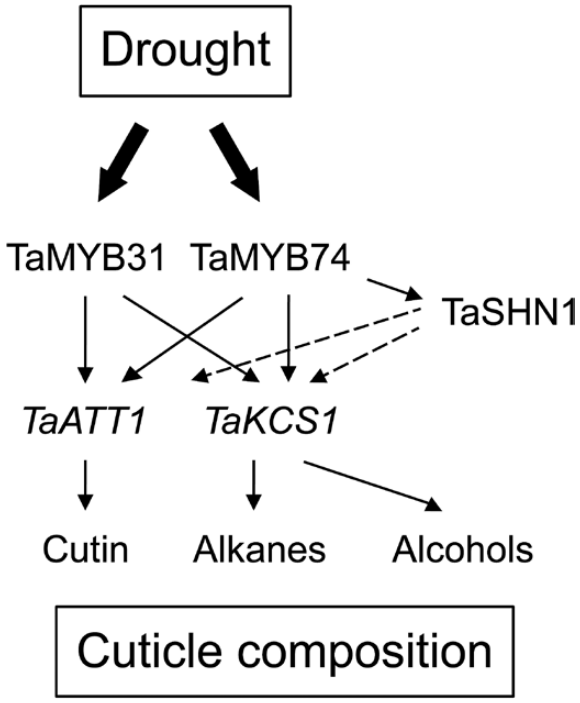

Scheme 1. The proposed roles of TaMYB31 and TaMYB74 in the regulation of cuticle biosynthesis under drought. The dashed lines reflect the roles of TaSHN1 in regulating TaATT1 and TaKCS1 genes, and consequently the biosynthesis of cuticular wax components, based on our own and other data.

The *TaMYB74* gene in turn possibly plays a more general role in cuticle biosynthesis, which is in agreement with specific activation by TaMYB74 of the *SHN1* gene, and hence with a position of this TF upstream of *TaSHN1* in the hierarchy of cuticle biosynthesis regulators.

In summary, we revealed that β-diketones are the main compositional determinants in the two elite Australian wheat cultivars RAC875 and Kukri, underlying the glaucous and non-glaucous phenotypes, respectively. The concentration of β-diketones remained unchanged during growth of both cultivars under limited watering, while the content of other wax components, alkanes and primary alcohols, increased. These findings suggest that a combination of β-diketones and stress-stimulated accumulation of other cuticle compounds may make RAC875 more resistant to a water loss under drought. We demonstrated drought-inducible expression of four isolated wheat *MYB* genes. Products of three genes (*TaMYB74, TaMYB31*, and *TaMYB24*) operated as the activators of cuticle biosynthetic genes in wheat cells. Moreover, two functional MYB-responsive elements localized in the promoter region of the *SHN1* gene were specifically recognized by TaMYB74, but not by other MYB TFs. We revealed the protein structural determinants underlying the binding specificity of two identified functional DNA *cis*-elements by TaMYB74, one of the investigated wheat TFs. We have integrated our data with other observations, and propose a scheme that links drought, the investigated TFs, downstream cuticle-related biosynthetic genes, and cuticle wax components. Our results extend the knowledge on cuticle biosynthesis regulation in grasses and can potentially be

used for engineering of cereal crops with enhanced tolerance and performance under drought.

Supplementary data

Supplementary data are available at *JXB* online.

Figure S1. Schematic diagram of the cyclic drought experiment (modified from Harris *et al.*, 2016).

Figure S2. Amounts of wax components in RAC875 (RAC) and Kukri (KUK) grown under well-watered (WW) and mild drought (DR) conditions.

Figure S3. A schematic representation showing the gene structure of the six wheat MYB TFs investigated in this study.

Table S1. List of primers used in this study.

Table S2. Amino acid residues of TaMYB74 forming hydrogen bonds with 12 bp DNA *cis*-elements of MYBR1 (5'-AGGTGGTTATGC-3'/5'-GCATAACCACCT-3') and MYBR2 (5'-ATCTAACCACAT-3'/5'-ATGTGGTTAGAT-3'). The core binding sequence in *cis*-elements is underlined.

Acknowledgements

We thank Nannan Yang, Nataliya Kovalchuk, and Ursula Langridge for assistance. We are grateful to Dr Julie Hayes for critically reading the manuscript. HB is grateful to the China Scholarship Council for providing a postgraduate scholarship. This work was supported by the Australian Centre for Plant Functional Genomics, and by the Australian Research Council (to MH and SL), the Grains Research & Development Corporation, and the Government of South Australia.

References

Adamski NM, Bush MS, Simmonds J, Turner AS, Mugford SG, Jones A, Findlay K, Pedentchouk N, Wettstein-Knowles P, Uauy C. 2013. The *Inhibitor of wax 1 locus* (*Iw1*) prevents formation of β- and OH-β-diketones in wheat cuticular waxes and maps to a sub-cM interval on chromosome arm 2BS. The Plant Journal **74,** 989–1002.

Adato A, Mandel T, Mintz-Oron S, *et al*. 2009. Fruit-surface flavonoid accumulation in tomato is controlled by a SlMYB12-regulated transcriptional network. PLoS Genetics **5,** e1000777.

Aharoni A, Dixit S, Jetter R, Thoenes E, van Arkel G, Pereira A. 2004. The SHINE clade of AP2 domain transcription factors activates wax biosynthesis, alters cuticle properties, and confers drought tolerance when overexpressed in *Arabidopsis*. The Plant Cell **16,** 2463–2480.

Amalraj A, Luang S, Kumar MY, *et al*. 2016. Change of function of the wheat stress-responsive transcriptional repressor TaRAP2.1L by repressor motif modification. Plant Biotechnology Journal **14,** 820–832.

Ambawat S, Sharma P, Yadav NR, Yadav RC. 2013. MYB transcription factor genes as regulators for plant responses: an overview. Physiology and Molecular Biology of Plants **19,** 307–321.

Baldoni E, Genga A, Cominelli E. 2015. Plant MYB transcription factors: their role in drought response mechanisms. International Journal of Molecular Sciences **16,** 15811–15851.

Beisson F, Koo AJ, Ruuska S, Schwender J, Pollard M, Thelen JJ, Paddock T, Salas JJ, Savage L, Milcamps A. 2003. *Arabidopsis* genes involved in acyl lipid metabolism. A 2003 census of the candidates, a study of the distribution of expressed sequence tags in organs, and a web-based database. Plant Physiology **132,** 681–697.

Beisson F, Li-Beisson Y, Pollard M. 2012. Solving the puzzles of cutin and suberin polymer biosynthesis. Current Opinion in Plant Biology **15,** 329–337.

Bennett D, Izanloo A, Edwards J, Kuchel H, Chalmers K, Tester M, Reynolds M, Schnurbusch T, Langridge P. 2012*a*. Identification of novel quantitative trait loci for days to ear emergence and flag leaf glaucousness in a bread wheat (*Triticum aestivum* L.) population adapted to southern Australian conditions. Theoretical and Applied Genetics **124,** 697–711.

Bennett D, Izanloo A, Reynolds M, Kuchel H, Langridge P, Schnurbusch T. 2012*b*. Genetic dissection of grain yield and physical grain quality in bread wheat (*Triticum aestivum* L.) under water-limited environments. Theoretical and Applied Genetics **125,** 255–271.

Bernard A, Joubès J. 2013. *Arabidopsis* cuticular waxes: advances in synthesis, export and regulation. Progress in Lipid Research **52,** 110–129.

Borisjuk N, Hrmova M, Lopato S. 2014. Transcriptional regulation of cuticle biosynthesis. Biotechnology Advances **32,** 526–540.

Bowne JB, Erwin TA, Juttner J, Schnurbusch T, Langridge P, Bacic A, Roessner U. 2012. Drought responses of leaf tissues from wheat cultivars of differing drought tolerance at the metabolite level. Molecular Plant **5,** 418–429.

Cenci A, Chantret N, Kong X, Gu Y, Anderson OD, Fahima T, Distelfeld A, Dubcovsky J. 2003. Construction and characterization of a half million clone BAC library of durum wheat (*Triticum turgidum* ssp. durum). Theoretical and Applied Genetics **107,** 931–939.

Cha S, Song Z, Nikolau BJ, Yeung ES. 2009. Direct profiling and imaging of epicuticular waxes on *Arabidopsis thaliana* by laser desorption/ionization mass spectrometry using silver colloid as a matrix. Analytical Chemistry **81,** 2991–3000.

Christensen AH, Sharrock RA, Quail PH. 1992. Maize polyubiquitin genes: structure, thermal perturbation of expression and transcript splicing, and promoter activity following transfer to protoplasts by electroporation. Plant Molecular Biology **18,** 675–689.

Cominelli E, Sala T, Calvi D, Gusmaroli G, Tonelli C. 2008. Over-expression of the *Arabidopsis AtMYB41* gene alters cell expansion and leaf surface permeability. The Plant Journal **53,** 53–64.

Curtis MD, Grossniklaus U. 2003. A gateway cloning vector set for high-throughput functional analysis of genes in planta. Plant Physiology ***133***, 462–469.

Eini O, Yang N, Pyvovarenko T, *et al*. 2013. Complex regulation by APETALA2 domain-containing transcription factors revealed through analysis of the stress-responsive *TdCor410b* promoter from durum wheat. PLoS One **8,** e58713.

Emsley P, Lohkamp B, Scott WG, Cowtan K. 2010. Features and development of Coot. Acta Crystallographica Section D: Biological Crystallography **66,** 486–501.

Eswar N, Eramian D, Webb B, Shen MY, Sali A. 2008. Protein structure modeling with MODELLER. Methods in Molecular Biology **426,** 145–159.

Evans L, Wardlaw I, Fischer R. 1975. Wheat. In: Evans L, ed. Crop physiology: some case histories. Cambridge: Cambridge University Press, 101–150.

Febrero A, Fernández S, Molina-Cano JL, Araus JL. 1998. Yield, carbon isotope discrimination, canopy reflectance and cuticular conductance of barley isolines of differing glaucousness. Journal of Experimental Botany **49,** 1575–1581.

Fersht AR. 1987. The hydrogen bond in molecular recognition. Trends in Biochemical Sciences **12,** 301–304.

Fletcher SJ. 2014. qPCR for quantification of transgene expression and determination of transgene copy number. Methods in Molecular Biology **1145,** 213–237.

Folkers U, Berger J, Hulskamp M. 1997. Cell morphogenesis of trichomes in *Arabidopsis*: differential control of primary and secondary branching by branch initiation regulators and cell growth. Development **124,** 3779–3786.

Gilding EK, Marks MD. 2010. Analysis of purified glabra3-shapeshifter trichomes reveals a role for NOECK in regulating early trichome morphogenic events. The Plant Journal **64,** 304–317.

González A, Ayerbe L. 2010. Effect of terminal water stress on leaf epicuticular wax load, residual transpiration and grain yield in barley. Euphytica **172,** 341–349.

Guo L, Yang H, Zhang X, Yang S. 2013. Lipid transfer protein 3 as a target of MYB96 mediates freezing and drought stress in *Arabidopsis*. Journal of Experimental Botany **64,** 1755–1767.

Harris JC, Sornaraj P, Taylor M, Bazanova N, Baumann U, Lovell B, Langridge P, Lopato S, Hrmova M. 2016. Molecular interactions of the γ-clade homeodomain-leucine zipper class I transcription factors during the wheat response to water deficit. Plant Molecular Biology **90,** 435–452.

Hen-Avivi S, Savin O, Racovita R, *et al*. 2016. A metabolic gene cluster in the wheat *W1* and the barley *Cer-cqu* loci determines beta-diketone biosynthesis and glaucousness. The Plant Cell **28,** 1440–1460.

Higo K, Ugawa Y, Iwamoto M, Korenaga T. 1999. Plant cis-acting regulatory DNA elements (PLACE) database: 1999. Nucleic Acids Research **27,** 297–300.

Hiratsu K, Matsui K, Koyama T, Ohme-Takagi M. 2003. Dominant repression of target genes by chimeric repressors that include the EAR motif, a repression domain, in Arabidopsis. The Plant Journal **34,** 733–739.

Hrmova M, Lopato S. 2014. Enhancing abiotic stress tolerance in plants by modulating properties of stress responsive transcription factors. In: Tuberosa R, Graner A, Frison E, eds. Genomics of plant genetic resources. Dordrecht, The Netherlands: Springer, 291–316.

Izanloo A, Condon AG, Langridge P, Tester M, Schnurbusch T. 2008. Different mechanisms of adaptation to cyclic water stress in two South Australian bread wheat cultivars. Journal of Experimental Botany **59,** 3327–3346.

Jakoby MJ, Falkenhan D, Mader MT, Brininstool G, Wischnitzki E, Platz N, Hudson A, Hülskamp M, Larkin J, Schnittger A. 2008. Transcriptional profiling of mature Arabidopsis trichomes reveals that NOECK encodes the MIXTA-like transcriptional regulator MYB106. Plant Physiology **148,** 1583–1602.

Javelle M, Vernoud V, Depege-Fargeix N, Arnould C, Oursel D, Domergue F, Sarda X, Rogowsky PM. 2010. Overexpression of the epidermis-specific homeodomain-leucine zipper IV transcription factor Outer Cell Layer1 in maize identifies target genes involved in lipid metabolism and cuticle biosynthesis. Plant Physiology **154,** 273–286.

Jetter R, Kunst L. 2008. Plant surface lipid biosynthetic pathways and their utility for metabolic engineering of waxes and hydrocarbon biofuels. The Plant Journal **54,** 670–683.

Jetter R, Kunst L, Samuels AL. 2007. Composition of plant cuticular waxes. In: Riederer M, Muller C, eds. Annual Plant Reviews Volume 23: Biology of the Plant Cuticle. Oxford: Blackwell Publishing Ltd, 145–181.

Jiang I, Tsai CK, Chen SC, Wang SH, Amiraslanov I, Chang CF, Wu WJ, Tai JH, Liaw YC, Huang TH. 2011. Molecular basis of the recognition of the *ap65-1* gene transcription promoter elements by a Myb protein from the protozoan parasite *Trichomonas vaginalis*. Nucleic Acids Research **39,** 8992–9008.

Johnson PF, Sterneck E, Williams SC. 1993. Activation domains of transcriptional regulatory proteins. Journal of Nutritional Biochemistry **4,** 386–398.

Kosma DK, Murmu J, Razeq FM, Santos P, Bourgault R, Molina I, Rowland O. 2014. AtMYB41 activates ectopic suberin synthesis and assembly in multiple plant species and cell types. The Plant Journal **80,** 216–229.

Krieger E, Joo K, Lee J, Lee J, Raman S, Thompson J, Tyka M, Baker D, Karplus K. 2009. Improving physical realism, stereochemistry, and side-chain accuracy in homology modeling: four approaches that performed well in CASP8. Proteins: Structure, Function, and Bioinformatics **77,** 114–122.

La Rocca N, Manzotti PS, Cavaiuolo M, *et al*. 2015. The maize *fused leaves1* (*fdl1*) gene controls organ separation in the embryo and seedling shoot and promotes coleoptile opening. Journal of Experimental Botany **66,** 5753–5767.

Laskowski RA, MacArthur MW, Moss DS, Thornton JM. 1993. PROCHECK: a program to check the stereochemical quality of protein structures. Journal of Applied Crystallography **26,** 283–291.

Lee SB, Kim H, Kim RJ, Suh MC. 2014. Overexpression of *Arabidopsis MYB96* confers drought resistance in *Camelina sativa* via cuticular wax accumulation. Plant Cell Reports **33,** 1535–1546.

Lee SB, Suh MC. 2015*a*. Advances in the understanding of cuticular waxes in *Arabidopsis thaliana* and crop species. Plant Cell Reports **34,** 557–572.

Lee SB, Suh MC. 2015*b*. Cuticular wax biosynthesis is up-regulated by the MYB94 transcription factor in Arabidopsis. Plant and Cell Physiology **56,** 48–60.

Letunic I, Doerks T, Bork P. 2015. SMART: recent updates, new developments and status in 2015. Nucleic Acids Research **43,** D257–D260.

Li-Beisson Y, Shorrosh B, Beisson F, *et al*. 2013. Acyl-lipid metabolism. The Arabidopsis Book 8, e0133.

Lippold F, Sanchez DH, Musialak M, Schlereth A, Scheible WR, Hincha DK, Udvardi MK. 2009. AtMyb41 regulates transcriptional and metabolic responses to osmotic stress in Arabidopsis. Plant Physiology **149,** 1761–1772.

Lobell DB, Gourdji SM. 2012. The influence of climate change on global crop productivity. Plant Physiology **160,** 1686–1697.

Morran S, Eini O, Pyvovarenko T, Parent B, Singh R, Ismagul A, Eliby S, Shirley N, Langridge P, Lopato S. 2011. Improvement of stress tolerance of wheat and barley by modulation of expression of DREB/CBF factors. Plant Biotechnology Journal **9,** 230–249.

Nei M, Kumar S. 2000. Molecular evolution and phylogenetics. Oxford: Oxford University Press.

Oda M, Furukawa K, Ogata K, Sarai A, Ishii S, Nishimura Y, Nakamura H. 1997. Identification of indispensable residues for specific DNA-binding in the imperfect tandem repeats of c-Myb R2R3. Protein Engineering **10,** 1407–1414.

Oshima Y, Mitsuda N. 2013. The MIXTA-like transcription factor MYB16 is a major regulator of cuticle formation in vegetative organs. Plant Signaling and Behavior **8,** e26826.

Oshima Y, Shikata M, Koyama T, Ohtsubo N, Mitsuda N, Ohme-Takagi M. 2013. MIXTA-like transcription factors and WAX INDUCER1/SHINE1 coordinately regulate cuticle development in *Arabidopsis* and *Torenia fournieri*. The Plant Cell **25,** 1609–1624.

Porter JR, Semenov MA. 2005. Crop responses to climatic variation. Philosophical Transactions of the Royal Society B: Biological Sciences **360,** 2021–2035.

Pyvovarenko T, Lopato S. 2011. Isolation of plant transcription factors using a yeast one-hybrid system. In: Yuan L, Perry SE, eds. Plant transcription factors: methods and protocols. New York: Humana Press, 45–66.

Raffaele S, Vailleau F, Leger A, Joubès J, Miersch O, Huard C, Blee E, Mongrand S, Domergue F, Roby D. 2008. A MYB transcription factor regulates very-long-chain fatty acid biosynthesis for activation of the hypersensitive cell death response in *Arabidopsis*. The Plant Cell **20,** 752–767.

Reynolds M, Foulkes J, Furbank R, Griffiths S, King J, Murchie E, Parry M, Slafer G. 2012. Achieving yield gains in wheat. Plant, Cell and Environment **35,** 1799–1823.

Richards R, Rawson H, Johnson D. 1986. Glaucousness in wheat: its development and effect on water-use efficiency, gas exchange and photosynthetic tissue temperatures. Functional Plant Biology **13,** 465–473.

Saitou N, Nei M. 1987. The neighbor–joining method: a new method for reconstructing phylogenetic trees. Molecular Biology and Evolution **4,** 406–425.

Schneider LM, Adamski NM, Christensen CE, Stuart DB, Vautrin S, Hansson M, Uauy C, von Wettstein-Knowles P. 2016. The *Cer–cqu* gene cluster determines three key players in a β-diketone synthase polyketide pathway synthesizing aliphatics in epicuticular waxes. Journal of Experimental Botany **67,** 2715–2730.

Schymkowitz JWH, Rousseau F, Martins IC, Ferkinghoff-Borg J, Stricher F, Serrano L. 2005. Prediction of water and metal binding sites and their affinities by using the Fold-X force field. Proceedings of the National Academy of Sciences, USA **102,** 10147–10152.

Seo PJ, Lee SB, Suh MC, Park MJ, Go YS, Park CM. 2011. The MYB96 transcription factor regulates cuticular wax biosynthesis under drought conditions in *Arabidopsis*. The Plant Cell **23,** 1138–1152.

Seo PJ, Park CM. 2010. MYB96-mediated abscisic acid signals induce pathogen resistance response by promoting salicylic acid biosynthesis in *Arabidopsis*. New Phytologist **186,** 471–483.

Seo PJ, Park CM. 2011. Cuticular wax biosynthesis as a way of inducing drought resistance. Plant Signaling and Behavior **6,** 1043–1045.

Seo PJ, Xiang F, Qiao M, Park J-Y, Lee YN, Kim S-G, Lee Y-H, Park WJ, Park C-M. 2009. The MYB96 transcription factor mediates abscisic acid signaling during drought stress response in *Arabidopsis*. Plant Physiology **151,** 275–289.

Sippl MJ. 1993. Recognition of errors in three-dimensional structures of proteins. Proteins: Structure, Function, and Bioinformatics **17,** 355–362.

Stracke R, Werber M, Weisshaar B. 2001. The *R2R3-MYB* gene family in *Arabidopsis thaliana*. Current Opinion in Plant Biology **4,** 447–456.

Tamura K, Stecher G, Peterson D, Filipski A, Kumar S. 2013. MEGA6: molecular evolutionary genetics analysis version 6.0. Molecular Biology and Evolution **30,** 2725–2729.

Vishwanath SJ, Kosma DK, Pulsifer IP, Scandola S, Pascal S, Joubès J, Dittrich-Domergue F, Lessire R, Rowland O, Domergue F. 2013. Suberin-associated fatty alcohols in *Arabidopsis*: distributions in roots and contributions to seed coat barrier properties. Plant Physiology **163,** 1118–1132.

von Wettstein-Knowles P. 2012. Plant waxes. *eLS*. Chichester: John Wiley & Sons Ltd.

Wicker T, Schlagenhauf E, Graner A, Close TJ, Keller B, Stein N. 2006. 454 sequencing put to the test using the complex genome of barley. BMC Genomics **7,** 275.

Yang J, Isabel Ordiz M, Jaworski JG, Beachy RN. 2011. Induced accumulation of cuticular waxes enhances drought tolerance in *Arabidopsis* by changes in development of stomata. Plant Physiology and Biochemistry **49,** 1448–1455.

Yeats TH, Rose JK. 2013. The formation and function of plant cuticles. Plant Physiology **163,** 5–20.

Zhang JY, Broeckling CD, Blancaflor EB, Sledge MK, Sumner LW, Wang ZY. 2005. Overexpression of *WXP1*, a putative Medicago truncatula AP2 domain-containing transcription factor gene, increases cuticular wax accumulation and enhances drought tolerance in transgenic alfalfa (*Medicago sativa*). The Plant Journal **42,** 689–707.

Zhang JY, Broeckling CD, Sumner LW, Wang ZY. 2007. Heterologous expression of two Medicago truncatula putative ERF transcription factor genes, *WXP1* and *WXP2*, in *Arabidopsis* led to increased leaf wax accumulation and improved drought tolerance, but differential response in freezing tolerance. Plant Molecular Biology **64,** 265–278.

Zhang L, Zhao G, Jia J, Liu X, Kong X. 2012. Molecular characterization of 60 isolated wheat *MYB* genes and analysis of their expression during abiotic stress. Journal of Experimental Botany **63,** 203–214.

Zhang Z, Wang W, Li W. 2013. Genetic interactions underlying the biosynthesis and inhibition of β-diketones in wheat and their impact on glaucousness and cuticle permeability. PLoS One **8,** e54129.

Identification and characterisation of wheat drought-responsive MYB transcription factors involved in the regulation of cuticle biosynthesis

Huihui Bi[1], Sukanya Luang[1], Yuan Li[1], Natalia Bazanova[1], Sarah Morran[1], Zhihong Song[2], M. Ann Perera[2], Maria Hrmova[1]*, Nikolai Borisjuk[1], Sergiy Lopato[1]

[1]*Australian Centre for Plant Functional Genomics, School of Agriculture, Food and Wine, University of Adelaide, Glen Osmond, South Australia 5064, Australia*
[2]*W.M.Keck Metabolomics Research Laboratory, Iowa State University, Ames, IA 50011, USA*

Supplementary Introduction

Protection against extreme ultraviolet (UV) radiation, prevention of dehydration, tolerance to high salinity and cold stress, as well as resistance to pest and pathogens are reported as the major functions of the cuticle (Amid *et al*., 2012; Bourdenx *et al*., 2011; Goodwin and Jenks, 2005; Kosma *et al*., 2009; Kosma *et al*., 2010; Lee *et al*., 2014; Panikashvili *et al*., 2007; Shepherd and Wynne Griffiths, 2006; Uppalapati *et al*., 2012; Wang *et al*., 2014; Wang *et al*., 2012; Zhang *et al*., 2007). It is well documented that drought can induce increased wax depositions on the leaf and stem surfaces of many plant species, such as *Arabidopsis*, cotton, soybean, rice, sesame, rose, peanut, ficus and tree tobacco (*Nicotiana glauca*) (Bondada *et al*., 1996; Cameron *et al*., 2006; Jenks *et al*., 2001; Kim *et al*., 2007a; Kim *et al*., 2007b; Kim, 2008; Kosma *et al*., 2009; Samdur *et al*., 2003; Zhu and Xiong, 2013). A naturally occurring mutant of wild barley (*Hordeum spontaneum*), *eibi1*, which has a very thin cuticle layer, is sensitive to drought (Chen *et al*., 2011). Similarly, a rice EMS mutant *wsl2* has approximately 80% less total wax content and is also more sensitive to drought than wild type rice (Mao *et al*., 2012).

Supplementary Results

Gene cloning and the phylogenetic relationships of MYB TFs

Three of the cloned wheat genes, a homologue of *AtMYB106* and two homologues of

AtMYB96, encode either the same or highly similar protein sequences to TaMYB16 (GenBank accession AEV91158.1, 100% identity), TaMYB24 (GenBank accession AEV91147.1, 99% identity) and TaMYB31 (GenBank accession AEV91154.1, 98% identity), respectively (Zhang *et al.*, 2012). These very high levels of identity with protein sequences reported by Zhang *et al.* (2012) are suggestive of homeologues or cultivar- and/or allele-specific origins. These three genes will be referred to as *TaMYB16*, *TaMYB24* and *TaMYB31*. The other three cloned wheat genes that are homologous to *AtMYB41*, *AtMYB16* and *SlMYB12* are novel and, therefore, these three wheat gene sequences were named *TaMYB74*, *TaMYB77* and *TaMYB78*, respectively.

Selection of MYB genes that are regulated by water deficit

Before dehydration *TaMYB24* had about 1.5-fold higher basal level of expression in Kukri than in RAC875. However, after two hours of dehydration the basal level of expression dropped 3.5-fold in leaves of Kukri and 1.5-fold in RAC875. In the drought-sensitive cultivar Kukri, the number of transcripts continued to decrease with dehydration. By contrast, in the leaves of the drought-tolerant cultivar RAC875, the expression levels of *TaMYB24* returned to initial levels after seven hours of dehydration.

Gene expression levels of *TaMYB31* in the absence of drought in the flag leaves of both Kukri and RAC875 cultivars were equally low. After the first two hours of dehydration, the expression of *TaMYB31* increased about two-fold in both wheat cultivars. Subsequently, expression returned to initial levels in Kukri, but kept increasing in RAC875, where after seven hours of leaf dehydration, expression was around six-fold higher than initial levels (Fig. 4).

The expression levels of *TaMYB74* gene during dehydration were different in wheat cultivars with contrasting drought tolerance. The basal levels of *TaMYB74* expression were low in both cultivars. In Kukri, the number of transcripts increased rapidly to about four-fold after two hours of dehydration, compared to the initial number of transcripts, and remained at the same level during next five hours of dehydration. In RAC875, however, the number of transcripts increased gradually with dehydration and reached a similar level to Kukri of a five-fold increase after seven hours of leaf dehydration (Fig. 4).

The basal expression levels and responses to dehydration of *TaMYB77* were similar in Kukri and RAC875. After two hours of dehydration the relatively low basal level of *TaMYB77* expression decreased three-fold in both cultivars and the same number of *TaMYB77* transcripts prevailed until the end of the experiment (Fig. 4).

The induction of *TaMYB24*, *TaMYB31*, *TaMYB74* and *TaMYB77* expression by drought was investigated in the flag leaves of wheat cultivars Kukri and RAC875 during three consecutive cycles of drought (Fig. 5). Water status during the experiment and the time points of leaf sampling are shown in Supplementary Fig. S1. The basal levels of *TaMYB24* expression were much higher than those of the other three *MYB* genes. The overall levels of expression of *TaMYB24* under cyclic drought were about two-fold and 1.5-fold lower than those under sufficient watering of Kukri and RAC875, respectively.

In contrast, the expression levels of *TaMYB31* gene under mild drought conditions (5 days after last watering) were 2.5-fold higher than in well-watered Kukri plants compared to a 1.5-fold increase in transcripts in RAC875 plants. The numbers of *TaMYB31* transcripts decreased with time under both well-watered and drought conditions, suggesting a developmental dependency of *TaMYB31* expression.

In Kukri, the transcript numbers of *TaMYB74* were dramatically increased only at fourteenth day of the first cycle of drought, when drought was strong and wheat plants started to wilt; the similar increase in transcripts was repeated at the end of a second cycle of drought (day 23). Similarly, the significant increase of *TaMYB74* transcripts was observed in the RAC875 flag leaves at fourteenth day; however there was no response of this gene during the second cycle of drought.

The number of *TaMYB77* transcripts in Kukri started to decrease at the ninth day of the first drought cycle and continued until the fourteenth day. The numbers of transcripts were significantly decreased at the end of the second cycle of drought and returned to normal levels after re-watering. In RAC875, the number of transcripts under drought were overall slightly reduced compared to those under well-watered conditions, but were not dependent on drought strength.

Supplementary References

Amid A, Lytovchenko A, Fernie AR, Warren G, Thorlby GJ. 2012. The *sensitive to freezing3* mutation of *Arabidopsis thaliana* is a cold-sensitive allele of homomeric acetyl-CoA carboxylase that results in cold-induced cuticle deficiencies. Journal of Experimental Botany **63**, 5289-5299.

Bondada BR, Oosterhuis DM, Murphy JB, Kim KS. 1996. Effect of water stress on the epicuticular wax composition and ultrastructure of cotton (*Gossypium hirsutum* L.) leaf, bract, and boll. Environmental and Experimental Botany **36**, 61-69.

Bourdenx B, Bernard A, Domergue F, Pascal S, Léger A, Roby D, Pervent M, Vile D, Haslam RP, Napier JA, Lessire R, Joubès J. 2011. Overexpression of Arabidopsis ECERIFERUM1 promotes wax very-long-chain alkane biosynthesis and influences plant response to biotic and abiotic stresses. Plant Physiology **156**, 29-45.

Bowne JB, Erwin TA, Juttner J, Schnurbusch T, Langridge P, Bacic A, Roessner U. 2012. Drought responses of leaf tissues from wheat cultivars of differing drought tolerance at the metabolite level. Molecular Plant **5**, 418-429.

Cameron KD, Teece MA, Smart LB. 2006. Increased accumulation of cuticular wax and expression of lipid transfer protein in response to periodic drying events in leaves of tree tobacco. Plant Physiology **140**, 176-183.

Chen G, Komatsuda T, Ma JF, Nawrath C, Pourkheirandish M, Tagiri A, Hu Y-G, Sameri M, Li X, Zhao X. 2011. An ATP-binding cassette subfamily G full transporter is essential for the retention of leaf water in both wild barley and rice. Proceedings of the National Academy of Sciences of the United States of America **108**, 12354-12359.

Goodwin S, Jenks M. 2005. The plant cuticle involvement in drought tolerance. In: Jenks M, Hasegawa P, eds. *Plant Abiotic Stress*. Oxford: Blackwell Scientific Publishers, 14-36.

Jenks MA, Andersen L, Teusink RS, Williams MH. 2001. Leaf cuticular waxes of potted rose cultivars as affected by plant development, drought and paclobutrazol treatments. Physiologia Plantarum **112**, 62-70.

Kim KS, Park SH, Jenks MA. 2007a. Changes in leaf cuticular waxes of sesame (*Sesamum indicum* L.) plants exposed to water deficit. Journal of Plant Physiology **164**, 1134-1143.

Kim KS, Park SH, Kim DK, Jenks MA. 2007b. Influence of water deficit on leaf cuticular waxes of soybean (*Glycine max* [L.] Merr.). International Journal of Plant Sciences **168**, 307-316.

Kim KW. 2008. Visualization of micromorphology of leaf epicuticular waxes of the rubber tree *Ficus elastica* by electron microscopy. Micron **39**, 976-984.

Kosma DK, Bourdenx B, Bernard A, Parsons EP, Lü S, Joubès J, Jenks MA. 2009. The impact of water deficiency on leaf cuticle lipids of *Arabidopsis*. Plant Physiology **151**, 1918-1929.

Kosma DK, Nemacheck JA, Jenks MA, Williams CE. 2010. Changes in properties of wheat leaf cuticle during interactions with Hessian fly. The Plant Journal **63**, 31-43.

Lee SB, Kim H, Kim RJ, Suh MC. 2014. Overexpression of *Arabidopsis MYB96* confers drought resistance in *Camelina sativa* via cuticular wax accumulation. Plant Cell Reports **33**, 1535-1546.

Mao B, Cheng Z, Lei C, *et al.* 2012. Wax crystal-sparse leaf2, a rice homologue of WAX2/GL1, is involved in synthesis of leaf cuticular wax. Planta **235**, 39-52.

Panikashvili D, Savaldi-Goldstein S, Mandel T, Yifhar T, Franke RB, Höfer R, Schreiber L, Chory J, Aharoni A. 2007. The *Arabidopsis* DESPERADO/AtWBC11 transporter is required for cutin and wax secretion. Plant Physiology **145**, 1345-1360.

Samdur M, Manivel P, Jain V, Chikani B, Gor H, Desai S, Misra J. 2003. Genotypic differences and water-deficit induced enhancement in epicuticular wax load in peanut. Crop Science **43**, 1294-1299.

Shepherd T, Wynne Griffiths D. 2006. The effects of stress on plant cuticular waxes. New Phytologist **171**, 469-499.

Uppalapati SR, Ishiga Y, Doraiswamy V, Bedair M, Mittal S, Chen J, Nakashima J, Tang Y, Tadege M, Ratet P. 2012. Loss of abaxial leaf epicuticular wax in *Medicago truncatula irg1*/*palm1* mutants results in reduced spore differentiation of anthracnose and nonhost rust pathogens. The Plant Cell **24**, 353-370.

Wang J, Li W, Wang W. 2014. Fine mapping and metabolic and physiological characterization of the glume glaucousness inhibitor locus *Iw3* derived from wild wheat. Theoretical and Applied Genetics **127**, 831-841.

Wang Y, Wan L, Zhang L, Zhang Z, Zhang H, Quan R, Zhou S, Huang R. 2012. An ethylene response factor OsWR1 responsive to drought stress transcriptionally activates wax synthesis related genes and increases wax production in rice. Plant Molecular Biology **78**, 275-288.

Zhang JY, Broeckling CD, Sumner LW, Wang ZY. 2007. Heterologous expression of two *Medicago truncatula* putative ERF transcription factor genes, *WXP1* and *WXP2*, in *Arabidopsis* led to increased leaf wax accumulation and improved drought tolerance, but differential response in freezing tolerance. Plant Molecular Biology **64**, 265-278.

Zhang L, Zhao G, Jia J, Liu X, Kong X. 2012. Molecular characterization of 60 isolated wheat MYB genes and analysis of their expression during abiotic stress. Journal of Experimental Botany **63**, 203-214.

Zhu X, Xiong L. 2013. Putative megaenzyme DWA1 plays essential roles in drought resistance by regulating stress-induced wax deposition in rice. Proceedings of the National Academy of Sciences of the United States of America **110**, 17790-17795.

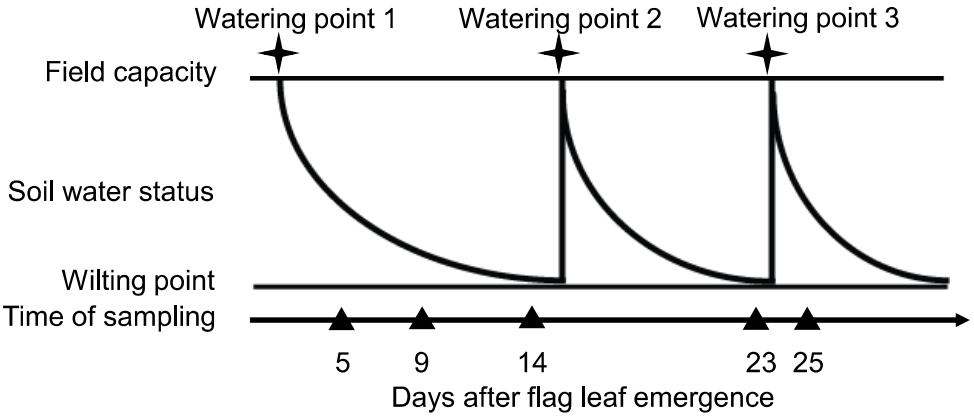

Supplementary Fig. S1

Schematic diagram of the cyclic drought experiment (modified from Bowne et al., 2012). Plants were watered at three time points as indicated by stars. Soil water content gradually decreased after watering until wilting point, at which water was re-applied. Leaf samples for RNA extraction were collected at five time points (5, 9, 14, 23 and 25 days after initial withholding of water), as indicated by triangles.

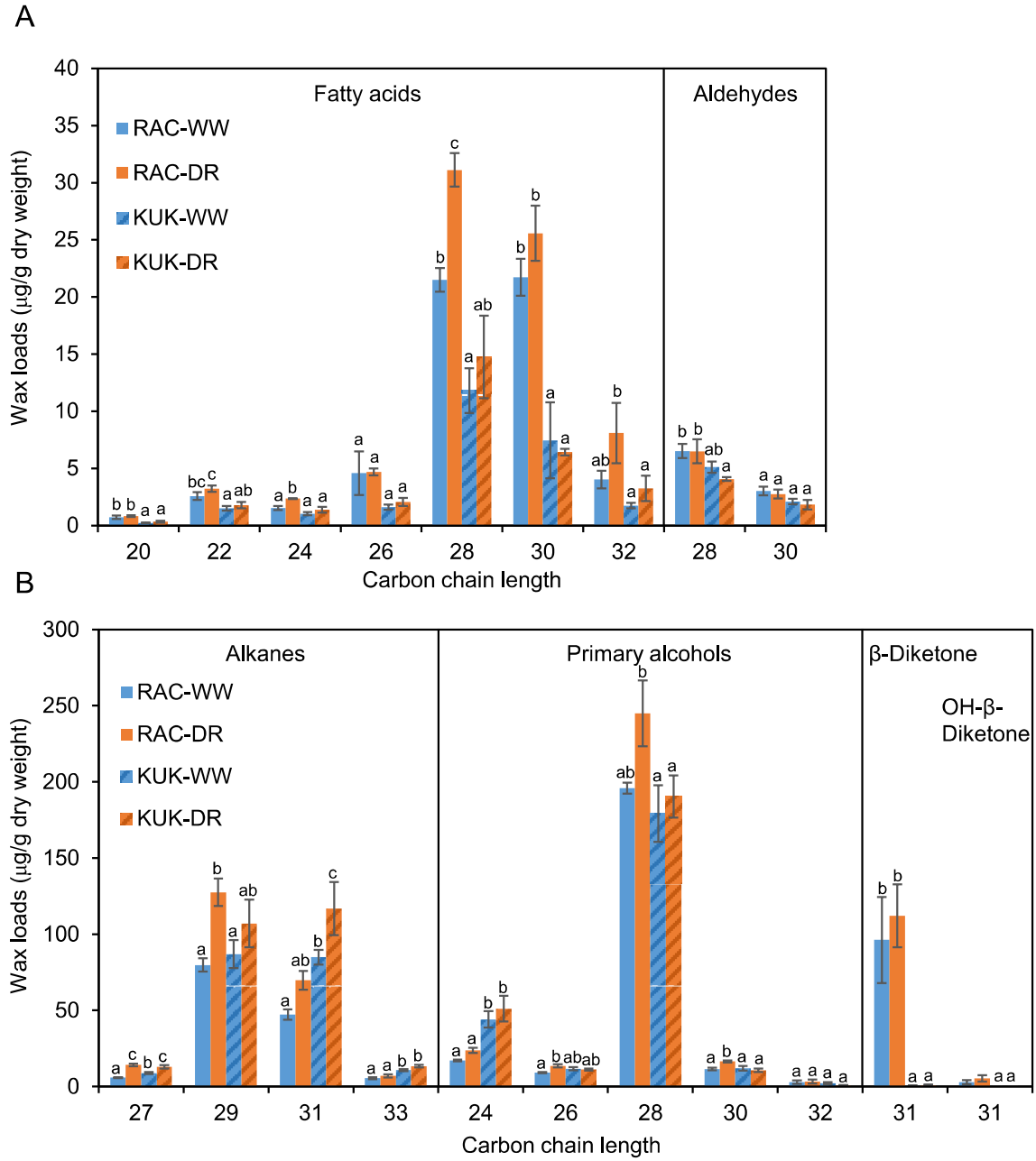

Supplementary Fig. S2

Amounts of wax components in RAC875 (RAC) and Kukri (KUK) grown under well-watered (WW) and mild drought (DR) conditions. A, Amounts of fatty acids and aldehydes. B, Amounts of alkanes, primary alcohols and β-diketones. Low amounts of C23, C25 alkanes, C20, C22, C34 primary alcohols and resorcinols in both cultivars, grown under the two conditions, are not shown but were included in the calculations of total wax loads (Fig. 1F). Means and standard errors were calculated from three replicates. Two-way ANOVA with the Fisher's Least Significant Difference *post hoc* test was conducted using GenStat. Small letters on the top of error bars indicate differences that are not significant at the 5% level.

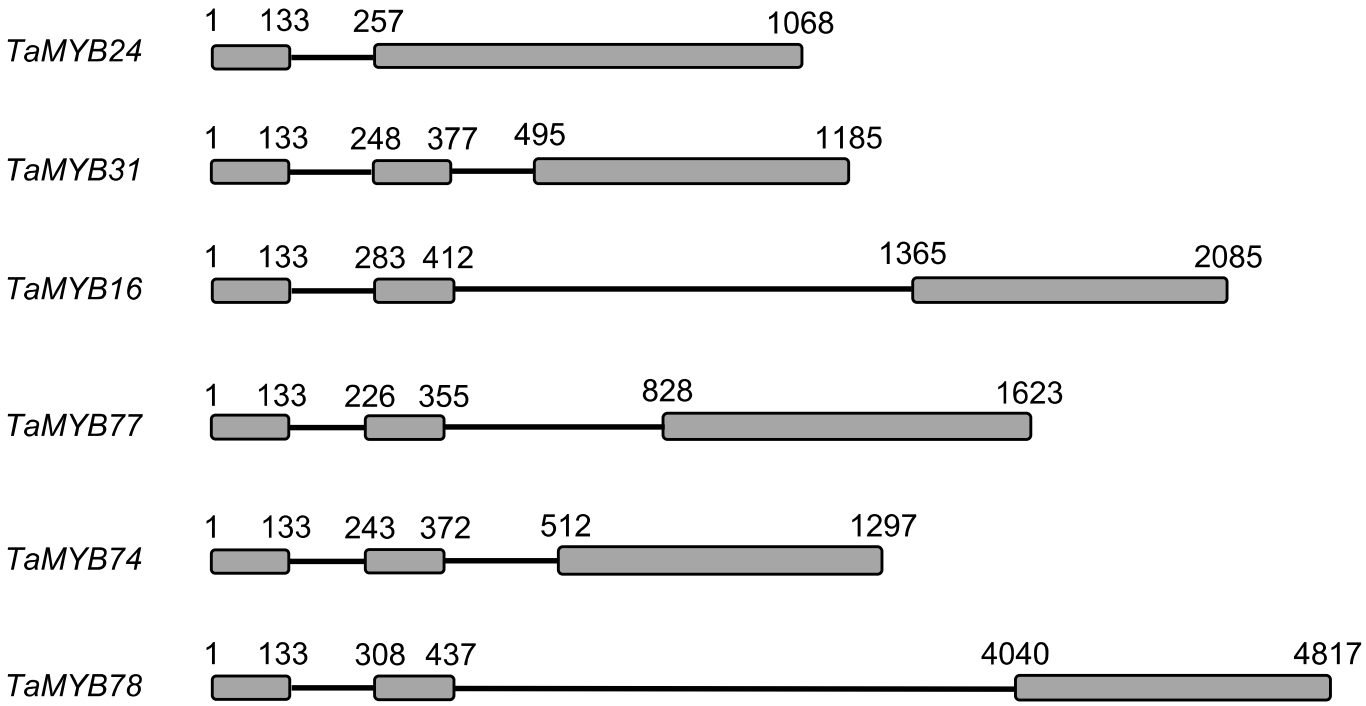

Supplementary Fig. S3

A schematic representation showing the gene structure of the six wheat MYB TFs investigated in this study. The positions of introns and exons, represented by lines and boxes, respectively, are indicated in each gene.

Supplementary Table S1. List of primers used in this study. The directional TOPO cloning overhang CACC, restriction enzyme sites and protection nucleotides are in bold.

Primer purposes	Genes (CDS) or promoters	Forward primer	Reverse primer
Cloning MYB TFs	*TaMYB16*	TTCGTTCGTGGGAGCGTTAG	CAAAGCATGTGCAGAGGTCG
		CACCATGGGGCGATCGCCGTGCT	TCAGAACTCTGGCGCCG
	TaMYB24	CAGTCCCCTCTCCTCACCTC	GTTAGGTGGGCATGCAGTGA
		CACCATGGGGAGGCCGCCGTGCT	CTAGAAAGGGTAGCCCAGG
	TaMYB31	TGTGCCTAGCCAGCCAAG	CCCAGCTCGATCTAAATCACC
		CACCATGGGGAGGCCTCCGTGCT	TTAGAAGAACTCACTGGGGTC
	TaMYB74	ACTCCAGCTGCGAGACAAAC	CTCGGTCGGTAGTACGTGATG
		CACCATGGGGCGCGCGCCGTG	CTACATGTAGTCGCTCACATCCAG
	TaMYB77	GCAGCATATTACGCCACTCC	CGACCTGTCGATGAAGCAG
		CACCATGGGGCGATCACCATG	CTAGAGAAATGCTGGTGG
	TaMYB78	GTATACAAGGGCCGCCATG	ACACCTGCTTTGCAATGGG
		CACCATGGGGAGGGCGCCGTGCT	TCAGCACGCGTCGGAGAG
Cloning promoters	*TaKCS1*	GTACGAAATCTCTCCAAGTCTTCC	GGATCTTGACGATGATGCTGG
		CACCCCAAGTCTTCCCCATGC	GGATCTCGAGACGTACG
	TaATT1	CAGACAAATGTTACATGCGGAG	GATCCACTCGTGCATGTCCTC
		CACCGGGTACTAGAGAAGAGAGCCATG	TGCCGGCCTCCCTG
	TdSHN1	**CACC**ATGGTGCAACCCAAGAAGAAGTTCC	TCAGACGACGAAGCTACCTTCTTCTCCA
		ACCTGCCTTCGCCTTGACAC	GCTCAGCAGCTCCTCGATCA
		CACCATCCACCATCTCAGCCAAAATAC	GGAGGCAGAAGACAAGAGCGAGAT
Gene expression	*TaMYB16*	GACAGAGGAGGAGAAGAACTAC	GTCGCCAGCACTCAGAAC
	TaMYB24	ACCGTGCCAAGTTATCAAGG	TAAGTAACACAGGAGACCAAGG
	TaMYB31	TGGAGAACTGGCTGCTTG	CGTACTTAGAAGAACTCACTGG
	TaMYB74	CAGATGCTCCTCCCTTGG	GTGATCCTGGTGTAGTTGC
	TaMYB77	ACCAACTTCAATCACTCTG	ATCGCTTCTCAACTTACAC
	TaMYB78	AGAAACAATAGCAAAGCAGGTG	CTCAGACGCCATATACGACTC
Yeast hybrid	*TaMYB16*	**GAAGAATTC**ATGGGGCGATCGCCGTGCTG	**GGAGGATCC**TCAGAACTCTGG
	TaMYB16D1	**GAAGAATTC**ATGGGGCGATCGCCGTGCTG	**GGAGGATCC**TCAAAGCAGCCCGGTGAAG
	TaMYB16D2	**GAAGAATTC**ATGGGGCGATCGCCGTGCTG	**GGAGGATCC**TCAGTACGCCTGCATGG

	TaMYB24	**GAAGAATTC**ATGGGGAGGCCGCCGTGCTG	**GGAGGATCC**CTAGAAAGGGTAGCCCAG
	TaMYB24D1	**GAAGAATTC**ATGGGGAGGCCGCCGTGCTG	**GGAGGATCC**TAGAACGCGGACCCCAGCGCAC
	TaMYB31	**GAAGAATTC**ATGGGGAGGCCTCC	**GGAGGATCC**TTAGAAGAACTCACTGG
	TaMYB31D1	**GAAGAATTC**ATGGGGAGGCCTCC	**GGAGGATCC**TTACAGCATGGAGAACG
	TaMYB31D2	**GAAGAATTC**ATGGGGAGGCCTCC	**GGAGGATCC**TTAGGGAGTCTGCGCTG
	TaMYB74	**GAAGAATTC**ATGGGGCGCGCGCC	**GGAGGATCC**CTACATGTAGTCGCTCACATCC
	TaMYB74D1	**GAAGAATTC**ATGGGGCGCGCGCC	**GGAGGATCC**TACGCGTGAACCAGG
	TaMYB77	**GAAGAATTC**ATGGGGCGATCACCATG	**GGAGGATCC**CTAGAGAAATGCTGGTGG
	TaMYB77D1	**GAAGAATTC**ATGGGGCGATCACCATG	**GGAGGATCC**CTAGCTTCTCAACTTACACG
	TaMYB78	**GAAGAATTC**ATGGGGAGGGCGCCGTGCTG	**GGAGGATCC**TCAGCACGCGTCGGAGAG
	TaMYB78D1	**GAAGAATTC**ATGGGGAGGGCGCCGTGCTG	**GGAGGATCC**TCATGCTGTAACGCTGCTGG
	TaMYB78D2	**GAAGAATTC**ATGGGGAGGGCGCCGTGCTG	**GGAGGATCC**TCAGAGGACACCAGTCTGATCAAC
TdSHN1 promoter deletions	*SHN1D1*	**CACC**GCTCAAGGCTTCTG	TTGTTCTGCCTGTC
	SHN1D2	**CACC**GTACCTGACCTGTTG	TTGTTCTGCCTGTC
	SHN1D3	**CACC**TCTCGGGATCTGATC	TTGTTCTGCCTGTC
	SHN1D4	**CACC**CACCGACAGTCCAC	TTGTTCTGCCTGTC
	SHN1D5	**CACC**GACTACCTACGCATC	TTGTTCTGCCTGTC
	SHN1D6	**CACC**GCAGAGGCAAGTAC	TTGTTCTGCCTGTC

Supplementary Table S2. Amino acid residues of TaMYB74 forming hydrogen bonds with 12-bp DNA *cis*-elements of MYBR1 (5'-AGGTGGTTATGC-3'/5'-GCATAACCACCT-3') and MYBR2 (5'-ATCTAACCACAT-3'/5'-ATGTGGTTAGAT-3'). Core binding sequences in *cis*-elements are underlined.

Residues	Number of hydrogen bonds with MYBR1 and their distances in Å[1]									DNA phospho-diester backbone	Number
	Sense strand (5'-3')							Antisense strand (5'-3')			
	T_4	G_5	G_6	T_7	T_8	A_9	T_{10}	$A_{6'}$	$C_{7'}$		
Lys13	-	-	-	-	-	-	-	-	-	2 (2.9; 3.3)	2
Lys14	-	-	-	1 (2.9)	-	-	-	-	-	-	1
Trp17	-	-	-	-	-	-	-	-	-	1 (3.0)	1
Arg48	-	-	-	-	-	-	-	-	-	1 (3.5)	1
Lys51	-	-	-	-	1 (3.1)	1 (3.1)	1 (2.9)	-	-		3
Arg54	-	-	-	-	-	-	-	-	-	1 (2.9)	1
Arg56	-	-	-	-	-	-	-	-	-	1 (3.0)	1
Asn87	-	-	-	-	-	-	-	-	-	1 (3.1)	1
Trp89	-	-	-	-	-	-	-	-	-	1 (2.8)	1
Ser90	-	-	-	-	-	-	-	-	-	1 (3.2)	1
Asn102	-	-	1 (3.5)	-	-	-	-	-	-	-	1
Lys105	-	-	1 (2.8)	-	-	-	-	1 (3.2)	1 (3.5)	-	3
Asn106	-	1 (3.0)	-	-	-	-	-	-	-	-	1
Asn109	1 (3.6)	-	-	-	-	-	-	-	-	-	1
Arg115	-	-	-	-	-	-	-	-	-	2 (2.8; 3.2)	2
Total	1	1	2	1	1	1	1	1	1	11	20

Residues	Number of hydrogen bonds with MYBR2 and their distances in Å[1]									DNA phospho-diester backbone	Number
	Antisense strand (5'-3')							Sense strand (5'-3')			
	$T_{4'}$	$G_{5'}$	$G_{6'}$	$T_{7'}$	$T_{8'}$	$A_{9'}$	$G_{10'}$	A_6	C_7		
Lys13	-	-	-	-	-	-	-	-	-	1 (2.8)	1
Lys14	-	-	1 (3.5)	-	-	-	-	-	-	-	1
Trp17	-	-	-	-	-	-	-	-	-	1 (2.9)	1
Arg48	-	-	-	-	-	-	-	-	-	-	-
Lys51	-	-	-	-	-	1 (3.3)	1 (3.0)	-	-	-	2
Arg54	-	-	-	-	-	-	-	-	-	1 (3.1)	1
Arg56	-	-	-	-	-	-	-	-	-	1 (2.8)	1
Asn87	-	-	-	-	-	-	-	-	-	1 (3.2)	1
Trp89	-	-	-	-	-	-	-	-	-	1 (2.8)	1
Ser90	-	-	-	-	-	-	-	-	-	1 (2.8)	1
Asn102	-	-	1 (3.3)	-	-	-	-	1 (3.6)	-	-	2
Lys105	-	-	1 (2.8)	-	-	-	-	1 (3.6)	1 (3.6)	-	3
Asn106	-	1 (3.0)	-	-	-	-	-	-	1 (3.4)	-	2
Asn109	-	-	-	-	-	-	-	-	-	-	-
Arg115	-	-	-	-	-	-	-	-	-	1 (2.8)	1
Total	-	1	3	-	-	1	1	2	2	8	18

[1]Separations equal to or less than 3.6 Å are indicated in brackets.

Chapter 4 Wheat drought-responsive WXPL transcription factors regulate cuticle biosynthesis genes

Statement of Authorship

Title of Paper	Wheat drought-responsive WXPL transcription factors regulate cuticle biosynthesis genes
Publication Status	☐ Published ☐ Accepted for Publication ☑ Submitted for Publication ☐ Unpublished and Unsubmitted w ork w ritten in manuscript style
Publication Details	Bi H, Luang Sukanya, Li Y, Bazanova N, Hrmova M, Borisjuk N, Lopato S. Wheat drought-responsive WXPL transcription factors regulate cuticle biosynthesis genes. Submitted to Plant Molecular Biology.

Principal Author

Name of Principal Author (Candidate)	Huihui Bi		
Contribution to the Paper	Designed the experiments with supervisors, performed experiments, analysed data and wrote the manuscript with supervisors.		
Overall percentage (%)	55%		
Certification:	This paper reports on original research I conducted during the period of my Higher Degree by Research candidature and is not subject to any obligations or contractual agreements with a third party that would constrain its inclusion in this thesis. I am the primary author of this paper.		
Signature		Date	13/09/2016

Co-Author Contributions

By signing the Statement of Authorship, each author certifies that:

i. the candidate's stated contribution to the publication is accurate (as detailed above);
ii. permission is granted for the candidate in include the publication in the thesis; and
iii. the sum of all co-author contributions is equal to 100% less the candidate's stated contribution.

Name of Co-Author	Sukanya Luang		
Contribution to the Paper	Performed and analysed the molecular model.		
Signature		Date	13/09/16

Name of Co-Author	Yuan Li		
Contribution to the Paper	Performed Q-PCR and normalised the data.		
Signature		Date	1/09/2016

Name of Co-Author	Natalia Bazanova
Contribution to the Paper	Performed yeast work for transcriptional activity and DNA-binding assays.
Signature	Date 12.09.2016

Name of Co-Author	Maria Hrmova
Contribution to the Paper	Supervised the development of experiments and analyses of data, edited the manuscript and acted as the corresponding author.
Signature	Date 01-09-2016

Name of Co-Author	Nikolai Borisjuk
Contribution to the Paper	Supervised the development of experiments and analyses of data, edited the manuscript.
Signature	Date 31-8-2016

Name of Co-Author	Sergiy Lopato
Contribution to the Paper	Conceived and designed the experiments, supervised the development of experiments and analyses of data, wrote the manuscript.
Signature	Date 12/09/2016

Wheat drought-responsive WXPL transcription factors regulate cuticle biosynthesis genes [S]

Huihui Bi, Sukanya Luang, Yuan Li, Natalia Bazanova, Maria Hrmova*, Nikolai Borisjuk, Sergiy Lopato

From the Australian Centre for Plant Functional Genomics, University of Adelaide, Waite Campus, Glen Osmond, South Australia 5064, Australia

[S] This article contains Figures 1-7, and Scheme 1, Tables 1-2, and Supporting Figure 1 and Supporting Tables 1-3.

The total word count of the manuscript is 8,895, including legend descriptions and excluding References.

*To whom correspondence should be addressed; E-mail: maria.hrmova@adelaide.edu.au; Tel.: +61 8 8313 7160; Fax: +61 8 8313 7102.

Abbreviations: 3D, three-dimensional; ABA, abscisic acid; DOPE, discrete optimised protein energy; GFP, green fluorescent protein; HD-Zip IV, homeodomain-leucine zipper class IV; IWGSC, International Wheat Genome Sequencing Consortium; LEA, late embryogenesis abundant; MOF, modeller objective function; Q-PCR, quantitative PCR; Ta, *Triticum aestivum*; TF(s), transcription factor(s); WXP, WAX PRODUCTION; WXPL,WXP-like; Y1H, yeast-1-hybrid.

Keywords: Abiotic stress; Cuticle; DREB transcription factors; Drought; Molecular model; MYB transcription factors; Transcription factor networks.

GeneBank accession numbers: *TaWPXL1A* - KX611869; *TaWPXL1B* - KX611870; *TaWPXL1D* - KX611871; *TaWPXL2B* - KX611872; *TaWPXL2D* - KX611873.

Abstract

The cuticle forms a hydrophobic waxy layer that covers plant organs and provides protection from biotic and abiotic stresses. Transcription of genes responsible for cuticle formation is regulated by several types of transcription factors (TFs). Five orthologous to *WAX PRODUCTION* (*WXP1* and *WXP2*) genes from *Medicago truncatula* were isolated from a cDNA library prepared from flag leaves and spikes of drought tolerant wheat (*Triticum aestivum,* breeding line RAC875) and designated *TaWXP-like* (*TaWXPL*) genes. Tissue-specific and drought-responsive expression of *TaWXPL1D* and *TaWXPL2B* was investigated by quantitative RT-PCR in two Australian wheat genotypes, RAC875 and Kukri, with contrasting glaucousness and drought tolerance. Rapid dehydration and/or slowly developing cyclic drought induced specific expression patterns of *WXPL* genes in flag leaves of the two cultivars RAC875 and Kukri. TaWXPL1D and TaWXPL2B proteins acted as transcriptional activators in yeast and in wheat cell cultures, and conserved sequences in their activation domains were localised at their C-termini. The involvement of wheat WXPL TFs in regulation of cuticle biosynthesis was confirmed by transient expression in wheat cells, using the promoters of wheat genes encoding two cuticle biosynthetic enzymes, the 3-ketoacyl-CoA-synthetase and the cytochrome P450 monooxygenase. Using the yeast 1-hybrid (Y1H) assay we also demonstrated the differential binding preferences of TaWXPL1D and TaWXPL2B towards three stress-related DNA *cis*-elements. Protein structural determinants underlying binding selectivity were revealed using comparative 3D molecular modelling of AP2 domains in complex with *cis*-elements. A scheme is proposed, which links the roles of WXPL and cuticle-related MYB TFs in regulation of genes responsible for the synthesis of cuticle components.

Introduction

Environmental stresses, such as limited water supply, high salinity and extreme temperatures, impair significantly grain yields (Porter and Semenov 2005). Minimising yield losses associated with these challenges could be achieved by strategic research to increase understanding of the physiological and molecular mechanisms of plant responses to stresses, and by applying this understanding to the development of plants with improved stress tolerance (Hrmova and Lopato 2014; Reynolds et al. 2012).

Two Australian wheat genotypes, Kukri and RAC875, which deliver similar grain yields and quality in optimal growing environments, show a drastic yield difference under cyclic drought conditions typical for most wheat growing regions in Australia; the glaucous advanced breeding line, RAC875 out-yields glaucousless Kukri by 24%. These two genotypes have been subjected to intensive

physiological, genetic and metabolomics investigations, which have revealed a stronger ability of RAC875 to maintain tissue water potential under drought, associated with the glaucous surface coverage of RAC875 (Bennett et al. 2012a; Bennett et al. 2012b; Bowne et al. 2012; Izagloo et al. 2008). Our recent comparative studies on the morphological and biochemical properties of leaf cuticles of RAC875 and Kukri cultivars demonstrated that better drought tolerance of RAC875 correlates with a number of cuticle properties, such as shape and load of cuticle wax crystals, biochemical composition, cuticle thickness, and that some of these features are regulated by drought-responsive MYB TFs (Bi et al. 2016).

There is a range of experimental evidence demonstrating the involvement of a variety of TFs in regulation of cuticular wax biosynthesis, transport and accumulation (Beisson et al. 2003; Jetter and Kunst 2008; Jetter et al. 2006; Li-Beisson et al. 2010). Most of these TFs belong to one of three plant families: the APETALA2/ethylene-responsive factor (AP2/ERF) family, the myeloblastosis (MYB) family, or homeodomain-leucine zipper class IV (HD-Zip IV) factors (Borisjuk et al. 2014). Cuticle-related TFs were identified and characterised for their regulation of cuticle-associated genes in a number of plant species, including *Arabidopsis*, rice, barley, maize, *Medicago*, soybean, tomato and wheat (Bi et al. 2016; Borisjuk et al. 2014; Buxdorf et al. 2014; Giménez et al. 2015; La Rocca et al. 2015; Sela et al. 2013; Xu et al. 2016). Over-expression of several cuticle-related TFs altered cuticle deposition and/or composition, changed cuticle structure and permeability, and in many cases increased stress tolerance of transgenic plants (Aharoni et al. 2004; Javelle et al. 2010; Seo et al. 2011; Seo and Park 2011; Zhang et al. 2005, 2007).

The AP2/ERF superfamily, which is involved in regulation of plant development and responses to biotic and abiotic stresses (Elliott et al. 1996; Licausi et al. 2013), is one of the largest families of TFs in plants. It comprises AP2, ERF, Dehydration Responsive Element Binding (DREB) and Related to ABI3/VP1 (RAV) subfamilies, which were classified based on the number and sequence differences of AP2 domains and the presence of additional DNA binding domains (Mizoi et al. 2012). ERFs have a single AP2 domain, which usually binds an ethylene responsive *cis*-element, designated as a GCC-box (AGCCGCC) (Ecker 1995). In some cases, ERFs can also bind C-repeat elements (GACGCC), which are usually recognised by DREB proteins (Eini et al. 2013).
WAX PRODUCTION (WXP1 and WXP2) TFs from the legume *Medicago truncatula* are members of the AP2/ERF superfamily, and have been reported to participate in regulation of cuticle biosynthesis (Zhang et al. 2005, 2007). These TFs have a low level of protein sequence identity to members of the WIN1/SHN1 clade of the ERFs, which belong to a clade of intensively studied transcriptional regulators of cuticle biosynthesis and distribution (Aharoni et al. 2004; Buxdorf et al. 2014; Kannangara et al. 2007; Sela et al. 2013; Shi et al. 2011, 2013; Xu et al. 2016). Expression of

both *WXP* genes is abscisic acid (ABA)-dependent and controlled by drought, while *WXP1* is also strongly up-regulated by cold (Zhang et al. 2005).

Strong constitutive expression of *WXP1* in transgenic *Medicago sativa* (alfalfa) as well as expression of both *WXP1* and *WXP2* in transgenic *Arabidopsis* led to significantly increased cuticular wax deposition on plant leaves, which could be visually detected (Zhang et al. 2005, 2007). Metabolomics analysis of leaf cuticle composition of *WXP1* and *WXP2* transgenic *Arabidopsis* lines revealed several differences in contents and chain length distributions of various wax components. For example, the amount of n-alkanes, a major wax component of *Arabidopsis* leaves, increased in both *WXP1* and *WXP2* transgenic *Arabidopsis* compared to control plants. However, the content of primary alcohols increased in *WXP1* plants but decreased in *WXP2* plants. Changes were also detected in physical cuticle properties. A chlorophyll leaching assay showed no changes in leaf cuticle permeability of the *WXP1 Arabidopsis* plants but decreased permeability in *WXP1* transgenic alfalfa, while cuticle permeability of the *WXP2 Arabidopsis* plants was increased. Expression levels of three *FATTY SCID ELONGASE* (*FAE*)-like genes and two *LACERATA* (*LCR*, encoding cytochrome P450 monooxygenases) genes from the cuticle biosynthesis pathway were significantly higher in the *WXP1* transgenic alfalfa plants than in control plants (Zhang et al. 2005). Drought tolerance of all alfalfa and *Arabidopsis* transgenic *WXP* lines was considerably enhanced compared to control plants. By contrast, freezing tolerance improvement was observed only for the *WXP1* transgenic *Arabidopsis* lines, while the *WXP2* plants were more sensitive to low temperature than control wild type (WT) plants (Zhang et al. 2007). However, a direct connection between changes in cuticle properties and freezing tolerance were not demonstrated in the latter report. In addition, expression of *WXP1* in alfalfa and *WXP2* in *Arabidopsis* strongly interfered with growth and development of transgenic plants. No negative influence of *WXP1* expression occurred on the developmental phenotype of transgenic *Arabidopsis*, suggesting *WXP1* may be a promising candidate gene for engineering of drought and frost tolerance in some plant species (Zhang et al. 2005, 2007).

Several orthologues WXP proteins are described in the literature. Amongst them is RAP2.4 from *Arabidopsis* (Lin et al. 2008; Rae et al. 2011; Shaikhali et al. 2008). Initially RAP2.4 was found to be involved in mediating light and ethylene signalling (Lin et al. 2008), as it acts as redox-sensor and a transducer of redox information (Shaikhali et al. 2008). Expression of the *RAP2.4* gene was found to be down-regulated by light, but up-regulated by salt and drought stresses (Ferreira et al. 2013; Lin et al. 2008; Rae et al. 2011). Another WXP orthologue, *ZmDBF1*, is induced by ABA and drought and the product of this gene regulated the drought-inducible *ZmRab17* gene by direct binding to DRE (ACCGAC) *cis*-element in its promoter (Kizis and Pagès 2002). The soybean

GmDREB2 gene is responsive to ABA treatment, drought, high salinity, and low temperature. GmDREB2 activates expression of downstream genes in transgenic *Arabidopsis* by binding to DRE elements and increases free proline contents in transgenic tobacco (Chen et al. 2007). An orthologue of WXP2, BpDREB2 from the woody plant *Broussonetia papyrifera*, has three characteristic domains/motifs: AP2, a nuclear localisation signal and a C-terminal acidic activation domain. It specifically binds to a DRE sequence in the Y1H assay. The expression of *BpDREB2* gene is strongly induced by dehydration and high salinity. Constitutive expression of *BpDREB2* in transgenic *Arabidopsis* conferred tolerance to salt and freezing without causing growth retardation (Sun et al. 2014). A WXP2-like gene *GhDBP2*, encoding a DREB (A-6) subfamily protein, was isolated from seedlings of cotton (*Gossypium hirsutum*). *GhDBP2* transcripts were strongly induced in cotton cotyledons by ABA treatment, drought, high salinity, and low temperature. GhDBP2 bound a DRE *cis*-element in the promoter region of the stress-inducible Late Embryogenesis Activated (LEA) gene, *LEA D113*, and in transient expression assays in tobacco cells it activated reporter gene expression driven by the *LEA D113* promoter (Huang et al. 2008). Although involvement of MtWXP orthologues in drought response has been repeatedly demonstrated in a number of species, no data on their participation in regulation of the cuticle biosynthesis have been reported.

Recently, we have identified wheat drought-regulated TFs from the MYB family and characterised their involvement in regulation of cuticle biosynthesis (Bi et al. 2016). In this study we describe wheat homologues of WXP1 and WXP2, designated TaWXP-like (TaWXPL) TFs. The expression patterns of two *TaWXPL* genes were studied in different wheat tissues and in leaves of two wheat genotypes with contrasting drought tolerance under the conditions of rapid dehydration and under cyclic drought. Transactivation properties of TaWXPL1D and TaWXPL2B TFs were demonstrated in yeast and wheat cell culture, and positions of conserved activation domains (ADs) were localised. DNA-binding selectivity of WXPL proteins was demonstrated and structural determinants of AP2 domains underlining this specificity were revealed for both TFs using 3D molecular modelling. Involvement of TaWXPL1D and TaWXPL2B TFs in the control of cuticle biosynthesis was confirmed by demonstrating their ability to activate the promoters of cuticle biosynthesis-related genes in transient expression assays.

Materials and Methods

Plant material and cultivation

Plants of the wheat (*Triticum aestivum*) genotypes RAC875 and Kukri, previously described by Izanloo et al. (2008), were grown in a greenhouse in 112 x 76 x 50 cm containers, equipped with an

automatic watering system and continuous monitoring of soil water potential (Amalraj et al. 2015). For the cyclic drought experiment, drought-tolerant RAC875 and drought-sensitive Kukri were grown and cyclic drought treatment was applied as described by Harris et al. (2016).

Cloning of the wheat orthologues of WXP TFs

Protein sequences of MtWXP1 and MtWXP2 were retrieved from the National Centre for Biotechnology Information (NCBI, Bethesda, MD, USA), using accession numbers summarised by Borisjuk et al. (2014). To identify the closest wheat homologues, MtWXP sequences were used to search in NCBI and International Wheat Genome Sequencing Consortium (IWGSC) sequence databases linked to the Blast Portal at the Australian Centre for Plant Functional Genomics (ACPFG, University of Adelaide, Australia). The closest wheat genes to MtWXP1 and MtWXP2 were DREB responsive factor (DRF)-like genes, designated *DRFL1* and *DRFL2*. Five sequences (presumably protein products of homeologous genes) of these two groups were deposited in NCBI by other research group, but no functional characterisation of these genes has been reported. Six homeologues of *DRFL1* and *DRFL2* genes were found in the IWGSC databases. These were used to design homeologue-specific primers (Supporting Table S1) for gene amplification by nested PCR from cDNA pools prepared from leaves and spikes of the drought-tolerant wheat genotype RAC875 subjected to drought. PCR products were cloned into the pENTR/D-TOPO vector (Life Technologies, Victoria, Australia) as previously described (Bi et al. 2016). Protein sequence identity analyses of translated cDNAs (Table 1) were calculated using the Needleman-Wunsch algorithm (McWilliam et al. 2013).

Construction of the evolutionary relationships of proteins with single AP2-domain

To construct a phylogenetic tree of ERF and DREB factors (Fig. 1), we used 106 wheat sequences from the Plant Transcription Factor Database (Jin et al. 2014; http://planttfdb.cbi.pku.edu.cn), together with five wheat WXPL proteins (products of genes cloned in this study), two (WXP1 and WXP2) query proteins from the legume *Medicago truncatula* (Mt), and proteins with high protein sequence homology to WXP proteins from *Asparagus officinalis* (Ao), *Arabidopsis thaliana* (At), *Broussonetia papyrifera* (Bp), *Gossypium hirsutum* (Gh), *Glycine max* (Gm) and *Zea maize* (Zm). In the first instance, a total of 161 sequences were retrieved; 55 sequences were removed because they did not contain starting methionine. The names of previously published wheat ERFs and DREB TFs were used together with their accession numbers. The evolutionary history of representative ERF and DREB proteins was inferred using the Neighbor-Joining method (Saitou and Nei 1987). Evolutionary distances were computed using the p-distance method (Nei and Kumar 2000) (with

1,000 bootstrap replications), and expressed in units of numbers of residue differences per site. All positions containing gaps and missing data were eliminated. Evolutionary analyses were conducted in MEGA6 (Tamura et al. 2013).

Gene expression analysis in different wheat tissues, under dehydration and cyclic drought

Gene expression of wheat *WXPL* genes was investigated in detached leaves subjected to rapid dehydration, and in plants subjected to cyclic drought as described by Bi et al. (2016). Quantitative RT-PCR (Q-PCR) analysis was performed on cDNA samples as described previously (Fletcher 2014) using gene specific primers listed in Supporting Table 1. Three of four wheat genes, encoding for actin, cyclophilin, elongation α factor and glyceraldehyde-3-phosphate dehydrogenase, were used for normalisation of expression (Fletcher 2014). Selection of the most appropriate three normalisation genes was based on pairwise comparisons among the four genes for each dataset. To analyse tissue specificity of gene expression, we also utilised a cDNA series prepared from different tissues of *T. aestivum* cv. Chinese Spring (Morran et al. 2011). Three biological and three technical replicates were used in all gene expression analysis experiments.

In-yeast activation assay and localisation of activation domains

Sets of full length and partial coding sequences (CDS) for *TaWPXL1D* were amplified by PCR with *Eco*RI and *Bam*HI restriction sites introduced in forward and reverse primers, respectively, and cloned in the same restriction sites of the pGBKT7 vector (Scientifix, Victoria, Australia). In the case of *TaWPXL2B*, *Nde*I and *Eco*RI restriction sites were used for cloning because a *Bam*HI site was found inside the CDS of *TaWPXL2B*. Each set included the full-length CDS, and versions with truncations at the 5' or 3' ends. All primer sequences are listed in Supporting Table 1. A transcriptional activation assay in yeast (*Saccharomyces cerevisiae*) was performed as described by Eini et al. (2013). Yeast transformants were first selected on synthetic defined (SD)/-Trp medium to prove that transformation of the pGBKT7 construct in yeast cells occurred. The yeast culture was replica-plated onto SD2 (-Trp, -His) medium containing 5 mM 3-Amino-1,2,4-Triazol (3AT). The ability of full-length or truncated wheat WPXL proteins to activate expression of the *HIS3* gene led to yeast growth on the selective medium.

Assessment of DNA-binding selectivity of WXPL TFs using a Y1H assay

The full length coding regions of *TaWXPL1D* and *TaWXPL2B* were amplified by PCR using the same pairs of primers as for the in-yeast activation assay, and cloned to the respective restriction sites of the pGADT7 vector (Supporting Table 1). Each of the resultant constructs was transformed

into Y187 wild-type yeast (*S. cerevisiae*), and each of four strains derived from Y187 (yDRE, yCRT, yGCC and yHDZ1), that were prepared by integration of constructs containing tandem repeats of DRE, CRT, GCC-box and HDZ1 *cis*-elements, respectively. These repeats were inserted upstream of the yeast minimal promoter and the *HIS3* gene (Pyvovarenko and Lopato 2011). Yeast transformants carrying the plasmids were selected on SD/-Leu medium and replica-plated to SD2 (-Leu, -His) medium containing 10 mM 3AT. The ability of transformants to grow on the SD2 medium suggested an interaction of TaWXPL proteins with a respective *cis*-element. Y187 and yHDZ1 strains were used as negative controls. The rate of yeast growth observed for each of the evaluated *cis*-element/WXPL protein combination was reproducible in three technical replicates.

Domain boundary and post-translation modification analyses and sequence alignments

Domain boundary distributions were determined using SMART (Letunic et al. 2015). Sequence alignments between WXPL protein sequences were performed using Annotator (Gille et al. 2014) and ProMals3D (Pei et al. 2008). Predictions of post-translation modifications (phosphorylation, N-glycosylation, nuclear localisation motifs) were performed using the ExPASy Bioinformatics Resource Portal (Gasteiger et al. 2003).

Homology modelling of wheat WXPL1D and WXPL2B TFs

Structural models of wheat WXPL1D and WXPL2B, using the *Arabidopsis thaliana* protein AtERF1 in complex with the GCC-box (Protein Data Bank accession 1GCC) as a template (Allen et al. 1998), were generated through the MODELLER 9.16 (Sali and Blundell 1993). Nucleotide variations required in the DNA template from AtERF1 were introduced using Coot (Emsley et al. 2010). Fifty models of each WXPL were generated using the starting coordinates of AtERF1, and models with the lowest scores of the Modeller Objective Function (MOF) (Shen and Sali 2006), and Discrete Optimised Protein Energy (DOPE) (Eswar et al. 2008) were selected. These models were optimised through energy minimisation using FoldX (Schymkowitz et al. 2005). Final models were evaluated by ProSa2003 (Sippl 1993) and PROCHECK programs (Laskowski et al. 1993) to evaluate stereochemical quality and G-factors. Ramachandran statistics and G-factor (Laskowski et al. 1993), and ProSa2003 z-score (Sippl 1993) parameters are summarised in Supporting Table 2.

Assessment of promoter activation by WXPL TFs in a wheat transient expression assay

A transient expression assay was performed using *Triticum monoccocum* L. suspension cell culture, according to the procedure established by Eini et al. (2013). In this assay, cultivated wheat cells were co-bombarded with a vector expressing one of the wheat *WXPL* genes and a construct containing the

β-glucuronidase reporter gene (*GUS*) fused to a promoter containing DREB, CBF and/or ERF binding sites. GUS expression from the WXPL-activated promoter was quantified 48 hours after bombardment. Promoters of three wheat cuticle biosynthesis-related genes: 3-ketoacyl CoA synthetase (*TaKCS1*; Acc. KU737579), cytochrome P450 monooxygenase (*TaATT1*; Acc. KU737578) and SHINE 1 TF (*TdSHN1*; Acc. KU737580), were cloned into the *GUS* expression vector pMDC164 and were used as targets for activation by WXPL TFs (Bi et al. 2016). Vectors for expression of WXPL proteins were constructed by recombinational cloning of *TaWXPL1D* and *TaWXPL2B* CDS into the pUbi vector (Bi et al. 2016). The pUbi-GFP construct was generated in a similar way and used as a negative control in all transient expression experiments. DREB and ERF specific *cis*-elements (DRE, CRT and GCC-box) in promoters were predicted using the Plant *Cis*-acting Regulatory DNA Elements database (PLACE, University of Pittsburgh, US) (Higo et al. 1999).

Statistical analysis of data

Statistical data analyses of gene expression levels under dehydration and cyclic drought were performed using two-way ANOVA with the Fisher's Least Significant Difference post-hoc test in GenStat 16th Edition (VSN International Ltd, Hemel Hempstead, UK). Transient expression assay data were analysed using Student's t-tests.

Results

Gene cloning and the phylogenetic relationships of WXPL TFs with ERFs and DREB proteins

Five homeologues of two wheat *WXPL* genes, *WXPL1* and *WXPL2*, which may potentially be involved in regulation of cuticle biosynthesis under drought, were cloned by nested PCR from leaves and spikes of the drought-tolerant wheat genotype RAC875. The protein sequences of two known cuticle regulators from *Medicago truncatula*, WXP1 and WXP2, were used to identify the closest wheat homologues as described in Materials and Methods. We intended to clone all three homeologues of each of these two wheat genes, but were able to clone only two homeologues of WXPL2. Details of the cloned wheat *WXPL* genes, including their names, accession numbers, protein sequence identities to MtWXP1 and MtWXP2, and chromosomal locations of respective genes are summarised in Table 1. Blast analysis of coding sequences of five wheat *WXPL* cDNAs using the IWGSC NRGene Assembly database linked to the Blast Portal, indicated that all *WXPL* genes are intron-less, and therefore cannot be regulated by alternative splicing. Investigation of the evolutionary relationships between 130 ERF/DREB members, including two WXPs from *Medicago*

truncatula and products of the five cloned *WXPL* homeologues showed that TaWXPL1 homeologues grouped with MtWXP1, while TaWXPL2 homeologues grouped with MtWXP2 (Fig. 1A). Two wheat sequences from the Plant Transcription Factor Database (Tae043463 and Tae006260) also grouped within the MtWXP2 clade. These two sequences share 94.3% sequence identity and 96.1% sequence similarity, and are localised on chromosomes 4D and 4A, respectively; these locations were obtained by searching the IWGSC NRGene Assembly. Although these sequences differed from the WXPL1 and WXPL2 proteins, they exhibited high sequence conservation in the AP2 domains and C-terminal regions (Supporting Figure 1). We have experimentally identified these C-terminal regions as activation domains (see below).

One wheat homeologue from each clade (TaWXPL1D and TaWXPL2B) was selected for further characterisation. When TaWXPL1D and TaWXPL2B were aligned using the Needleman-Wunsch algorithm (McWilliam et al. 2013) across 35 C-terminal residues, a high sequence identity (69% identity, 86% similarity) was noted in C-terminal domains (Fig. 1B). This may indicate that both proteins exhibit similar activation regions, and may have similar protein binding properties.

Expression of *WXPL* genes in wheat tissues

Expression of *TaWXPL1D* and *TaWXPL2B* was examined using Q-PCR in various tissues of *T. aestivum* cv Chinese spring (Fig. 2). The *TaWXPL1D* gene showed highest transcript levels in anthers and pistils before anthesis and moderate levels in leaves and other tested tissues. The expression pattern of *TaWXPL2B* gene had some similarity to that of its homologue, *TaWXPL1D*, but overall the levels of *TaWXPL2B* expression were low. The highest number of *TaWXPL2B* transcripts was observed in bracts, while lower levels of expression were found in pistils, anthers and leaves. In other tested tissues the transcript levels of *TaWXPL2B* were very low.

Influence of water deficit on expression of wheat *WXPL* genes

Expression of *TaWXPL1D* and *TaWXPL2B* was analysed by Q-PCR (i) in detached flag leaves of Kukri and RAC875 that were subjected to rapid dehydration, and (ii) in flag leaves of the same two cultivars growing under cyclic drought. The first experiment was designed to reveal rapid transient responses on dehydration. The second experiment focused on determining gene expression during long-lasting and repeatable cycles of drought.

Difference in glaucousness of flag leaves and peduncles of drought-sensitive Kukri and drought-tolerant RAC875 were observed (Fig. 3A), reflecting differences in content and structure of their epicuticular waxes (Bi et al. 2016).

During rapid dehydration, the *TaWXPL1D* gene was upregulated, while *TaWXPL2B* was downregulated (Fig. 3B). Regulation of both genes occurred differently in Kukri and RAC875. Upregulation of *TaWXPL1D* in drought-sensitive Kukri was weak and statistically insignificant, although the basal level of expression of this gene in flag leaves of Kukri was 3-fold higher than basal levels of expression in flag leaves of RAC875. In contrast to Kukri, *TaWXPL1D* in leaves of drought-tolerant RAC875 was rapidly induced by dehydration. A six-fold increase in transcript number was observed after two hours of stress, and over the next five hours, transcript numbers continued to slowly increase (Fig. 3B).

Dehydration-induced changes in expression of *TaWXPL2B* also occurred differently in the two wheat genotypes. The basal level of expression of *TaWXPL2B* in flag leaves of Kukri was about 1.6-fold higher than basal levels of expression in RAC875. In Kukri, the number of transcripts decreased rapidly by about 3.5-fold compared to the initial number of transcripts after two hours of dehydration and remained at the same level during next five hours of dehydration. However, in RAC875, the number of transcripts slightly decreased during the first 4 hours of dehydration and after next 3 hours returned to initial level (Fig. 3B).

The induction of *TaWXPL1D* and *TaWXPL2B* expression by drought was investigated in flag leaves of wheat genotypes Kukri and RAC875 during three consecutive cycles of drought (Fig. 4). Flag leaf samples were collected at the beginning, in the middle and at the end of the first drought cycle, than at the end of the second drought cycle, and finally, a short time after the second re-watering (Bi et al. 2016). No induction of the *TaWXPL1D* gene in Kukri by drought was observed. However, this gene was transiently up-regulated in RAC875 until the fifth day of the first drought cycle, and then quickly returned to its initial level of expression. By contrast, the *TaWXPL2B* gene in Kukri it was activated early by drought and at the end of the first drought cycle started to return to initial levels of expression, remained at the same level at the end of the second drought cycle and again returned to initial levels a short time after re-watering (Fig. 4). Drought-inducible regulation of this gene in flag leaves of RAC875 was not observed.

Domain structure and the activation properties of WXPL TFs

Domain organisation of wheat WXPL proteins was investigated using the SMART protein domain analysis tool (Letunic et al. 2015). Each of wheat WXPL TFs was predicted to contain a single AP2 DNA-binding domain, localised approximately in the middle of proteins, and two (TaWXPL1) to five (TaWXPL2) low-complexity domains that were between eight to 58 residues long. Up to 38 Tyr and Ser phosphorylation sites were identified in the TaWXPL1 sequences following the AP2 domain, while in TaWXPL2 sequences, more than 50 Tyr and Ser phosphorylation sites were found,

predominatly present in the N-terminal regions and before the AP2. At least three N-glycosylation sites were found in TaWXPL1 sequences; one site in the middle of the AP2 and two sites following the AP2 domain. In TaWXPL2 sequences, two N-glycosylation sites were identified, both of which preceded AP2. No nuclear localisation signals were predicted in WXPL sequences. AP2 domains exibited the features characteristic of DNA binding function, with a prevalance of positively charged arginine and lysine residues.

The presence and positions of activation domains (ADs) in wheat WXPL proteins were examined in yeast. Full-length and truncated *WXPL* genes at the 5' or 3' coding regions were fused to the sequence-encoding binding domain (BD) of yeast GAL4 TF. Constructs were used to transform yeast cells, and the presence of ADs in TFs was revealed as the ability of the yeasts to grow on a selective medium. Both full-length TaWXPL1D and TaWXPL2B proteins provided strong transcriptional activation of the yeast *HIS3* gene, the product of which supports yeast growth on selective medium deficient in histidine (Fig. 5A). Truncation D1 decreased the TaWXPL1D transactivation activity, and completely removed the ability of TaWXPL2B to activate the reporter gene. D2 truncations of TaWXPL1D and TaWXPL2B abolished the activation properties of both proteins, suggesting that significant portions of proteins responsible for transcriptional activation are located at the C-termini of WXPL proteins.

We also predicted the presence of transcriptional ADs in WXPL proteins, based on knowledge that ADs are usually (but not always) enriched in acidic amino acid residues and contain glutamine-rich and proline-rich motifs (Johnson et al. 1993). The alignment of 14 sequences, of the branch highlighted in blue lines in the phylogenetic tree in Fig. 1A, revealed the presence of a conserved motif/domain (Fig. 1B), characteristic of only WXPL TFs from wheat and other plants. The presence of several absolutely conserved hydrophobic and charged residues indicated that these domains may adopt a similar fold. We predicted (Scratch Protein Predictor; Cheng et al. 2005) that this domain exhibits significant disorder, but carrying a C-terminal α-helix. A description of this C-terminal domain could not be found in ProDom (Bru et al. 2005) or SMART (Letunic et al. 2015) databases, although a 15-residue motif xFxLxKxPSxEIDWx was identified in the MEME suite (Bailey et al. 2009). We have termed this domain the 'WaX-production C-terminal Domain' (WXCD).

The DNA binding specificity of the TaWXPL1D and TaWXPL2B proteins

The DNA binding specificity of TaWXPL1D and TaWXPL2B was analysed using a Yeast 1-hybrid (Y1H) assay. Plasmids encoding GAL4 activation domain (AD) fusion proteins were used in the assay. The TaWXPL1D-GAL4 plasmids were transformed into yeast strain Y187 and each of four

derivatives of this strain containing an integrated genomic DNA reporter gene under minimal yeast promoter with four repeats of one of the plant specific *cis*-elements DRE, CRT, GCC-box or HDZ1 (resultant strains were designated as yDRE, yCRT, yGCC and yHDZ1, respectively). Y187 and yHDZ strains were used as negative controls. The Y1H assay (Fig. 5B) revealed that both wheat WXPL proteins can recognise the *cis*-elements DRE, CRT and GCC-box, wich were earlier reported as elements specific for DREB TFs and/or ERFs (Baker et al. 1994; Ohme-Takagi and Shinshi 1995; Yamaguchi-Shinozaki and Shinozaki 1994). However, there were significant differences in the strength of protein-DNA binding between the two WXPL proteins. Interaction of TaWXPL1D with the CRT element was stronger than with the two other elements, which bound this protein with equally low eficiency. By contrast, TaWXPL2B showed very strong interaction with DRE, signigicantly weaker interaction with CRT and weak interaction with the GCC-box element (Fig. 5B).

Homology modelling of wheat WXPL1D and WXPL2B TFs

Domain boundaries analyses of wheat TaWXPL1D and TaWXPL2B proteins showed the presence of AP2 domains (with well-defined boundaries), and between two and five low-complexity domains. An alignment of the template (AtERF1) and the two wheat AP2 WXPL sequences (Fig. 6A) indicates that there is a high level of sequence identity between the investigated proteins. AP2 of the AtERF1 template shares 70% (with TaWXPL1D) and 75% (with TaWXPL2B), and 83% (with both TaWXPL proteins) sequence identity and similarity. The positions of ten identical residues and secondary structure element distributions between the template and target sequences indicate the presence of three β-sheets and one α-helix.

To understand variations in binding of the two wheat WXPL proteins with the DNA *cis*-elements CRT (5′-GCCGAC-3′/5'-GTCGGC-3'), DRE (5'-ACCGAC-3'/5'-GTCGGT-3') and GCC (5'-GCCGCC-3'/5'-GGCGGC-3'), we generated 3D models of AP2 domains of wheat TFs using AtERF1 as the template (PDB accession 1GCC in complex with the GCC box). The AP2 models of both WXPL proteins consist of a three-stranded anti-parallel β-sheet and an α-helix that is positioned almost in parallel to the β-sheet (Fig. 6B). The wheat WXPL proteins bound to the major groove of *cis*-elements *via* charge/polar (Arg, Glu, and Thr) and hydrophobic (Trp) residues in the three-stranded β-sheet, and *via* a Tyr residue from the α-helix. The Arg residue is predicted to bind the first bases of DNA sense strands (G_1 or A_1), while Thr and Trp always interact with the phosphate backbone (Fig. 6B, Supporting Table 3). However, in this model, the Arg residues of TaWXPL1D and TaWXPL2B interacted with first bases ($G_{1'}$) of antisense strands. The residues of TaWXPL1D

and TaWXPL2B involved in interactions to CRT elements were found to be similar (Supporting Table 3), except that no interactions of Glu187 and Arg196 with the respective $C_{3'}$ and G_4 bases were found for TaWXPL2B. TaWXPL2B bound the DRE *cis*-element more specifically than CRT, because Arg179 not only contacted to the first base (A_1) in the sense strand, but also it interacted with its complementary base ($T_{6'}$) in the antisense strand. Moreover, Arg189 bonded to the A_5 base to increase the binding specificity. Investigation of interactions with the GCC *cis*-element revealed that the nucleobases of G_1, $G_{1'}$ and $C_{3'}$ made contacts to Arg115, Arg125 and Glu123 for TaWXPL1D, and to Arg179, Arg189 and Glu187 for TaWXPL2B, respectively. Additionally, TaWXPL1D formed hydrogen bonds to $G_{2'}$ and $G_{4'}$ of the GCC *cis*-element through Arg125 and Arg113, respectively, but these bonds were not found in the TaWXPL2B/GCC complex. It was notable that in the TaWXPL2a/GCC complex, Arg176 and Arg196 contacted G_4 or $G_{5'}$ bases, and hydrogen bond separations between residues and nucleobases or the sugar-phosphate backbone varied between 2.5 Å to 3.5 Å (Supporting Table 3).

Activation of promoters of cuticle biosynthesis-related genes by WXPL TFs

Three promoters of cuticle biosynthesis-related genes were cloned either by nested PCR using genomic DNA of *T. aestivum* as template (*TaATT1* and *TaKCS1* promoters), or *via* screening of a BAC library of *T. durum* (*TdSHN1* promoter) (Bi et al. 2016). Promoters were inserted upstream of the *GUS* reporter gene and resulting constructs were used in transient expression assays. These assays were conducted to confirm the involvement of wheat *WXPL* genes in regulation of cuticle biosynthesis. Transient expression assays were performed by co-bombardment of suspension cell culture of *T. monoccocum* L., with constructs containing the *GUS* gene driven by each of the tested promoters (reporter constructs), and constructs containing each WXPL TF gene driven by the constitutive polyubiquitin promoter (effector constructs) (Fig. 7A). TaMYB74 (Bi et al. 2016) driven by polyubiquitin promoter was used as a positive control in the case of *TdSHN1* promoter activation. The *GFP* gene cloned under the polyubiquitin promoter was used as a negative control to reveal basal levels of promoter activity in wheat cells.

As shown in Fig. 7B, TaWXPL1D activated two promoters, *TaKCS1* and *TaATT1*, while TaWXPL2B activated only the *TaKCS1* promoter. Although the *TdSHN1* promoter was strongly activated by TaMYB74 (Bi et al. 2016), it was not activated by either of the wheat WXPL proteins (data not shown).

Discussion

The main function of cuticle, and of cuticular waxes in particular, is protection against excessive solar irradiation and conservation of internal plant water (Yeats and Rose 2013). In this work, two Australian wheat cultivars, RAC875 (glaucous, drought tolerant) and Kukri (non-glaucous, drought sensitive), previously characterised in terms of cuticle structure and composition as well as transcriptional regulation of cuticle biosynthesis by drought-regulated MYB TFs (Bi et al. 2016), were used with the aim to: (i) identify genes encoding wheat orthologues of WXP TFs that potentially may be involved in regulation of cuticular wax biosynthesis pathways under drought, (ii) functionally characterise wheat *WXP*-like genes and gene products, and (iii) to show the ability of wheat WXPL TFs to activate promoters of genes involved in cuticle biosynthesis.

Phylogenetic analysis of DREB/ERF proteins (Fig. 1) indicated that the five WXPL proteins cloned from the advanced breeding line RAC875 were grouped in two clades, together with WXP1 and WXP2 TFs from *Medicago truncatula* (Zhang et al. 2005, 2007). Alignments of protein sequences of wheat WXPL proteins (Supporting Figure 1) revealed that the *TaWXPL1* cDNAs isolated from RAC875 are represented by all three homeologous genes (letters at the end of gene/protein names reflect their belonging to A, B or D genome of hexaploid wheat), while only two homeologues of *TaWXPL2* (B and D) were cloned. No significant differences in protein sequence were found between the homeologues which could potentially influence protein structure or function. Therefore, two representatives, *TaWXPL1D* and *TaWXPL2B*, one from each clade were selected for further characterisation.

It is notable, that the wheat genome contains a third type of *WXPL* genes (Tae043463 and Tae006260), which in our phylogenetic analysis grouped to the MtWXP2 clade, and which have a C-terminal activation domain similar to TaWXPL1 and TaWXPL2 (Fig. 1B). All WXPL homologues reported for different plant species grouping to the MtWXPL1 and MtWXP2 clades (Huang et al. 2008; Kizis and Pagès 2002; Lin et al. 2008; Liu et al. 2010; Rae et al. 2011; Shaikhali et al. 2008; Sun et al. 2014) are responsive to drought and some other abiotic stresses.

The analysis of gene activity in different tissues of wheat plants grown under optimal well-watered conditions, revealed both similarities and differences in the expression patterns of *TaWXPL1D* and *TaWXPL2B* (Fig. 2). There were relatively high levels of *TaWXPL1D* gene expression in all tested tissues, in contrast to a more tissue-specific pattern of TaWXPL2B. This may suggest a broad involvement of the product of *TaWXPL1D* in regulation of biochemical and physiological processes in wheat. By contrast, TaWXPL2B in the absence of stress may participate mostly in gene regulation in specific wheat tissues. Notable differences in levels of expression of *TaWXPL1D* and *TaWXPL2B* were observed in bracts. The highest expression levels of both genes were found in flowers.

Transcripts of both *WXP* genes from legume *Medicago truncatula* (Zhang et al. 2005, 2007), *RAP2.4* from *Arabidopsis* (Lin et al. 2008), *ZmDBF1* from maize (Kizis and Pagès 2002), *GmDREB2* from soybean (Chen et al. 2007), and other *WXP* homologues were reported to be up-regulated by ABA and abiotic stresses. We have compared expression of wheat WXPL genes under two different regimes of dehydration in two wheat genotypes with contrast drought tolerance. The impact on TF genes during stress is often rapid and transient: after some time the levels of transcripts return to initial levels, even if the stress factor is persisting. Therefore, changes in expression of TF genes with a short transient response are sometimes difficult to detect if the stress, e.g. drought, develops slowly. For these reasons we used two regimes of low water stress: rapid dehydration and slowly developing cyclic drought (Bi et al. 2016). The aim of the first experiment was to detect rapid and transient changes in expression of *WXPL* genes. The aim of the second experiment was to detect long-lasting and late-occurring changes in expression levels of *WXPL* genes under the conditions of two successive cycles of drought.

We found that both wheat *WXPL* genes are regulated by dehydration and drought. Similarly to drought-regulated cuticle-related *MYB* genes (Bi et al. 2016), reasonable correlation was observed for wheat *WXPL* genes for expression patterns under two regimes of dehydration in both Kukri and RAC875, with the exception of *TaWXPL2B* in Kukri. The *TaWXPL2B* gene in Kukri was clearly downregulated by rapid dehydration and transiently upregulated in the first cycle of drought, but was not significantly affected in RAC875 under the same dehydration regimes. Such behaviour may suggest that *TaWXPL2B* is regulated differently by different components of drought, and that expression of this gene depends on the component that prevails during a particular type or time of stress. *TaWXPL2B* may be an early-activated type of regulatory gene, which is initially triggered by something that is yet not clear under conditions of low level of dehydration, but later downregulated by increasing dehydration of drought-sensitive plants. The RAC875 cultivar is much better protected against drought, particularly the dehydration component, than Kukri. This characteristic was recently demonstrated by water-loss and chlorophyll-leaching tests (Bi et al. unpublished data). Therefore drought-responsive regulation of *TaWXPL2B* expression in RAC875 might not be required for the acquisition of drought tolerance.

The patterns of expression of *TaWXPL2B* and *TaMYB24* (Bi et al. 2016) are surprisingly similar in both studied wheat cultivars, suggesting their cooperation in activation of the same gene pools during dehydration.

The *TaWXPL1D* gene was not affected by either rapid dehydration or cyclic drought in the drought sensitive Kukri, but it was clearly upregulated under both stress regimes in the drought tolerant RAC875. This suggests a role of this gene in the development of high drought tolerance of RAC875.

TaWXPL1D may be an exciting candidate for engineering of enhanced drought tolerance. It would be interesting to overexpress this gene in Kukri or another drought-sensitive wheat genotype under a moderate constitutive or drought-responsive promoter, and to compare stress tolerance of the generated transgenic lines with stress tolerance of wild type plants.

As previously reported, the *Arabidopsis* orthologue of TaWXPL2 proteins, RAP2.4, can bind to different stress-responsive elements in gene promoters, including the ethylene-responsive GCC-box, dehydration-responsive element (DRE) (Lin et al. 2008) and the CGCG core of a CE3-like element (Shaikhali et al. 2008). Using a Y1H assay we have demonstrated that both WXPL proteins can bind to each of three tested *cis*-elements specific for ERFs and/or DREB TFs, but that they show obvious sequence binding preferences. The TaWXPL1D protein demonstrated higher affinity for the CRT (GCCGAC) element compared to two other *cis*-elements, DRE (ACCGAC) and GCC-box (GCCGCC), which this protein bound with similar low efficiency (Fig. 5A). By contrast, TaWXPL2B clearly preferred DRE to other tested elements, interacted less efficiently with CRT and even less efficiently with the GCC-box. Small differences in protein sequences were found between the AP2 domains of TaWXPL1D and TaWXPL2B, which are sufficient to provide different DNA-binding specificity and hence activation of diverse groups of target genes. Analysis of molecular models of protein-DNA interactions revealed possible bases of different binding strengths. To understand why TaWXPL1D better binds CRT (GCCGAC) and TaWXPL2B stronger binds DRE (ACCGAC), one should consider that a total of 13 and 14 respective hydrogen bonds to nucleobases are formed in protein-DNA complexes. In other words, there are different hydrogen bond distributions in both complexes; it has been estimated that a loss of one hydrogen bond corresponds to approximately 1 kcal/mol (Fersht 1987). In the TaWXPL2B/DRE complex two unique hydrogen bonds are formed to nucleobases, while in the TaWXPL1D/CRT complex, one less hydrogen bond is present and simultaneously Arg125 forms two nearly identical hydrogen bonds to the antisense DNA strand (Supporting Table 3). Notably, no differences in the number of DNA phospho-diester backbone bonds were found between the two protein complexes.

Wheat WXPL proteins act as transcriptional activators. The C-terminal activation domains, WXCDs, were initially identified at the C-termini of all analysed WXP-like proteins (including representatives from other plants) as conserved sequences. The proposed function of WXCDs as activation domains was confirmed in in-yeast activation assays using truncated versions of TaWXPL1D and TaWXPL2B proteins (Fig. 5A).

A transient expression assay in wheat suspension cells was used to confirm the participation of drought-affected wheat WXPL TFs in transciptional activation of cuticle-related genes (Fig. 7). For these purposes, previously described promoters of *TaATT1*, *TaKCS1* and *TdSHN1* genes (Bi et

al. 2016) were tested as promoters of potential target genes of wheat WXPL TFs. The *TaATT1* gene encodes an enzyme from the cutin biosynthetic pathway, the *TaKCS1* gene encodes an enzyme from the wax biosynthetic pathway, and *TdSHN1* encodes a regulator of wax biosynthesis (Borisjuk et al. 2014). In our assay, the TaWXPL1D protein activated two (*TaATT1* and *TaKCS1*) promoters, and TaWXPL2B protein activated one (*TaKCS1*) promoter, and therefore both TFs may be considered as true cuticle biosynthesis-related regulators in wheat. Neither WXPL TFs activated the *TdSHN1* promoter. Hence, the WXPL TFs demonstrated selectivity in target gene activation and can potentially collaborate with cuticle biosynthesis-related MYB TFs during activation of the *TaATT1* and *TaKCS1* promoters.

The results of promoter activation in wheat cells are in a good agreement with the results of DNA binding selectivity obtained in the Y1H assay. *In silico* analysis of the promoter sequences of *TaATT1*, *TaKCS1* and *TdSHN1* (including 5'-UTRs) identified different representations of CRT, DRE and GCC-box elements (Table 2). It is plausible that TaWXPL2B, which demonstrated the highest affinity for DRE in the Y1H assay, requires this specific element for promoter activation, as it activated the *TaKCS1* promoter containing two DRE elements but did not activate the *TaATT1* promoter, which has no DRE elements. By contrast, TaWXPL1D showed highest affinity for CRT in the Y1H assay, and activated both *TaATT1* and *TaKCS1* promoters, which have four and two CRT elements, respectively. Inability of either of wheat WXPL TFs to activate the *TdSHN1* promoter is a logical consequence of the absence of the corresponding *cis*-elements. A single DRE of this promoter might be inactive because of its position or adjacent sequences; alternatively the activation through these elements requires cooperation of DREB/ERF with other TFs/co-factors, which may be essential for a strong binding and/or activation of the *TdSHN1* promoter.

The transient expression assay we used for confirmation and analysis of wheat cuticle-related TFs is relatively robust, rapid and reliable. The use of a wheat cell suspension culture for transient expression is a good option for the preliminary confirmation of regulatory effects of TFs on particular promoters, and also provides a convenient method for verification of DNA constructs for stable gene overexpression or for component delivery in emerging genome editing technologies (Baltes and Voytas 2015). This approach provides several other advantages, including the possibility to test promoter activation by two or more TFs simultaneously and to identify functional *cis*-elements on promoters (Bi et al. 2016; Eini et al. 2013).

Scheme 1 is an extended version of an earlier published scheme (Bi et al. 2016). It summarises our findings of the activation of cuticle biosynthetic pathways in wheat by drought-inducible TFs TaWXPL1, TaWXPL2, TaMYB31 and TaMYB74, homologues of the well-characterised cuticle biosynthesis regulators MtWXP1 and MtWXP2 (Zhang et al. 2005, 2007), AtMYB96 (Seo et al.

2011) and AtMYB41 (Cominelli et al. 2008). Expression of all four wheat TFs was upregulated by drought and/or dehydration, and three of them activated both *ATT1* and *KCS1* genes through direct binding to their promoters, albeit with different efficiencies (Bi et al. 2016). Further experiments are required to elucidate cooperative regulation of the *TaATT1* and *TaKCS1* promoters by WXPL and MYB TFs.

In conclusion, differences in expression patterns of *TaWXPL2B* and *TaWXPL1D* under dehydration together with variances in DNA binding selectivity of the corresponding proteins strongly advocate the possible involvement of wheat WXPL TFs in regulation of different sets of genes related to cuticle biosynthesis, although some overlap in function may exist. Transient expression assay data, demonstrating activation of the *TaKCS1* promoter by both WXPL TFs but activation of the *TaATT1* promoter only by TaWXPL1D, strongly support this hypothesis. Characterisation of WXP homologues in other plant species suggests that in addition to regulating cuticle amount and quality as we have demonstrated in this study, wheat WXPL TFs could also confer drought tolerance through different pathways, *e.g.* through the modulation of water homeostasis by downregulation of aquaporin genes (Rae et al. 2011) or by increasing free proline content (Chen et al. 2007). Further research should be aimed at investigation of other WXPL roles in wheat.

Acknowledgments

We thank Dr Julie Hayes for critically reading the manuscript. The China Scholarship Council and the University of Adelaide are acknowledged for providing HB a joint postgraduate scholarship. This work was supported by the Australian Centre for Plant Functional Genomics, and by the Australian Research Council (to MH and SL), the Grains Research & Development Corporation and the Government of South Australia.

Author contributions statement: HB performed most of the experiments. NB and YL assisted with experiments. SLu and MH performed molecular modelling. SLo, NBo and MH guided research and wrote the manuscript.

Compliance with ethical standards: Conflict of interest Authors declare that they have no conflict of interest.

References

Aharoni A, Dixit S, Jetter R, Thoenes E, van Arkel G, Pereira A (2004) The SHINE clade of AP2 domain transcription factors activates wax biosynthesis, alters cuticle properties, and confers drought tolerance when overexpressed in *Arabidopsis*. Plant Cell 16:2463-2480

Allen MD, Yamasaki K, Ohme-Takagi M, Tateno M, Suzuki M (1998) A novel mode of DNA recognition by a beta-sheet revealed by the solution structure of the GCC-box binding domain in complex with DNA. EMBO J 17:5484-5496

Amalraj A, Luang S, Kumar MY, Sornaraj P, Eini O, Kovalchuk N, Bazanova N, Li Y, Yang N, Eliby S, Langridge P, Hrmova M, Lopato S (2016) Change of function of the wheat stress-responsive transcriptional repressor TaRAP2.1L by repressor motif modification. Plant Biotechnol J 14:820-832

Bailey TL, Bodén M, Buske FA, Frith M, Grant CE, Clementi L, Ren J, LI WW, Noble WS (2009) MEME SUITE: tools for motif discovery and searching. Nucleic Acids Res 37:W202-W208

Baker SS, Wilhelm KS, Thomashow MF (1994) The 5′-region of *Arabidopsis thaliana cor15a* has *cis*-acting elements that confer cold-, drought-and ABA-regulated gene expression. Plant Mol Biol 24:701-713

Baltes NJ, Voytas DF (2015) Enabling plant synthetic biology through genome engineering. Trends Biotechnol 33:120-131

Beisson F, Koo AJ, Ruuska S, Schwender J, Pollard M, Thelen JJ, Paddock T, Salas JJ, Savage L, Milcamps A, Mhaske VB, Cho Y, Ohlrogge JB (2003) *Arabidopsis* genes involved in acyl lipid metabolism. A 2003 census of the candidates, a study of the distribution of expressed sequence tags in organs, and a web-based database. Plant Physiol 132:681-697

Bennett D, Izanloo A, Reynolds M, Kuchel H, Langridge P, Schnurbusch T (2012a) Genetic dissection of grain yield and physical grain quality in bread wheat (*Triticum aestivum* L.) under water-limited environments. Theor Appl Genet 125:255-271

Bennett D, Izanloo A, Edwards J, Kuchel H, Chalmers K, Tester M, Reynolds M, Schnurbusch T, Langridge P (2012b) Identification of novel quantitative trait loci for days to ear emergence and flag leaf glaucousness in a bread wheat (*Triticum aestivum* L.) population adapted to southern Australian conditions. Theor Appl Genet 124:697-711

Bi H, Luang S, Li Y, Bazanova N, Morran S, Song Z, Perera MA, Hrmova M, Borisjuk N, Lopato S Identification and characterization of wheat drought-responsive MYB transcription factors involved in the regulation of cuticle biosynthesis. J Exp Bot, doi:10.1093/jxb/erw298

Borisjuk N, Hrmova M, Lopato S (2014) Transcriptional regulation of cuticle biosynthesis. Biotechnol Adv 32:526-540

Bowne JB, Erwin TA, Juttner J, Schnurbusch T, Langridge P, Bacic A, Roessner U (2012) Drought responses of leaf tissues from wheat cultivars of differing drought tolerance at the metabolite level. Mol Plant 5:418-429

Bru C, Courcelle E, Carrère S, Beausse Y, Dalmar S, Kahn D (2005) The ProDom database of protein domain families: more emphasis on 3D. Nucleic Acids Res 33:D212-D215

Buxdorf K, Rubinsky G, Barda O, Burdman S, Aharoni A, Levy M (2014) The transcription factor SlSHINE3 modulates defense responses in tomato plants. Plant Mol Biol 84:37-47

Chen M, Wang QY, Cheng XG, Xu ZS, Li LC, Ye XG, Xia LQ, Ma YZ (2007) GmDREB2, a soybean DRE-binding transcription factor, conferred drought and high-salt tolerance in transgenic plants. Biochem Biophys Res Commun 353:299-305

Cheng J, Randall A, Sweredoski M, Baldi P (2005) SCRATCH: A protein structure and structural feature prediction server. Nucleic Acids Res 33:W72-W76

Cominelli E, Sala T, Calvi D, Gusmaroli G, Tonelli C (2008) Over-expression of the Arabidopsis *AtMYB41* gene alters cell expansion and leaf surface permeability. Plant J 53:53-64

Cui F, Brosché M, Lehtonen MT, Amiryousefi A, Xu E, Punkkinen M, Valkonen JP, Fujii H, Overmyer K (2016) Dissecting abscisic acid signaling pathways involved in cuticle formation. Mol Plant 9:926-938

Ecker JR (1995) The ethylene signal transduction pathway in plants. Science 268:667-675

Eini O, Yang N, Pyvovarenko T, Pillman K, Bazanova N, Tikhomirov N, Eliby S, Shirley N, Sivasankar S, Tingey S, Langridge P, Hrmova M, Lopato S (2013) Complex regulation by Apetala2 domain-containing transcription factors revealed through analysis of the stress-responsive *TdCor410b* promoter from durum wheat. PloS One 8:e58713

Elliott RC, Betzner AS, Huttner E, Oakes MP, Tucker WQ, Gerentes D, Perez P, Smyth DR (1996) *AINTEGUMENTA*, an *APETALA2*-like gene of *Arabidopsis* with pleiotropic roles in ovule development and floral organ growth. Plant Cell 8:155-168

Emsley P, Lohkamp B, Scott WG, Cowtan K (2010) Features and development of Coot. Acta Crystallogr D66:486-501

Eswar N, Eramian D, Webb B, Shen MY, Sali A (2008) Protein structure modeling with MODELLER. Methods Mol Biol 426:145-159

Ferreira Neto JR, Pandolfi V, Guimaraes FC, Benko-Iseppon AM, Romero C, Silva RL, Rodrigues FA, Abdelnoor RV, Nepomuceno AL, Kido EA (2013) Early transcriptional response of soybean contrasting accessions to root dehydration. PLoS One 8:e83466

Fersht AR (1987) The hydrogen bond in molecular recognition. Trends Biochem Sci 12:301-304

Fletcher SJ (2014) qPCR for quantification of transgene expression and determination of transgene copy number. Methods Mol Biol 1145:213-237

Gasteiger E, Gattiker A, Hoogland C, Ivanyi I, Appel RD, Bairoch A (2003) ExPASy: the proteomics server for in-depth protein knowledge and analysis. Nucleic Acids Res 31:3784-3788

Gille C, Fähling M, Wey B, Wiel T, Gille A (2014) Alignment-annotator web server: rendering and annotating sequence alignments. Nucleic Acids Res 42:W3-W6

Giménez E, Dominguez E, Pineda B, Heredia A, Moreno V, Lozano R, Angosto T (2015) Transcriptional activity of the MADS box *ARLEQUIN*/*TOMATO AGAMOUS-LIKE1* gene is required for cuticle development of tomato fruit. Plant Physiol 168:1036-1048

Harris JC, Sornaraj P, Taylor M, Bazanova N, Baumann U, Lovell B, Langridge P, Lopato S, Hrmova M (2016) Molecular interactions of the gamma-clade homeodomain-leucine zipper class I transcription factors during the wheat response to water deficit. Plant Mol Biol 90:435-452

Higo K, Ugawa Y, Iwamoto M, Korenaga T (1999) Plant *cis*-acting regulatory DNA elements (PLACE) database: 1999. Nucleic Acids Res 27:297-300

Hrmova M, Lopato S (2014) Enhancing abiotic stress tolerance in plants by modulating properties of stress responsive transcription factors. In: Genomics of Plant Genetic Resources (Tuberosa R, Graner A, Frison E, eds.), Springer Netherlands, 515 pp, Volume 2, Part II: Crop productivity, food security and nutritional quality, pp 291-316

Huang B, Jin L, Liu JY (2007) Identification and characterization of the novel gene *GhDBP2* encoding a DRE-binding protein from cotton (*Gossypium hirsutum*). J Plant Physiol 165:214-223

Javelle M, Vernoud V, Depege-Fargeix N, Arnould C, Oursel D, Domergue F, Sarda X, Rogowsky PM (2010) Overexpression of the epidermis-specific homeodomain-leucine zipper IV transcription factor Outer Cell Layer1 in maize identifies target genes involved in lipid metabolism and cuticle biosynthesis. Plant Physiol 154:273-286

Jetter R, Kunst L (2008) Plant surface lipid biosynthetic pathways and their utility for metabolic engineering of waxes and hydrocarbon biofuels. Plant J 54:670-683

Jetter R, Kunst L, Samuels AL (2006) Composition of plant cuticular waxes. Blackwell Publishing, Oxford

Jin J, Zhang H, Kong L, Gao G, Luo J (2014) PlantTFDB 3.0: a portal for the functional and evolutionary study of plant transcription factors. Nucleic Acids Res 42: D1182-7

Johnson PF, Sterneck E, Williams SC (1993) Activation domains of transcriptional regulatory proteins. J Nutr Biochem 4:386-398

Kannangara R, Branigan C, Liu Y, Penfield T, Rao V, Mouille G, Höfte H, Pauly M, Riechmann JL, Broun P (2007) The transcription factor WIN1/SHN1 regulates Cutin biosynthesis in *Arabidopsis thaliana*. Plant Cell 19:1278-1294

Kizis D, Pagès M (2002) Maize DRE-binding proteins DBF1 and DBF2 are involved in *rab17* regulation through the drought-responsive element in an ABA-dependent pathway. Plant J 30:679-89

La Rocca N, Manzotti PS, Cavaiuolo M, Barbante A, Dalla Vecchia F, Gabotti D, Gendrot G, Horner DS, Krstajic J, Persico M, Rascio N, Rogowsky P, Scarafoni A, Consonni G (2015) The maize *fused leaves1* (*fdl1*) gene controls organ separation in the embryo and seedling shoot and promotes coleoptile opening. J Exp Bot 66:5753-5767

Laskowski RA, Macarthur MW, Moss DS, Thornton JM (1993) PROCHECK: a program to check the stereochemical quality of protein structures. J Appl Crystall 26:283-291

Letunic I, Doerks T, Bork P (2015) SMART: recent updates, new developments and status in 2015. Nucleic Acids Res 43:D257-260

Li-Beisson Y, Shorrosh B, Beisson F, Andersson MX, Arondel V, Bates PD, Baud S, Bird D, Debono A, Durrett TP, Franke RB, Graham IA, Katayama K, Kelly AA, Larson T, Markham JE, Miquel M, Molina I, Nishida I, Rowland O, Samuels L, Schmid KM, Wada H, Welti R, Xu C, Zallot R, Ohlrogge J (2010) Acyl-lipid metabolism. The Arabidopsis book / American Society of Plant Biologists 8:e0133

Licausi F, Ohme-Takagi M, Perata P (2013) APETALA2/Ethylene Responsive Factor (AP2/ERF) transcription factors: mediators of stress responses and developmental programs. New Phytol 199:639-649

Lin RC, Park HJ, Wang HY (2008) Role of *Arabidopsis* RAP2.4 in regulating light- and ethylene-mediated developmental processes and drought stress tolerance. Mol Plant 1:42-57

Liu Y, Chen H, Zhuang D, Jiang D, Liu J, Wu G, Yang M, Shen S (2010) Characterization of a DRE-binding transcription factor from Asparagus (*Asparagus officinalis* L.) and its overexpression in *Arabidopsis* resulting in salt-and drought-resistant transgenic plants. Int J Plant Sci 171:12-23

Mizoi J, Shinozaki K, Yamaguchi-Shinozaki K (2012) AP2/ERF family transcription factors in plant abiotic stress responses. Biochim Biophys Acta 1819:86-96

Morran S, Eini O, Pyvovarenko T, Parent B, Singh R, Ismagul A, Eliby S, Shirley N, Langridge P, Lopato S (2011) Improvement of stress tolerance of wheat and barley by modulation of expression of DREB/CBF factors. Plant Biotechnol J 9:230-249

Nei M, Kumar S (2000) Molecular Evolution and Phylogenetics. Oxford University Press Inc, New York, NY

Ohme-Takagi M, Shinshi H (1995) Ethylene-inducible DNA binding proteins that interact with an ethylene-responsive element. Plant Cell 7:173-182

Porter J, Semenov M (2005) Crop responses to climatic variation. Philos Trans R Soc Biol Sci 360:2021–2035

Pei JM, Tang M, Grishin NV (2008) PROMALS3D web server for accurate multiple protein sequence and structure alignments. Nucleic Acids Res 36:W30–W34

Pyvovarenko T, Lopato S (2011) Isolation of plant transcription factors using a yeast one-hybrid system. Methods Mol Biol 754:45-66

Rae L, Lao NT, Kavanagh TA (2011) Regulation of multiple aquaporin genes in Arabidopsis by a pair of recently duplicated DREB transcription factors. Planta. 234:429-444

Reynolds M, Foulkes J, Furbank R, Griffiths S, King J, Murchie E, Parry M, Slafer G (2012) Achieving yield gains in wheat. Plant Cell Env 35:1799-1823

Saitou N, Nei M (1987) The neighbor-joining method: a new method for reconstructing phylogenetic trees. Mol Biol Evol 4:406-425

Sali A, Blundell TL (1993) Comparative protein modelling by satisfaction of spatial restraints. J Mol Boil 234: 779-815

Schymkowitz JW, Rousseau F, Martins IC, Ferkinghoff-Borg J, Stricher F, Serrano L (2005) Prediction of water and metal binding sites and their affinities by using the Fold-X force field. Proceed Natl Acad Sci USA 102:10147-10152

Shen MY, Sali A. (2006) Statistical potential for assessment and prediction of protein structures. Protein Sci 15:2507-2524

Sela D, Buxdorf K, Shi JX, Feldmesser E, Schreiber L, Aharoni A, Levy M (2013) Overexpression of AtSHN1/WIN1 provokes unique defense responses. PLoS One 8:e70146

Seo PJ, Lee SB, Suh MC, Park MJ, Go YS, Park CM (2011) The MYB96 transcription factor regulates cuticular wax biosynthesis under drought conditions in Arabidopsis. Plant Cell 23:1138-1152

Seo PJ, Park CM (2011) Cuticular wax biosynthesis as a way of inducing drought resistance. Plant Signal Behav 6:1043-1045

Shaikhali J, Heiber I, Seidel T, Ströher E, Hiltscher H, Birkmann S, Dietz KJ, Baier M (2008) The redox-sensitive transcription factor Rap2.4a controls nuclear expression of 2-Cys peroxiredoxin A and other chloroplast antioxidant enzymes. BMC Plant Biol 8:48

Shi JX, Adato A, Alkan N, He Y, Lashbrooke J, Matas AJ, Meir S, Malitsky S, Isaacson T, Prusky D, Leshkowitz D, Schreiber L, Granell AR, Widemann E, Grausem B, Pinot F, Rose JK, Rogachev I, Rothan C, Aharoni A (2013) The tomato SlSHINE3 transcription factor regulates fruit cuticle formation and epidermal patterning. New Phytol 197: 468-480

Shi JX, Malitsky S, De Oliveira S, Branigan C, Franke RB, Schreiber L, Aharoni A (2011) SHINE transcription factors act redundantly to pattern the archetypal surface of Arabidopsis flower organs. PLoS Genet 7:e1001388

Sippl MJ (1993) Recognition of errors in three-dimensional structures of proteins. Proteins 17:355-362

Sun J, Peng X, Fan W, Tang M, Liu J, Shen S (2014) Functional analysis of *BpDREB2* gene involved in salt and drought response from a woody plant *Broussonetia papyrifera*. Gene 535:140-149

Tamura K, Stecher G, Peterson D, Filipski A, Kumar S (2013) MEGA6: Molecular Evolutionary Genetics Analysis version 6.0. Mol Biol Evol 30:2725-2729

McWilliam H, Li W, Uludag M, Squizzato S, Park YM, Buso N, Cowley AP, Lopez R (2013) Analysis tool web services from the EMBL-EBI. Nucleic Acids Res 41:W597-600

Xu Y, Wu H, Zhao M, Wu W, Xu Y, Gu D (2016) Overexpression of the transcription factors GmSHN1 and GmSHN9 differentially regulates wax and cutin biosynthesis, alters cuticle properties, and changes leaf phenotypes in *Arabidopsis*. Int J Mol Sci 17, pii: E587. doi: 10.3390/ijms17040587

Yamaguchi-Shinozaki K, Shinozaki K (1994) A novel *cis*-acting element in an *Arabidopsis* gene is involved in responsiveness to drought, low-temperature, or high-salt stress. Plant Cell 6: 251-264

Yang J, Isabel Ordiz M, Jaworski JG, Beachy RN (2011) Induced accumulation of cuticular waxes enhances drought tolerance in *Arabidopsis* by changes in development of stomata. Plant Physiol Biochem 49:1448-1455

Yeats TH, Rose JK (2013) The formation and function of plant cuticles. Plant Physiol 163:5-20

Zhang JY, Broeckling CD, Blancaflor EB, Sledge MK, Sumner LW, Wang ZY (2005) Overexpression of WXP1, a putative *Medicago truncatula* AP2 domain-containing transcription factor gene, increases cuticular wax accumulation and enhances drought tolerance in transgenic alfalfa (*Medicago sativa*). Plant J 42:689-707

Zhang JY, Broeckling CD, Sumner LW, Wang ZY (2007) Heterologous expression of two *Medicago truncatula* putative ERF transcription factor genes, *WXP1* and *WXP2*, in *Arabidopsis* led to increased leaf wax accumulation and improved drought tolerance, but differential response in freezing tolerance. Plant Mol Biol 64:265-278

Figure Legends

Figure 1. Phylogenetic analysis of ERF TFs. (A) The tree consists of 130 protein sequences, including five derived from cloned *TaWXPL* genes in this study, eight homologs from other species, 11 wheat ERF sequences retrieved from NCBI and 106 wheat ERF sequences from the PlantTFDB database (http://planttfdb.cbi.pku.edu.cn). Sequences were aligned by ClustalW and a bootstrap consensus tree was generated using the Neighbour-Joining method in MEGA6 (Tamura et al. 2013). The branch with protein sequences (indicated by dots) derived from cloned genes is highlighted in cyan. (B) Multiple sequence alignment (Gille et al. 2014) of 14 selected sequences (contained in the branch highlighted in blue lines in panel (A) illustrating a conserved WXCD domain. The black box indicates the boundaries of this domain, and the positions of conserved negatively (red) and positively (cyan) charged residues. Secondary structure elements (line: disordered region, α-helix: red/grey) are shown below the sequences.

Figure 2. Expression profiles of *TaWXPL1D* and *TaWXPL2B* in wheat tissues (cultivar Chinese Spring) revealed by Q-PCR. DAP - days after pollination; germ. - germinating. Error bars indicate the standard error of three biological replicates.

Figure 3. Expression of wheat *WXPL* genes in rapidly dehydrating flag leaves of two wheat genotypes, Kukri and RAC875, with contrasting drought tolerance. Expression of *TaWXPL1D* and *TaWXPL2B* was studied by Q-PCR. (A) Appearance of flag leaves, peduncles and spikes of Kukri and RAC875 plants. (B) Expression of wheat *WXPL* genes in rapidly dehydrating flag leaves. Flag leaf samples were sampled at awn emergence. Dehydration was performed using detached flag leaves incubated at ambient temperature for 0, 2, 4 and 7 hours (h). Two-way ANOVA with the Fisher's Least Significant Difference post-hoc test was conducted using GenStat. Error bars indicate the standard errors of three biological replicates.

Figure 4. Expression of wheat *WXPL* genes under cyclic drought in flag leaves of two wheat genotypes, Kukri and RAC875, with contrasting drought tolerance. Expression of *TaWXPL1D* and *TaWXPL2B* was studied by Q-PCR. Expression of genes was examined after 5, 9, 14, 23 and 25 days (d), using either well-watered (WW) or cyclic drought-exposed (DR) plants. Three cycles of drought were applied at 0, 15 and 24 days; times of watering and two re-watering events are indicated with arrows. Two-way ANOVA with the Fisher's Least Significant Difference post-hoc test was conducted using GenStat. Error bars indicate the standard errors of three biological replicates.

Figure 5. Analysis of activation (A) and DNA-binding (B) properties of the TaWXPL1D and TaWXPL2B proteins. (A) Transcriptional activation assays and the localisation of activation domains of wheat WXPL proteins. The assay was performed in yeast using full-length and N- or C-terminal truncated WXPL TFs fused to a binding domain (BD) of yeast GAL4 TF. An empty pGBKT7 plasmid was used as a negative control. -Trp represents SD medium lacking tryptophan (selection for plasmid presence) and -Trp/-His, 5mM 3AT refers to the SD medium without tryptophan and histidine but containing 5mM 3-amino-1,2,4-triazole (3AT) (selection for activation of the yeast *HIS3* gene). Domain structures and positions of truncations are indicated in the right part of Fig. 5A. AP2 - APETALA 2 DNA binding domain. D1, D2 and D3 represent removed protein fragments; the residue positions of truncation positions are indicated. (B) DNA-binding selectivity of wheat WXPL proteins shown in the Y1H assay. Each of the constructs expressing recombinant AD-WXPL proteins was transformed into each of four yeast strains (based on Y187) with integrated tandem repeats of DRE, CRT, GCC-box and HDZ1 *cis*-elements upstream of a minimal promoter of the reporter gene. Yeast transformants carrying the plasmids were selected on synthetic defined (SD) (-Leu) medium and replica-plated to SD2 (-Leu, -His, 10mM 3AT) medium. The ability of transformants to grow on SD2 medium suggested an interaction of wheat WXPL proteins with corresponding *cis*-elements.

Figure 6. Molecular features of wheat WXPL proteins in complex with DNA *cis*-elements. (A) The sequence alignment of AP2 domains of TaWXPL1D, TaWXPL2B and AtERF1. Identical residues between the template and target sequences are coloured; colouring based on the properties of the amino acid residues. Secondary structure elements are indicated above the sequences (C: coil, S: sheet, H: α-helix). Boxed residues indicate the positions of residues that form interactions with DNA *cis*-elements. (B) Ribbon representations show the disposition of secondary structures, where antiparallel strands carry the residues that contact DNA *cis*-elements. Structural models of TaWXPL1D and TaWXPL2B are coloured in green and cyan, respectively. The antisense strands of CRT 5′-GTCGGC-3′, DRE 5′-GTCGGT-3′, and GCC 5′-GGCGGC-3′ *cis*-elements are shown in sticks, whereby the sixth bases ($C_{6'}$ or $T_{6'}$) are coloured in cpk yellow. The nucleobases at the first (G_1 or A_1), fourth (G_4) and fifth (A_5) positions of DNA sense strands are shown in sticks, and the first nucleobases are coloured in cpk yellow. Interactions between amino acid residues and DNA *cis*-elements are shown as dashed lines at 2.5 Å to 3.5 Å separations.

Figure 7. Activation of promoters of cuticle-related genes *TaATT1* and *TaKCS1* by wheat WXPL TFs, as revealed by a transient expression assay in a wheat suspension culture. (A) Schematic showing DNA constructs used in the transient expression assay. The reporter *GUS* gene was driven by one of two promoters of cuticle biosynthesis genes, *TaATT1* or *TaKCS1*. In effector constructs, wheat *WXPL* genes were cloned under the control of the ubiquitin promoter. *GFP* served as a negative control. (B) Activation of *GUS* expression fused with promoters of *TaATT1* and *TaKCS1* by WXPL factors. Each reporter construct was co-bombarded with each effector and *GFP* construct into a wheat suspension culture. Student's t-test was performed for significant analysis of data. *, $P<0.05$; **, $P<0.01$. Error bars indicate the standard error of three replicates.

Scheme 1. The proposed roles of TaWXPL1D and TaWXPL2B TFs in regulation of cuticle biosynthesis during wheat response to drought. This scheme is a modification of a previously published scheme described in Bi et al. (2016).

Supporting Figure Legend

Supporting Figure 1. Multiple sequence alignment of wheat WXPL proteins from MtWXP1 and MtWXP2 clades suggests the presence of products of three homologous genes: the first group comprises homeologues of the *TaWXPL1* gene, the second group comprises homeologues of the *TaWXPL2* gene, while the remainder of the sequences are protein products of the third, yet uncharacterised *WXPL* gene. APETALA2 (AP2) domain and C-terminal activation domain are underlined.

Table 1. Cloned wheat *WXPL* genes. Their locations on wheat chromosomes are based on *in silico* analysis using the IWGSC NRGene Assembly database.

Cloned wheat genes	GenBank accession number	Length of CDS (bp)	Genetic location	Protein sequence identity to MtWXP1	Protein sequence identity to MtWXP2
TaWXPL1A	KX611869	855	5AL	35.6%	37.4%
TaWXPL1B	KX611870	855	5BL	35.4%	38.3%
TaWXPL1D	KX611871	855	5DL	36.1%	38.0%
TaWXPL2B	KX611872	1002	6BL	36.8%	43.1%
TaWXPL2D	KX611873	1011	6DL	37.4%	42.9%

Table 2. Numbers of DREB- and ERF-specific *cis*-elements in promoters of cuticle biosynthesis-related genes, and their status of activation by wheat WXPL TFs (*cf*. Fig. 7B).

Promoter	Number of CRTs	Number of DREs	Number of GCC-boxes	Activation by TaWXPL1D	Activation by TaWXPL2B
TaKCS1	2	2	-	+	+
TaATT1	4	-	3	+	-
TdSHN1	-	1	-	-	-

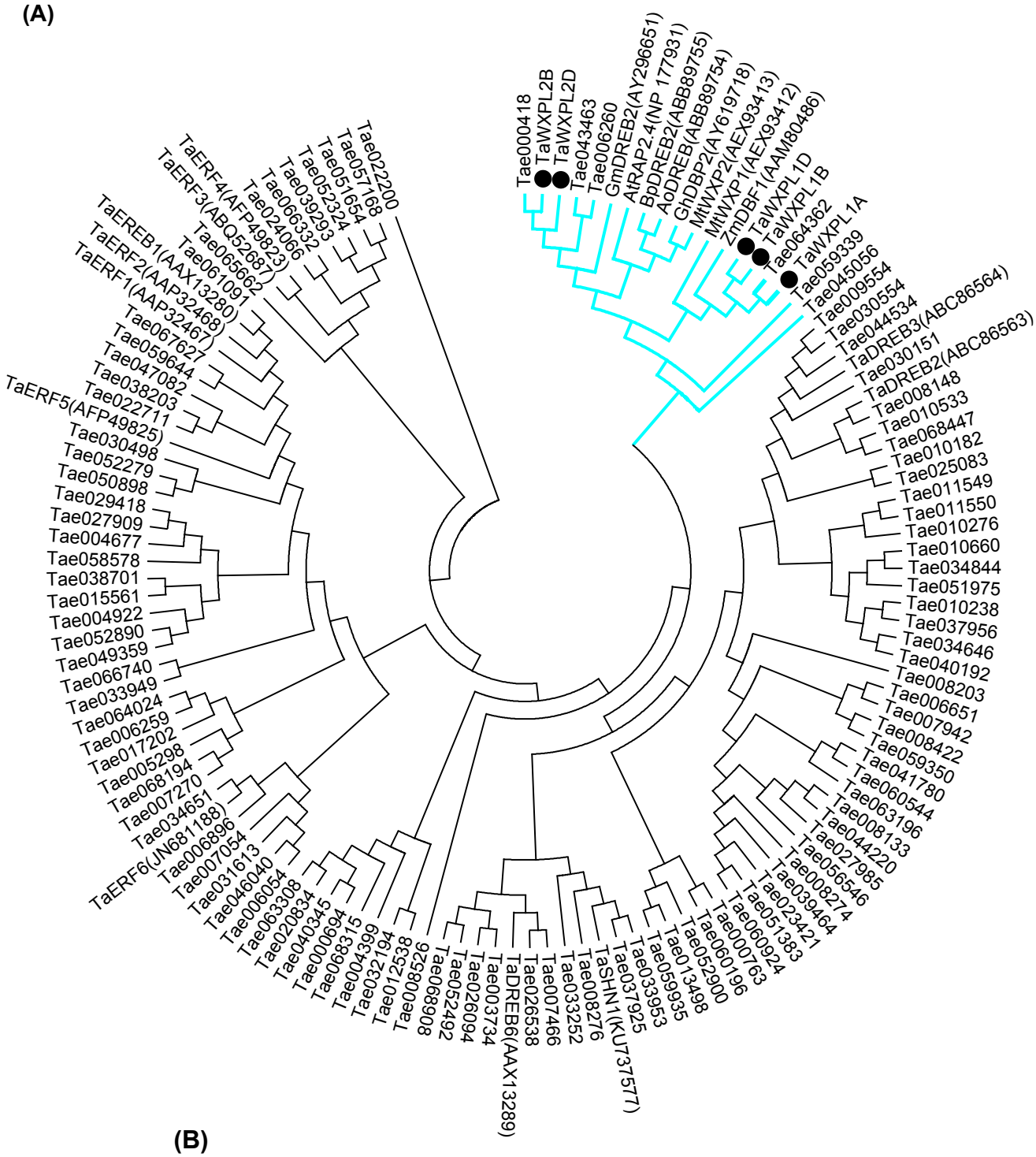
(A)
Tae000418
TaWXPL2B
TaWXPL2D
Tae043463
Tae006260
GmDREB2(AY296651)
AtRAP2.4(NP 177931)
BpDREB2(ABB89755)
AoDREB(ABB89754)
GhDBP2(AY619718)
MtWXP2(AEX93413)
MtWXP1(AEX93412)
ZmDBF1(AAM80486)
TaWXPL1D
TaWXPL1B
TaWXPL1A
Tae064362
Tae059339
Tae045056
Tae009554
Tae030554
Tae044534
TaDREB3(ABC86564)
TaDREB2(ABC86563)
Tae030151
Tae008148
Tae010533
Tae068447
Tae010182
Tae025083
Tae011549
Tae011550
Tae010276
Tae010660
Tae034844
Tae051975
Tae010238
Tae037956
Tae034646
Tae040192
Tae008203
Tae006651
Tae007942
Tae008422
Tae059350
Tae041780
Tae060544
Tae063196
Tae008133
Tae044220
Tae027985
Tae056546
Tae008274
Tae039464
Tae023421
Tae051383
Tae060924
Tae000763
Tae060196
Tae052900
Tae013498
Tae059935
Tae033953
Tae037925
TaSHN1(KU737577)
Tae033252
Tae008276
Tae007466
TaDREB6(AAX13289)
Tae026538
Tae003734
Tae026094
Tae052492
Tae008526
Tae068908
Tae012538
Tae032194
Tae004399
Tae068315
Tae000694
Tae040345
Tae020834
Tae063308
Tae006054
Tae046040
Tae031613
Tae007054
Tae006896
TaERF6(JN681188)
Tae034651
Tae007270
Tae068194
Tae005298
Tae017202
Tae006259
Tae064024
Tae033949
Tae066740
Tae049359
Tae052890
Tae004922
Tae015561
Tae038701
Tae058578
Tae004677
Tae027909
Tae029418
Tae050898
Tae052279
Tae030498
TaERF5(AFP49825)
Tae022711
Tae038203
Tae047082
Tae059644
Tae067627
TaERF1(AAP32467)
TaERF2(AAP32468)
TaEREB1(AAX13280)
Tae061091
Tae065662
TaERF3(ABQ52687)
TaERF4(AFP49823)
Tae024066
Tae066332
Tae039293
Tae052324
Tae051654
Tae057168
Tae022200
(B)
TaWXPL1A 238 PAATTAAEVPEMQQLDFSEAPWD-----EAACFALTKYPSYEIDWDSLLAAN
TaWXPL1B 238 PAATTAADVPEMQQLDFSEAPWD-----EAACFALTKYPSYEIDWDSLLATN
TaWXPL1D 238 PATTTAAEVPEMQQLDFSEAPWD-----EAACFALTKYPSYEIDWDSLLATN
TaWXPL2B 293 PTP----PVPEMEKLDFTEAPWD-----ESETFHLRKYPSVEIDWDSILS--
TaWXPL2D 296 PTP----PVPEMEKLDFTEAPWD-----ESETFHLRKYPSVEIDWDSILS--
MtWXP1 330 SDD--SSPLSDLTFGEFAEPQWEN----GFEQFNLQKFPSYEIDWASL----
GhDBP2 302 EGSAVSSPLSDLTFSDFDEQPWPE-VVSSSETFMLSKYPS-EIDWDSILKA-
ZmDBF1 177 PTPVVAPPVADMGQLDFSEVPWD-----EDESFVLRKYPSYEIDWDALLSN-
AoDREB 199 N-----SPVSEIESLDFNEVPWD-----ETEDFVLRKYPSYEIDWDSILSSA
BpDREB2 292 SS----SPESDVTLLDFSDS-----HWDGNENFGLGKYPSVEIDWDAL----
GmDREBb 269 SS----SPESSVTFLDFSDFSDSNNQWDEMENFGLEKFPSVEIDWEAI----
AtRAP2 294 AG---SSPLSDLTFADPEEPPQ------WNETFSLEKYPSYEIDWDSILA--
Tae043463 240 EVSSCSDVVPEMQLLDFSEAPWD--------ESLLRKYPSLEIDWDAILP--
Tae006260 240 EVSSCSDVVPEMQLLDFSEAPWD--------ESLLRKYPSLEIDWDAILS--

Figure 1

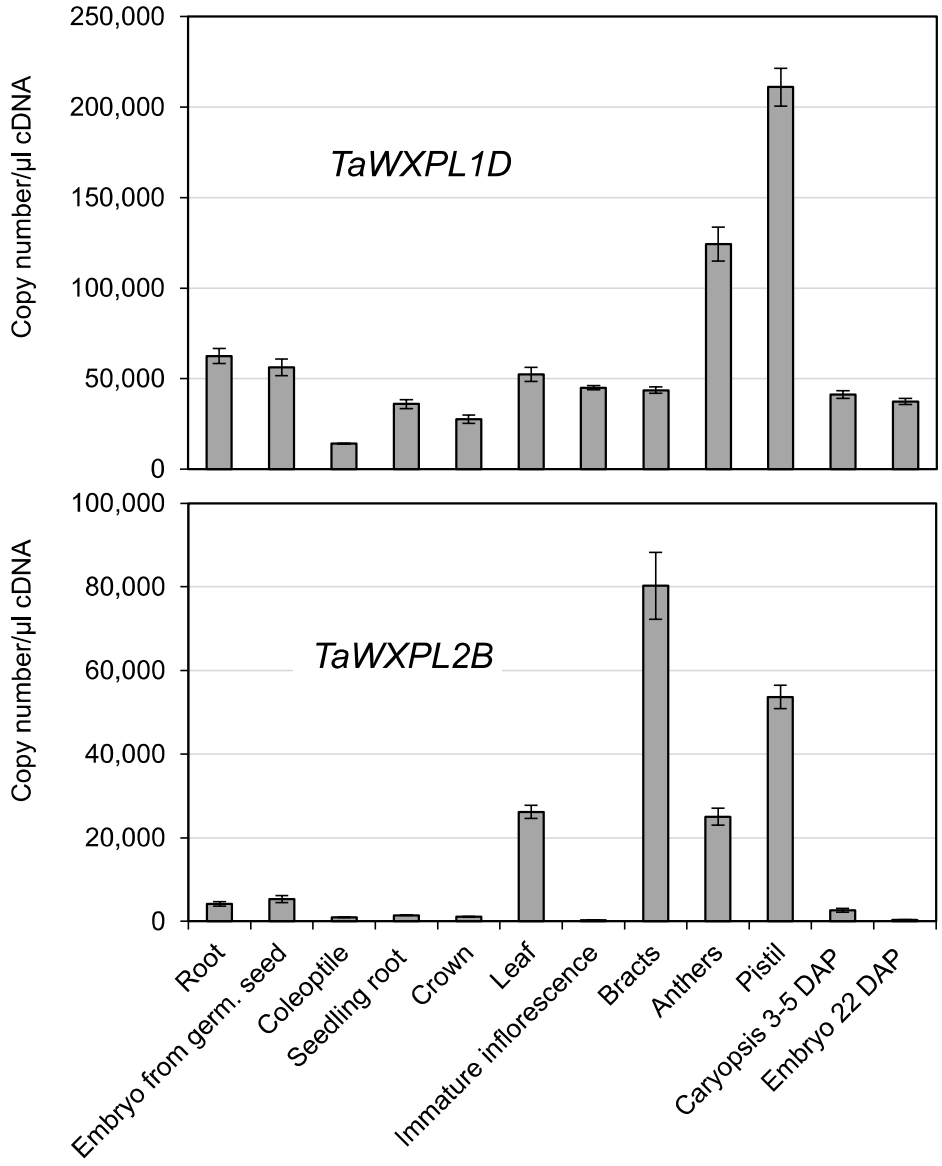
TaWXPL1D
Copy number/µl cDNA
250,000
200,000
150,000
100,000
50,000
0
TaWXPL2B
Copy number/µl cDNA
100,000
80,000
60,000
40,000
20,000
0
Root
Embryo from germ. seed
Coleoptile
Seedling root
Crown
Leaf
Immature inflorescence
Bracts
Anthers
Pistil
Caryopsis 3-5 DAP
Embryo 22 DAP

Figure 2

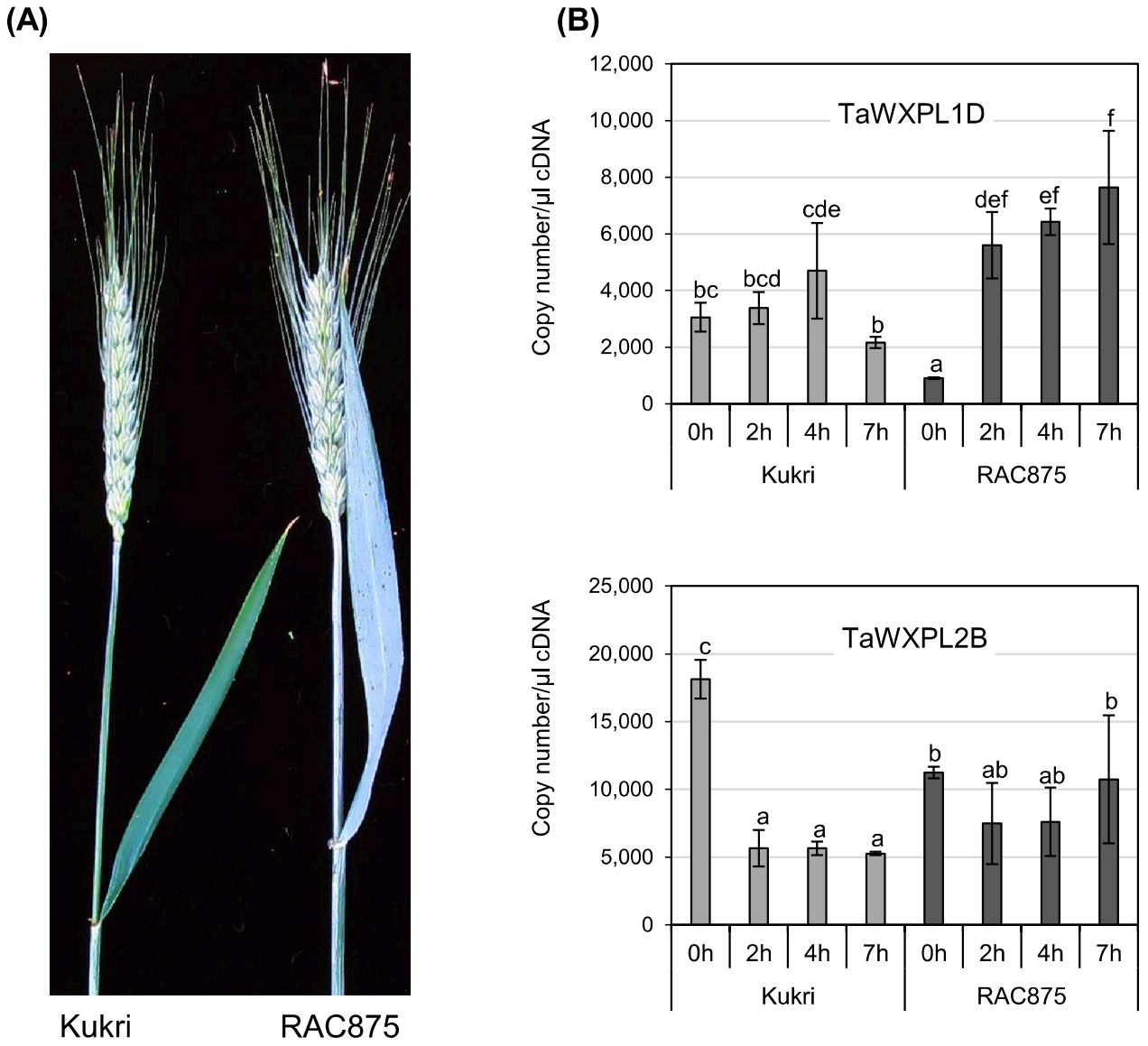
(A)
(B)
Kukri
RAC875
TaWXPL1D
Copy number/µl cDNA
12,000
10,000
8,000
6,000
4,000
2,000
0
bc
bcd
cde
b
a
def
ef
f
0h
2h
4h
7h
0h
2h
4h
7h
Kukri
RAC875
TaWXPL2B
Copy number/µl cDNA
25,000
20,000
15,000
10,000
5,000
0
c
a
a
a
b
ab
ab
b
0h
2h
4h
7h
0h
2h
4h
7h
Kukri
RAC875

Figure 3

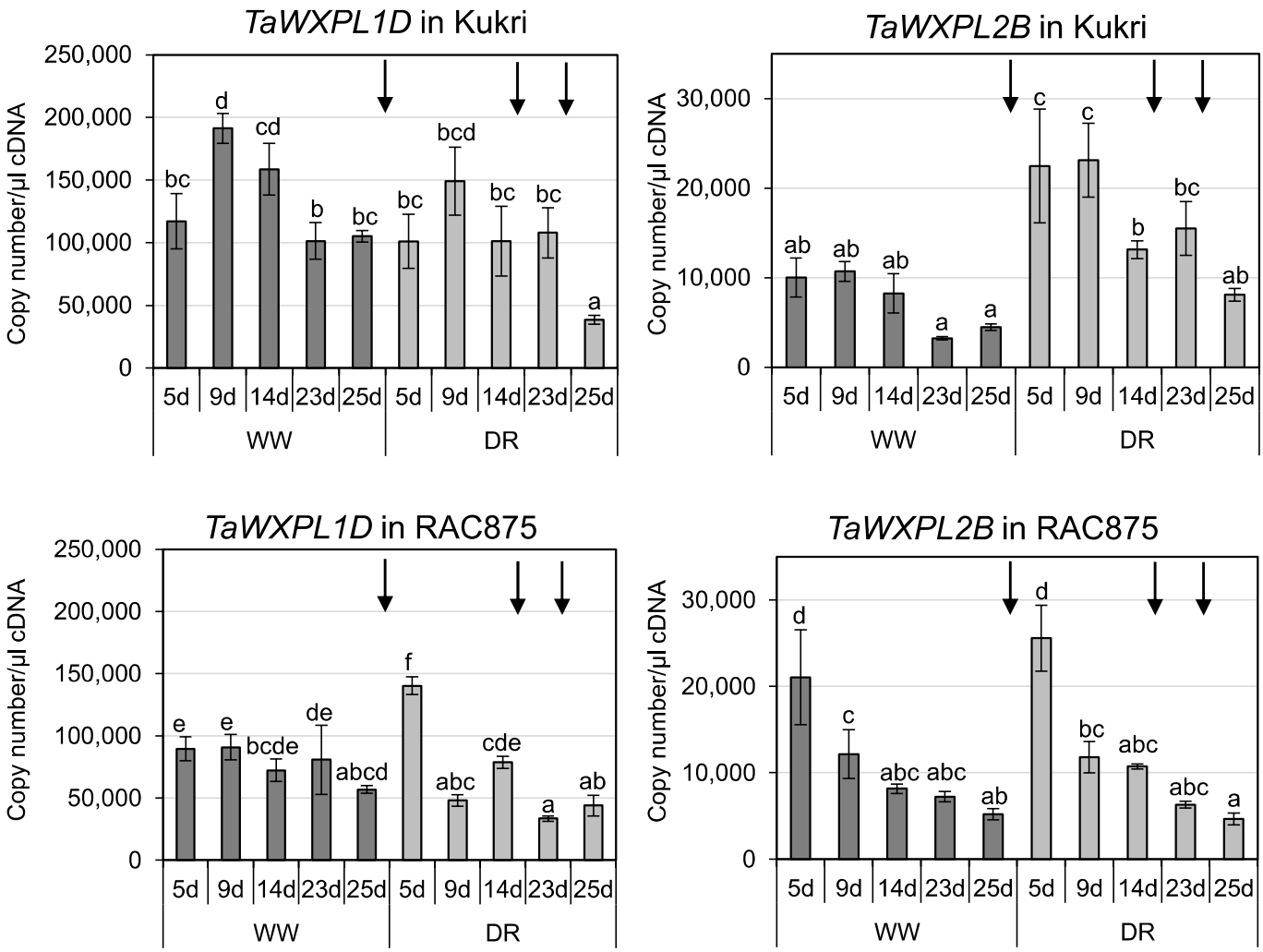
TaWXPL1D in Kukri
Copy number/µl cDNA
250,000
200,000
150,000
100,000
50,000
0
bc d cd b bc bc bcd bc bc a
5d 9d 14d 23d 25d 5d 9d 14d 23d 25d
WW DR
TaWXPL2B in Kukri
Copy number/µl cDNA
30,000
20,000
10,000
0
ab ab ab a a c c b bc ab
5d 9d 14d 23d 25d 5d 9d 14d 23d 25d
WW DR
TaWXPL1D in RAC875
Copy number/µl cDNA
250,000
200,000
150,000
100,000
50,000
0
e e bcde de abcd f abc cde a ab
5d 9d 14d 23d 25d 5d 9d 14d 23d 25d
WW DR
TaWXPL2B in RAC875
Copy number/µl cDNA
30,000
20,000
10,000
0
d c abc abc ab d bc abc abc a
5d 9d 14d 23d 25d 5d 9d 14d 23d 25d
WW DR

Figure 4

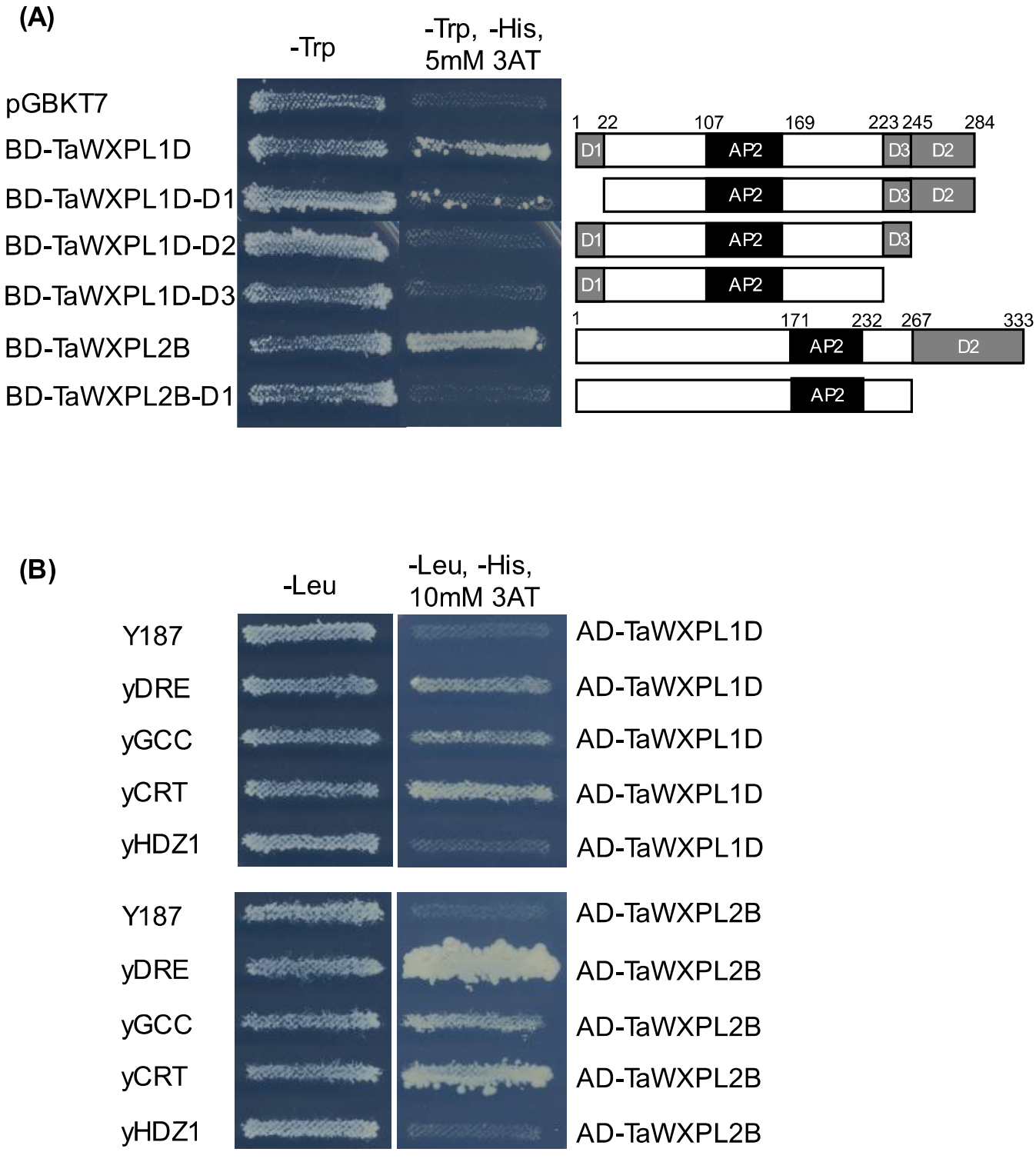
(A)
-Trp
-Trp, -His,
5mM 3AT
pGBKT7
BD-TaWXPL1D
BD-TaWXPL1D-D1
BD-TaWXPL1D-D2
BD-TaWXPL1D-D3
BD-TaWXPL2B
BD-TaWXPL2B-D1
1 22 107 169 223 245 284
D1
AP2
D3
D2
1 171 232 267 333
(B)
-Leu
-Leu, -His,
10mM 3AT
Y187
yDRE
yGCC
yCRT
yHDZ1
AD-TaWXPL1D
AD-TaWXPL2B

Figure 5

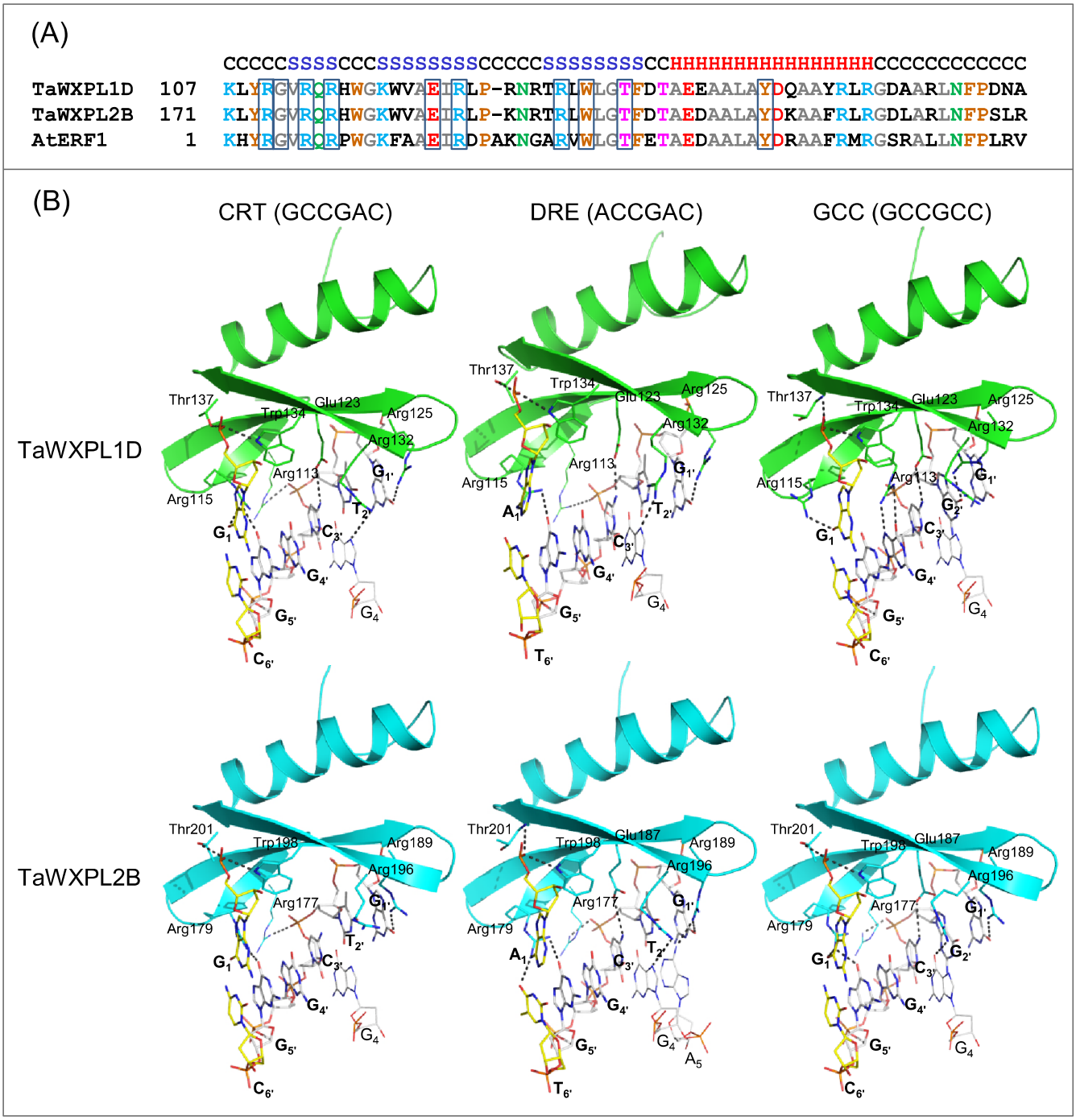
(A)
CCCCCSSSSCCCSSSSSSSSCCCCCSSSSSSSSCCHHHHHHHHHHHHHHHHCCCCCCCCCCCC
TaWXPL1D 107 KLYRGVRQRHWGKWVAEIRLP-RNRTRLWLGTFDTAEEAALAYDQAAYRLRGDAARLNFPDNA
TaWXPL2B 171 KLYRGVRQRHWGKWVAEIRLP-KNRTRLWLGTFDTAEDAALAYDKAAFRLRGDLARLNFPSLR
AtERF1 1 KHYRGVRQRPWGKFAAEIRDPAKNGARVWLGTFETAEDAALAYDRAAFRMRGSRALLNFPLRV
(B)
CRT (GCCGAC)
DRE (ACCGAC)
GCC (GCCGCC)
TaWXPL1D
TaWXPL2B
Thr137
Trp134
Glu123
Arg125
Arg132
Arg113
Arg115
Thr201
Trp198
Glu187
Arg189
Arg196
Arg177
Arg179

Figure 6

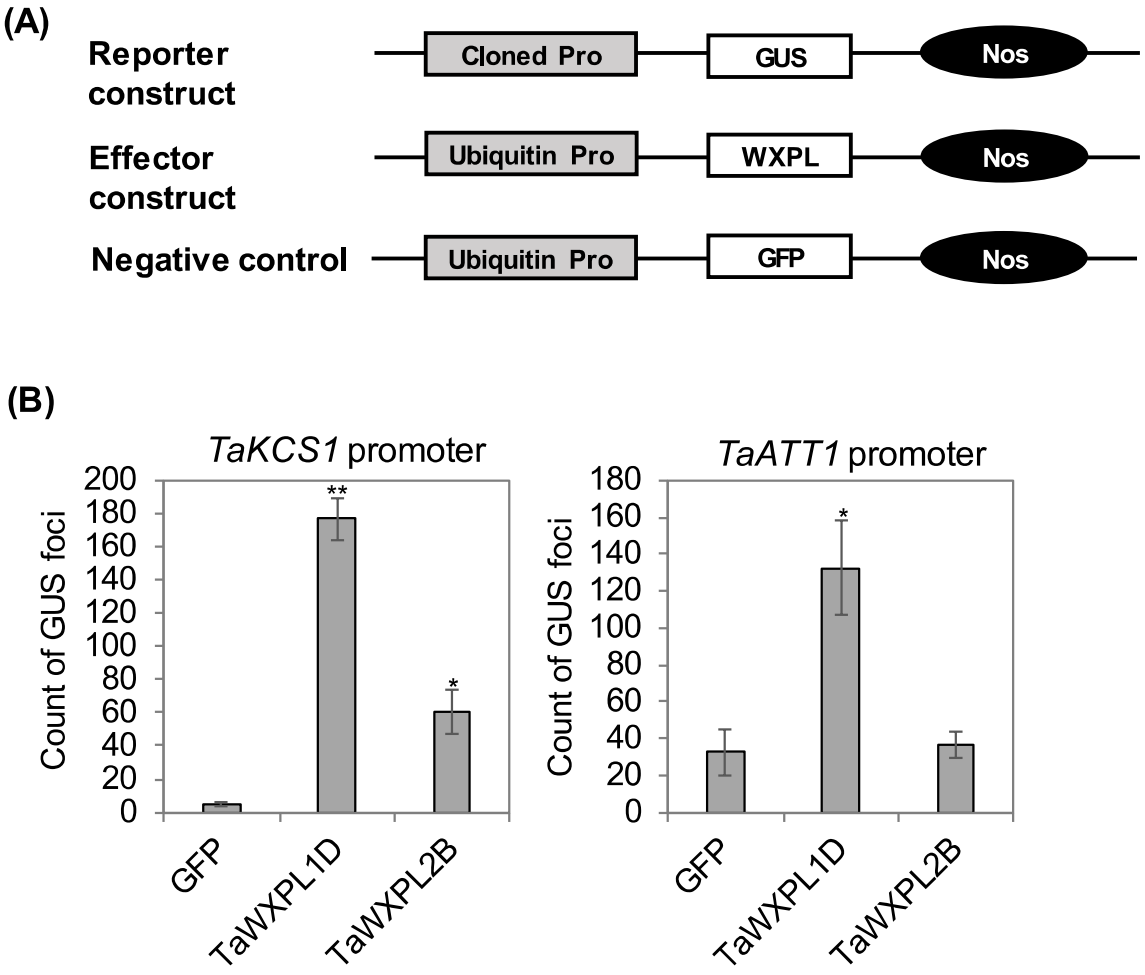
(A)
Reporter construct
Cloned Pro
GUS
Nos
Effector construct
Ubiquitin Pro
WXPL
Nos
Negative control
Ubiquitin Pro
GFP
Nos
(B)
TaKCS1 promoter
Count of GUS foci
200
180
160
140
120
100
80
60
40
20
0
**
*
GFP
TaWXPL1D
TaWXPL2B
TaATT1 promoter
Count of GUS foci
180
160
140
120
100
80
60
40
20
0
*
GFP
TaWXPL1D
TaWXPL2B

Figure 7

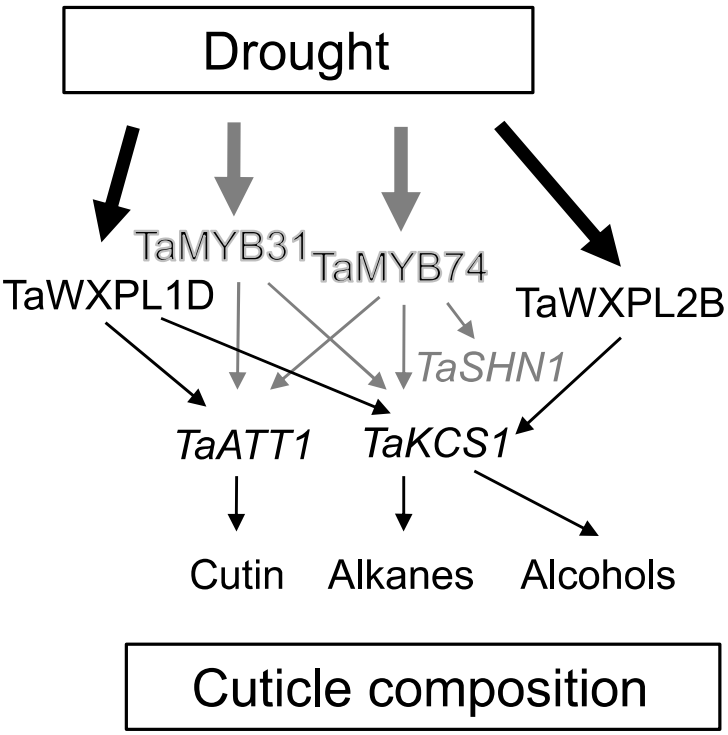
Drought
TaMYB31
TaMYB74
TaWXPL1D
TaWXPL2B
TaSHN1
TaATT1
TaKCS1
Cutin
Alkanes
Alcohols
Cuticle composition

Scheme 1

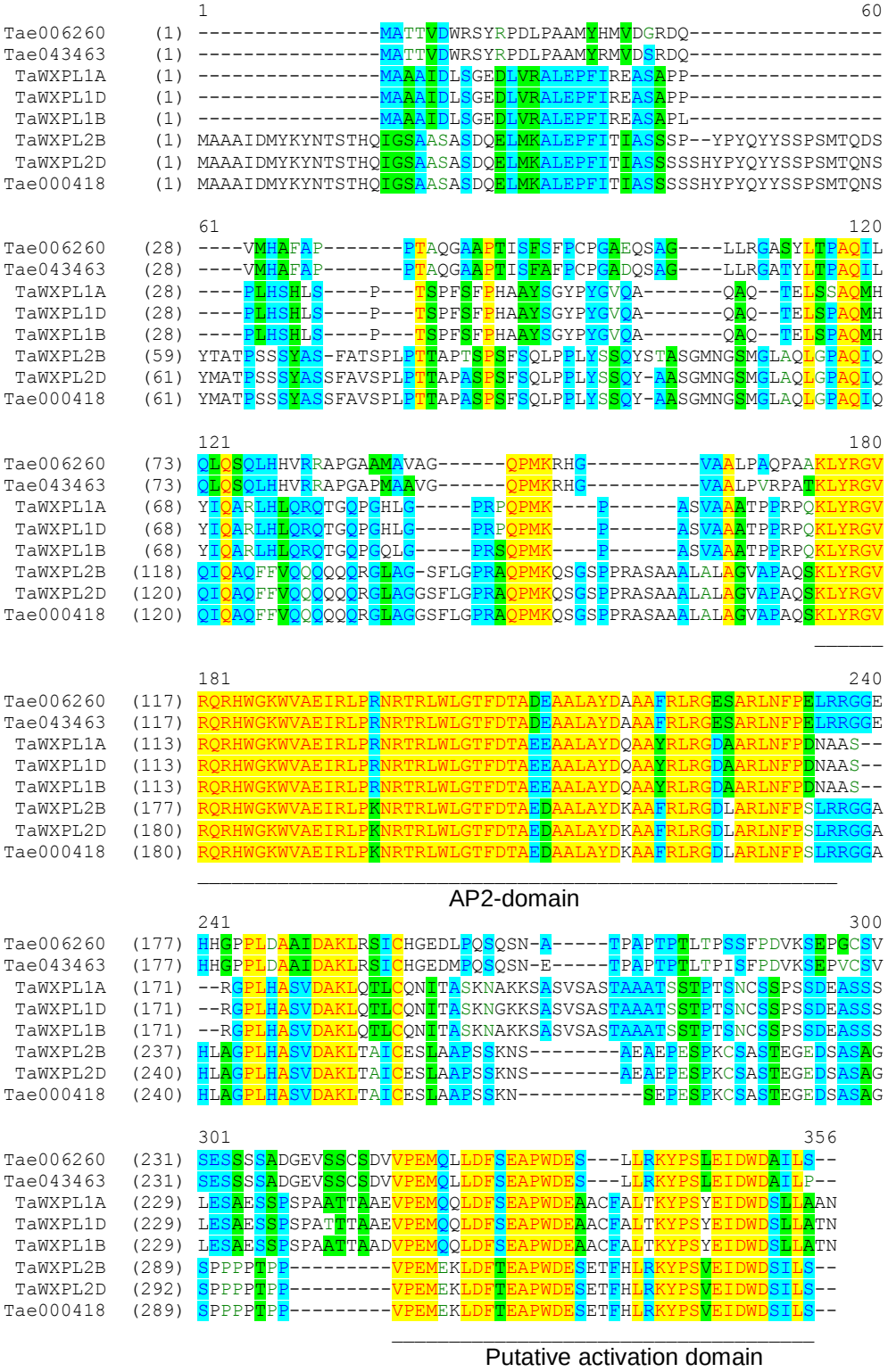

Supporting Figure 1

Supporting Table 1. List of primers used in this study. The directional TOPO cloning overhang (CACC), restriction enzyme sites and protection nucleotides are in bold.

Primer purposes	Genes	Forward primer	Reverse primer
Cloning of *TaWXPL* genes	*TaWXPL1A*	TCCAGGGGCTCCAGATCTGTTCG	GACGGACTAACCAAACCCTACCAC
		CACCATGGCTGCCGCTATAGATCTGTCC	CTAATTGGCGGCGAGAAGCGAGTC
	TaWXPL1B	CCCTATTCGTCTCCTTGTTCACC	GACGGTAGTAATAGTAGCTGACGG
		CACCATGGCTGCAGCTATAGATCTGTCC	CTAATTGGTGGCGAGAAGCGAATC
	TaWXPL1D	CCTGTTCGTCTCCTTGTTCACG	ACGGACTAACCAAACCCTACCCAC
		CACCATGGCTGCCGCTATAGATCTGTCC	CTAATTGGTGGCGAGAAGCGAGTC
	TaWXPL2B	CCCTTGTAGTTCGTCCGAATTATTC	TCTTACTAAACACCACTGGCTAC
		CACCATGGCCGCTGCCATAGACATGTAC	TCACGACAGGATGGAGTCCCAGTC
	TaWXPL2D	CGCTCTCCTCTTGCTCGGGATC	TCTTACTAAACACCACTGGCTAC
		CACCATGGCCGCTGCCATAGACATGTAC	TCACGACAGGATGGAGTCCCAGTC
Gene expression	*TaWXPL1D*	CCTGTTCGTCTCCTTGTTCACG	CGCCTGGCCGATTACTACAG
	TaWXPL2B	GCTATGATGTAATTTCTCTTTCG	CACTGGCTACTTACTGCTAC
Yeast 1-hybrid and in-yeast activation assays	*TaWXPL1D*	**GAAGAATTC**ATGGCTGCCGCTATAGATCTG	**GGAGGATCC**CTAATTGGTGGCGAGAAGC
	TaWXPL1D-D1	**GAAGAATTC**ATGGCCTCTGCCCCCCCTC	**GGAGGATCC**CTAATTGGTGGCGAGAAGC
	TaWXPL1D-D2	**GAAGAATTC**ATGGCTGCCGCTATAGATCTG	**GGAGGATCC**TATGCTGCGGTGGTGGTG
	TaWXPL1D-D3	**GAAGAATTC**ATGGCTGCCGCTATAGATCTG	**GGAGGATCC**TAGGAGGACGGCGAGGAGCAG
	TaWXPL2B	**CATCATATG**GCCGCTGCCATAGAC	**GAAGAATTC**ACGACAGGATGGAGTCC
	TaWXPL2B-D1	**CATCATATG**GCCGCTGCCATAGAC	**GAAGAATTC**AGGCCGAGTTCTTGGACGAG

Supporting Table 2. Evaluation of AP2 TaWXPL structural models in complex with CRT, DRE and GCC *cis*-elements, and the AtERF1 template. Discrete Optimised Protein Energy (DOPE)/Modeller Object Function (MOF) (Modeller 9.16), Ramachandran statistics (allowed residues from PROCHECK), G-factor (from PROCHECK) and z-score (ProSa2003) parameters are given.

Model/DNA complex	DOPE/MOF	Allowed residues	G-factors	z-score
TaWXPL1D/CRT	-4845.91/561.45	100	-0.2	-5.47
TaWXPL1D/DRE	-4842.21/538.62	100	-0.2	-5.44
TaWXPL1D/GCC	-4743.61/527.67	100	-0.1	-5.63
TaWXPL2B/CRT	-4838.09/516.73	100	-0.1	-5.23
TaWXPL2B/DRE	-4857.21/537.41	100	-0.2	-4.82
TaWXPL2B/GCC	-4834.81/522.40	100	-0.1	-5.27
AtERF1	-4916.53/-	100	-0.2	-5.54

Supporting Table 3. Hydrogen bonds of AP2 of TaWXPL1D and TaWXPL2B with CRT (5'-GCCGAC-3'/5'-GTCGGC-3'), DRE (5'-ACCGAC-3'/5'-GTCGGT-3') and GCC (5'-GCCGCC-3'/5'-GGCGGC-3') *cis*-elements.

Residues	**Number of hydrogen bonds with CRT and distances in Å[1]**									**DNA phospho-diester backbone**	**Number**
	CRT										
	G_1	**C_2**	**G_4**	**A_5**	**$G_{1'}$**	**$T_{2'}$**	**$C_{3'}$**	**$G_{5'}$**	**$C_{6'}$**		
TaWXPL1D											
Arg110	-	-	-	-	-	-	-	-	-	1 (2.9)	1
Gly111	-	-	-	-	-	-	-	-	-	1 (2.7)	1
Arg113	-	-	-	-	-	-	-	-	-	1 (2.6)	1
Arg115	1 (2.9)	-	-	-	-	-	-	1 (2.9)	-	-	2
Glu123	-	-	-	-	-	-	1 (3.4)	-	-	-	1
Arg125	-	-	-	-	2 (2.8, 2.9)	-	-	-	-	-	2
Arg132	-	-	1 (3.4)	-	-	-	-	-	-	1 (2.9)	2
Trp134	-	-	-	-	-	-	-	-	-	1 (3.1)	1
Thr137	-	-	-	-	-	-	-	-	-	1 (2.5)	1
Tyr148	-	-	-	-	-	-	-	-	-	1 (2.8)	1
Total	1	0	1	0	2	0	1	1	0	7	13
TaWXPL2B											
Arg174	-	-	-	-	-	-	-	-	-	1 (2.8)	1
Gly175	-	-	-	-	-	-	-	-	-	1 (2.7)	1
Arg177	-	-	-	-	-	-	-	-	-	1 (3.1)	1
Arg179	1 (3.1)	-	-	-	-	-	-	1 (3.0)	-	-	2
Glu187	-	-	-	-	-	-	-	-	-	-	0
Arg189	-	-	-	-	1 (3.0)	-	-	-	-	1 (3.0)	2
Arg196	-	-	-	-	-	-	-	-	-	1 (2.6)	1
Trp198	-	-	-	-	-	-	-	-	-	1 (2.9)	1
Thr201	-	-	-	-	-	-	-	-	-	1 (3.1)	1
Tyr212	-	-	-	-	-	-	-	-	-	1 (2.7)	1
Total	1	0	0	0	1	0	0	1	0	8	11

[1] The separations equal or less than 3.5 Å are indicated in brackets.

Residues	Number of hydrogen bonds with DRE and distances in Å[1]									DNA phospho-diester backbone	Number
	DRE										
	A_1	**C_2**	**G_4**	**A_5**	**$G_{1'}$**	**$T_{2'}$**	**$C_{3'}$**	**$G_{5'}$**	**$T_{6'}$**		
TaWXPL1D											
Arg110	-	-	-	-	-	-	-	-	-	1 (2.9)	1
Gly111	-	-	-	-	-	-	-	-	-	1 (2.7)	1
Arg113	-	-	-	-	-	-	-	-	-	1 (3.4)	1
Arg115	1 (2.5)	1 (3.5)	-	-	-	-	-	1 (2.9)	-	-	3
Glu123	-	-	-	-	-	-	1 (3.3)	-	-	-	1
Arg125	-	-	-	-	1 (2.9)	-	-	-	-	1 (2.9)	2
Arg132	-	-	2 (2.7, 2.8)	-	-	1 (3.1)	-	-	-	-	3
Trp134	-	-	-	-	-	-	-	-	-	1 (2.9)	1
Thr137	-	-	-	-	-	-	-	-	-	1 (3.1)	1
Tyr148	-	-	-	-	-	-	-	-	-	1 (2.7)	1
Total	1	1	2	0	1	1	1	1	0	7	15
TaWXPL2B											
Arg174	-	-	-	-	-	-	-	-	-	1 (2.9)	1
Gly175	-	-	-	-	-	-	-	-	-	1 (2.7)	1
Arg177	-	-	-	-	-	-	-	-	-	1 (2.7)	1
Arg179	1 (2.6)	-	-	-	-	-	-	1 (3.0)	1 (3.3)	-	3
Glu187	-	-	-	-	-	-	1 (3.5)	-	-	-	1
Arg189	-	-	-	1 (2.9)	1 (2.8)	-	-	-	-	-	2
Arg196	-	-	1 (3.3)	-	-	-	-	-	-	1 (2.9)	2
Trp198	-	-	-	-	-	-	-	-	-	1 (3.1)	1
Thr201	-	-	-	-	-	-	-	-	-	1 (3.2)	1
Tyr212	-	-	-	-	-	-	-	-	-	1 (2.5)	1
Total	1	0	1	1	1	0	1	1	1	7	14

[1] The separations equal or less than 3.5 Å are indicated in brackets.

Residues	Number of hydrogen bonds with GCC and distances in Å[1]									DNA phospho-diester backbone	Number
	GCC										
	G_1	C_2	G_4	C_5	$G_{1'}$	$G_{2'}$	$C_{3'}$	$G_{4'}$	$G_{5'}$		
TaWXPL1D											
Arg110	-	-	-	-	-	-	-	-	-	-	0
Gly111	-	-	-	-	-	-	-	-	-	1 (2.7)	1
Arg113	-	-	-	-	-	-	-	2 (2.9, 3.5)	-	-	2
Arg115	1 (2.6)	-	-	-	-	-	-	-	-	-	1
Glu123	-	-	-	-	-	-	1 (3.5)	-	-	-	1
Arg125	-	-	-	-	1 (2.7)	1 (2.7)	-	-	-	-	2
Arg132	-	-	-	-	-	-	-	-	-	1 (2.9)	1
Trp134	-	-	-	-	-	-	-	-	-	1 (3.1)	1
Thr137	-	-	-	-	-	-	-	-	-	1 (3.1)	1
Tyr148	-	-	-	-	-	-	-	-	-	1 (2.6)	1
Total	1	0	0	0	1	1	1	2	0	5	11
TaWXPL2B											
Arg174	-	-	-	-	-	-	-	-	-	1 (2.9)	1
Gly175	-	-	-	-	-	-	-	-	-	1 (2.7)	1
Arg177	-	-	-	-	-	-	-	-	-	1 (2.9)	1
Arg179	1 (2.3)	-	-	-	-	-	-	-	1 (2.6)	-	2
Glu187	-	-	-	-	-	-	1 (3.4)	-	-	-	1
Arg189	-	-	-	-	1 (3.0)	-	-	-	-	-	1
Arg196	-	-	1 (2.9)	-	-	-	-	-	-	-	1
Trp198	-	-	-	-	-	-	-	-	-	1 (3.1)	1
Thr201	-	-	-	-	-	-	-	-	-	1 (3.1)	1
Tyr212	-	-	-	-	-	-	-	-	-	1 (3.5)	1
Total	1	0	1	0	1	0	1	0	1	6	11

[1] The separations equal or less than 3.5 Å are indicated in brackets.

Chapter 5 Molecular and functional characterization of the wheat SHN1 transcription factor

5.1 Introduction

In addition to its primary function in resisting water loss, the cuticle plays multiple roles in biotic and abiotic stress response as a physical barrier protecting plants against pathogens, pests, heat, frost and UV radiation (reviewed in Borisjuk *et al.* 2014; Yeats and Rose 2013). The cuticle is also essential for plant development as it forms physical boundaries between organs. A group of mutants with defects in cuticle biosynthesis, such as the *bodyguard* mutant (Kurdyukov *et al.* 2006), the *atwbc11* mutant (Luo *et al.* 2007) and the maize *fused leaves1* (*fdl1*) mutant (La Rocca *et al.* 2015) exhibited organ fusions.

The product of the *WAX INDUCER1 (WIN1) /SHINE1 (SHN1)* gene belongs to the AP2/EREBP (ERF) family of TFs. The importance of the WIN1/SHN1 TF for regulation of cuticle biosynthesis and abiotic and biotic stresses has been demonstrated in several plant species. Overexpression of *AtWIN/SHN* genes in transgenic *Arabidopsis* altered cuticular wax composition and cuticle properties, conferred a brilliant, shiny green leaf phenotype and increased drought tolerance in transgenic *Arabidopsis* lines (Aharoni *et al.* 2004; Broun *et al.* 2004). Gene expression analysis revealed that several wax biosynthetic genes, such as *ECERIFERUM1* (*CER1*), *ECERIFERUM2* (*CER2*), and *3-ketoacyl-CoA synthetase* (*KCS1*), were induced in *WIN1*/*SHN1* transgenic *Arabidopsis* plants. Constitutive overexpression of *WIN1*/*SHN1* in *Arabidopsis* resulted in obvious morphological changes in transgenic plants compared to wild type plants. These changes included slower growth rates, smaller plant sizes, delayed flowering and increased sterility. Moreover, the degree of alteration was clearly associated with the strength of *WIN1* overexpression in transgenic plants (Broun *et al.* 2004). Various changes in *Arabidopsis* leaf morphology were also recently reported as a result of overexpression of ten *SHN* homologues isolated from *Glycine max* (Xu *et al.* 2016).

Kannangara *et al.* (2007) found that *WIN1/SHN1* overexpression influenced cutin production in *Arabidopsis*. In an attempt to explain the function of *WIN1/SHN1*, Kannangara *et al.* (2007) found that induction of *WIN1/SHN1* overexpression rapidly up-regulated a number of genes that are involved, or likely to be involved, in cutin biosynthesis. In contrast, wax biosynthetic genes *CER1*, *KCS1* and *CER2* were late induced by WIN1/SHN1. It was demonstrated *in planta* that WIN1/SHN1 directly bound to the promoter of *LACS2*, a cutin pathway gene encoding a long-chain acyl-CoA synthetase (Kannangara *et al.* 2007).

A *WIN/SHN* gene regulates lipid biosynthesis in developing caryopsis. Taketa *et al.* (2008) found that the *Nud* gene from barley, encoding a homologue of the *Arabidopsis WIN1/SHN1* gene, controlled the covered (hulled) / naked (hulless) caryopsis phenotypes of barley. These authors detected a lipid layer on the pericarp epidermis in hulled barley but not in hulless barley and concluded that the lipid layer, controlled by the *Nud* gene, was a critical difference between hulled and hulless phenotypes.

Another orthologue of *Arabidopsis WIN1/SHN1* gene, *OsWR1*, was found in rice (Wang *et al.* 2012). Transcript analysis demonstrated that *OsWR1* is induced by ABA, drought, and high salinity. *OsWR1* overexpression and RNA interference analyses revealed increased and decreased drought tolerance, respectively. These findings were consistent with changes in water loss and chlorophyll leaching properties in transgenic rice lines compared with those of control plants.

Plant cuticular waxes affect the exchange of gases and water between plants and the environment. Yang *et al.* (2011) investigated the correlation between wax accumulation and drought tolerance in transgenic *Arabidopsis*. They found that inducible overexpression of *WIN1/SHN1* gene led not only to alterations of the cuticle, but also to reduction of both stomatal density and index in leaves of transgenic *Arabidopsis* lines compared to those of control plants. Quantitative RT-PCR analysis in transgenic plants revealed increased levels of expression of wax biosynthetic genes and decreased expression of genes involved in stomatal development. These results suggested that reduction of stomata number together with quantitative and qualitative changes of cutin and cuticular wax might be the major contributors to the drought tolerance conferred by the expression of *WIN1/SHN1* gene.

In this study, we characterised the wheat orthologue of the *Arabidopsis WIN1/SHN1* gene. The analyses included investigation of transactivation properties and DNA-binding selectivity of the gene product, as well as generation and analysis of the *WIN1*/*SHN1*-overexpressing transgenic wheat plants. We examined water loss rates, stomatal density, leaf cuticular wax composition, as well as evaluation of plant growth and development and yield components using T_2 and T_3 lines grown under conditions of sufficient and limited watering.

5.2 Materials and methods

5.2.1 Phylogenetic analysis and sequence alignment

To conduct phylogenetic analysis of TaSHN1, we used 133 ERF proteins, including 12 SHNs, 5 TaWXPLs, 10 wheat ERF family proteins retrieved from NCBI and 106 wheat ERF proteins from Plant Transcription Factor Database (PlantTFDB, http://planttfdb.cbi.pku.edu.cn/). In total 161 amino acid sequences were retrieved from PlantTFDB. 55 sequences without methionine as the first amino acid were removed. Amino acid sequences were aligned by ClustalW and a bootstrap consensus tree using the maximum likelihood method was generated using MEGA 6 (Tamura *et al.* 2013). The alignment of six SHN TFs in Figure 5.1B was made in Vector NTI (11.5.2; Invitrogen, California, United States) using default parameters.

5.2.2 Transcriptional activation and DNA-binding assays in yeast

The procedures for transcriptional activation assays were as described by Bi *et al.* (2016) (See Chapter 3). The DNA-binding assay was performed using a modified yeast one-hybrid (Y1H) method described by Lopato *et al.* (2006). pGADT7-TaSHN1 construct was transformed into a yeast strain AH109, and a positive transformant was mated with a modified yeast strain Y187 (negative control) as well as four other modified Y187 strains with DRE, GCC-box, CRT and HDZ1 DNA *cis*-elements inserted in the yeast genomic DNA as part of the reporter constructs. Tandem repeats of DRE, GCC-box, CRT and HDZ1 *cis*-elements were cloned upstream of the *His* reporter gene in pINT-3NBHis vector (kindly provided by Prof. P. Ouwerkerk). The sequences of the DNA *cis*-elements can be found in Table 5.1.

Table 5.1 Sequences of DNA cis-elements used in analysis of DNA-binding selectivity of TaSHN1.

DNA *cis*-elements	DNA sequences[1,2]	References
DRE	GGCCGCTACCGACATTACCGACATTACCGACATTACCGACATA	Pyvovarenko and Lopato, 2011
GCC-box	GGCCGCCCACAAAGCCGCCGCCGTTAGACCACAAAGCCGCCGCCGTTAGAA	Unpublished
CRT	GGCCGCGCCGACGCCGACGCCGACGCCGACA	Pyvovarenko and Lopato, 2011
HDZ1	GGCCGCCAATCATTGCAATCATTGCAATCATTGCAATCATTGA	Pyvovarenko and Lopato, 2011

[1] Core elements are underlined.

[2] DRE, CRT and HDZ1 were named as "DRE, AtERD1", "CRT" and "HD-Zip class II", respectively, as defined by Pyvovarenko and Lopato (2011).

5.2.3 Construction of expression cassette and wheat transformation

The vector for wheat transformation of *TaSHN1* gene was constructed using the same approach as described by Bi *et al.* (2016) (See Chapter 3). The coding sequence of *TaSHN1* was firstly cloned into the pENTR-D-TOPO vector (Life Technologies, Victoria, Australia) and then inserted downstream of a maize polyubiquitin promoter in the modified pMDC32 vector (Curtis and Grossniklaus 2003), designated as pUbi, using the Gateway recombination system. The resulting 4237 bp long expression cassette, *pUbi-TaSHN1-NOS*, was cut from the pUbi vector using *Pme*I and *Asi*SI restriction endonucleases and purified by agarose gel electrophoresis. The DNA fragment for *TaSHN1* expression was co-transformed with a fragment of a hygromycin selection cassette (*pUbi-Hyg-NOS*) into the Australian elite wheat cultivar (*Triticum aestivum* cv. Gladius) using biolistic bombardment as described by Kovalchuk *et al.* (2009) and Ismagul *et al.* (2014).

5.2.4 Transgene detection and estimation of copy number

The presence of the transgene in the genomes of transformed wheat lines was pre-selected on the hygromycin containing medium, and estimation of transgene copy number was carried out both by Q-PCR and Southern blot hybridization. For Q-PCR analysis, the DNA extraction and amplification of specific fragments were performed as described by Fletcher (2014). Sequences of primers and dual-labelled probes, respectively targeting *nopaline synthase* (*NOS*) terminator (transgene) and *Puroindoline-b* (control gene), are listed in Table 5.2. A previously generated wheat transgenic plant with a single copy of the *NOS* terminator was used as a single copy reference. *Puroindoline-b* was used as a control gene (Fletcher 2014).

Table 5.2 Sequences of primers and probes used in Q-PCR.

Target	Target type	Oligo Name	Sequence (5′-3′)	Amplicon size (bp)	Reference
NOS terminator	Transgene	NOSTX_F	CTTAAGATTGAATCCTGTTGCCGGTC	225	Fletcher (2014)
		NOSTX_R	CGAATTCAGTAACATAGATGACACCGC		
		TxNOS probe green	AGCGCGCAAACTAGGATAAA		
Puroindoline-b	Low-copy control gene	Pinb_F	ATTTTCCAGTCACCTGGCCC	92	Li *et al.* (2004)
		Pinb_R	TGCTATCTGGCTCAGCTGC		
		Pinb_probe	ATGGTGGAAGGGCGGCTGTGA		

For Southern blot hybridisation, the genomic DNA was extracted using a method modified from Pallotta *et al.* (2000). Modifications are as follows: A large (diameter 9 mm) and three small (diameter 3 mm) ball bearings were added into the collection tubes with collected leaf samples. After freezing in liquid nitrogen, the samples were ground using MS 3 digital vortex mixer (IKA, Staufen, Germany). After addition of phenol/chloroform/iso-amylalcohol (25:24:1) mix, the samples were shaken using a RSM6 rotary mixer (Ratek Instruments, Victoria, Australia) for 10 minutes. DNAs were digested with *Eco*RV at 37 °C for 5 hours, run on a 1.0% agarose gel, blotted onto a Hybond N+ nylon membrane (GE Healthcare Life Sciences, NSW, Australia) and subjected to hybridisation with a ^{32}P-labelled DNA probe following standard methods. An in-house probe (2x 35S, 354 bp) targeting part of the backbone of the 4237 bp transformed DNA fragment was used. Primers for amplifying this probe are listed in Table 5.3.

Table 5.3 Sequences of primers used in preparation of the probe for Southern blot hybridisation[1].

Forward primer sequence	Reverse primer sequence	Amplicon size (bp)
CAACATGGTGGAGCACGAC	GCGTCATCCCTTACGTCAGTGGAG	354

[1] This pair of primers produced two PCR products of 681 bp and 354 bp in length. The 354 bp PCR product was purified and used as a probe.

5.2.5 Analysis of transgene expression

Expression of the transgene was examined by both Northern blot hybridisation and Reverse Transcription Polymerase Chain Reaction (RT-PCR). For both methods, total RNAs were isolated from leaf tissues using a Direct-zol RNA MiniPrep Kit (Zymo Research, CA, USA). The Northern blot (or RNA gel blot) was performed as described by (Sambrook and Russell 2001). RNAs were run on a 1.76% agarose gel with 1.3% formaldehyde. RNAs on the gel were blotted onto a Hybond N+ nylon membrane (GE Healthcare Life Sciences). The membrane was subjected to hybridisation with a ^{32}P-labelled DNA probe. Primers for preparation of this probe are listed in Table 5.4.

RT-PCR was used to confirm the transgene expression in T_2 plants. For this purpose, a pair of primers derived from the 3′-end of *TaSHN1* CDS (forward) and *NOS* terminator (reverse) were used (Table 5.4). cDNA synthesis was performed using 1.5 μg of purified total RNA and SuperScript III Reverse Transcriptase kit (Life Technologies, Victoria, Australia) according to the manufacturer's instructions. Wheat *Glyceraldehyde-3-phosphate dehydrogenase* (*TaGAP*) was used as a control gene. Primers for *TaGAP* are listed in Table 5.4.

Table 5.4 Sequences of primers used for preparation of the probe for Northern blot hybridisation and RT-PCR.

Primer purposes	Forward primer sequence	Reverse primer sequence	Amplicon size (bp)
Northern blot probe	GAAGGTAGCTTCGTCG	CCCATCTCATAAATAACGTC	267
RT-PCR transgene	CAGTCCACAGTGTCAGCAAC	GTTTGAACGATCGGGGAAATTC	266
RT-PCR *TaGAP* control gene	TTCAACATCATTCCAAGCAGCA	CGTAACCCAAAATGCCCTTG	223

5.2.6 Plant growth and sampling

The commercial Australian bread wheat variety Gladius plants and the derived transgenic lines overexpressing *TaSHN1* were grown in a randomized block design in 112 × 76 × 50 cm containers under well-watered conditions and drought, as described by Bi *et al.* (2016) (See Chapter 3). Six centimetres from the lower parts of flag leaf blades were collected 10 days after anthesis and used for quantitative and qualitative analyses of wax components. The weight of leaf samples was estimated immediately after detachment and then they were immersed into liquid nitrogen and stored at -80 ºC until wax was extracted

with chloroform. For yield components analysis, plant height and biomass, flowering time, number of spikes and seeds, and seed weight were recorded.

5.2.7 Assessment of water loss rates

Flag leaves were collected 10 days after anthesis, and the weight of each leaf was measured immediately before it was placed into a collection tube. Leaves were dehydrated in opened collection tubes at room temperature (23 °C) for 12 hours; weight of each leaf was measured every hour. Then leaves were dried in 37 °C incubator for 72 hours. Leaf weight after drying was taken as dry weight. Water loss rates were calculated as weight loss per hour and per dry weight of flag leaves.

5.2.8 Leaf surface imprints for assessment of stomatal density

Leaf surface imprints were prepared and analysed following the procedures described in Chapter 2. Counts were made from each of five images of each of the imprints from four biological replicates.

5.2.9 Quantification of cuticular waxes by GC-MS

For wax component analysis, leaf materials were retrieved from -80 °C freezer and warmed at room temperature for 2 minutes to ambient temperature. Leaves were immersed in 4 ml chloroform for 30 seconds, rinsed again for 30 seconds with 4 ml chloroform. The two extracts were pooled into a glass vial and dried under a stream of nitrogen. GC-MS was performed in Prof. Dabing Zhang's lab in the School of life sciences and biotechnology of Shanghai Jiao Tong University using the method described by Zhu *et al.* (2013). Dried samples were dissolved in 1 ml chloroform and 50 µl of internal standard (C24 alkane; 10 mg/ 50 ml) were added to the solution. Wax samples were then evaporated under a stream of nitrogen to a final volume of 100 µl. Trimethylsilyl groups were introduced to free hydroxyl and carboxyl groups in waxes by addition to each wax sample of 20 µl pyridine and 20 µl BSTFA [*N*,*O*-bis(trimethylsilyl)trifluoroacetamide] and following incubation of the reaction mix at 70°C for 40 minutes. Wax solutions were transferred to a GC vial and analysed by GC-FID (Agilent Technologies, California, United States) and GC-MS, Agilent GC coupled to an Agilent 5973N mass selective detector.

5.2.10 SEM and TEM

The waxy surfaces of leaves were examined using a scanning electron microscope (SEM) at the Adelaide Microscopy Waite Facility. Flag leaf blades were collected 10 days after

anthesis. Several segments of approximately 4mm × 3mm were cut from the middle of the leaves close to the major vein and freeze-dried overnight in an Alpha 1-2 LDplus freeze dryer (Christ, Germany), attached to a holder using the Tissue Tek OCT compound (ProSciTech Pty Ltd, QLD, Australia) mixed with carbon dag (Acheson ANZ Pty. Ltd., NSW, Australia) (in 1:1 ratio; carbon dag is a kind of conductive carbon paint). They were loaded onto the stage of a Philips XL30 Field Emission Scanning Electron Microscope and examined.

The cuticle layer was examined by a transmission electron microscope (TEM) of leaf segments taken at similar locations from the same leaf as used for SEM examination. The detailed procedures were described in Chapter 2.

5.3 Results

5.3.1 TaSHN1 is a wheat orthologue of AtSHN1

The coding sequence of *TaSHN1* (Accession KU737577) was isolated previously by PCR (Bi *et al*., 2016) (See Chapter 3). TaSHN1 is a wheat orthologue of AtSHN1 and has the highest protein sequence identity with the rice orthologue of AtSHN1, OsWR1 (Figure 5.1A). Protein alignment of six closely related SHNs showed that TaSHN1 contains the highly conserved AP2 domain with sequence features characteristic to ERF-type TFs, and has two additional conserved motifs characteristic for all members of SHN clade. These are a conserved middle motif ("mm") and a conserved C-terminal motif ("cm"), which were defined by Aharoni *et al.* (2004) (Figure 5.1B).

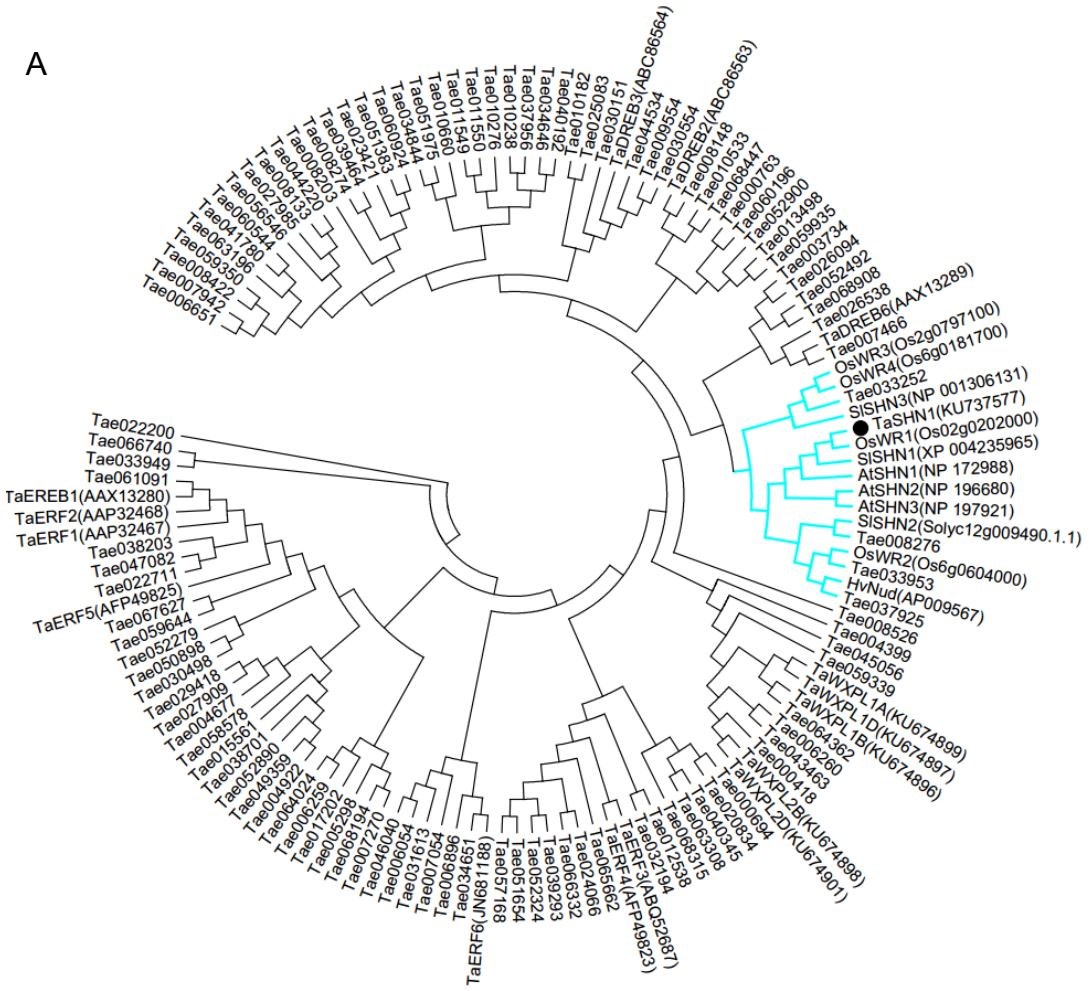
A
Tae022200
Tae066740
Tae033949
Tae061091
TaEREB1(AAX13280)
TaERF2(AAP32468)
TaERF1(AAP32467)
Tae038203
Tae047082
Tae022711
TaERF5(AFP49825)
Tae067627
Tae059644
Tae052279
Tae050898
Tae030498
Tae029418
Tae027909
Tae004677
Tae058578
Tae015561
Tae038701
Tae052890
Tae049359
Tae004922
Tae064024
Tae006259
Tae017202
Tae052298
Tae068184
Tae007270
Tae046040
Tae006054
Tae031613
Tae007054
Tae006896
Tae034651
TaERF6(JN681188)
Tae057168
Tae051654
Tae052324
Tae039293
Tae066332
Tae024066
Tae065662
TaERF4(AFP49823)
TaERF3(ABQ52687)
Tae032194
Tae012538
Tae063308
Tae040345
Tae020834
Tae000694
TaWXPL2D(KU674901)
TaWXPL2B(KU674898)
Tae000418
Tae043463
Tae006260
Tae064362
TaWXPL1B(KU674896)
TaWXPL1D(KU674897)
TaWXPL1A(KU674899)
Tae059339
Tae045056
Tae004399
Tae008526
Tae037925
HvNud(AP009567)
Tae033953
OsWR2(Os6g0604000)
Tae008276
SlSHN2(Solyc12g009490.1.1)
AtSHN3(NP 197921)
AtSHN2(NP 196680)
AtSHN1(NP 172988)
SlSHN1(XP 004235965)
OsWR1(Os02g0202000)
TaSHN1(KU737577)
SlSHN3(NP 001306131)
Tae033252
OsWR4(Os6g0181700)
Tae007466
TaDREB6(AAX13289)
Tae026538
Tae068908
Tae052492
Tae026094
Tae003734
Tae059935
Tae013498
Tae060196
Tae000763
Tae068447
Tae010533
Tae008148
TaDREB2(ABC86563)
Tae030554
Tae009554
Tae044534
TaDREB3(ABC86564)
Tae030151
Tae025083
Tae040192
Tae010182
Tae034846
Tae037956
Tae010238
Tae010276
Tae011550
Tae011549
Tae010660
Tae051975
Tae034844
Tae060924
Tae051383
Tae023421
Tae039464
Tae008274
Tae008203
Tae044220
Tae008133
Tae021985
Tae056546
Tae060544
Tae041780
Tae063196
Tae059350
Tae008422
Tae007942
Tae006651

B

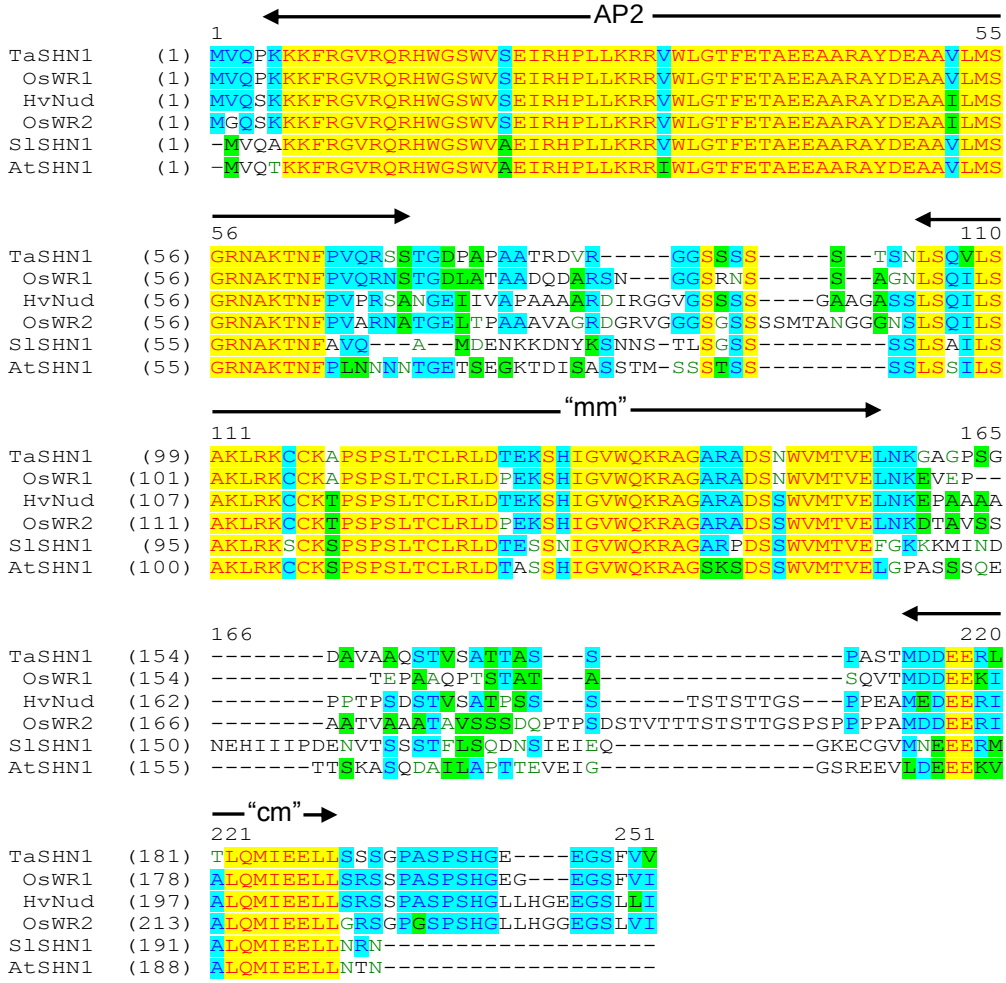

Figure 5.1 TaSHN1 is a wheat orthologue of AtSHN1.

(A) Phylogenetic analysis of plant SHN, and wheat ERF TFs retrieved from NCBI and PlantTFDB. Os, *Oryza sativa*; Hv, *Hordeum vulgare*; At, *Arabidopsis thaliana*; Sl, *Solanum lycopersicum*. (B) TaSHN1 contains an AP2 domain. "mm", a conserved middle motif; "cm", a conserved C-terminal motif.

5.3.2 TaSHN1 is a transcriptional activator and binds to specific DNA *cis*-elements

The transcriptional activation activity of TaSHN1 was examined in yeast. The ability of a modified yeast strain Y187 to grow on the selection medium lacking tryptophan (-Trp) indicated the successful transformation of pGBKT7 or pGBKT7-TaSHN1 (Figure 5.2A). The Y187 containing pGBKT7 plasmid could not grow on the selection medium lacking tryptophan and histidine (-Trp/-His) with 5 mM 3-amino-1,2,4-triazole (3-AT) since no transcription factors in this strain could activate the transcription of the *His* selection gene. The capability of the Y187 containing pGBKT7-TaSHN1 construct to grow on -Trp/-His

+ 5 mM 3-AT medium indicated that the successfully expressed recombinant protein, BD-TaSHN1 (BD, binding domain of yeast GAL4 TF), activated the expression of the *His* gene. Thus, TaSHN1 has an activation domain and acts as a transcriptional activator.

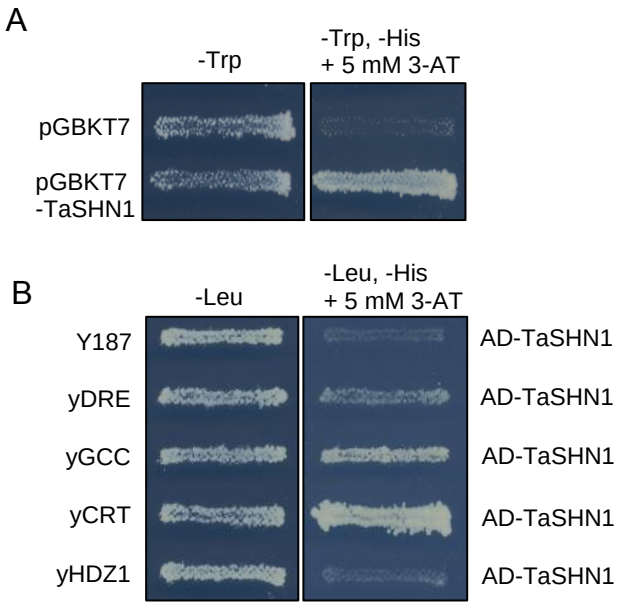

Figure 5.2 TaSHN1 is a transcriptional activator and binds to specific DNA elements. (A) Transcriptional activation assay in yeast. –Trp, the synthetic defined medium lacking tryptophan. -Trp/-His+5 mM 3-AT, the synthetic defined medium lacking tryptophan and histidine with 5 mM 3-amino-1,2,4-triazole (3-AT). (B) TaSHN1 binds to DRE, GCC and CRT DNA elements. HDZ1 is a negative control. –Leu, the synthetic defined medium lacking leucine. - Leu/-His+5 mM 3-AT, the synthetic defined medium lacking leucine and histidine with 5 mM 3-amino-1,2,4-triazole (3-AT).

It is known that ERFs specifically bind to a GCC-box and some also bind CRT DNA *cis*-elements, while DREB TFs specifically recognise DREs and CRT sequences (Eini *et al.* 2013). The affinities of TaSHN1 to these three *cis*-elements were determined using the Y1H assay (Figure 5.2B). The ability of either a yeast strain Y187 (negative control) or its versions with different *cis*-elements (DRE, GCC-box, CRT and HDZ1) integrated as a parts of reporter constructs in the yeast genome, to grow on the selection medium lacking leucine (-Leu), indicated that these strains were successfully mated with AH109 strain containing pGADT7-TaSHN1 since the pGADT7 vector harbours a *Leu* selection gene (Figure 5.2B). The yeast strains on -Leu media were replica plated to -Leu/-His + 5 mM 3-AT media. The growth of yDRE, yGCC and yCRT strains on these media indicated that TaSHN1 could interact with DRE, GCC-box and CRT *cis*-elements although with

very different strengths. Interaction with DRE was weak, interaction with GCC-box was moderate and with the CRT element was strong.

5.3.3 Generation and selection of *TaSHN1* transgenic wheat lines

To investigate the biological function of the *TaSHN1* gene in wheat, we generated wheat transgenic plants overexpressing *TaSHN1* under the control of a maize polyubiquitin promoter. In total, 50 independent transgenic lines were produced; the presence and copy numbers of transgene were determined in all T_0 plants using quantitative real-time PCR (Q-PCR). The expression of the transgene was examined in 16 lines with 0-3 copies and one line with 9 copies by Northern blot hybridisation (Figure 5.3A). Six lines (Lines 8, 10, 17, 36, 42 and 43; indicated by arrows in Figure 5.3A) containing 1-2 copies of the transgene and exhibiting different strength of gene expression were selected for further analysis. Southern blot hybridisation was performed with these six lines to confirm the copy number of the transgene obtained by Q-PCR (Figure 5.3B). Both methods of copy number estimation gave the same results for Lines 8, 10, 17 and 43. Transgene expression levels were re-assessed in the T_1 generation where segregation of the transgene occurred (Figure 5.3C). Finally, four sub-lines (indicated by arrows in Figure 5.3C) with the highest expression of the *TaSHN1* were selected for further analysis. In the T_2 generation, the presence of the *TaSHN1* transgene was verified by PCR for all 32 plants per line used for yield component analyses (data not shown). The expression of the transgene was confirmed by RT-PCR in the plants subjected to quantification of cuticular waxes (Figure 5.3D).

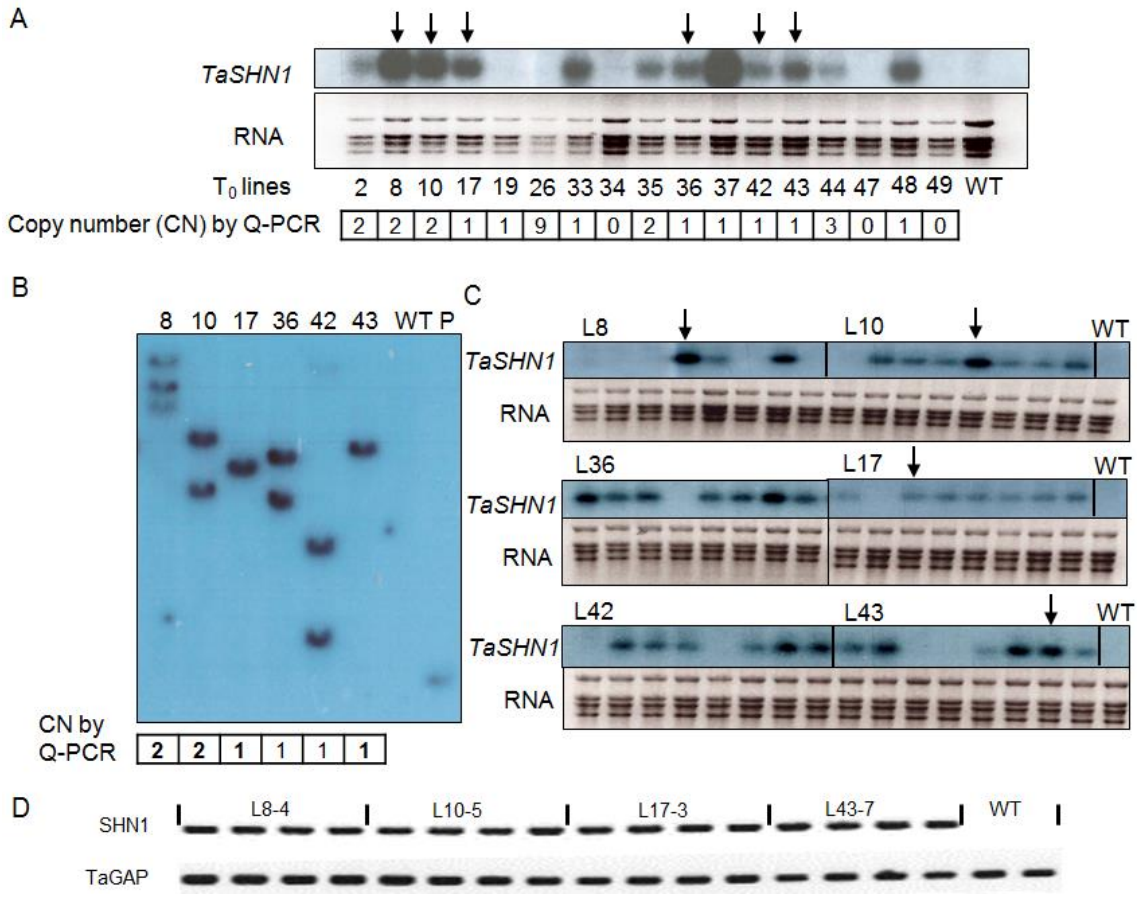

Figure 5.3 Copy number and expression of the transgene in transgenic wheat lines. (A) Expression of the transgene in T_0 lines assessed by Northern blot hybridisation and copy number of the transgene determined by Q-PCR. Black arrows indicate the lines selected for T_1 analysis. (B) Transgene copy number estimated by Southern blot hybridisation in selected T_0 lines. WT, wild type wheat cv. Gladius. P, positive control. (C). Expression of the transgene in T_1 progeny of selected T_0 lines. Eight plants per line were analysed for gene expression. Black arrows indicate the lines selected for T_2 analysis. WT, wild type wheat cv. Gladius. (D). Expression of the transgene in T_2 progeny of selected T_1 lines revealed by RT-PCR. These four samples per line were from the same plants subjected to cuticular wax quantification analysis. TaGAP (Glyceraldehyde-3-phosphate dehydrogenase) was used as a control gene. WT, wild type wheat cv. Gladius.

5.3.4 Overexpression of *TaSHN1* decreased water loss rates and stomatal density

The four selected T_2 lines together with WT plants were grown in two large containers; one container was well-watered during the entire experiment, while mild drought was

applied to another container. We selected three lines (Lines 10, 17 and 43) for analyses of water loss, stomatal density and cuticular waxes.

Non-stomatal water loss is a physiological trait directly associated with the plant cuticle, and assessment of water loss from detached leaves has been widely used to reflect cuticle related changes. We determined water loss rates of detached leaves of *TaSHN1* transgenic and WT control plants grown under both well-watered (WW) and drought (DR) conditions (Figure 5.4A). In the first hour after detachment, leaf water loss rates of WW Lines 10 and 17 were significantly lower than that of WT plants (P <0.01), and in the second hour leaf water loss rates of all three tested lines at WW conditions were lower than for WT (P <0.05). For the remaining time points, the differences in water loss rates between transgenic lines and WT were small, albeit in a few cases they were statistically significant. For plants grown under DR, however, water loss rates of detached leaves in all three transgenic lines were significantly lower than those of WT (P <0.05) at nearly all time points.

Stomatal density was examined on both sides of leaves from plants grown under the same watering regimes as in the water loss test (Figure 5.4B). On the abaxial side, stomatal densities were significantly reduced in WW Lines 10 and 17 compared with WT, by 19.9% and 12.7%, respectively, while they were 21.1%, 19.2% and 11.1% lower in DR Lines 10, 17 and 43, respectively. On the adaxial side, the density was significantly reduced only in the DR Line 43.

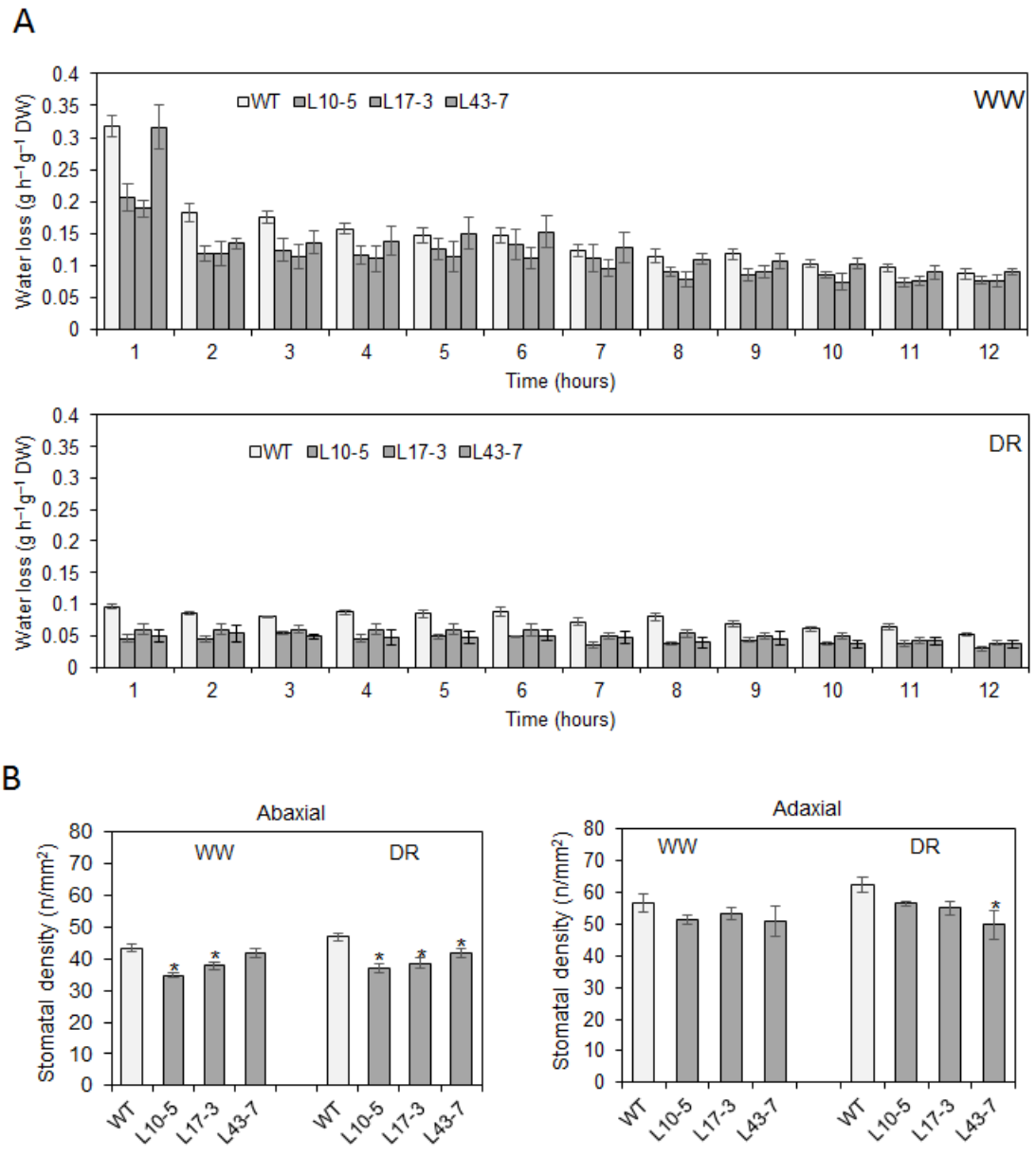

Figure 5.4 Water loss rates and stomatal density.

(A) Mean water loss rates (+/- SE) of flag leaves detached from wild type (WT) and transgenic wheat lines grown under well-watered (WW) conditions and mild drought (DR) (n=4). (B) Mean stomatal density (+/- SE) on the abaxial and adaxial surfaces of flag leaves collected from WT and transgenic wheat lines grown under WW and DR (n=4). Means and standard errors were counted in each of five images per leaf imprint from each of four biological replicates. Asterisks indicate significant differences at 5% level by Student's t-test.

5.3.5 Overexpression of *TaSHN1* influenced cuticular wax deposition on the leaf surface

To investigate how overexpression of *TaSHN1* affects cuticular waxes, the surfaces of flag leaves were observed under a scanning electron microscope in transgenic lines and WT controls (Figure 5.5). Under 150x magnification, it was found that the surfaces of both transgenic lines and WT plants are covered with very dense cuticular waxes which made the surfaces look glaucous. Surprisingly, a number of cuticular papillae (one indicated by a red arrow in Figure 5.5) were observed on the surface of a Line 43 leaf, while they were never detected in WT plants. Under 1500x and 8000x magnification, wax depositions around stomata were examined. Lines 17 and 43 exhibited a less dense distribution of waxes than the WT and the wax crystalloids appeared shorter than on leaves of control plants.

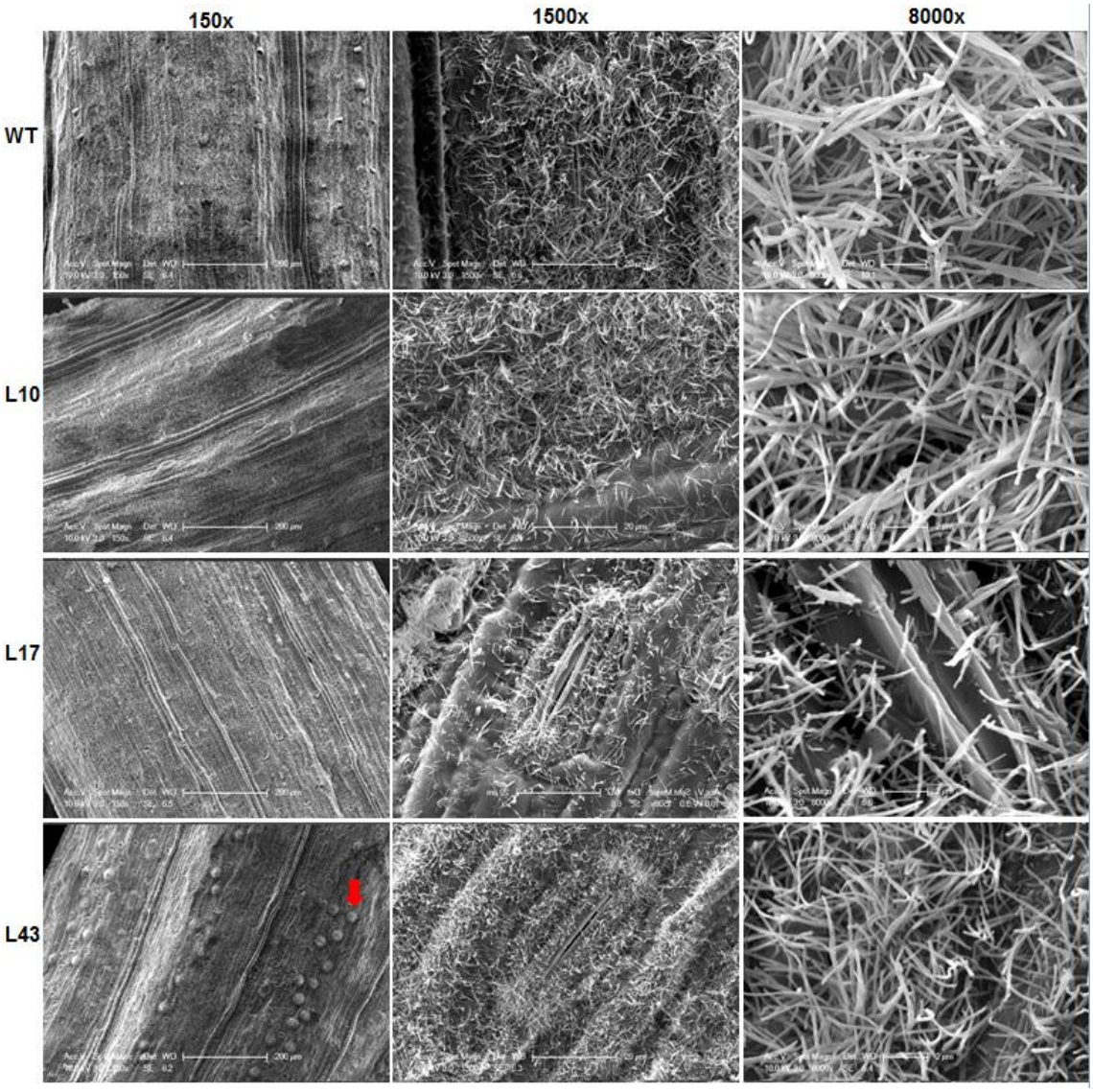

Figure 5.5 Observations of epicuticular waxes under scanning electron microscopy on the abaxial sides of flag leaves in transgenic lines and the wild type (WT) control. Leaf surfaces of WT, L10, L17 and L43 were observed under three different magnifications, 150x, 1500x and 8000x.

Cross-sections of cuticle layers were examined under a transmission electron microscope (Figure 5.6). No prominent differences were observed on either the abaxial side or the adaxial side of flag leaves between transgenic lines and the WT.

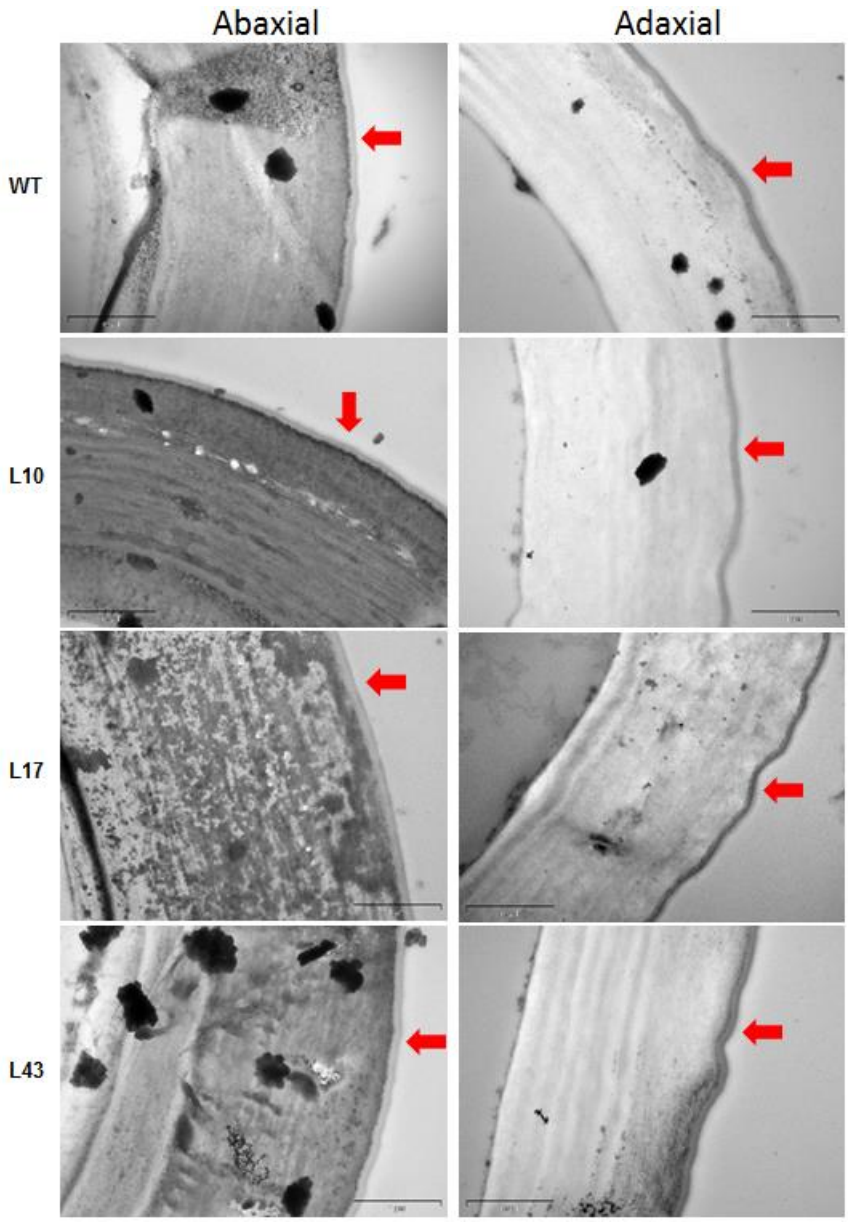

Figure 5.6 Observations of cuticle layer under transmission electron microscopy on the abaxial and adaxial sides of flag leaves in transgenic lines and the wild type (WT) control.

The very thin layers of the cuticle were indicated by red arrows.

5.3.6 Overexpression of *TaSHN1* altered cuticular wax accumulation

We quantified leaf epicuticular waxes using GC-MS for plants grown under both WW and DR (Figure 5.7). Under WW conditions, the total amounts of leaf epicuticular waxes were significantly reduced in Lines 17 and 43 compared with those in WT, by 35.6% ($P < 0.01$) and 16.5% ($P < 0.05$), respectively. These decreases in total wax amounts were mainly a result of significant decreases in contents of β-diketones in Lines 17 and 43, which were 71.0% ($P < 0.01$) and 53.1% ($P < 0.01$), respectively. Another significant

difference between transgenic lines and WT plants was in contents of aldehydes, which were significantly increased in Lines 10 ($P < 0.01$) and 43 ($P < 0.05$).

Overall, similar differences in compositions of leaf epicuticular waxes were found between DR transgenic lines and WT control plants as between WW transgenic lines and control plants, although some differences existed in particular transgenic lines. For instance, the amount of alkanes in Line 43 was significantly increased in DR transgenic plants compared with WT, but not in WW plants.

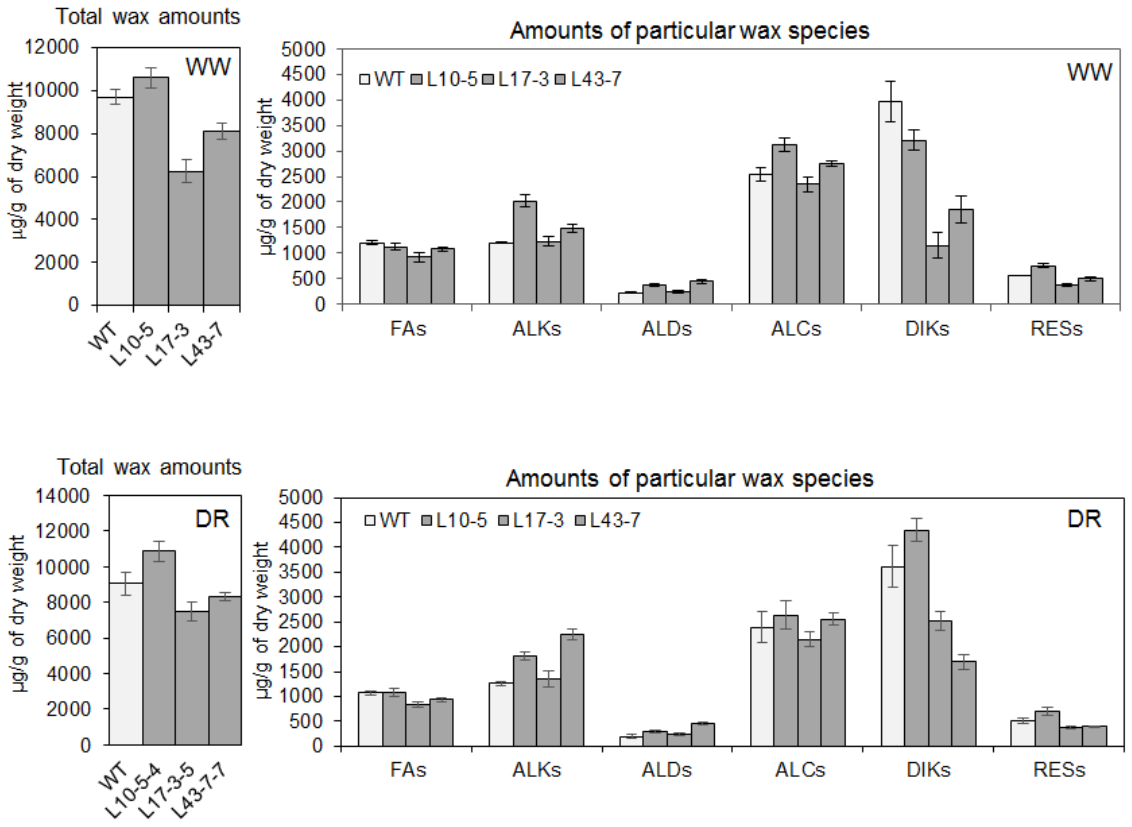

Figure 5.7 Epicuticular waxes (µg g-1) and composition on flag leaves of wild type (WT) wheat plants and transgenic wheat lines grown under well-watered (WW) conditions and mild drought (DR).

FAs - fatty acids, ALKs - alkanes, ALDs - aldehydes, ALCs - primary alcohols, DIKs – β-diketones, RESs - Resorcinols. Means and standard errors (indicated by bars) were calculated from four replicates.

Analysis of the quantity of individual wax components, revealed significant increases in amounts of C29 alkane, C26 and C28 aldehydes, and C24 and C26 primary alcohols in transgenic Lines 10 and 43 grown at WW conditions compared to those of WT controls (Figure 5.8). Similar changes occurred in these two lines under DR, with the exception of C28 aldehyde, the amount of which slightly increased only in Line 10 (Figure 5.9).

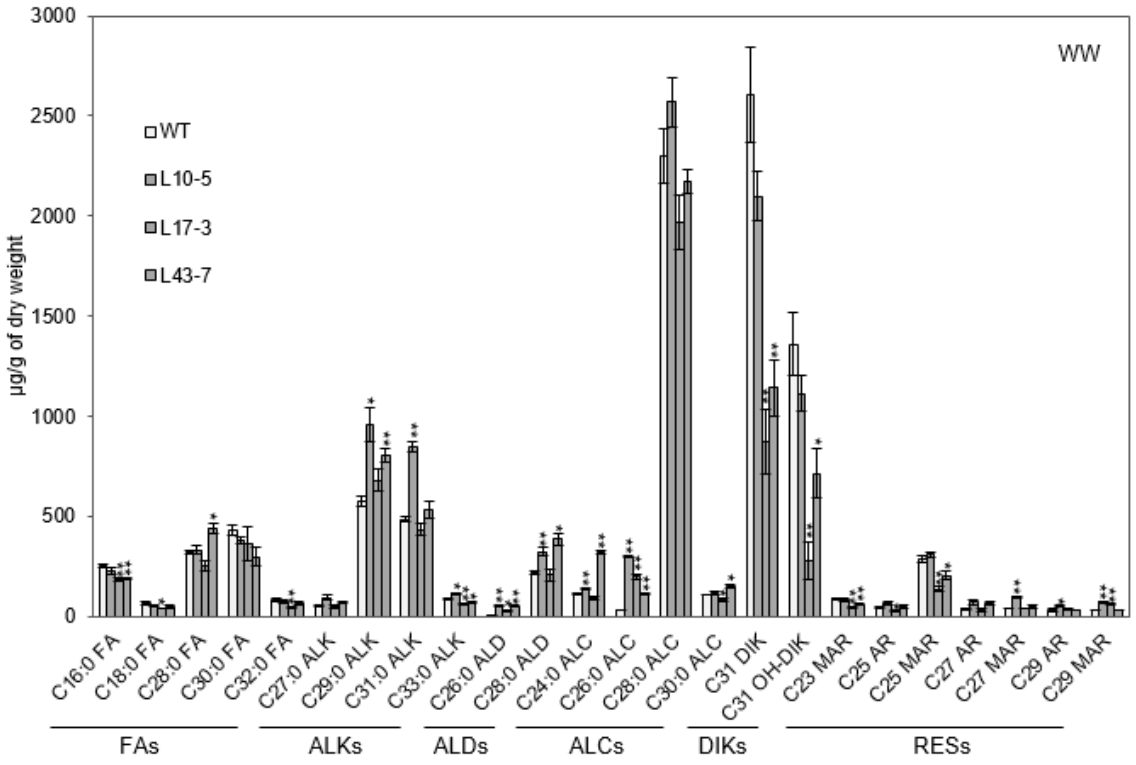

Figure 5.8 Individual wax components (µg g-1) on the flag leaves of the wild type control (WT) and transgenic lines grown under well-watered condition (WW).

Very low amounts of C20:0 FA, C22:0 FA and C24:0 FA are not shown but included in the calculations of amounts of wax species and total wax loads in Figure 5.7. FA, fatty acid; ALK, alkane; ALD, aldehyde; ALC, primary alcohol; DIK, β-diketone; MAR, methylalkylresorcinol; AR, alkylresorcinol; RES, resorcinol. Student's t-test was performed for statistical analysis of significance. * (in vertical direction) indicates significant difference at $P < 0.05$, ** (in vertical direction) indicates significant difference at $P < 0.01$.

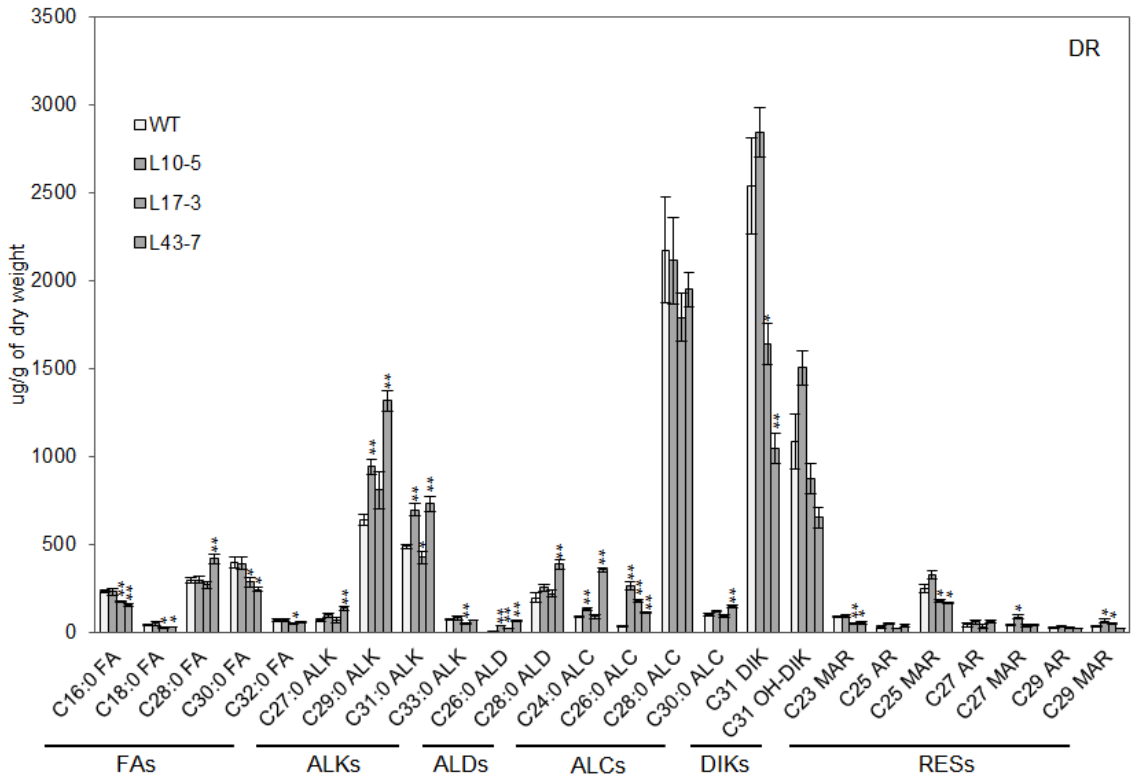

Figure 5.9 Individual wax components (µg g-1) on the flag leaves of wild type control (WT) and transgenic lines grown under mild drought (DR).

Very low amounts of C20:0 FA, C22:0 FA and C24:0 FA are not shown but are included in the calculations of amounts of wax species and total wax loads in Figure 5.7. FA, fatty acid; ALK, alkane; ALD, aldehyde; ALC, primary alcohol; DIK, β-diketone; MAR, methylalkylresorcinol; AR, alkylresorcinol; RES, resorcinol. Student's t-test was performed for statistical analysis of significance. * (in vertical direction) indicates significant difference at P <0.05, ** (in vertical direction) indicates significant difference at P <0.01.

5.3.7 Overexpression of *TaSHN1* affected plant biomass and yield

To get insight into the effects of *TaSHN1* on plant growth and development, we examined a series of yield related traits of T_2 transgenic lines grown under both WW and DR conditions. Surprisingly, the dry biomass and seed weight per plant (yield) appeared to be greatly increased in transgenic Lines 8 and 43 compared to control plants (Figure 5.10). The reason for the yield increase was an increase of spike and seed numbers per plant in transgenic lines. To confirm these data, we repeated these analyses using T_3 progenies of the same transgenic lines (Figure 5.11). The increases of plant biomass, seed number per plant and yield was observed for three (Lines 8, 10 and 43) of four tested lines. Seed

number per plant was well-correlated with increases in the plant biomass and grain yield, suggesting this trait as the main contributor to the yield increases.

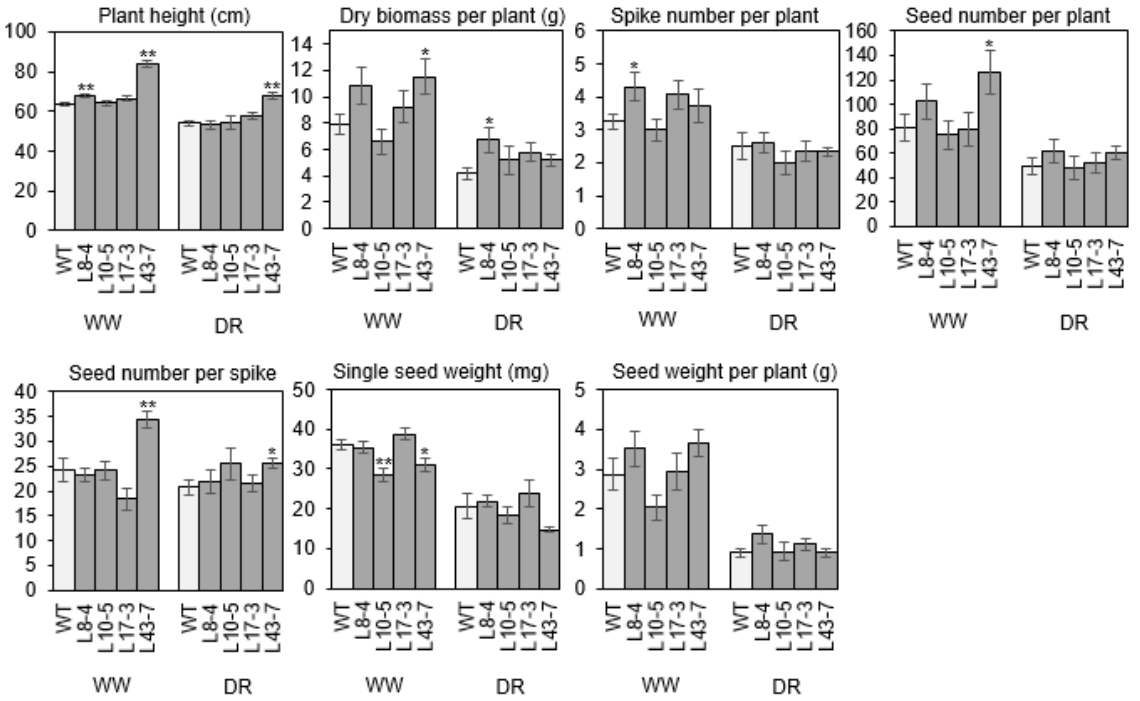

Figure 5.10 Yield components of T2 transgenic lines (means +/- SE, n=4).

Student's t-test was performed for statistical analysis of significance. * indicates significant difference at $P < 0.05$, ** indicates significant difference at $P < 0.01$.

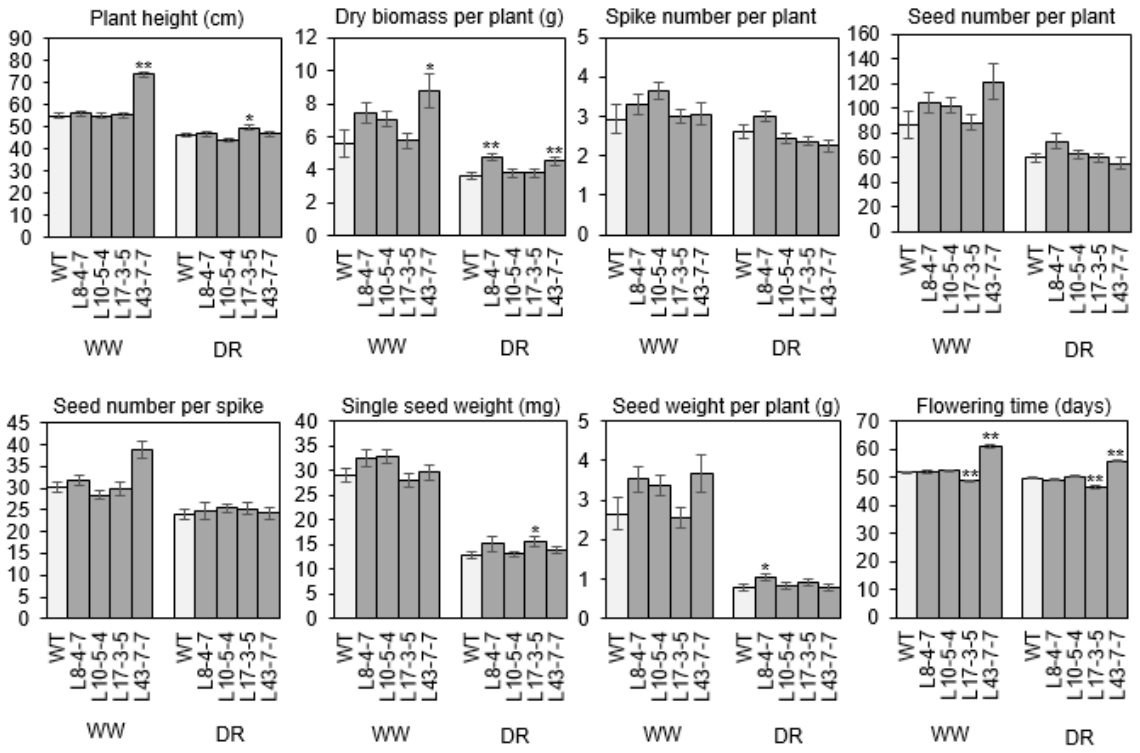

Figure 5.11 Yield components of T3 transgenic lines (means +/- SE, n=4).

Student's t-test was performed for statistical analysis of significance. * indicates significant difference at $P < 0.05$, ** indicates significant difference at $P < 0.01$.

In addition, rolling of leaves, distortion of spikes (as a result of organ fusion) and formation of additional spikelets (indicated by red arrows in Figure 5.12B) were observed in Line 10 plants (Figure 5.12).

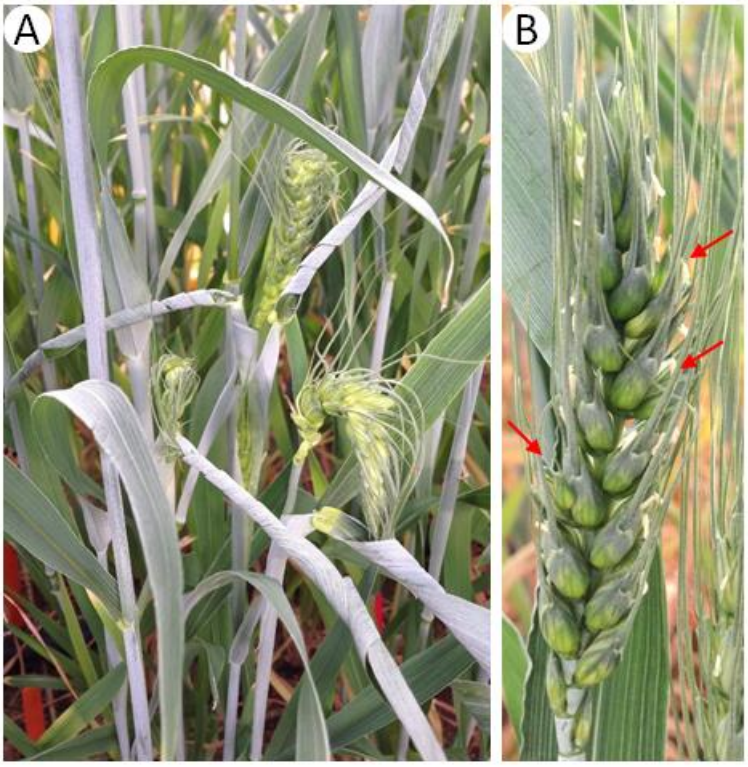

Figure 5.12 Phenotypic alterations in wheat transgenic plants (Line 10).
(A) Leaf rolling and spike distortion. (B) Formation of additional spikelets.

5.4 Discussion

Phylogenetic analysis of SHN related proteins with wheat AP2/ERF proteins grouped TaSHN1 into the same clade with SHN-like TF from other species and revealed at least four more wheat SHN TFs in the databases (Tae033252, Tae008276, Tae033953, Tae037925) (Figure 5.1A). TaSHN1 has the highest protein sequence identity, 81.4%, to OsWR1, a rice orthologue of AtSHN1, while a barley SHN-clade protein, HvNud, is phylogenetically close to OsWR2. In addition to the highly conserved AP2 domain, SHN proteins contain conserved "mm" and "cm" motifs which were defined by Aharoni *et al.* (2004). The function of these motifs in SHN proteins has not yet been clarified. Overexpression of *At5g25190*, whose gene product was classified into the same group as SHNs, did not exhibit the typical, glossy SHINE phenotype. This might result from the

incomplete “mm” motif in At5g25190 (Aharoni *et al.* 2004). Taketa *et al.* (2008) found that HvNud, a barley orthologue of AtSHN/WIN, controls adhering hulls in barley grain by regulating a lipid biosynthesis pathway. These authors revealed that one of the hulless caryopsis mutants is a result of a mutation in the valine residue at position 134, which is situated inside the “mm” motif of Nud. This finding suggests an important role of the “mm” motif in the regulation of the lipid biosynthetic pathways. The function of “cm” motif was not reported, however, it might be interesting to test whether this motif acts as a C-terminal transcriptional activation domain, similar to the ADs that we have identified in the wheat WXPL TFs (See Chapter 4).

Arabidopsis SHN TFs, AtSHN1, AtSHN2 and AtSHN3, were classified into Group V of the ERF subfamily of the AP2/ERF TF superfamily (Nakano *et al.* 2006). Members of this subfamily have a single AP2 domain which usually binds an ethylene responsive DNA *cis*-element, known as a GCC-box (AGCCGCC) (Ecker 1995). However, for some ERFs, such as CaERFLP1 (Lee *et al.* 2004), GmERF3 (Zhang *et al.* 2009) and TaERF6 (Eini *et al.* 2013), binding to CRT and/or DRE sequences were also reported. Another subfamily of the AP2/ERF TF superfamily with single AP2 domain, DREB/CBF, binds only DRE (ACCGAC) and CRT (GCCGAC) elements. In this study, we found that TaSHN1 could bind GCC-box, DRE, and CRT elements with clear preference for the CRT element (Figure 5.2). The weakest binding was observed for DRE, suggesting that the SHN proteins are rather ERFs than DREB TFs. Interestingly, the TaWXPL TFs (characterised in Chapter 4) which belong to Group I of the DREB/CBF subfamily (Nakano *et al.* 2006) were also revealed to bind all three DNA elements tested in this study. However, the weakest binding in the case of TaWXPLs was to GCC-box, which confirmed the fact that WXPL proteins are phylogenetically closer to the DREB subfamily than to ERFs. Comparative analyses of AP2 domains of wheat WXPL and SHN TFs using molecular models might provide additional explanations for differences in binding selectivity of these two groups of TFs to particular DNA elements.

One of the objectives of this study was to explore the options for using SHN to enhance drought tolerance in wheat as has been observed in *Arabidopsis* (Aharoni *et al.* 2004; Yang *et al.* 2011). The decreases in water loss rates in the first two hours after leaf detachment from transgenic plants grown under WW conditions probably resulted from the significant decreases in stomatal density (Figure 5.4). Aharoni *et al.* (2004) found that overexpression of *AtSHN1/WIN1* also altered epidermal cell differentiation, including reduction of both pavement cell density and stomatal density on the abaxial side of

overexpression lines. Results of Yang *et al.* (2011) confirmed that expression of genes involved in wax formation was increased after the induction of *WIN1/SHN1* gene, whereas expression of selected genes involved in stomatal development was decreased. The more significant differences in water loss rates between transgenic lines and WT plants grown under drought stress could not be explained only by corresponding changes of stomatal density in these plants. One possible explanations might be that TaSHN1 induced also other unknown defence responses to drought. Results of Voisin *et al.* (2009) suggested that dysfunction of the cuticle in cuticular mutants triggers a remodelling of the cuticle and cell wall and activation of defences to abiotic and biotic stresses.

We observed leaf rolling and spikelet fusion in the transgenic wheat line 10 (Figure 5.12). These alterations in plant morphology and cell adhesion are typical for a group of cuticular mutants, in addition to *AtSHN1* overexpression lines (Aharoni *et al.* 2004; Kurdyukov *et al.* 2006; Lolle *et al.* 1992; Wellesen *et al.* 2001). Variations in wax amounts (Figure 5.7) and yield components (Figure 5.10, Figure 5.11) among independent transgenic lines can be explained by the different strength of transgene expression in selected lines as a result of the insertion position in the genome. Line 10 was initially selected as a line with a high level of transgene transcription, while Lines 17 and 43 produced medium numbers of transgene transcripts (Figure 5.3). Overall, alterations in wheat organ development and cuticular wax accumulation confirmed the expression of the TaSHN1 at the protein level.

We demonstrated that *TaSHN1* overexpression in wheat increased the content of C29/C31 alkanes, C26/C28 aldehydes and C24/C26 primary alcohols in cuticular waxes (Figure 5.8). These changes in accumulation of particular wax components were in agreement with results of AtSHN1 in *Arabidopsis* (Aharoni *et al.* 2004). The *Arabidopsis shn* transposon activation mutant exhibited 2.2, 9.0 and 2.8 fold increases of leaf aldehydes, alkanes and primary alcohols amounts, respectively, compared to WT plants (Aharoni *et al.* 2004). It might be worth mentioning that the *shn* mutant enhanced the expression of two flanking genes, one of which was *SHN1* and chosen as the candidate for further studies.

The content of β-diketones significantly decreased in *TaSHN1* wheat transgenic plants compared to control WT plants (Figure 5.7Fig. 5). This finding on regulation of β-diketones biosynthesis by TaSHN1 is novel, because β-diketones are not present in the cuticular waxes of most studied model plants, such as *Arabidopsis*, rice and maize. In wheat, β-diketones are synthesized through a third pathway that is different from the other

two cuticular wax biosynthetic pathways, which were originally discovered in model plants: the acyl reduction (or alcohol-forming) pathway and the decarbonylation (or alkane-forming) pathway (Hen-Avivi *et al.* 2016; Zhang *et al.* 2013). All three pathways, however, rely on common fatty acid precursors (Borisjuk *et al.* 2014; Yeats and Rose 2013); the observed shift in wax composition could be explained therefore by competition for precursors, assuming that TaSHN1 stimulates alcohol/alkane biosynthesis at the expense of β-diketones. Information about genes encoding three key enzymes involved in the pathway of β-diketone biosynthesis have been reported recently for wheat and barley (Hen-Avivi *et al.* 2016; Schneider *et al.* 2016). Analyses of expression levels of these genes in *TaSHN1* transgenic lines or studies on the promoter regulation of these genes by TaSHN1 in transient expression assays could confirm the results presented here.

The physiological and biochemical changes seen in transgenic plants overexpressing *TaSHN1* suggest that these lines may show enhanced drought tolerance. The initial trials in controlled environments are encouraging but require field confirmation. The transgenic lines were produced in the background of the cultivar Gladius which is regarded as highly adapted to the low-yielding and drought prone environments in southern Australia (Fleury *et al.* 2010). Therefore, any improvement in the performance of this line under drought would be highly relevant to breeding programs.

In summary, we demonstrated that TaSHN1 acts as a transcriptional activator and binds all three tested *cis*-elements, albeit with different strengths. Overexpression of *TaSHN1* in transgenic wheat altered epicuticular wax composition and deposition, and decreased stomatal density and rates of water loss from detached leaves. Although the precise biological function of TaSHN1 requires further investigation, our current results strongly suggest that TaSHN1 plays a role in wax synthesis, epidermal cell differentiation and plant water conservation.

Chapter 6 General discussion

Drought has been a limiting factor in wheat production worldwide, and particularly in regions of southern and western Australia. Studies in plant biology for improvement of wheat stress tolerance and performance under drought have focussed on identification and analyses of drought-related physiological traits and candidate genes involved in the drought response. The plant cuticle plays multiple roles in protection from abiotic and biotic stresses. However, limited studies were performed on elucidation of the role of the wheat cuticle in resistance to dehydration. This PhD project was designed to: 1) explore different aspects of leaf cuticle in wheat cultivars with contrasting drought tolerance and glaucousness at conditions of sufficient and limited watering in an effort to establish a relationship between cuticle composition, structure, permeability and plant drought tolerance, and 2) identify and characterise drought-responsive wheat genes encoding regulators of the cuticle biosynthesis. In this chapter, the significance of the work and potential directions for future research are discussed.

Significance of the work

Significant differences were detected in the cuticle's ability to resist water loss, as evaluated by water loss rates from detached flag leaves. In particular, we found glaucous and drought tolerant wheat lines had much lower residual transpiration rates than the non-glaucous and drought sensitive control, Kukri. This finding suggests the importance of glaucousness in resisting non-stomatal water loss, although the precise value of this trait for drought and grain yield remains to be determined. Therefore, glaucousness as an adaptive, visual trait that can be easily scored for breeding selection, deserves attention. Our data also suggest the importance of other characteristics of the wheat cuticle under stress, such as the drought-adaptive increase in the amount of alkanes in cuticular wax and the increase of the thickness of the cuticle. These findings on the impact of drought on wheat cuticle are novel and should provide new opportunities for manipulation of leaf surface traits related to drought tolerance.

We identified several wheat genes encoding drought-responsive members of two TF families, which, potentially, can be used for improvement of wheat performance under drought stress via manipulation of cuticle properties and related mechanisms. The interest in related mechanisms was stimulated by studies that showed that some cuticle synthesis-related TFs in other species play multiple roles in response to drought and osmotic stress; AtMYB41 and AtMYB96, the respective homologues of TaMYB74 and TaMYB31, are among them. In this study, *TaMYB31* and *TaMYB74* were strongly up-regulated by both

rapid dehydration and slowly-developing drought in two wheat genotypes, RAC875 and Kukri. The up-regulation of *TaMYB31* by rapid dehydration was stronger in drought-tolerant RAC875 than in drought-sensitive Kukri. This suggests that *TaMYB31* is one of the contributors to the high drought tolerance of RAC875 and thus make it a good candidate for future study. In contrast, no differences were observed for the *TaMYB74* gene in maximal levels of induction between the two wheat genotypes, suggesting *TaMYB74* might play a universal role under drought. Similar to *TaMYB31*, the *TaWXPL1D* gene was not affected in Kukri but was clearly up-regulated in drought tolerant RAC875 under both stress conditions and thus represents a promising candidate for drought tolerance improvement.

Results of studies on protein domain structure, selectivity of DNA binding and mechanisms of target gene activation of drought-responsive cuticle-related MYB and WXPL TFs provide valuable data for future genome editing projects. These projects could aim at increased or decreased expression of a regulatory gene or alterations in the activity or specificity of its product to achieve modulation of expression of particular groups of the cuticle-related genes.

We identified two functional MYB-responsive DNA *cis*-elements in the promoter of the *TdSHN1* gene. This finding might lead to identification of new drought-responsive wheat *MYB* genes by screening cDNA libraries prepared from drought treated plant tissues using the yeast one-hybrid method with functional *cis*-elements as bait.

Data obtained in this work on decreases of water loss rates and stomatal density, and alterations in wax composition that occurred on leaves of *TaSHN1*-overexpressing wheat lines compared to leaves of control plants strongly suggest that TaSHN1 plays an important role(s) in plant water retention under drought. These results also support the conservation of the *SHN1* function in different species and confirm the effectiveness of identification of wheat genes by homology cloning of key genes identified and characterised in other species. This approach and the results obtained are particularly important for crop improvement through genetic engineering and genome editing, because the direct identification of wheat genes responsible for drought-related traits using tools of forward genetics, such as mutagenesis and QTL analyses, is still slow and difficult.

Improved performance of transgenic *TaSHN1* wheat lines compared to control plants can be considered as a significant first step on the way to produce wheat with increased grain yield, although confirmation in field trials is required. It would be important to note that

the transgenic lines were produced in Gladius, an elite Australian cultivar of bread wheat, which is highly adapted to the drought prone and low-yielding environments in southern Australia. The improvement of drought tolerance and performance under drought should be more obvious and significant if the drought-sensitive Kukri was used as a recipient cultivar for plant transformation. However, for a new technology to be useful, we must demonstrate that it offers advantages over and above what has been achieved by conventional breeding. In other words, demonstrating enhanced drought tolerance in a drought sensitive line is of far less value than showing improvements in a drought tolerant variety.

Taken together, this PhD project generated new knowledge at physiological, biochemical and molecular levels about the cuticle of wheat genotypes with contrasting drought tolerance and glaucousness, which were grown under optimal conditions and drought. The work presented here identified promising candidate genes for wheat drought tolerance improvement.

Possible research directions

Our findings suggest a positive role of glaucousness in resisting non-stomatal water loss in drought tolerant wheat lines. It is important to note that our study has focused on Australian elite lines. It is known that the biosynthesis of cuticular waxes is affected by a range of environmental conditions, such as light, temperature, osmotic stress and altitude. It would be interesting to explore the role of glaucousness in a large set of wheat genotypes with different levels of glaucousness and drought tolerance and from a wide range of cultivation areas.

Localization of water barrier properties in the epicuticular and intracuticular waxes of wheat cuticle should enhance our understanding of the water barrier property of the cuticle and its relationship with cuticle composition and structure. Recently, Jetter and Riederer (2016) found that the transpiration barrier property of cuticle was mainly formed by the intracuticular wax, while the epicuticular wax might also play a role depending on the cuticle composition of specific species. In addition, they found that the barrier was mainly associated with VLCFA derivatives rather than alicyclic wax compounds (e. g. triterpenoids, steroids, or tocopherols). It is reasonable to expect that the wheat cuticle is a good water barrier since only VLCFA derivatives were found in epicuticular wax. However, does the wheat leaf cuticle have similar compositions of epicuticular and

intracuticular waxes? How significant are the contributions of epicuticular and intracuticular waxes to wheat cuticle transpiration?

Three of the cloned wheat TF genes, TaMYB31, TaMYB74 and TaWXPL1D, were revealed to be strongly responsive to dehydration and drought and thus represent exciting candidate genes for wheat drought improvement. Further functional studies of these genes are required, for example, through overexpression using wheat transformation, and through gene silencing by means of virus-induced gene silencing (VIGS), interfering RNA or genome editing. A number of successful examples of characterisation of genes in wheat using VIGS via barley stripe mosaic virus (BSMV) and genome editing via a CRISPR-Cas system have been reported. The experiments should include evaluation of drought tolerance and grain yield, and exploration of the underlying mechanisms, for example, through identification of genes involved in the response pathway by RNA-seq analysis and identification of interacting partners by co-immunoprecipitation (Co-IP).

References (excluding Chapters 3 and 4)

Aarts M, Keijzer CJ, Stiekema WJ, Pereira A (1995) Molecular characterization of the *CER1* gene of *Arabidopsis* involved in epicuticular wax biosynthesis and pollen fertility. The Plant Cell 7:2115-2127

Abe H, Urao T, Ito T, Seki M, Shinozaki K, Yamaguchi-Shinozaki K (2003) *Arabidopsis* AtMYC2 (bHLH) and AtMYB2 (MYB) function as transcriptional activators in abscisic acid signaling. The Plant Cell 15:63-78

Adamski NM et al. (2013) The *Inhibitor of wax 1* locus (*Iw1*) prevents formation of β- and OH-β-diketones in wheat cuticular waxes and maps to a sub-cM interval on chromosome arm 2BS. The Plant Journal 74:989-1002

Adato A et al. (2009) Fruit-surface flavonoid accumulation in tomato is controlled by a SlMYB12-regulated transcriptional network. PLoS Genetics 5:e1000777

Aharoni A, Dixit S, Jetter R, Thoenes E, van Arkel G, Pereira A (2004) The SHINE clade of AP2 domain transcription factors activates wax biosynthesis, alters cuticle properties, and confers drought tolerance when overexpressed in *Arabidopsis*. The Plant Cell 16:2463-2480

Amalraj A et al. (2016) Change of function of the wheat stress-responsive transcriptional repressor TaRAP2.1L by repressor motif modification. Plant Biotechnology Journal 14:820-832

Baldoni E, Genga A, Cominelli E (2015) Plant MYB transcription factors: their role in drought response mechanisms. International journal of molecular sciences 16:15811-15851

Barthlott W, Neinhuis C, Cutler D, Ditsch F, Meusel I, Theisen I, Wilhelmi H (1998) Classification and terminology of plant epicuticular waxes. Botanical Journal of the Linnean Society 126:237-260

Bennett D et al. (2012) Identification of novel quantitative trait loci for days to ear emergence and flag leaf glaucousness in a bread wheat (*Triticum aestivum* L.) population adapted to southern Australian conditions. Theoretical and Applied Genetics 124:697-711

Bernard A et al. (2012) Reconstitution of plant alkane biosynthesis in yeast demonstrates that *Arabidopsis* ECERIFERUM1 and ECERIFERUM3 are core components of a very-long-chain alkane synthesis complex. The Plant Cell 24:3106-3118

Bernard A, Joubes J (2013) *Arabidopsis* cuticular waxes: advances in synthesis, export and regulation. Progress in lipid research 52:110-129

Bi H et al. (2016) Identification and characterization of wheat drought-responsive MYB transcription factors involved in the regulation of cuticle biosynthesis. Journal of Experimental Botany, doi:10.1093/jxb/erw298

Blum A (1975) Effect of the Bm gene on epicuticular wax deposition and the spectral characteristics of sorghum leaves. SABRAO Journal of Breeding and Genetics 7:45-52

Blum A (1988) Plant breeding for stress environments. CRC Press, Boca Raton, Florida

Bodner G, Nakhforoosh A, Kaul H-P (2015) Management of crop water under drought: a review. Agronomy for Sustainable Development 35:401-442

Bondada BR, Oosterhuis DM, Murphy JB, Kim KS (1996) Effect of water stress on the epicuticular wax composition and ultrastructure of cotton (*Gossypium hirsutum* L.) leaf, bract, and boll. Environmental and Experimental Botany 36:61-69

Borisjuk N, Hrmova M, Lopato S (2014) Transcriptional regulation of cuticle biosynthesis. Biotechnology Advances 32:526-540

Bourdenx B et al. (2011) Overexpression of *Arabidopsis ECERIFERUM1* promotes wax very-long-chain alkane biosynthesis and influences plant response to biotic and abiotic stresses. Plant Physiology 156:29-45

Bowne JB, Erwin TA, Juttner J, Schnurbusch T, Langridge P, Bacic A, Roessner U (2012) Drought responses of leaf tissues from wheat cultivars of differing drought tolerance at the metabolite level. Molecular plant 5:418-429

Broun P, Poindexter P, Osborne E, Jiang CZ, Riechmann JL (2004) WIN1, a transcriptional activator of epidermal wax accumulation in *Arabidopsis*. Proceedings of the National Academy of Sciences of the United States of America 101:4706-4711

Buxdorf K, Rubinsky G, Barda O, Burdman S, Aharoni A, Levy M (2014) The transcription factor SlSHINE3 modulates defense responses in tomato plants. Plant Molecular Biology 84:37-47

Cameron KD, Teece MA, Smart LB (2006) Increased accumulation of cuticular wax and expression of lipid transfer protein in response to periodic drying events in leaves of tree tobacco. Plant Physiology 140:176-183

Cha S, Song Z, Nikolau BJ, Yeung ES (2009) Direct profiling and imaging of epicuticular waxes on *Arabidopsis thaliana* by laser desorption/ionization mass spectrometry using silver colloid as a matrix. Analytical chemistry 81:2991-3000

Chai M et al. (2016) A class II KNOX gene, *KNOX4*, controls seed physical dormancy. Proceedings of the National Academy of Sciences of the United States of America 113:6997-7002

Chen G et al. (2011) An ATP-binding cassette subfamily G full transporter is essential for the retention of leaf water in both wild barley and rice. Proceedings of the National Academy of Sciences of the United States of America 108:12354-12359

Chen X, Goodwin SM, Boroff VL, Liu X, Jenks MA (2003) Cloning and characterization of the *WAX2* gene of *Arabidopsis* involved in cuticle membrane and wax production. The Plant Cell 15:1170-1185

Clarke J, Richards R (1988) The effects of glaucousness, epicuticular wax, leaf age, plant height, and growth environment on water loss rates of excised wheat leaves. Canadian Journal of Plant Science 68:975-982

Cominelli E, Sala T, Calvi D, Gusmaroli G, Tonelli C (2008) Over-expression of the *Arabidopsis AtMYB41* gene alters cell expansion and leaf surface permeability. The Plant Journal 53:53-64

Curtis MD, Grossniklaus U (2003) A gateway cloning vector set for high-throughput functional analysis of genes in planta. Plant Physiology 133:462-469

Delude C, Moussu S, Joubès J, Ingram G, Domergue F (2016) Plant surface lipids and epidermis development. In: Nakamura Y, Li-Beisson Y (eds) Lipids in plant and algae development. Springer International Publishing, Switzerland, pp 287-313

Denic V, Weissman JS (2007) A molecular caliper mechanism for determining very long-chain fatty acid length. Cell 130:663-677

Dubos C, Stracke R, Grotewold E, Weisshaar B, Martin C, Lepiniec L (2010) MYB transcription factors in *Arabidopsis*. Trends in Plant Science 15:573-581

Ecker JR (1995) The ethylene signal transduction pathway in plants. Science 268:667

Eini O et al. (2013) Complex regulation by Apetala2 domain-containing transcription factors revealed through analysis of the stress-responsive *TdCor410b* promoter from Durum Wheat. PLoS One 8:e58713

Ensikat H, Boese M, Mader W, Barthlott W, Koch K (2006) Crystallinity of plant epicuticular waxes: electron and X-ray diffraction studies. Chemistry and physics of lipids 144:45-59

Fabre G et al. (2016) The ABCG transporter PEC1/ABCG32 is required for the formation of the developing leaf cuticle in *Arabidopsis*. New Phytologist 209:192-201

Febrero A, Fernández S, Molina-Cano JL, Araus JL (1998) Yield, carbon isotope discrimination, canopy reflectance and cuticular conductance of barley isolines of differing glaucousness. Journal of Experimental Botany 49:1575-1581

Fletcher SJ (2014) qPCR for quantification of transgene expression and determination of transgene copy number. Methods in Molecular Biology 1145:213-237

Fleury D, Jefferies S, Kuchel H, Langridge P (2010) Genetic and genomic tools to improve drought tolerance in wheat. Journal of Experimental Botany 61:3211-3222

Folkers U, Berger J, Hulskamp M (1997) Cell morphogenesis of trichomes in *Arabidopsis*: differential control of primary and secondary branching by branch initiation regulators and cell growth. Development 124:3779-3786

Ford KL, Cassin A, Bacic A (2011) Quantitative proteomic analysis of wheat cultivars with differing drought stress tolerance. Frontiers in Plant Science 2:44

Fujita Y et al. (2005) AREB1 is a transcription activator of novel ABRE-dependent ABA signaling that enhances drought stress tolerance in *Arabidopsis*. The Plant Cell 17:3470-3488

Gilding EK, Marks MD (2010) Analysis of purified glabra3-shapeshifter trichomes reveals a role for NOECK in regulating early trichome morphogenic events. The Plant Journal 64:304-317

González A, Ayerbe L (2010) Effect of terminal water stress on leaf epicuticular wax load, residual transpiration and grain yield in barley. Euphytica 172:341-349

Goodwin SM, Jenks MA (2005) Plant cuticle function as a barrier to water loss. In: Jenks M, Hasegawa P (eds) Plant Abiotic Stress. Blackwell Scientific Publishers, Oxford, pp 14-36

Greer S, Wen M, Bird D, Wu X, Samuels L, Kunst L, Jetter R (2007) The cytochrome P450 enzyme CYP96A15 is the midchain alkane hydroxylase responsible for formation of secondary alcohols and ketones in stem cuticular wax of *Arabidopsis*. Plant Physiology 145:653-667

Grncarevic M, Radler F (1967) The effect of wax components on cuticular transpiration-model experiments. Planta 75:23-27

Guo L, Yang H, Zhang X, Yang S (2013) Lipid transfer protein 3 as a target of MYB96 mediates freezing and drought stress in *Arabidopsis*. Journal of Experimental Botany 64:1755-1767

Hen-Avivi S et al. (2016) A metabolic gene cluster in the wheat *W1* and the barley *Cer-cqu* loci determines beta-diketone biosynthesis and glaucousness. The Plant Cell 28:1440-1460

Hill CB, Taylor JD, Edwards J, Mather D, Bacic A, Langridge P, Roessner U (2013) Whole-genome mapping of agronomic and metabolic traits to identify novel quantitative trait loci in bread wheat grown in a water-limited environment. Plant Physiology 162:1266-1281

Hiratsu K, Matsui K, Koyama T, Ohme-Takagi M (2003) Dominant repression of target genes by chimeric repressors that include the EAR motif, a repression domain, in *Arabidopsis*. The Plant Journal 34:733-739

Hoang MHT et al. (2012) Phosphorylation by AtMPK6 is required for the biological function of AtMYB41 in *Arabidopsis*. Biochemical and Biophysical Research Communications 422:181-186

Islam MA, Du H, Ning J, Ye H, Xiong L (2009) Characterization of *Glossy1*-homologous genes in rice involved in leaf wax accumulation and drought resistance. Plant Molecular Biology 70:443-456

Ismagul A, Iskakova G, Harris JC, Eliby S (2014) Biolistic transformation of wheat with centrophenoxine as a synthetic auxin. In: Fleury D, Whitford R (eds) Crop Breeding, vol 1145. Springer, New York, pp 191-202

Izanloo A, Condon AG, Langridge P, Tester M, Schnurbusch T (2008) Different mechanisms of adaptation to cyclic water stress in two South Australian bread wheat cultivars. Journal of Experimental Botany 59:3327-3346

Jäger K, Fábián A, Eitel G, Szabó L, Deák C, Barnabás B, Papp I (2014) A morpho-physiological approach differentiates bread wheat cultivars of contrasting tolerance under cyclic water stress. Journal of Plant Physiology 171:1256-1266

Jakoby MJ et al. (2008) Transcriptional profiling of mature *Arabidopsis* trichomes reveals that NOECK encodes the MIXTA-like transcriptional regulator MYB106. Plant Physiology 148:1583-1602

Javelle M, Vernoud V, Rogowsky PM, Ingram GC (2011) Epidermis: the formation and functions of a fundamental plant tissue. New Phytologist 189:17-39

Jefferson P, Johnson D, Asay K (1989) Epicuticular wax production, water status and leaf temperature in Triticeae range grasses of contrasting visible glaucousness. Canadian Journal of Plant Science 69:513-519

Jenks MA, Andersen L, Teusink RS, Williams MH (2001) Leaf cuticular waxes of potted rose cultivars as affected by plant development, drought and paclobutrazol treatments. Physiologia Plantarum 112:62-70

Jenks MA, Ashworth EN (1999) Plant epicuticular waxes: function, production, and genetics. Horticultural Reviews 23:1-68

Jenks MA, Joly RJ, Peters PJ, Rich PJ, Axtell JD, Ashworth EN (1994) Chemically induced cuticle mutation affecting epidermal conductance to water vapor and disease susceptibility in *Sorghum bicolor* (L.) Moench. Plant Physiology 105:1239-1245

Jenks MA, Tuttle HA, Eigenbrode SD, Feldmann KA (1995) Leaf epicuticular waxes of the *eceriferum* mutants in *Arabidopsis*. Plant Physiology 108:369-377

Jetter R, Kunst L, Samuels AL (2007) Composition of plant cuticular waxes. In: Riederer M, Muller C (eds) Annual Plant Reviews Volume 23: Biology of the Plant Cuticle. Blackwell Publishing Ltd, Oxford, pp 145-181

Jetter R, Riederer M (2016) Localization of the transpiration barrier in the epi-and intracuticular waxes of eight plant species: water transport resistances are associated with fatty acyl rather than alicyclic components. Plant Physiology 170:921-934

Jetter R, Sodhi R (2011) Chemical composition and microstructure of waxy plant surfaces: triterpenoids and fatty acid derivatives on leaves of *Kalanchoe daigremontiana*. Surface and Interface Analysis 43:326-330

Johnson DA, Richards RA, Turner NC (1983) Yield, water relations, gas exchange, and surface reflectances of near-isogenic wheat lines differing in glaucousness. Crop Science 23:318-325

Jung KH et al. (2006) *Wax-deficient anther1* is involved in cuticle and wax production in rice anther walls and is required for pollen development. The Plant Cell 18:3015-3032

Kannangara R et al. (2007) The transcription factor WIN1/SHN1 regulates cutin biosynthesis in *Arabidopsis thaliana*. The Plant Cell 19:1278-1294

Kim KS, Park SH, Jenks MA (2007a) Changes in leaf cuticular waxes of sesame (*Sesamum indicum* L.) plants exposed to water deficit. Journal of Plant Physiology 164:1134-1143

Kim KS, Park SH, Kim DK, Jenks MA (2007b) Influence of water deficit on leaf cuticular waxes of soybean (*Glycine max* [L.] Merr.). International Journal of Plant Sciences 168:307-316

Kooyers NJ (2015) The evolution of drought escape and avoidance in natural herbaceous populations. Plant Science 234:155-162

Kosma DK, Bourdenx B, Bernard A, Parsons EP, Lü S, Joubès J, Jenks MA (2009) The impact of water deficiency on leaf cuticle lipids of *Arabidopsis*. Plant Physiology 151:1918-1929

Kosma DK, Jenks MA (2007) Eco-physiological and molecular-genetic determinants of plant cuticle function in drought and salt stress tolerance. In: Jenks MA, Hasegawa PM, Jain SM (eds) Advances in molecular breeding toward drought and salt tolerant crops. Springer, Netherlands, pp 91-120

Kosma DK, Murmu J, Razeq FM, Santos P, Bourgault R, Molina I, Rowland O (2014) AtMYB41 activates ectopic suberin synthesis and assembly in multiple plant species and cell types. The Plant Journal 80:216-229

Kosma DK, Nemacheck JA, Jenks MA, Williams CE (2010) Changes in properties of wheat leaf cuticle during interactions with Hessian fly. The Plant Journal 63:31-43

Kovalchuk N et al. (2009) Characterization of the wheat endosperm transfer cell-specific protein TaPR60. Plant Molecular Biology 71:81-98

Kunst L, Samuels L (2009) Plant cuticles shine: advances in wax biosynthesis and export. Current Opinion in Plant Biology 12:721-727

Kurdyukov S et al. (2006) The epidermis-specific extracellular BODYGUARD controls cuticle development and morphogenesis in *Arabidopsis*. The Plant Cell 18:321-339

La Rocca N et al. (2015) The maize *fused leaves1* (*fdl1*) gene controls organ separation in the embryo and seedling shoot and promotes coleoptile opening. Journal of Experimental Botany 66:5753-5767

Langridge P, Reynolds MP (2015) Genomic tools to assist breeding for drought tolerance. Current Opinion in Biotechnology 32:130-135

Lee J-H, Hong J-P, Oh S-K, Lee S, Choi D, Kim W (2004) The ethylene-responsive factor like protein 1 (CaERFLP1) of hot pepper (Capsicum annuum L.) interacts in vitro with both GCC and DRE/CRT sequences with different binding affinities: possible biological roles of CaERFLP1 in response to pathogen infection and high salinity conditions in transgenic tobacco plants. Plant Molecular Biology 55:61-81

Lee SB, Kim H, Kim RJ, Suh MC (2014) Overexpression of *Arabidopsis MYB96* confers drought resistance in *Camelina sativa* via cuticular wax accumulation. Plant Cell Reports 33:1535-1546

Lee SB, Suh MC (2015a) Advances in the understanding of cuticular waxes in *Arabidopsis thaliana* and crop species. Plant Cell Reports 34:557-572

Lee SB, Suh MC (2015b) Cuticular Wax Biosynthesis is Up-Regulated by the MYB94 Transcription Factor in *Arabidopsis*. Plant and Cell Physiology 56:48-60

Levitt J (1980) Stress terminology. In: Turner NC, Kramer PJ (eds) Adaptation of plants to water and high temperature stress. Wiley, New York, pp 473-439

Li-Beisson Y et al. (2013) Acyl-lipid metabolism. In: Torii K et al. (eds) The Arabidopsis Book, vol 11. 2013/03/19 edn. The American Society of Plant Biologists, Rockville, p e0161. doi:10.1199/tab.0161

Li F et al. (2008) Identification of the wax ester synthase/acyl-coenzyme A: diacylglycerol acyltransferase WSD1 required for stem wax ester biosynthesis in *Arabidopsis*. Plant Physiology 148:97-107

Li H et al. (2010) Cytochrome P450 family member CYP704B2 catalyzes the ω -hydroxylation of fatty acids and is required for anther cutin biosynthesis and pollen exine formation in rice. The Plant Cell 22:173-190

Li Z, Hansen JL, Liu Y, Zemetra RS, Berger PH (2004) Using real-time PCR to determine transgene copy number in wheat. Plant Molecular Biology Reporter 22:179-188

Licausi F, Ohme-Takagi M, Perata P (2013) APETALA2/Ethylene Responsive Factor (AP2/ERF) transcription factors: mediators of stress responses and developmental programs. New Phytologist 199:639-649

Lippold F, Sanchez DH, Musialak M, Schlereth A, Scheible WR, Hincha DK, Udvardi MK (2009) AtMyb41 regulates transcriptional and metabolic responses to osmotic stress in *Arabidopsis*. Plant Physiology 149:1761-1772

Lobell DB, Gourdji SM (2012) The influence of climate change on global crop productivity. Plant Physiology 160:1686-1697

Lolle SJ, Cheung AY, Sussex IM (1992) *Fiddlehead*: an *Arabidopsis* mutant constitutively expressing an organ fusion program that involves interactions between epidermal cells. Developmental Biology 152:383-392

Lopato S, Bazanova N, Morran S, Milligan AS, Shirley N, Langridge P (2006) Isolation of plant transcription factors using a modified yeast one-hybrid system. Plant Methods 2:3

Lu P et al. (2015) Comparative fine mapping of the *Wax 1* (*W1*) locus in hexaploid wheat. Theoretical and Applied Genetics:1-9

Lü S, Song T, Kosma DK, Parsons EP, Rowland O, Jenks MA (2009) *Arabidopsis CER8* encodes long-chain acyl-CoA synthase 1 (LACS1) that has overlapping functions with LACS2 in plant wax and cutin synthesis. The Plant Journal 59:553-564

Luo B, Xue X-Y, Hu W-L, Wang L-J, Chen X-Y (2007) An ABC transporter gene of *Arabidopsis thaliana*, *AtWBC11*, is involved in cuticle development and prevention of organ fusion. Plant and Cell Physiology 48:1790-1802

Merah O, Deléens E, Souyris I, Monneveux P (2000) Effect of glaucousness on carbon isotope discrimination and grain yield in durum wheat. Journal of Agronomy and Crop Science 185:259-265

Mickelbart MV, Hasegawa PM, Bailey-Serres J (2015) Genetic mechanisms of abiotic stress tolerance that translate to crop yield stability. Nature Reviews Genetics 16:237-251

Millar AA, Kunst L (1997) Very-long-chain fatty acid biosynthesis is controlled through the expression and specificity of the condensing enzyme. The Plant Journal 12:121-131

Mizoi J, Shinozaki K, Yamaguchi-Shinozaki K (2012) AP2/ERF family transcription factors in plant abiotic stress responses. Biochimica et Biophysica Acta: Protein Structure and Molecular Enzymology 1819:86-96

Moose SP, Sisco PH (1996) *Glossy15*, an APETALA2-like gene from maize that regulates leaf epidermal cell identity. Genes & Development 10:3018-3027

Mulroy TW (1979) Spectral properties of heavily glaucous and non-glaucous leaves of a succulent rosette-plant. Oecologia 38:349-357

Nakano T, Suzuki K, Fujimura T, Shinshi H (2006) Genome-wide analysis of the ERF gene family in *Arabidopsis* and rice. Plant Physiology 140:411-432

Nawrath C (2006) Unraveling the complex network of cuticular structure and function. Current Opinion in Plant Biology 9:281-287

Ni Y, Guo Y, Han L, Tang H, Conyers M (2012) Leaf cuticular waxes and physiological parameters in alfalfa leaves as influenced by drought. Photosynthetica 50:458-466

Oliveira AF, Meirelles ST, Salatino A (2003) Epicuticular waxes from caatinga and cerrado species and their efficiency against water loss. Annals of the Brazilian Academy of Sciences 75:431-439

Oshima Y, Mitsuda N (2013) The MIXTA-like Transcription factor MYB16 is a major regulator of cuticle formation in vegetative organs. Plant Signaling & Behavior 8:e26826

Oshima Y, Shikata M, Koyama T, Ohtsubo N, Mitsuda N, Ohme-Takagi M (2013) MIXTA-like transcription factors and WAX INDUCER1/SHINE1 coordinately

regulate cuticle development in *Arabidopsis* and *Torenia fournieri*. The Plant Cell 25:1609-1624
Pallotta M, Graham R, Langridge P, Sparrow D, Barker S (2000) RFLP mapping of manganese efficiency in barley. Theoretical and Applied Genetics 101:1100-1108
Parsons EP et al. (2012) Fruit cuticle lipid composition and fruit post-harvest water loss in an advanced backcross generation of pepper (*Capsicum* sp.). Physiologia Plantarum 146:15-25
Pollard M, Beisson F, Li Y, Ohlrogge JB (2008) Building lipid barriers: biosynthesis of cutin and suberin. Trends in Plant Science 13:236-246
Prior S, Pritchard S, Runion G, Rogers H, Mitchell R (1997) Influence of atmospheric CO_2 enrichment, soil N, and water stress on needle surface wax formation in *Pinus palustris* (Pinaceae). American Journal of Botany 84:1070-1070
Pyvovarenko T, Lopato S (2011) Isolation of plant transcription factors using a yeast one-hybrid system. In: Yuan L, Perry SE (eds) Plant Transcription Factors: Methods and Protocols. Humana Press, New York, pp 45-66. doi:10.1007/978-1-61779-154-3
Raffaele S et al. (2008) A MYB transcription factor regulates very-long-chain fatty acid biosynthesis for activation of the hypersensitive cell death response in *Arabidopsis*. The Plant Cell 20:752-767
Rawson H, Clarke J (1988) Nocturnal transpiration in wheat. Functional Plant Biology 15:397-406
Richards R, Rawson H, Johnson D (1986) Glaucousness in wheat: Its development and effect on water-use efficiency, gas exchange and photosynthetic tissue temperatures. Functional Plant Biology 13:465-473
Ristic Z, Jenks MA (2002) Leaf cuticle and water loss in maize lines differing in dehydration avoidance. Journal of Plant Physiology 159:645-651
Rowland O, Zheng H, Hepworth SR, Lam P, Jetter R, Kunst L (2006) CER4 encodes an alcohol-forming fatty acyl-coenzyme A reductase involved in cuticular wax production in *Arabidopsis*. Plant Physiology 142:866-877
Rozema J, van de Staaij J, Björn LO, Caldwell M (1997) UV-B as an environmental factor in plant life: stress and regulation. Trends in Ecology & Evolution 12:22-28
Sakuma Y, Liu Q, Dubouzet JG, Abe H, Shinozaki K, Yamaguchi-Shinozaki K (2002) DNA-binding specificity of the ERF/AP2 domain of *Arabidopsis* DREBs, transcription factors involved in dehydration- and cold-inducible gene expression. Biochemical and Biophysical Research Communications 290:998-1009
Sambrook J, Russell DW (2001) Molecular cloning: a laboratory manual, 3rd Edition. vol 1. Cold Spring Harbour Laboratory Press, New York
Samdur M, Manivel P, Jain V, Chikani B, Gor H, Desai S, Misra J (2003) Genotypic differences and water-deficit induced enhancement in epicuticular wax load in peanut. Crop Science 43:1294-1299
Samuels L, Kunst L, Jetter R (2008) Sealing plant surfaces: cuticular wax formation by epidermal cells. Annual Review of Plant Biology 59:683-707
Sánchez FJ, Manzanares Ma, de Andrés EF, Tenorio JL, Ayerbe L (2001) Residual transpiration rate, epicuticular wax load and leaf colour of pea plants in drought conditions. Influence on harvest index and canopy temperature. European Journal of Agronomy 15:57-70
Schneider LM et al. (2016) The *Cer-cqu* gene cluster determines three key players in a β-diketone synthase polyketide pathway synthesizing aliphatics in epicuticular waxes. Journal of Experimental Botany 67:2715-2730
Schoppach R, Sadok W (2012) Differential sensitivities of transpiration to evaporative demand and soil water deficit among wheat elite cultivars indicate different strategies for drought tolerance. Environmental and Experimental Botany 84:1-10

Schreiber L, Riederer M (1996) Ecophysiology of cuticular transpiration: comparative investigation of cuticular water permeability of plant species from different habitats. Oecologia 107:426-432

Sela D, Buxdorf K, Shi JX, Feldmesser E, Schreiber L, Aharoni A, Levy M (2013) Overexpression of *AtSHN1/WIN1* provokes unique defense responses. PLoS One 8:e70146

Seo PJ, Lee SB, Suh MC, Park MJ, Go YS, Park CM (2011) The MYB96 transcription factor regulates cuticular wax biosynthesis under drought conditions in *Arabidopsis*. The Plant Cell 23:1138-1152

Seo PJ, Park CM (2010) MYB96-mediated abscisic acid signals induce pathogen resistance response by promoting salicylic acid biosynthesis in *Arabidopsis*. New Phytologist 186:471-483

Seo PJ, Park CM (2011) Cuticular wax biosynthesis as a way of inducing drought resistance. Plant Signaling & Behavior 6:1043-1045

Seo PJ et al. (2009) The MYB96 transcription factor mediates abscisic acid signaling during drought stress response in *Arabidopsis*. Plant Physiology 151:275-289

Shepherd T, Wynne Griffiths D (2006) The effects of stress on plant cuticular waxes. New Phytologist 171:469-499

Shewry P (2009) Wheat. Journal of Experimental Botany 60:1537-1553

Shi JX, Malitsky S, De Oliveira S, Branigan C, Franke RB, Schreiber L, Aharoni A (2011) SHINE transcription factors act redundantly to pattern the archetypal surface of *Arabidopsis* flower organs. PLoS Genetics 7:e1001388

Sinclair JB, Dhingra OD (1995) Basic plant pathology methods. CRC press, Florida

Stracke R, Werber M, Weisshaar B (2001) The *R2R3-MYB* gene family in *Arabidopsis thaliana*. Current Opinion in Plant Biology 4:447-456

Taketa S et al. (2008) Barley grain with adhering hulls is controlled by an ERF family transcription factor gene regulating a lipid biosynthesis pathway. Proceedings of the National Academy of Sciences of the United States of America 105:4062-4067

Tamura K, Stecher G, Peterson D, Filipski A, Kumar S (2013) MEGA6: molecular evolutionary genetics analysis version 6.0. Molecular Biology and Evolution 30:2725-2729

Tsunewaki K (1962) Monosomic analysis of synthesized hexaploid wheats. The Japanese Journal of Genetics 37:155-168

Tsunewaki K, Ebana K (1999) Production of near-isogenic lines of common wheat for glaucousness and genetic basis of this trait clarified by their use. Genes & Genetic Systems 74:33-41

Tulloch AP (1973) Composition of leaf surface waxes of *Triticum* species: Variation with age and tissue. Phytochemistry 12:2225-2232

Turner NC (1979) Drought resistance and adaptation to water deficits in crop plants. In: Mussell H, Staples RC (eds) Stress physiology in crop plants. John Wiley & Sons, New York, pp 344-372

Uppalapati SR et al. (2012) Loss of abaxial leaf epicuticular wax in *Medicago truncatula irg1/palm1* mutants results in reduced spore differentiation of anthracnose and nonhost rust pathogens. The Plant Cell 24:353-370

Urao T, Yamaguchi-Shinozaki K, Urao S, Shinozaki K (1993) An *Arabidopsis* myb homolog is induced by dehydration stress and its gene product binds to the conserved MYB recognition sequence. The Plant Cell 5:1529-1539

Vogg G, Fischer S, Leide J, Emmanuel E, Jetter R, Levy AA, Riederer M (2004) Tomato fruit cuticular waxes and their effects on transpiration barrier properties: functional characterization of a mutant deficient in a very-long-chain fatty acid β-ketoacyl-CoA synthase. Journal of Experimental Botany 55:1401-1410

Voisin D et al. (2009) Dissection of the complex phenotype in cuticular mutants of *Arabidopsis* reveals a role of SERRATE as a mediator. PLoS Genetics 5:e1000703

von Wettstein-Knowles P (1972) Genetic control of β-diketone and hydroxy-β-diketone synthesis in epicuticular waxes of barley. Planta 106:113-130

von Wettstein-Knowles P (1979) Genetics and biosynthesis of plant epicuticular waxes. In: Applelqvist L, Liljenberg C (eds) Advances in the biochemistry and physiology of plant lipids. Elsevier/North-Holland Biomedical Press, New York, pp 1-26

von Wettstein-Knowles P (1995) Biosynthesis and genetics of waxes. In: Hamilton RJ (ed) Waxes: chemistry, molecular biology and functions. . The Oily Press, Dundee, pp 91-130

von Wettstein-Knowles P (2012) Plant Waxes. In: eLS. John Wiley & Sons, Ltd. doi:10.1002/9780470015902.a0001919.pub2

Wang M et al. (2016) Three *TaFAR* genes function in the biosynthesis of primary alcohols and the response to abiotic stresses in *Triticum aestivum*. Scientific Reports 6:25008

Wang Y et al. (2012) An ethylene response factor OsWR1 responsive to drought stress transcriptionally activates wax synthesis related genes and increases wax production in rice. Plant Molecular Biology 78:275-288

Wang Y, Wang M, Sun Y, Hegebarth D, Li T, Jetter R, Wang Z (2015a) Molecular Characterization of *TaFAR1* Involved in Primary Alcohol Biosynthesis of Cuticular Wax in Hexaploid Wheat. Plant and Cell Physiology 56:1944-1961

Wang Y et al. (2015b) FAR5, a fatty acyl-coenzyme A reductase, is involved in primary alcohol biosynthesis of the leaf blade cuticular wax in wheat (*Triticum aestivum* L.). Journal of Experimental Botany 66:1165-1178

Wang ZY, Xiong L, Li W, Zhu JK, Zhu J (2011) The plant cuticle is required for osmotic stress regulation of abscisic acid biosynthesis and osmotic stress tolerance in *Arabidopsis*. The Plant Cell 23:1971-1984

Wellesen K et al. (2001) Functional analysis of the *LACERATA* gene of *Arabidopsis* provides evidence for different roles of fatty acid ω-hydroxylation in development. takeProceedings of the National Academy of Sciences of the United States of America 98:9694-9699

Weng H, Molina I, Shockey J (2010) Organ fusion and defective cuticle function in a *lacs1 lacs2* double mutant of *Arabidopsis*. Planta 231:1089-1100

Xu Y, Wu H, Zhao M, Wu W, Xu Y, Gu D (2016) Overexpression of the transcription factors GmSHN1 and GmSHN9 differentially regulates wax and cutin biosynthesis, alters cuticle properties, and changes leaf phenotypes in *Arabidopsis*. International journal of molecular sciences 17:587

Xu Z, Zhou G (2008) Responses of leaf stomatal density to water status and its relationship with photosynthesis in a grass. Journal of Experimental Botany 59:3317-3325

Xu ZS, Chen M, Li LC, Ma YZ (2011) Functions and application of the AP2/ERF transcription factor family in crop improvement. Journal of Integrative Plant Biology 53:570-585

Yang J, Isabel Ordiz M, Jaworski JG, Beachy RN (2011) Induced accumulation of cuticular waxes enhances drought tolerance in *Arabidopsis* by changes in development of stomata. Plant Physiology and Biochemistry 49:1448-1455

Yeats TH, Rose JK (2013) The formation and function of plant cuticles. Plant Physiology 163:5-20

Zhang G, Chen M, Li L, Xu Z, Chen X, Guo J, Ma Y (2009) Overexpression of the soybean *GmERF3* gene, an AP2/ERF type transcription factor for increased

tolerances to salt, drought, and diseases in transgenic tobacco. Journal of Experimental Botany 60:3781-3796

Zhang JY, Broeckling CD, Blancaflor EB, Sledge MK, Sumner LW, Wang ZY (2005) Overexpression of *WXP1*, a putative *Medicago truncatula* AP2 domain-containing transcription factor gene, increases cuticular wax accumulation and enhances drought tolerance in transgenic alfalfa (*Medicago sativa*). The Plant Journal 42:689-707

Zhang JY, Broeckling CD, Sumner LW, Wang ZY (2007) Heterologous expression of two *Medicago truncatula* putative ERF transcription factor genes, *WXP1* and *WXP2*, in *Arabidopsis* led to increased leaf wax accumulation and improved drought tolerance, but differential response in freezing tolerance. Plant Molecular Biology 64:265-278

Zhang Z, Wang W, Li W (2013) Genetic interactions underlying the biosynthesis and inhibition of β-diketones in wheat and their impact on glaucousness and cuticle permeability. PLoS One 8:e54129

Zhu L, Shi J, Zhao G, Zhang D, Liang W (2013) *Post-meiotic deficient anther1* (*PDA1*) encodes an ABC transporter required for the development of anther cuticle and pollen exine in rice. Journal of Plant Biology 56:59-68